Dissecting the Mechanisms of Joka2 Mediated Defence-Related Autophagy

Yasin Tumtas

Imperial College of Science, Technology and Medicine

(Imperial College London)

Department of Life Sciences

A thesis submitted for the degree of

Doctor of Philosophy

March 2020

Declaration of originality:

I declare that this thesis is a result of author's own work. All the data and conclusions have been analysed and formulated by the author. Any external contributions are indicated and acknowledged appropriately. This study has been conducted at Imperial College London, between March 2016 and March 2019, and it has not been submitted for any other degree.

Copyright Declaration:

The copyright of this thesis rests with the author. Unless otherwise indicated, its contents are licensed under a Creative Commons Attribution-NonCommercial 4.0 International Licence (CC BY-NC). Under this licence, you may copy and redistribute the material in any medium or format. You may also create and distribute modified versions of the work. This is on the condition that: you credit the author and do not use it, or any derivative works, for a commercial purpose. When reusing or sharing this work, ensure you make the licence terms clear to others by naming the licence and linking to the licence text. Where a work has been adapted, you should indicate that the work has been changed and describe those changes. Please seek permission from the copyright holder for uses of this work that are not included in this licence or permitted under UK Copyright Law.

ABSTRACT

Phytophthora infestans forms infection structures, haustoria, that enable translocation of virulence proteins, effectors. Invaded cells respond with a spatially confined defence response known as focal immunity, a poorly understood process that is implicated in the concentration of plant immune responses around haustoria. *P. infestans* counteracts this by deploying PexRD54, an effector that antagonizes Joka2 mediated immunity across the extra-haustorial membrane (EHM). However, how Joka2 contributes to immunity and molecular mechanisms enhancing resistance remain unknown. In this study, I dissect the role of Joka2 in defence-related autophagy. I first investigated recruitment of defence-related host autophagy machinery, including the plant autophagy cargo receptor Joka2 and ATG9 towards the EHM (Chapter 3), I showed that trafficking of Joka2 perihaustorial region is necessary for Joka2-mediated immunity. Then, I identified candidate Joka2 interactors which were obtained from a mass spectrometry analyses of Joka2 pull-downs. Remarkably, this revealed potential Joka2 interactors, including defence-related enzymes and signalling components that are implicated in both basal plant immunity and effector triggered immunity. By using a co-immunoprecipitation approach, I validated that PAL and MAP kinases 3, 6, and 9 interact with Joka2 *in vivo*, but not PDX. I showed that PAL-Joka2 interaction is UBA domain dependent and MAPK-Joka2 association is through the uncharacterized domain(s) of Joka2 (Chapter 4). Consistent with this, Joka2 co-expression together with MAPK cascade activation stabilised MAPKs protein levels which shows MAPKs are not autophagy substrates recruited by Joka2. Furthermore, abundant Joka2 enhanced hypersensitive response triggered by these MAPK's pathway (Chapter 5). I also found that Joka2 loses its ability to contribute to immunity upon removal of the domain responsible for MAPK binding, indicating that Joka2-MAPK interaction is essential for activation of defence-related autophagy. These results implicate selective autophagy in plant focal immunity and suggest more complex functions for autophagy than the widely known degradative roles.

TABLE OF CONTENTS

CHAPTER 1 - INTRODUCTION.....13

1.1 Food Security.....14

1.2 Plant Innate Immunity.....15

1.2.1 *Phytophthora infestans*, its infections strategy and effectors.....15

1.2.2 The plant innate immunity.....18

1.3 Overview of Cellular Degradation Systems.....20

1.3.1 Ubiquitin proteasome system.....20

1.3.2 Lysosomal degradation pathway.....21

1.4 Macroautophagy: An Overview.....22

1.4.1 Key steps within autophagy.....23

1.5 The role of antimicrobial autophagy in immunity.....25

1.6 The role of selective autophagy in innate immunity.....30

1.7 Proteomics Screening to Investigate Potential Joka2 Interactors.....37

1.8 AIMS.....38

CHAPTER 2 - MATERIALS AND METHODS.....40

2.1 Maintenance of *Nicotiana benthamiana* and *Phytophthora infestans*.....40

2.2 Generation of cloning and silencing plasmid constructs.....40

2.3 Agroinfiltration and Transient gene-expression assays in *N. benthamiana* 45

2.4 Confocal Microscopy.....45

2.5 Infection Assays.....45

2.6 Co-immunoprecipitations.....46

2.7 Crude protein extraction.....47

2.8 SDS-PAGE, Transferring of proteins and Western blot 47

2.9 Hairpin gene silencing and Virus-induced gene silencing (VIGS) 50

2.10 Reverse transcription PCR (RT-PCR) 51

2.11 Recombinant protein expression 51

2.12 Recombinant protein purification 52

2.13 *P. infestans* extract preparation and PAMP treatment 53

2.14 Measurement and analysis of cell death 53

CHAPTER 3 - HOST AUTOPHAGY MACHINERY ENHANCES FOCAL DEFENCE RESPONSES…… 54

3.1 INTRODUCTION 55

3.2 AIM 56

3.3 RESULTS 57

3.3.1 Defence-related selective autophagy mediated by Joka2 is diverted towards haustoria 57

3.3.2 Accumulation of perihaustorial ATG8CL-autophagosomes is dependent on the core autophagy machinery 67

3.3.3 Haustoria are hotspots for autophagosome biogenesis 68

3.4 DISCUSSION 73

CHAPTER 4 – VALIDATION OF JOKA2 INTERACTORS 76

4.1 INTRODUCTION 77

4.1.1 Mitogen-activated protein kinases in plant immunity 77

4.1.2 Phenylalanine ammonia-lyase and its role in plant defence 80

4.1.3 Vitamin B6 synthesizing enzyme in plant stress tolerance 81

4.2 AIM 82

4.3 RESULTS 83

4.3.1 Identification of Joka2 targets 83

4.3.2 Silencing of MAPK3 and PAL weakens plant immunity against *P. infestans* 84

4.3.3 MAP3, MAPK6 and MAPK9 colocalise with Joka2 but not PDX or PAL.....86

4.3.4 MAP kinase 3, 6, and 9 interact with Joka2 92

4.3.5 Exploring Joka2 domains that are responsible for MAPKs and PAL interaction....94

4.3.6 Impact of Joka2 on regulating MAPK3 and MAPK6 protein stability.....111

4.4 DISCUSSION 118

CHAPTER 5 – CONTRIBUTION OF JOKA2 TO PLANT IMMUNITY BY STABILISING MAPK3/6 AND ENHANCING PROGRAMMED CELL DEATH 128

5.1 INTRODUCTION 129

5.2 AIM 132

5.3 RESULTS 133

5.3.1 Impact of NBR1 domain on Joka2-MAPK association and plant immunity 133

5.3.2 Joka2 might serve as a scaffold for immune related proteins in MAPK signalling pathway....140

5.3.3 Joka2 stabilises MAPK3/6 and enhances programmed cell death 144

5.4 DISCUSSION 152

CHAPTER 6 - GENERAL DISCUSSION AND FUTURE PERSPECTIVES....157

APPENDIX 166

REFERENCES....174

LIST OF TABLES

Figure 1.1. Schematic representation of infection site of *Phytophthora infestans*.....16

Figure 1.2. Processing of ATG8 to form autophagosomes 23

Figure 1.3. *P. infestans* effector PexRD54 outcompetes Joka2 and facilitates the virulence of the pathogen. 31

Figure 1.4. Domain architecture of Joka2 and its human autophagy cargo receptors homologues, p62 and NBR1 33

Figure 1.5. Protein sequence alignment of Joka2 homologs in *S. tuberosum* (StJoka2A and StJoka2B) and *N. benthamiana* (NbJoka2A, NbJoka2B, NbJoka2C and NbJoka2D).35

Figure 1.6. Phylogenetic tree of Joka2 homologs in *S. tuberosum* and *N. benthamiana*. 36

Figure 3.1. Joka2-mediated autophagy is directed towards the haustoria 60

Figure 3.2. The ZZ and NBR1 domains are not essential for perihaustorial localization of Joka2.....62

Figure 3.3. Ordered structure probability of Joka2 63

Figure 3.4. Joka2 lacking PB1-ZZ domains affect *P. infestans* growth 64

Figure 3.5. Joka2 localizes to ATG8c-autophagosomes found at perihaustorial region via its AIM domain. 65

Figure 3.6. Joka2 and ATG8CL degradation slows down during *P. infestans* infection or after PAMP treatment.....67

Figure 3.7. ATG9 colocalises with Joka2-autophagosomes/aggregates. 69

Figure 3.8. ATG9-labelled vesicles/autophagosomes accumulate around haustoria and Joka2 puncta colocalises with them 71

Figure 3.9. ATG9 contributes to plant immunity against *P. infestans* 72

Figure 4.1. Silencing *MAPK3* and *PAL* in *N. benthamiana* leaves leads to augmented pathogen growth 85

Figure 4.2. Silencing *PAL* in *N. benthamiana* causes *P. infestans* to cause less necrosis. 86

Figure 4.3. Joka2 does not co-localise with PAL or PDX *in planta* 87

Figure 4.4. Colocalisation of Joka2 puncta with its candidate MAPK interactors in presence of ATG8CL-autophagosomes 90

Figure 4.5. Colocalisation of Joka2 puncta with its candidate MAPK interactors during infection 92

Figure 4.6 Validation of MAPK3, MAPK6, and MAPK9-Joka2 association *in planta* 93

Figure 4.7. MAPK3 and MAPK6 interact with Joka2 regardless of the tag used to pulldown 94

Figure 4.8. MAPK3 interacts with Joka2 regardless of Joka2's polyubiquitin binding ability 95

Figure 4.9. MAPK3 interacts with Joka2UBA1,2 and reveals a high molecular weight band 97

Figure 4.10. Only functional UBA domains pull down polyubiquitin 98

Figure 4.11. MAPK3 does not interact with Joka2 via PB1 or ZZ domains 99

Figure 4.12. MAPK3-Joka2 interaction is diminished upon removal of PB1, ZZ and NBR1 domains 101

Figure 4.13. Removal of only NBR1 domain significantly reduces Joka2-MAPK3 interaction 103

Figure 4.14. Removal of only NBR1 domain significantly reduces Joka2-MAPK3 interaction 104

Figure 4.15. MAPK6 interacts with Joka2 and mutants lacking ZZ and NBR1 domains 106

Figure 4.16. PAL interacts with both wild type Joka2 and all truncated mutants 107

Figure 4.17. PAL interacts with both wild type Joka2 and its UBA domains regardless of their polyubiquitin binding abilities 108

Figure 4.18. PAL interacts with both wild type Joka2 and its UBA domains regardless of their polyubiquitin binding abilities 110

Figure 4.19. MAPK levels might be affected by Joka2 overexpression 112

Figure 4.20. Joka2 overexpression does not affect MAPK3 protein levels *in planta*....113

Figure 4.21. Inhibition of autophagy seems to not alter MAPK stability.....114

Figure 4.22. Silencing Joka2 in plants may cause protein stability of MAPK3 115

Figure 4.23. Validation of silencing of Joka2 in *N. benthamiana* by using VIGS. 117

Figure 4.24. VIGS of *StJoka2* also knocks down *NbJoka2* 117

Figure 5.1 Phylogenetic tree of plant MAPKs 130

Figure 5.2. NBR1 domain of Joka2 is the site of MAPK3 interaction. 134

Figure 5.3. MAPK6 does not have an affinity to NBR1 domain 135

Figure 5.4. Pairwise comparison of *N. benthamiana* MAPK3 and MAPK6 136

Figure 5.5. Removal of NBR1 abolishes Joka2-mediated plant immunity against *P. infestans* 137

Figure 5.6. MAPK3 and NBR1 can be expressed in bacteria and purified with cobalt columns 139

Figure 5.7. SDS-PAGE of fractions obtained after size exclusion chromatography of His-tagged NBR1 and MAPK3 140

Figure 5.8. Joka2 might be serving as a scaffold protein for MAPK3 and MAPK6 to form high molecular weight multiprotein complexes with MAPK9 142

Figure 5.9. Validation of Joka2 and MEK2 association *in planta* 143

Figure 5.10. Phosphorylated MAPK3/6 levels are highest 1 hour after treatment with *P. infestans* extract 144

Figure 5.11. The tagged proteins generated from *N. benthamiana* MAPK3 and MAPK6 can be phosphorylated by autoactive MEK2 and PAMP treatment 146

Figure 5.12. Joka2 enhances the protein stability of MAPK3/6 elevating phosphorylated MAPK levels 148

Figure 5.13. Joka2 enhances the protein stability of MAPK6 and increases MAPK6 phosphorylation by autoactive MEK2. 149

Figure 5.14. Joka2 enhances MEK2 mediated cell death 151

Figure 5.15. Validation of double silencing of MAPK3 and MAPK6 by the construct TRV2:MAPK3/6 151

Figure 6.1. Summary figure of how Joka2-mediated antimicrobial autophagy might function 160

Figure 7.1. ATG8CL autophagosomes localize to perihaustorial region *in planta* 166

Figure 7.2. Expression of ATG4 and ATG9 is required for proper accumulation of ATG8CL puncta around haustoria 168

Figure 7.3. Joka2 mRNA levels, specifically NbJoka2A, increases upon infection of *N. benthamiana* 169

Figure 7.4. Overexpression of ATG9 increases the frequency of haustoria surrounded by ATG8CL-autophagosomes 169

Figure 7.5. Overexpression of Joka2 destabilises MAPK9 170

Figure 7.6. Joka2 or Gus protein levels do not change with MAPK3 overexpression...171

Figure 7.7. Silencing *NbJoka2* might be affecting MAP kinase protein levels 172

Figure 7.8. RNAi-mediated silencing constructs of *MAPK3, MAPK6, MAPK9* and *PAL* successfully silenced target genes in plant.....172

Figure 7.9. Validation of silencing of *NbJoka2A* and double silencing of *NbMAPK3* and *NbMAPK6* 173

LIST OF FIGURES

Table 2.1. Primers used in this study.....42

Table 2.2. Antibodies used for western blotting 49

Table 4.1. Peptide hit counts from Mass Spectroscopy after EV, ATG8c and Joka2 co-immunoprecipitations in uninfected (mock) and infected conditions 84

Acknowledgement

First and foremost, I would like to thank my supervisor Tolga Bozkurt, for his support, patience and encouragement during my PhD. I have learnt a lot with his guidance and under his supervision, and I feel fortunate to complete my studies in his lab.

I owe special thanks to my long-term lab mates, Pooja Pandey, Alex Leary and Cian Duggan for their never-ending help starting from the very beginning of my PhD. Zac Savage, Eleonora Moratto, Enoch Yuen and Tarhan Ibrahim have joined the lab later but I greatly enjoyed their friendship and support. Although they did not hang out in our lab for long, which was such a pity, I am grateful to be friends with Elisa Fantino and Nattapong Sanguankiattichai. I am also grateful for those amazing future scientists, Sherry (Wen) Yin, Ioanna Morianou, Camilla Molinari, and Amber Connerton who were unlucky to have me as a mentor in their undergraduate final year or in their graduate projects. I would like to thank all those people for turning SAF building into a loving environment. I will miss all of them and our countless coffees, lunches and socials.

I cannot thank enough to my beloved friends, Tugce Elif Ceran Arslan and Y. Murat Kadioglu, for being there for me during my darkest and happiest moments in those years. I also cannot pay my depts to Paul Girvan because of his phycological support and gargantuan helpfulness before and during my thesis writing period. My life in Imperial College and in London would not be the same without them.

I would like to thank The Scientific and Technological Research Council of Turkey (TUBITAK) and British Council for supporting me with Newton-Katip Çelebi Fund Programme during the first three year of my doctoral studies.

And finally, I sincerely thank my family for their love and support! They have been always patient and caring in my long academic career path. I lost my grandfather, but I gained a nephew in those years when I was away from them. I feel blessed to have them in all those highs and lows, ups and downs.

CHAPTER 1 - INTRODUCTION

1.1 Food Security

Food security is one of the most important concerns for the growing human population. Over the past several decades, the proportion of the global population without access to adequate food has thankfully steadily declined. However, it has become clear that within the past few years this decline has levelled off, with approximately 10% of people worldwide suffering from undernourishment (Savary, S. *et al.*, 2012).

The reasons for this halt in decline are likely manifold. Changes in land utilization, particularly putting land towards more energy intensive food sources (e.g. meat) to meet the changes in dietary preferences of rapidly developing countries results in less efficient use of land (Godfray, H. C. J. *et al.*, 2010b). Effects from climate change add to this issue via losses to useable land due to abiotic factors (droughts, floods, salinity etc.).

For the decline in undernourishment to continue, simply using more land for agriculture is not likely to be a viable option. We therefore need to find other ways to increase crop production, while also recognising the need to preserve what has already been harvested. Estimations of food wastage have been reported to be 30 to 40%, which interestingly does not appear to vary between the developing or developed world (Godfray, H. C. J. *et al.*, 2010a).

A further piece of the food security puzzle lies with plant pathogens. While estimations vary, at least 10% of crop losses are attributed to plant pathogens (Strange, R. N. *et al.*, 2005). Among them, filamentous plant pathogens cause most devastating plant diseases and threaten global food security by leading vast economic losses on important crop species as well as environmental damage in natural ecosystems (Liu, T. L. *et al.*, 2014). These disease-causing microorganisms cost billions of dollars annual loses to modern agriculture and severely hamper subsistence agriculture in developing countries. They are a group of eukaryotic pathogens including oomycetes (water moulds) and fungi, which form intimate interactions with their host plants.

1.2 Plant Innate Immunity

1.2.1 *Phytophthora infestans*, its infections strategy and effectors

Plant pathogens from time to time cause major outbreaks, which results in tragic and devastating social and economic consequences, and these epidemics can be traced back in recorded ancient history. The Irish potato famine is one of the most notorious among all plant diseases because of its occurrence in the relatively near past (the late 1840s). Late blight of potato was the cause of that catastrophe which is caused by the oomycete *Phytophthora infestans*, which still infests members of Solanaceous species, including potato and tomato (Derevnina, L. *et al.*, 2016). Currently, *P. infestans* is the most important pathogen that threatens potato production in the UK, and globally, with an estimated economic loss of 6.7 billion dollars annually (Nowicki, M. *et al.*, 2012). For example, the disease lead to almost 100% crop loss of tomato in South India after it had been detected in 2008 (Chowdappa, P. *et al.*, 2013). Since its genome was sequenced in 2009, it has become a model system to study filamentous pathogen-plant interactions (Haas, B. J. *et al.*, 2009; Raffaele, S. *et al.*, 2010).

Under high humidity, *P. infestans* spores secrete proteins to form a walled cyst which rapidly germinates and forms an appressorium. If the pathogen manages to form an infection vesicle, filamentous structures called hyphae form and start to elongate in the apoplast. The sub-hyphal structures penetrating inside the cells are called haustoria and are responsible for the release of various infection elements and uptake of nutrients from the host. During invasion, the pathogen secretes various enzymes to degrade the cell wall, and proteins called effectors which change the plants molecular mechanisms to render the plants defence system susceptible to the pathogen attack. Effectors might be excreted into the apoplastic space of the tissue or directly inside the plant cells through haustoria depending on their target (Figure 1.1). Extracellular effectors can be cell wall-degrading enzymes, elicitors, toxins causing cell death, or enzymes inhibiting hydrolytic enzymes of the host.

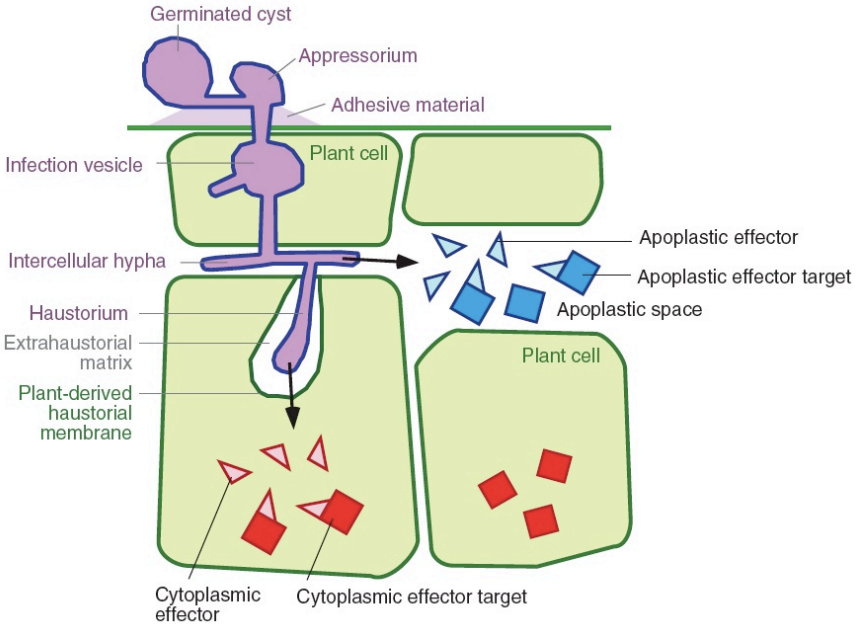


Figure 1.1. **Schematic representation of infection site of *Phytophthora infestans***. After attaching the host tissue surface, germinating zoospore of the oomycete forms an appressorium, which results in generation of infection vesicles after penetration. Once the cell is invaded, hyphae extend in the apoplastic region secreting apoplastic effectors, and invade other cells by specialized hyphal extensions called haustoria. These structures are hubs to release effector proteins and absorb nutrients from the host cell. Adapted from the Kamoun Lab web page (Hafren, Anders *et al.*, 2017).

Filamentous pathogens which are phylogenetically distinct from each other such as oomycetes, powdery mildew ascomycetes, and rust basidiomycetes have generated haustorium independently and adopted a similar life cycle (Bozkurt, T. O. *et al.*, 2020; Latijnhouwers, M. *et al.*, 2003). Although these structures are known to be crucial for the pathogen's survival and spread, we still do not clearly know the exchange of molecules and their delivery systems. However, evidence of sugar transporters, for example, at fungal haustoria show that those infection structures are also important nutrient uptake (Mendgen, K. *et al.*, 1988). The effectors which are macromolecules produced in pathogen cells but function in the host, can also be delivered from the haustoria. The effectors are mostly protein based macromolecules, however, those virulent factors include RNA molecules which are suppressing the plant immunity, which are mostly secreted from parasitic plants (Shahid, S. *et al.*, 2018).

Delivery systems of effectors especially RNAs are not fully dissected. One possible transport system can be extracellular vesicles (EVs) which have been observed in EHMx (extrahaustorial matrix) during fungal invasion (Micali, C. O. *et al.*, 2011). Not only the pathogens but also plants can also utilise EVs to subvert pathogens invasion (Cai, Q. *et al.*, 2018). Therefore, the potential of these EVs to EHMX has drawn attention to their transport systems and the content they carry.

Adopted fungal and oomycete pathogens devised ways and systems to transport their immunosuppressor effectors. Most of the effectors produced and translocated by oomycetes pathogens carry a conserved domain called RXLR motif followed by a secretion signal (Whisson, S. C. *et al.*, 2007). RXLR domain of the effector is not required for the function inside the plant cell, however, it is hypothesised that this domain is needed for effector's translocation from pathogen to host cell (Bozkurt, T. O. *et al.*, 2012). This motif undergoes proteolytic cleavage before entering the plant cell and mature effectors lack these domains (Wawra, S. *et al.*, 2017). Fungal effectors with the same domains have not been identified, yet. This shows that different delivery systems have evolved as fungal haustoria are separate cells compared to haustoria of oomycetes. Various means of transport of effectors from filamentous pathogens to host cells are proposed. Those would be via receptor-mediated endocytosis of EVs carrying effector and active transport.

When it comes to the composition of the extrahaustorial membrane, it differs significantly from the plasma membrane of the host cell. Haustoria are continuous lipid bilayer to plant plasma membrane. Although there is no known physical barrier, components of plasma membrane and EHM are substantially varying. Intriguingly, most of the membrane proteins are excluded from EHM, including known immune receptors (Lu, Y. J. *et al.*, 2012; Micali, C. O. *et al.*, 2011). On the other hand, there are few exceptions known to be present in both plasma and EHM, such as membrane associated remorin protein REM1.3 and vesicle fusion protein SYT1 (Bozkurt, Tolga O. *et al.*, 2014). The protein content can also vary depending on the pathogen, for example, the plasma membrane-bound pattern recognition receptor (PRR), FLS2, is found on the EHM of *Hyaloperonospora arabidopsidis* (HPA) however haustoria formed by *Phytophthora*

infestans do not contain FLS2 (Lu, Y. J. *et al.*, 2012). Distributions of these membrane proteins to microdomains revealed that EHM has non-uniform interface.

Some haustoria of the pathogens are targeted by the focal to be covered by cell wall materials to form callose immunity (Caillaud, M. C. *et al.*, 2014). This physical defence layer prevents pathogen's access to nutrients from the host cell and protects the defence pathways. However, some adopted pathogens, e.g. *P. infestans*, avoid callose deposition by unidentified ways.

How infected cell deliver the defence related components and proteins to the pathogen entry site is poorly understood. It is considered that various vesicular pathways are diverted to EHM region. The proteins in EHM is can start their journey from plasma membrane, vacuolar membrane, EVs, plasmodesmata or ER (Bozkurt, Tolga O. *et al.*, 2014; Dagdas, Y. F. *et al.*, 2018). For example, late endocytic protein, small GTPase RabG3c, is found to be diverted to EHM of *P. infestans* (Bozkurt, T. O. *et al.*, 2015; Lu, Y. J. *et al.*, 2012). Although some PRRs are also diverted to EHM, it is not clear if those receptors are still active at EHM or they are inactivated by the pathogen (Bozkurt, T. O. *et al.*, 2015).

1.2.2 The plant innate immunity

Plants do not have mobile immune cells or an adaptive immune system as animals do; their defence system is mainly based on the innate immunity of individual cells and systemic signals emerging from injured parts or infection sites (Jones, J. D. *et al.*, 2006). The plant innate immune system can be thought of as being roughly governed via two branches of receptors: extracellular transmembrane pattern recognition receptors (PRRs) and intracellular nucleotide-binding/leucine-rich-repeat (NB-NLR) receptors (Jones, J. D. *et al.*, 2006). PRRs are cell surface receptors, and they are one of the first layers of the defence mechanism. These proteins are mostly receptor-like kinases (RLKs) or receptor-like proteins (RLPs). Plant cells can detect pathogenic threats through PRRs that are specialised detecting widely conserved molecules which are called microorganism/pathogen-associated molecular patterns (MAMPs or PAMPs) (Giraldo, M. C. *et al.*, 2013; Yi, M. *et al.*, 2013). Activation of Pattern-triggered immunity (PTI) by

PAMPs is believed to be the major factor that prevents non-adapted pathogens to colonize plants (Cui, H. *et al.*, 2015). Adapted pathogens, on the other hand, have evolved strategies to dampen plant defence systems. Pathogens deploy an arsenal of macromolecules, termed effectors, which interfere with host defence and contribute to virulence (Figure 1.1).

Phytophthora species have been shown to encode for hundreds of effectors. One of the effector class is with conserved RxLR motif, which is followed by EER sequence within 30 amino acids at N-terminus of the protein, is secreted from the pathogen and translocated to the host (Anderson, R. G. *et al.*, 2015; Birch, P. R. *et al.*, 2008). However, some effectors can be detected by surface immune receptors or cytoplasmic NB-NLR receptors which activate effector-triggered immunity (ETI, NLR-triggered immunity) (Win, J. *et al.*, 2012). Along with PTI, ETI increases antimicrobial defence by activating downstream signalling pathways and generally triggering a plant specific cell death known as the hypersensitive response (HR) that hampers pathogen growth (Cui, H. *et al.*, 2015; Yi, M. *et al.*, 2013).

Defence against those pathogens, however, initiates even before infection structures of the pathogens are able to contact plant cells. Plants can sense pathogen penetration attempts or contact and reprogram their cytoskeleton to mediate cytoplasmic streaming of the endomembrane system towards pathogen contact sites, enable targeted secretion of defence related compounds and deploy cell wall components. Formation of cell wall appositions called papillae followed by cytoskeletal re-organisation can prevent pathogen penetration attempts, resulting in a phenomenon known as focal immunity (Collinge, D. B., 2009; Yi, M. *et al.*, 2013). Nevertheless, adapted pathogens can overcome the focal immune responses by deploying effector proteins.

One of the focal immunity responses is trafficking of autophagy-related vesicles, autophagosomes, or proteins to the pathogen site (Dagdas, Y. F. *et al.*, 2018). It is a highly conserved eukaryotic cellular process which enables removal of cellular components and microbes via engulfment in double membraned autophagosomes (Lamb, C. A. *et al.*, 2013). This process can be selective for in various occasions, for

example, during pathogen invasion and autophagosomes found at perimicrobial interfaces (Haldar, A. K. *et al.*, 2014; Real, E. *et al.*, 2018; Thurston, T. L. *et al.*, 2012). Dagdas *et al.* showed that defence-related antimicrobial autophagy proteins Joka2 (plant NBR1) and ATG8 (isoform C) target the EHM of *P. infestans* (Dagdas, Y. F. *et al.*, 2016). The pathogen was found to be avoiding this defence system by secreting an effector, PexRD54, which inhibits Joka2-mediated plant immunity. Autophagy mechanism seems to be involving in intricate immune functions at the host-pathogen interfaces.

1.3 Overview of Cellular Degradation Systems

Cells are fastidious in their maintenance of homeostasis. This steady state is maintained for many cellular variables, such as (but by no means limited to) ions, pH and protein levels; the last of which is deemed important enough to warrant its own proteostasis. Homeostasis of protein levels within the cell is achieved through regulation at many junctures, including regulation at the gene level, during transcription and translation or through regulation of post translational modifications. In addition to all these controls along the biosynthetic pathway, the cell also has methods by which it can degrade and recycle proteins when required.

The eukaryotic cell has two major protein degradation pathways available to it to maintain protein homeostasis: lysosomal proteolysis and the ubiquitin proteasome pathway. Through these pathways the cell can remove misfolded or aggregated proteins as well as proteins that are no longer required or that are non-functional, and in doing so recycle the components for new uses.

1.3.1 Ubiquitin proteasome system

The ubiquitin proteasome pathway is the major route for selective degradation of proteins in the eukaryotic cell. It involves the tagging of a prospective protein for degradation with ubiquitin. Ubiquitin is a 76 amino acid protein that is highly conserved throughout all eukaryotes. Proteins are ubiquitinated through the actions of three enzymes in a multistep process involving ubiquitin activation (E1), transfer to a ubiquitin

conjugating enzyme (E2) and then a final transfer mediated by ubiquitin ligase (E3) to the protein for degradation.

After several rounds of ubiquitinylation, addition of a poly-ubiquitin tail is achieved. The protein is then recognised by the proteasome, which isolates it from the rest of the cytoplasm where it can be safely degraded by proteases. By having a large diversity of different E3 ligases the cell can achieve specificity in that each E3 ligase is generally responsible for recognition of a specific protein. Thus, the ubiquitin proteasome pathway can be thought of as a highly targeted system for selective removal of proteins.

1.3.2 Lysosomal degradation pathway

The lysosome is a membrane bound organelle that uses a combination of low pH along with a variety of proteases to degrade cellular material which is transported into it. Material can either enter the lysosome from the extracellular space through endocytosis and subsequent fusion of these endosomes with the lysosome, or alternatively material can come from within the cell's own cytosol. The latter is termed autophagy, literally self-eating.

Autophagy can be further subclassified into three categories: (1) chaperone mediated autophagy, (2) microautophagy, and (3) macroautophagy (Feng, Y. *et al.*, 2014). Chaperone mediated autophagy is characterised by proteins (typically containing a specific amino acid motif) being directed towards the lysosome via a chaperone, where the protein is unfolded and passed through the lysosomal membrane without the formation of additional vesicles. In contrast, microautophagy occurs through invagination of the lysosomal membrane, capturing the nearby cytosolic components in a small intraluminal vesicle. The final type of autophagy, macroautophagy, is perhaps the most studied of the three autophagic processes and is characterised by the *de novo* formation of a unique double layered membrane compartment called an autophagosome. This autophagosome envelops material to be degraded and then fuses with the lysosome, releasing the inner membrane and its cargo into the lysosome for degradation. The formation of this autophagosome and the material it envelops is

precisely controlled by a finely tuned orchestra of proteins. As we shall explore throughout this thesis, some of these autophagy protein players have been co-opted into also serving roles within plant pathology.

1.4 Macroautophagy: An Overview

Macroautophagy, (which will subsequently be referred as simply autophagy) is a ubiquitous catabolic cellular process required to recycle excess or dysfunctioning organelles as well as other cellular content (Klionsky, D. J., 2007; Stolz, A. *et al.*, 2014). Autophagy can be both selective and non-selective. The latter is sometimes also referred to as bulk autophagy and is generally upregulated as a response to starvation. In contrast, selective autophagy targets a specific cargo for degradation. Both of these autophagy pathways play a crucial role in the survival of all eukaryotic organisms by degrading unnecessary cellular compartments within the cell, and thereby supplying building blocks for cellular remodelling and energy to sustain basic cellular activities, especially during stress conditions (Klionsky, D. J., 2007).

The first proteins involved in regulating autophagy were discovered in yeast and were subsequently termed Atg (autophagy-related) proteins (Tsukada, M. *et al.*, 1993). In total, over 30 genes related to autophagy have been identified in yeast, with many homologous genes having subsequently been identified in other eukaryotes, (though somewhat confusingly these homologs are referred to by different names).(Ohsumi 2014) Of the 30 or so yeast autophagy genes, 18 are considered to make up the 'core' autophagy genes. These core *ATG* genes encode the fundamental machinery required for the formation of the unique double membraned autophagosome and are thus common to both selective and non-selective autophagy pathways (Nakatogawa, H. *et al.*, 2009). Through study of these core *ATG* genes they have been grouped into five subcatogories: the Atg1 kinase, phosphatidylinositol-3-kinase complex, the ubiquitin-like Atg8 and Atg12 conjugation systems and the multi transmembrane protein Atg9.

1.4.1 Key steps within autophagy

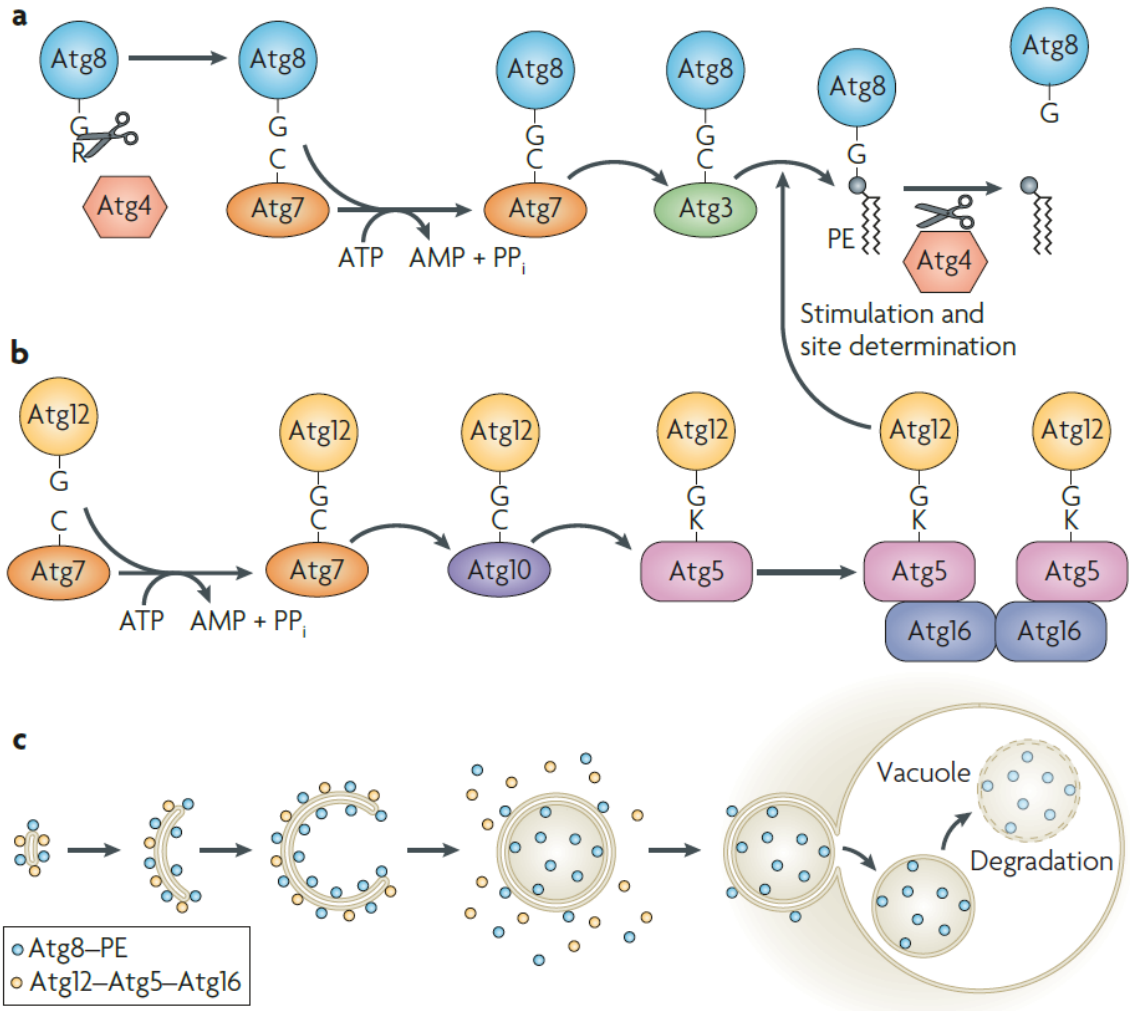


Figure 1.2. Processing of ATG8 to form autophagosomes. (A-C) Cleavage, lipidation and conjugation of mature ATG8 proteins for biogenesis of autophagosomes. Image was adopted from (Nakatogawa, H. et al., 2009). (The permission to reuse the contents is under the license number 4922390004580 (Copyright Clearance Center Inc., U.S.)).

Autophagosome biogenesis initiates after activation of the ATG1 complex which is responsible for formation of the initial membranous structure, the phagophore. Subsequently, ATG1 phosphorylates the phosphatidylinositol-3-kinase (PI3K) complex which recruits other core proteins in order to proceed with nucleation of the phagophore assembly site (Figure 1.2).

The growing membrane of the phagophore is decorated with modified ATG8 which has been cleaved by ATG4 to reveal C-terminal glycine amino acid for further reactions.

ATG8 is lipidated (conjugated to phosphatidylethanolamine (PE)) by ATG7 (an E1 enzyme), ATG3 (an E2 enzyme) and ATG12-ATG5-ATG16 (E3 enzyme-like) complex. ATG12-ATG5-ATG16 (E3 enzyme-like) complex is generated through subsequent enzymatic reactions where the process is mediated by ATG7 and ATG10 (an E2 enzyme) proteins (Kaur, J. *et al.*, 2015). Atg12–Atg5–Atg16 complex preferentially stays on the outer surface of the newly forming autophagosome membrane and dissociates from the membrane upon completion of the autophagosome biogenesis. Anchored ATG8s on the inner membrane serve as a docking site for autophagy cargo receptors, or proteins to be degraded, whereas the outer membrane-bound ATG8s mediate transport and fusion of the autophagosomes. After fusing with other membranous compartments, such as lysosomes, ATG8 can be recycled to the cytoplasm via ATG4 action (Yu, Z. Q. *et al.*, 2012).

Although the biogenesis and the membrane source of autophagosomes are still unknown, several compartments including Golgi apparatus, mitochondria, ER and plasma membrane are reported to provide the membrane material (Axe, E. L. *et al.*, 2008; Hailey, D. W. *et al.*, 2010; Hayashi-Nishino, M. *et al.*, 2009; Ravikumar, B. *et al.*, 2010). ATG9, the only described multi-transmembrane ATG protein, is required for the assembly of the pre-autophagosomal structure (or phagophore assembly site, PAS) and is therefore thought to contribute to autophagosome biogenesis through membrane trafficking. In yeast clusters of Atg9 containing vesicles and tubules have been reported (Mari, M. *et al.*, 2010), which appear to re-localise to the PAS upon autophagy initiation, presumably acting as an initial membrane source. There is also evidence that Atg9 can cycle between the PAS and structures such as mitochondria with the implication being that this can provide a means of transporting lipids to the expanding phagophore (Reggiori, F. *et al.*, 2005). As Atg9 is recruited early in the process of autophagosome development it is often used as a marker for identifying autophagosomes within the cell. ATG9, after fusing to form the PAS, stays at the outer autophagosomal membrane and it is recycled when the autophagosomes fuse with the vacuole (Papinski, D. *et al.*, 2014) . The autophagosomal growth after initiation might not depend solely on ATG9-labelled vesicles but might also need other phospholipid sources as well (Le Bot, N., 2012).

A lipid modified form of ATG8 (also known in mammals as microtubule-associated protein 1 light chain 3 (LC3) or GABARAB) coats the autophagosomal membranes in order to mediate cargo recruitment and autophagosome biogenesis and transport. For this reason, it has been extensively used as a marker for autophagosome biogenesis and transport (Klionsky, D. J. *et al.*, 2011). The ATG8 protein which is encoded by a single copy gene in yeast is expanded in plants and animals. For example. the model plant *Arabidopsis* encodes nine different ATG8 isoforms (Park, E. *et al.*, 2014) whereas at least 8 different isoforms have been detected in *N. benthamiana* (Kellner, R. *et al.*, 2016). Although autophagy was initially considered as a bulk degradation process, recent studies have revealed that autophagy can be highly selective by capturing specific cargo through tightly regulated autophagy cargo receptors (Stolz, A. *et al.*, 2014). It is believed that different ATG8 isoforms differently bind to a range of specific autophagy cargo receptors or adaptors to mediate diverse selective autophagic pathways (Kellner, R. *et al.*, 2016).

1.5 The role of antimicrobial autophagy in immunity

Autophagy is not only a degradation pathway but it also involved in various cellular functions linked to membrane-vesicle trafficking such as endocytosis, phagocytosis, conventional and unconventional secretory pathways, even non-membrane related functions such as immune responses, cell death, and so forth (Galluzzi, L. *et al.*, 2019) (Jiang, S. *et al.*, 2013). Among the unconventional ways of autophagy, one of them is getting attention as it is crucial for fighting against the pathogens. In the early studies, for instance, it has been observed that autophagy deficient mammalian cells were more susceptible to *Streptococcus* bacteria (Hofius, D. *et al.*, 2011). Similarly, stimulation of autophagy decreased the survival of *Mycobacterium tuberculosis* in macrophages (Gutierrez, M. G. *et al.*, 2004). Since the pathogens co-evolved with their hosts, some devised effectors to interfere with autophagy. For example, wild type *Shigella* bacteria targets autophagy to escape from host defence, whereas, mutant type lacking the appropriate effector is entrapped via autophagy and becomes less infectious (Ogawa, M. *et al.*, 2005).

Although the internal clearance of pathogens is well-known in mammalian systems, the role of autophagy in plant resistance is still not well-understood (Deretic, V. *et al.*, 2009). In plants, many studies concluded that mutant lines of autophagy-related (ATG) proteins are more susceptible to viruses, bacteria and fungi (Hofius, D. *et al.*, 2011). Although autophagy has been associated with hypersensitive response, a form of cell death triggered upon activation of ETI that restricts pathogen growth, its role in plant-microbe interactions remain largely unknown (Teh, O. K. *et al.*, 2014).

Contradictory reports on autophagy and its contribution to the development of hypersensitive response exist. This might be because of targeting the core autophagy proteins in the studies, in which multiple molecular machineries were affected. With The emergence of new studies on more specific molecular pathways in selective autophagy will help to clarify the role of autophagy in HR responses in plants.

Early studies in the field reported that autophagy can enhance HR responses at the infection site but limit the spread of cell death in unaffected area (Patel, S. *et al.*, 2008). When some autophagy genes were knocked down (such as *PI3K*/*VPS34, ATG3, ATG6*, and *ATG7)* an enhanced spread of HR was observed when the plant was challenged with Tobacco Mosaic virus (TMV). Similar observations showed that autophagy deficient lines of Arabidopsis when an effector from *Pseudomonas syringae* pv*. tomato DC3000* (Pst DC3000), AvrRpm1, was recognized by a resistance protein, RPM1. Similarly, Arabidopsis *atg* loss-of-function mutants exaggerated the spread of cell death when infected by necrotrophic type of fungi, *Alternaria brassicicola* or *B. cinerea (Lai, Z. et al., 2011).*

In contrast, some studies showed that there was not uncontrolled cell death upon infection of *atg* mutants of *Arabidopsis* with avirulent pathogens (Coll, N. S. *et al.*, 2014; Hofius, D. *et al.*, 2009). On the contrary, HR was reduced and delayed in *Arabidopsis* plants when inoculated with avirulent Pst DC3000 (*AvrRps4*) or the avirulent isolate of *Hyaloperonospora arabidopsidis* (oomycete pathogen) (Hofius, Daniel *et al.*, 2009). Some earlier studies showed that perturbation of HR occurred in autophagy-deficient lines of plants when both T and C type NLR immune receptors were activated (Hofius, Daniel *et al.*, 2009). These findings shed light on the specificity of delayed HR. In general, the controversial results from those experiments were thought to be related to the age

of the plants used in the experimental setups. Older plants were showing more and uncontrolled cell death, whereas, younger plants showed slightly delayed not spreading of HR (Yoshimoto, K. *et al.*, 2009), which suggests cellular stress built up over time causes spreading HR in older autophagy mutants.

Phytopathogens can be generally grouped by the mechanism through which the pathogen extracts nutrition from its host. If the pathogen requires living tissue it is termed a biotroph, while conversely if the pathogen feeds off dead tissue it is considered to be a necrotroph. There are also phytopathogens that can be considered as hemibiotrophs, which are characterised by an initial stage of biotrophic interaction with their host, before moving onto a necrotrophic stage. *P. infestans*, the Irish potato gamine pathogen, which was introduced earlier is an example of such a hemibiotrophic pathogen.

Given the varied nature of how pathogens can extract nutrition from their hosts (biotrophy vs necrotrophy), it is perhaps unsurprising that the role of bulk autophagy within the host can lead to different outcomes depending on the nature of the invading pathogen. For example, many threads of evidence point towards the conclusion that upregulation of autophagy has a positive role in defence against necrotrophic pathogens (Katsiarimpa, A. *et al.*, 2013; Lai, Z. *et al.*, 2011; Lenz, H. D. *et al.*, 2011). Conversely, it has been shown that plants containing mutations which render them autophagy defective are better able to defend against biotrophic attack (Lenz *et al.*, 2011). How bulk autophagy contributes to the defence of the host against pathogen attack therefore appears to be mechanistically diverse and depend on the pathogen in question.

There are few studies showing the effect of inhibition of autophagy in crop plants (Tang, J. *et al.*, 2018). For instance, when plant autophagy is disturbed by autophagy inhibiting chemicals such as 3-methhyladenine (3-MA), banana plants became more susceptible to *Fusarium oxysporum f.* sp. *cubense* (Wei, Y. *et al.*, 2017). Similarly, interfering with *ATG8* gens in cassava, led to compromised resistance in the plants against *Xanthomonas axonopodis pv manihotis* (*Xam*) (Yan, Y. *et al.*, 2017; Zeng, H. *et al.*, 2018). *ATG8j*-silenced wheat plants became more susceptible to an avirulent fungus*, Puccinia striiformis f.* sp. *tritici* (*Pst*) race CRY23 (Mamun, M. A. *et al.*, 2018). Interestingly, although silencing of

ATG6 in wheat hindered the immunity in a resistant plant line carrying a resistance gene *Pm21*, the basal immunity of the plants were enhanced against powdery mildew pathogen *Blumeria graminis f. sp. tritici* (*Bgt*) in a susceptible plant line (Yue, J. *et al.*, 2015). These results show the involvement of autophagy in plant immunity yet do not clarify how the mechanisms underlying this process cause the physiological effects that we observe.

In addition to how bulk autophagy contributes to plant immunity, selective autophagy also has a role to play. Having co-evolved with their pathogens, plants have utilised selective autophagy to target pathogen proteins in an attempt to prevent pathogen spread. In response, the pathogens have developed ways around this and even gone as far as co-opting host autophagy for their own benefit. This has resulted in an evolutionary arms race. For example, it has been demonstrated that in response to infection by the Cauliflower mosaic virus *Arabidopsis* can utilise NBR1 to target capsid proteins and transported them to autophagosomes for degradation (Hafren, Anders *et al.*, 2017). This plant protective antiviral response is countered by the virus, which attempts to evade degradation by forming autophagy-resistant virus inclusion bodies. Additionally, the virus also goes one step further; virus-triggered non-selective autophagy helps the infected plant survive and as a result extends the timespan of virus production. This extended timespan also increases the chance of transmission to other plants, resulting in this 'survival function' of the plant ultimately ending up doing more harm than good to the plant community.

Various regulatory elements in autophagy during pathogen attack have been identified. (Leary, A. Y. *et al.*, 2019). The transcription factor WRKY33, for instance, interacts with ATG18a and induces transcription of ATG18a during infection of *Arabidopsis* by *Botrytis* (Lai, Z. *et al.*, 2011). Similar to WRKY33, WRKY20 was found to bind to several ATG8 variants such as ATG8a, ATG8f and ATG8h in cassava (Yan, Y. *et al.*, 2017). When the plant is infected by *Xanthomonas axonopodis pv manihotis* (*Xam*) which causes cassava bacterial blight, WRKY20 expression is induced during the pathogen attack and the transcription factor WRK20 binds to *ATG8a* promoter to activate transcription of *ATG8a.* Complementary to these findings, silencing of WRK20 made cassava more susceptible

to bacterial blight, which suggested the requirement of autophagy-WRKY20 interaction for plant immunity.

A plant strategy utilizing autophagy to degrade viral elements related to dsRNA-induced RNA silencing was discovered in many studies (Agius, C. *et al.*, 2012; Nakahara, K. S. *et al.*, 2012). Similarly, an earlier study found that a tobacco protein targets an RNA silencing suppressor type of protein to be degraded by autophagy. However, as pathogens hijacks host autophagy for the pathogen's benefit, they can use host autophagy to degrade host's own proteins. For example, in response to infection by Polerovirus the plant uses the RNA-induced silencing complex (RISC) to degrade viral RNAs. However, the Polerovirus then generates an RNA silencing suppressor, which has been reported to mediate the autophagic degradation of an essential component of the plants RNA-induced silencing complex (Derrien, B. *et al.*, 2012a).

Another example of how a pathogen evades host immunity is the fungal pathogen *Sclerotinia sclerotiorum,* which suppresses plant immunity by secreting autophagy inhibiting phytotoxins such as oxalic acid (OA) in *Arabidopsis* and tomato (Kabbage, M. *et al.*, 2013). OA was found to be inhibiting autophagy as *ATG4*, *ATG8f* and *ATG8g* levels were lowered significantly upon the pathogen inoculation. OA-defective mutant strain of the *S. sclerotiorum* lost its pathogenicity, however, inhibition of plant autophagy rescued the infection ability of the pathogen on tomato (Kabbage, M. *et al.*, 2013). Through this method the pathogen uses the hosts autophagy pathway to degrade the host's key line of defence against infection.

There are more evidences that host autophagy can be utilized as an antimicrobial mechanism in plants against viruses. For instants, rgs-CaM (regulator of gene silencing-calmodulin-like protein) in tobacco targets the viral elements to be degraded by autophagy. Those elements, RSSs, are utilized to suppress RNA silencing in plants which is the primary defence mechanism against the spreading viruses (Nakahara, K. S. *et al.*, 2012). Similarly, the cotton ATG8 targets the viral RSSs of CLCuMuV (cotton leaf curl Multan virus), which is called βC1. Moreover, ATG6 can supress the spread of turnip mosaic virus (TuMV) by targeting NIb, a viral RNA-dependent RNA polymerase (RdRp) (Li, F. *et al.*, 2018).

Numerous examples exist where plants have used autophagy to fend of pathogen attack, while the same pathogens have equally used the same autophagic process for their own benefit. This constant struggle between plant and pathogen has led to an intricate web, that at times can appear intractable. Much remains to be addressed, particularly regarding the molecular mechanisms of autophagy in plant-pathogen interactions.

1.6 The role of selective autophagy in innate immunity

Autophagy cargo receptors are the link between the proteins, generally to be degraded, to the autophagy machinery. They implicated in cell autonomous immunity in both plants and animals (Huang, J. *et al.*, 2014). One such plant autophagy cargo receptor, Joka2, contributes to immunity against *P. infestans,* whereas *P. infestans* secreted RxLR effector PexRD54 subverts Joka2's positive role in immunity (Figure 1.3) (Dagdas, Y. F. *et al.*, 2016). PexRD54 enables this by depleting Joka2 out of ATG8CL complexes as it has a better ATG8-Interacting Motif in terms of binding affinity. Joka2 with a mutant AIM which does not bind to ATG8, does not fully contribute to resistance against *P. infestans*. Similarly, PexRD54 with an unfunctional AIM region does not enhance the virulence of the pathogen (Dagdas, Y. F. *et al.*, 2016).

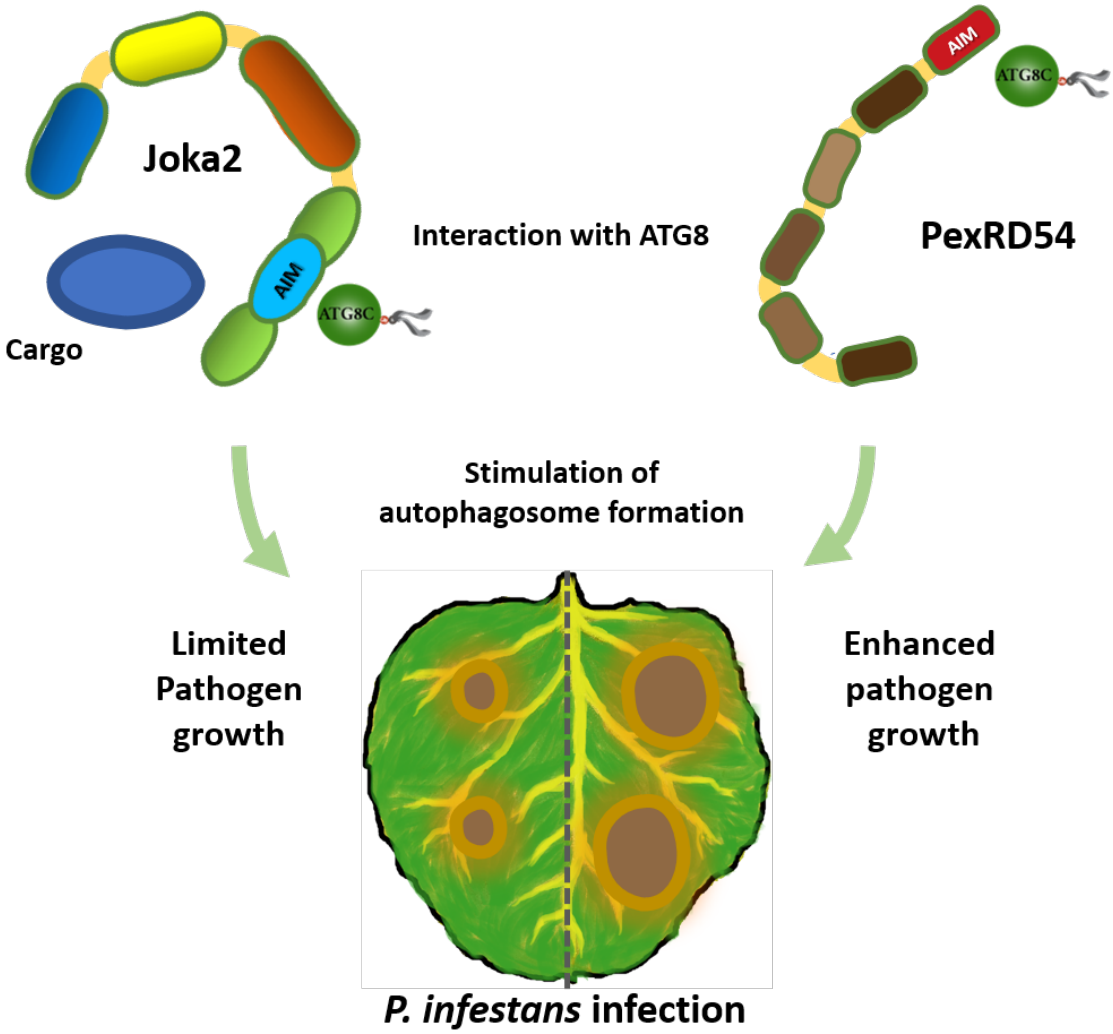


Figure 1.3. *P. infestans* effector PexRD54 outcompetes Joka2 and facilitates the virulence of the pathogen. Both host autophagy cargo protein Joka2 and pathogen effector PexRD54 stimulate autophagosome formation. Whilst Joka2 limits the spread of *P. infestans* on *N. benthamiana* leaf, PexRD54 causes susceptibility on the plant leaf.

An antiviral role of Joka2 was shown by Hafren and his co-authors (2017). In that study, they investigated how Joka2 limited spreading of Cauliflower mosaic virus (CaMV) and showed that the interaction of Joka2 with capsid protein P4 of CaMV lead to autophagic clearance of the viral particles. Similarly, Joka2 was found to be interacting with HCpro (a viral RSS helper component proteinase) of turnip mosaic virus (TuMV) leading to degradation of the viral element via selective autophagy (Hafren, A. *et al.*, 2018). It is not clear whether Joka2 directly binds to HCpro, however, the interaction between the

two proteins seems to depend on ubiquitin binding ability of Joka2. Because mutations on Joka2's ubiquitin binding domain (UBA2) lowers the colocalization of Joka2 and HCpro in the cells (Hafren, A. *et al.*, 2018).

Viruses, however, co-evolved to avoid degradation by host autophagy through targeting autophagy machinery. For instance, some viruses like CaMV generate inclusion bodies to prevent recognition by Joka2. Intriguingly, it is known that CaMV triggers non-selective autophagy to slow down senescence of the plant to increase the chance of spreading by the help of aphids (Hafren, A. *et al.*, 2017). TuMV deploys virulence factor, VPg, which induces degradation of defence related proteins in the plants (Cheng, X. *et al.*, 2017). VPg was also reported to antagonise Joka2 and so that prevents degradation of the viral RSS HCpro (Hafren, A. *et al.*, 2018). Similar to VPg, P0 form polerovirus causes degradation of ARGONAUTE 1 (component of RNA-induced silencing complex) via host autophagy, which is thought to occur through ubiquitin system (Derrien, B. *et al.*, 2012b). Rice stripe virus (RSV) targets a host protein that is inhibiting cell to cell spread of virus and causes its degradation through autophagy machinery (Fu, S. *et al.*, 2018). Barley stripe mosaic virus (BSMV) follows a different strategy and inhibits the interaction between core autophagy proteins ATG7 and ATG8 by encoding γb protein, therefore, interferes with the host autophagy (Yang, M. *et al.*, 2018).

The nature of the selective cargo recruited by Joka2 and how it contributes to immunity against filamentous pathogens remains unknown (Dagdas, Y. F. *et al.*, 2016). Like other autophagy cargo receptors, Joka2 interacts with the ATG8c-like (ATG8c throughout the report) isoform of the core autophagy protein ATG8 (Dagdas, Y. F. *et al.*, 2016; Noda, N. N. *et al.*, 2008). Previous work revealed that both Joka2 and PexRD54 compete for binding to the ATG8CL isoform but not ATG8IL. Joka2 in plants is homologous to human p62/SQSTM1/Sequestosome-1 and a neighbour of the BRCA gene 1 (NBR1) cargo receptors (Zientara-Rytter, K. *et al.*, 2011)(Figure 1.4). In humans, p62 has been mostly studied because it has been observed in many toxic, chronic and degenerative diseases with protein aggregates. Although those homologs are generally observed to colocalise with polyubiquitinated proteins or other aggregates, p62 also interacts with non-ubiquitinated proteins to mediate cellular signalling (Zientara-Rytter, K. *et al.*, 2011). In

animals whose autophagy is inhibited, proteins start to accumulate within the cells which triggers UPS. However, long term inhibition of autophagy cuased ubiqutinated proteins to form aggregates bound by p62, which also inhinbits proteosomal degredation. Those complexes can also sequester proteasomes which further inhibits protein degradation (Ji, C. H. *et al.*, 2017; Korolchuk, V. I. *et al.*, 2009).

In terms of protein domain organization and function, Joka2 carries signatures of a hypothetical hybrid of p62 and NBR1 (Figure 1.4). After embarking, the cargo and Joka2 and its human homologs interact with ATG8 to be engulfed by autophagosomes and degraded. A common feature shared by these autophagy cargo receptors are the phox/Bem1p (PB1), ZZ-typ zinger finger, C-terminal ubiquitin association domain (UBA), and a motif with uncharacterized function. ZZ domain of p62 interacts with arginylated chaperon such as BiP (which is induced by misfolded proteins) and cytoplasmic R-BiP is associated with cargoes and bind to ZZ domain of p62, facilitating p62 self polymerization and interaction with LC3.

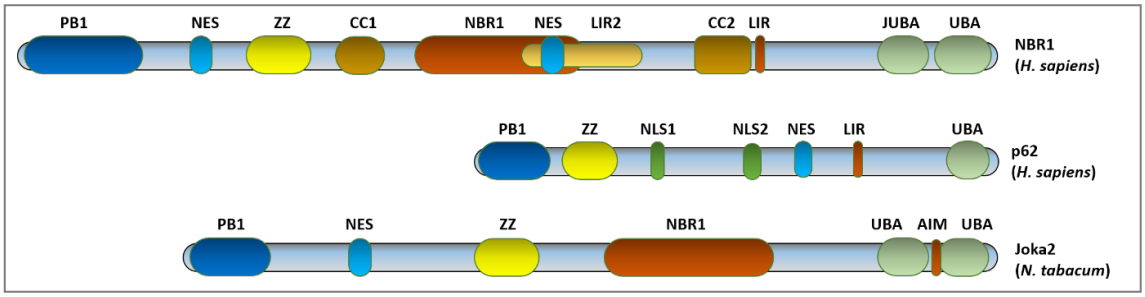
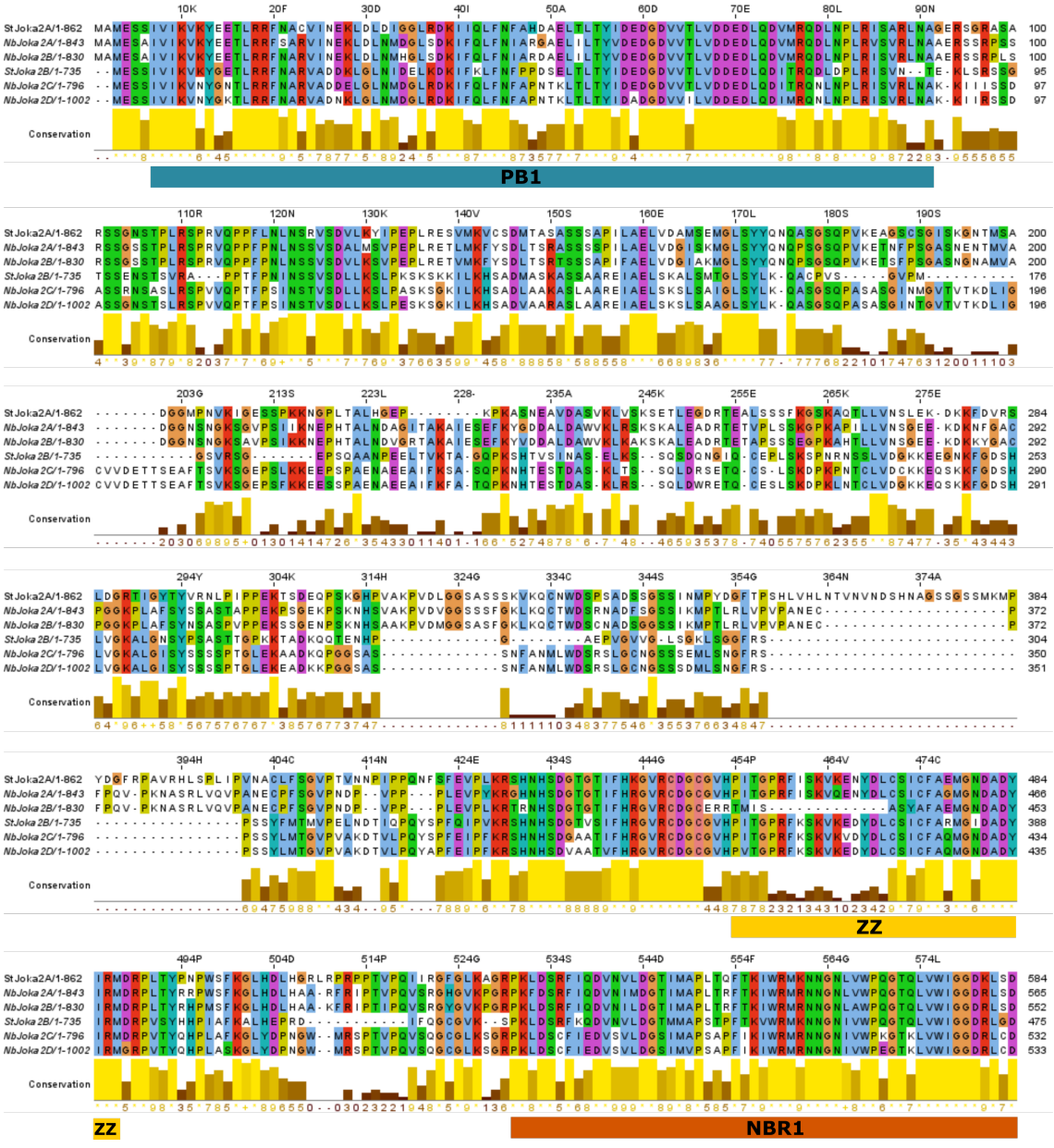


Figure 1.4. Domain architecture of Joka2 and its human autophagy cargo receptors homologues, p62 and NBR1. PB1: phox/Bem1p, NES: Nuclear export signal, NLS: Nuclear localisation signal, CC: Coiled-coil region, UBA: ubiquitin-binding domain, JUBA: amphipathic helical domain, ZZ: ZZ-type zinc finger domain, NBR1: Neighbour of BRCA1 gene 1 (domain with unknown function), LIR: LC3-interacting region, AIM: ATG8-interacting motif.

I found four full length predicted Joka2 proteins (Figure 1.5) in *N. benthamiana* proteome from Solgenomics database (Fernandez-Pozo, N. *et al.*, 2015a). When, the four homologs of Joka2 from *N. benthamiana* are aligned with *S. tuberasum* Joka2 proteins (A and B), the known domains of plant NBR1 from the literature are highly conserved between homologs and two species (Figure 1.5).



(Figure caption is in the next page)

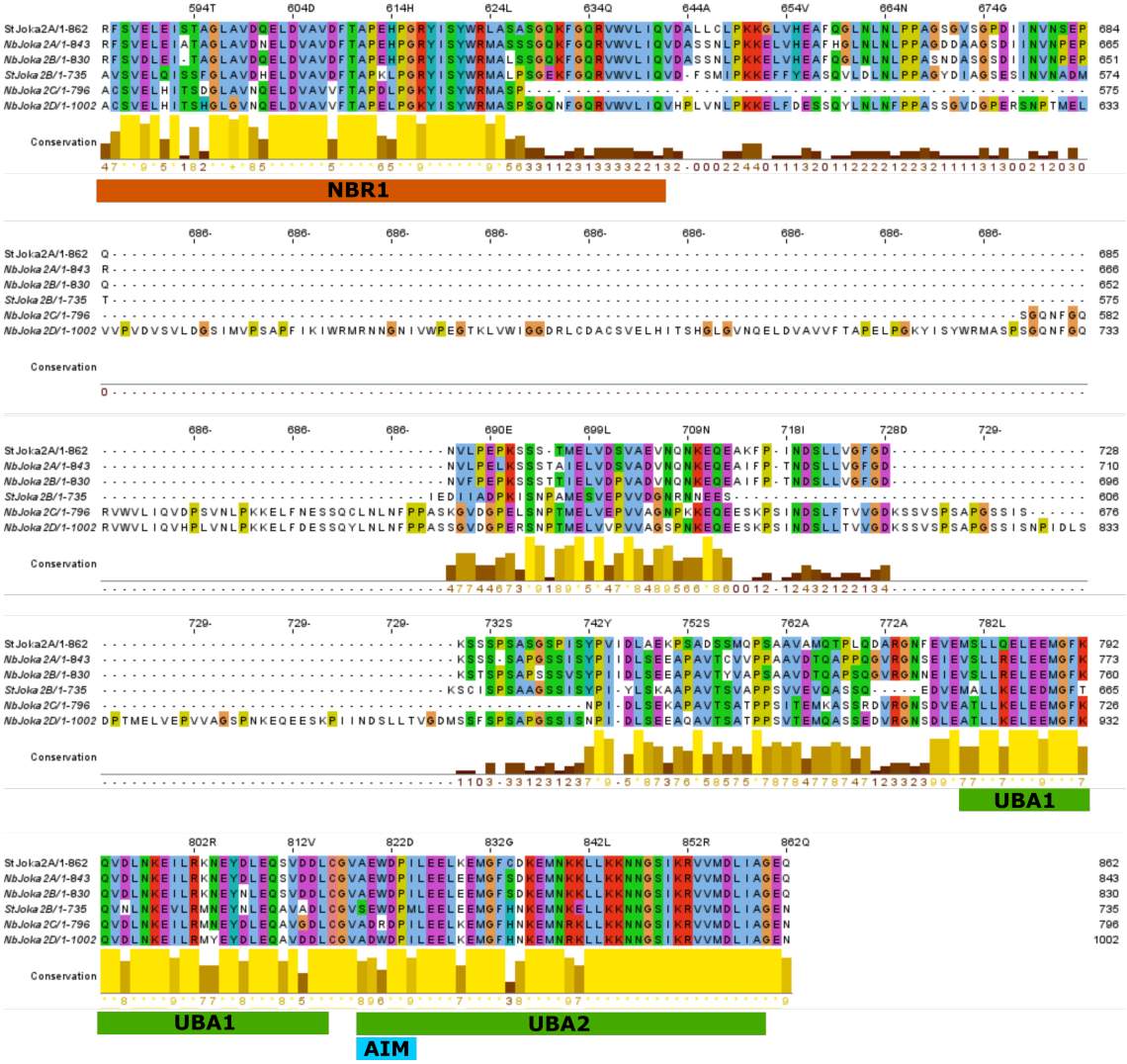


Figure 1.5. Protein sequence alignment of Joka2 homologs in *S. tuberosum* (StJoka2A and StJoka2B) and *N. benthamiana* (NbJoka2A, NbJoka2B, NbJoka2C and NbJoka2D). Sequences of Joka2 homologs in *S. tuberosum* and *N. benthamiana* were aligned with Clustal Omega and analysed by Jalview (Waterhouse, A. M. *et al.*, 2009). Matching amino acids with similar properties are highlighted in individual colours. PB1, ZZ, NBR1 and UBA domains are indicated based on StJoka2A. ATG8-intreracting Motif (AIM) is localised in the UBA2 domain.

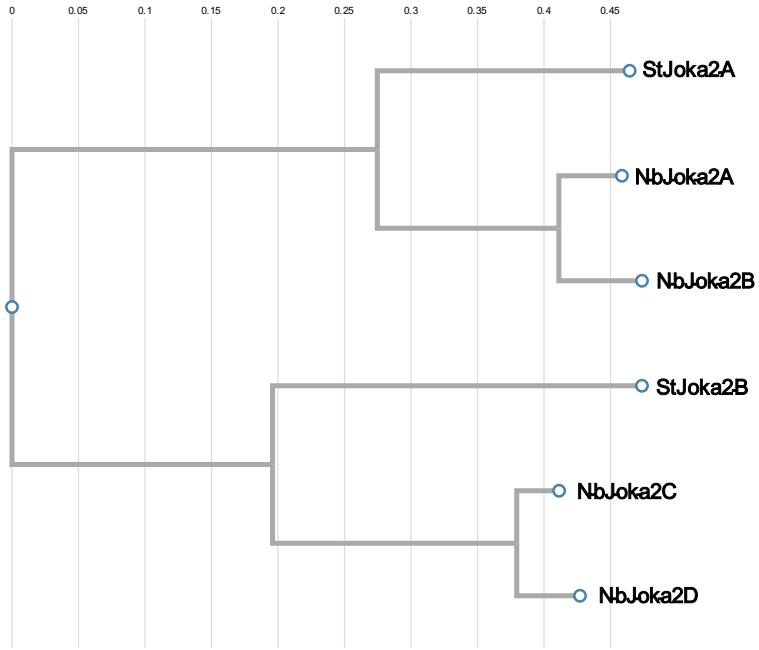


Figure 1.6. Phylogenetic tree of Joka2 homologs in *S. tuberosum* and *N. benthamiana*. Protein sequence of *S. tuberosum* and *N. benthamiana* Joka2 orthologs are aligned and analysed by using ClustalW (Waterhouse, A. M. *et al.*, 2009). *N. benthamiana* Joka2A and Joka2B are more homologous to StJoka2A, whereas, NbJoka2C and NbJoka2D sequences are more similar to *S. tuberosum* Joka2B.

In addition cargo-bound p62 induces autophagosome biogenesis (Ji, C. H. *et al.*, 2017). UBA2 domain in tobacco Joka2 has been shown to have affinity to ubiquitinated proteins (Zientara-Rytter, K. *et al.*, 2014). These cargo receptors also have a hydrophobic LIR (AIM) conserved domain consisting of a Y/WXXI/L motif that is required for interaction with ATG8 and to be recruited to autophagosomes (Zientara-Rytter, K. *et al.*, 2011). NBR1 forms a heterodimer with p62 via its PB1 domain and a homodimer via its N-terminal CC region (Lamark, T. *et al.*, 2003; Waters, S. *et al.*, 2009). Similarly, Joka2 forms homodimers via PB1-PB1 or PB1-UBA interactions. Joka2 has been observed to be involved in plant immunity against pathogens in different studies. Having been previously mentioned, Joka2 provides an advantage to *N. benthamiana* leaves when it was overexpressed, however the effector from the oomycete pathogen was overtaking the binding of Joka2 to ATG8CL and thus enabling successful invasion. Joka2 was shown to be also directly involved in degradation of virus-forming capsid proteins of CaMV to cease viral spread in Arabidopsis plants, which supports the findings for Joka2-mediated

autophagy against the pathogens (Hafren, Anders *et al.*, 2017). Another intriguing instance from a different type of pathogen, *Pseudomonas syringae* bacteria, demonstrated the importance of Joka2 (Ustun, S. *et al.*, 2018). While bacterial effector exploits autophagy to eliminate proteasomes to make the plants more susceptible, the same mechanism, autophagy, was also demonstrated to be used by the host and lessens the bacterial invasion by using a Joka2-dependent process. However, in most of those studies the common point is that the underlying mechanism of how Joka2 mediates resistance is poorly understood.

1.7 Proteomics Screening to Investigate Potential Joka2 Interactors

The study that had revealed the association of PexRD54 and ATG8CL was a result of proteomics screen of PexRD54 pull-down. As PexRD54 is an effector protein secreted by *P. infestans*, the target of the effector could be anything, which cannot be predicted due to its unfamiliar protein structure to plant proteins. Therefore, flag-tagged PexRD54 was transiently expressed in N. *benthamiana* leaves and the protein samples from those leaves and also from control group were used in immunoprecipitation (IP) experiments. Liquid chromatography tandem mass spectroscopy (LC-MS/MS) analyses of these IPs suggested that PexRD54 was associating with several ATG8 variants and some other proteins related to vesicular trafficking. A similar approach is used to identify the potential interactors of Joka2. As the mechanism of how Joka2 enhances plant immunity is not clear, finding out Joka2's cargoes or regulatory interactors would allow us to illuminate the ways how Joka2 functions during normal conditions or pathogen attack.

Protein-protein interactions can be studied by using various techniques. Conventional methods to purify the proteins involve chromatography such as ion exchange chromatography, size exclusion chromatography and affinity chromatography. To be more selective antibody-based methods like western blotting and ELISA can be carried out. Electrophoresis techniques such as two-dimensional gel electrophoresis can help to study protein complexes, too. However, those techniques are limited to known numbers of proteins. Therefore, more sensitive methods such as mass spectroscopy has been

utilised to analyse the complex protein mixtures with the advancement in the technology (Aslam, B. *et al.*, 2017). With the help of an appropriate approach, a whole set of interactors of a particular protein can be revealed with such sensitive techniques.

1.8 AIMS

The goal of my PhD study was to characterize the host processes required for accommodation of filamentous plant pathogens inside the plant cells. I mainly focused on recently discovered autophagy mediated plant defence, which is targeted by filamentous pathogen, *P. infestans*. Dagdas *et al.* showed that overexpression of Joka2 leads to stimulation of autophagosome formation and enhances plant immunity (Dagdas, Y. F. *et al.*, 2016). Yet, how Joka2 contributes to defence during *P. infestans* host colonization is unknown. Therefore, I employed a multidisciplinary approach including genetics, cell biology and biochemistry to study the mechanisms of defence-related autophagy which is mediated by the autophagy cargo receptor Joka2. As a model pathosystem, I used the solanaceous model plant *Nicotiana benthamiana* that can be infected by haustoria forming oomycete pathogens such as the Irish potato famine pathogen. To dissect the mechanisms of Joka2-mediated immunity, I pursued following specific objectives:

(i) Determining the subcellular dynamics of Joka2-mediated selective autophagy during infection. Preliminary work had showed ATG8CL/Joka2-labelled autophagosomes accumulated around the haustoria. Thus, I determined to continue the extent to which defence related autophagy was diverted to host-microbe interface and dissect the autophagy components involved in this process.

(ii) The second aim was to identify the Joka2 cargo and its transport route during infection. The rationale behind this objective was based on the preliminary data which I observed that Joka2-labelled vesicles accumulate around perihaustorial region. This implies that Joka2 could recruit defence-related components that contribute to resistance to prevent pathogen penetration. Alternatively, Joka2 might recruit a signalling complex to haustoria to stimulate defence related signalling. I worked on identifying the Joka2-cargo targeted to pathogen interface and investigated the

transport mechanisms involved in this process. I focused on identifying the roles and associations of potential Joka2 interactors, which were identified through a proteomics screen in infected plants. I investigated the nature of interaction between Joka2 and its confirmed interactors. In order to do that I focused on to find out the domains responsible for this interaction this association. I investigated their potential roles in Joka2-mediated autophagy defence system.

(iii) The third aim was to investigate the link between PTI and Joka2-mediated antimicrobial autophagy**.** How Joka2-mediated autophagy is activated during infection is unknown. Execution of PTI responses following immune recognition on the cell surface relies on downstream signalling events including mitogen-activated protein kinase (MAPK) pathways. Interestingly, the Joka2-interactor screen revealed several MAPKs downstream of PTI signalling. Therefore, I investigated how activation or suppression of PTI signalling affected.

CHAPTER 2 - MATERIALS AND METHODS

2.1 Maintenance of *Nicotiana benthamiana* and *Phytophthora infestans*

N. benthamiana plants were grown and maintained on organic compost and vermiculite (3:1) mixture in a growth chamber with long light intensity (16 hours light/ 8 hours dark photoperiod) at 22-24°C with 50% relative humidity.

P. infestans strain 88069 cultures were grown and maintained on rye sucrose agar medium at 18°C in the dark for 13-21 days prior to use for infection of *N. benthamiana* leaves as described (Song, J. *et al.*, 2009).

2.2 Generation of cloning and silencing plasmid constructs

Target sequences were amplified using Phusion proof-reading DNA polymerase (New England Biolabs), and primers were designed so that overhangs compatible with either Gibson assembly (GA) or Golden Gate (GG) assembly systems (Table 2.1). I used Gibson assembly for generating overexpression plasmids and Golden Gate assembly for hairpin and virus-induced gene silencing vectors. I used the tagged Joka2, Joka2^{AIM}, ATG8CL and REM1.3 constructs from previous projects, which were amplified from *S. tuberosum* cDNA (Bozkurt, T. O. *et al.*, 2014; Dagdas, Y. F. *et al.*, 2016), whereas, I generated tagged ATG9, MAPK3/6/9, MEK2, PAL, and PDX from *N. benthamiana* cDNA. PCR amplified DNA products were purified using Wizard SV gel and PCR clean up kit (Promega). All the fusion constructs were generated by altering pK7WGF2 plasmid; N-terminal fluorescent protein tag fusion was obtained by excising a fragment after EcoRV digestion and replacing it with GFP/BFP/RFP/HA/Myc sequence followed by a linker sequence and EcoRV restriction sites, and C-terminal fusion of GFP/BFP/RFP/HA/Myc was made by digesting pK7WGF2 plasmid with EcoRV, and inserting GFP/BFP/RFP/HA/My sequence bearing EcoRV cutting site with a linker sequence. Then, C-terminal fusion constructs of Joka2:BFP, Joka2^{AIM}:BFP, ΔPB1:GFP, ΔPZ:GFP, ΔZZ:GFP, ΔPZN:GFP, UBAs:GFP, UBAs^{1,2}:GFP, EV:BFP, ATG9:GFP, MAPK9:GFP, and PAL:GFP, N-terminal GFP fusion construct of GFP:PDX, and their other HA, Flag or Myc-tagged versions, were generated by Gibson assembly of each gene PCR fragment into EcoRV digested vectors.

Hairpin RNAi silencing constructs of hpMAPK3, hpMAPK6, hpMAPK9, hpPDX, hpPAL and hpGus were generated by amplifying 300-500 base pairs of target mRNA region from cDNA of the plants. The pRNAiGG vector and the amplified sequences were digested with BsaI and ligated with T4 DNA ligase in a mixture containing ligase buffer. The cloned vectors lack ccdB suicide region but contain antibiotic resistance to kanamycin and chloramphenicol.

Vectors obtained after the Gibson assembly and Golden gate assembly were transferred to chemically competent DH5α cells by heat-shock at 42^{o}C for 60-90 seconds. Single transformant colonies were selected on LB plates containing 50 µg/mL kanamycin and 25 µg/mL chloramphenicol (after Golden gate assembly), or 100 µg/mL (after Gibson assembly). Recombinant colonies were selected by using colony PCR. Primer pairs GA_35s_F and GA_TERM_R2 were used for GA and TRV2gg_cPCR-F and TRV2gg_cPCR-R were used for TRV2 plasmids. Because pRNAiGG vector has two insertion sites P21-P22 and P24-P25 pairs were used to test the insertions. P23 was used for sequencing (Table 2.1). Plasmids were isolated from overnight cultures of single recombinant colonies (Promega Pure yield plasmid miniprep kit). Verified plasmids by sequencing were transformed to electrocompetent *Agrobacterium tumefaciens* using Micropulser (Bio-Rad). Transformed bacteria were grown on LB with appropriate antibiotics and additional 50 µg/mL rifampicin and tetracycline 30 µg/mL for selection of *A. tumefaciens*.

Table 2.1. Primers used in this study. Primers starting with GA are for overexpression, hp are for hairpin and virus-induced gene silencing, and RT are for RT-PCR.

Name	Sequence (5'- 3')
GA_Joka2_F1	CAGGCGGCCGCACTAGTGATATGGCTATGGAGTCATCTATTGTGATCAAGG
GA_Joka2_R1	GCAGATCCAGCAGATCCGATCTGCTCTCCAGCAATAAGATCCATCACAAC
GA_ΔPB1_F **GA_Joka2$^{\Delta 1-91}$_F**	CAGGCGGCCGCACTAGTGATGGGCGAAAGAAGCGGCAGAGCTTCA
GA_ΔPZ_F **GA_Joka2$^{\Delta 1-487}$_F**	CAGGCGGCCGCACTAGTGATGGATCGTCCTCTAACTTACCCGAATCCCT
GA_ΔPZN_F **GA_Joka2$^{\Delta 1-645}$_F**	CAGGCGGCCGCACTAGTGATGGATGCTTTATTATGCCTGCCAA
GA_UBAs_F **GA_Joka2$^{\Delta 1-779}$_F**	CAGGCGGCCGCACTAGTGATGTCTCTCCTCCAGGAGTTGG
GA_ΔZZ_F **GA_ Joka2$^{\Delta 445-487}$_F**	GACTATTTTCCATAAAGGTGATCGTCCTCTAACTTACCCG
GA_ΔZZ_R **GA_ Joka2$^{\Delta 445-487}$_R**	GTAAGTTAGAGGACGATCACCTTTATGGAAAATAGTCCCAGT
GA_ΔNBR1_F **GA_ Joka2$^{\Delta 529-642}$_F**	GGGTTGAAAGCAGGTCGGGATGCTTTATTATGCCTGCCAA
GA_ΔNBR1_R **GA_ Joka2$^{\Delta 529-642}$_R**	CAGGCATAATAAAGCATCCCGACCTGCTTTCAACCC
GA_UBAs_F	CAGGCGGCCGCACTAGTGATGTCTCTCCTCCAGGAGTTGG
GA_PDX_F	CTGGATCTGGAGAATTTGATGGCCGGAAGCGGTGT
GA_PDX_R	TAGCATGGCCGCGGGATCACTCGGAACGATTAGCATACCTC
GA_PAL1_R	GCAGATCCAGCAGATCCGATACAGATTGGAAGAGGTGC
GA_PAL1_F	CAGGCGGCCGCACTAGTGATGGCTGGTGTTGCACA
GA_MAPK3_R	GCAGATCCAGCAGATCCGATAACATATTCAGGATTCAGTGACAAA
GA_MAPK3_F	CAGGCGGCCGCACTAGTGATATGGCTGATGCAAATATGG
GA_MAPK6_R	GCAGATCCAGCAGATCCGATCATGTGCTGGTATTCAGGATT
GA_MAPK6_F	CAGGCGGCCGCACTAGTGATGGATGGTTCTGGTCAGC
GA_MAPK9_F	CAGGCGGCCGCACTAGTGATGGGGGGTGGTGGTACA

GA_MAPK9_R	GCAGATCCAGCAGATCCGATAGCATGGAGAGCAGCAACTT
GA_ATG9_F	CAGGCGGCCGCACTAGTGATGATGTTTGGTGGACAAAAAGG
GA_ATG9_R	GCAGATCCAGCAGATCCGATAACAAGATCTGAAGGATCTAACTTTC T
GA_MEK2_F	CAGGCGGCCGCACTAGTGATGCGACCTCTTCAACCACC
GA_MEK2_R	GCAGATCCAGCAGATCCGATAGAAGAAAAATGAGGCGGGGG
hp_Joka2_Fus_F1	ACCAGGTCTCAGGAGTGGTGCCGAACTCATACTCA
hp_Joka2_Fus_R1	ACCAGGTCTCAGATGAGGATGAGGCCCTTGAAGTC
hp_Joka2_Fus_F3	ACCAGGTCTCACATCCAAAAGACACTGTGCTGCCT
hp_Joka2_Fus_R3	ACCAGGTCTCATCGTTACTTGTGGAACGGTAGGGG
hp_ATG9_F	ACCAGGTCTCAGGAGAGGGTTGCTTGATGATGTGC
hp_ATG9_R	ACCAGGTCTCATCGTATTCCACAGCATCCATTCCAC
hp_ATG4_F	ACCAGGTCTCAGGAGGAACCAGGACCAAGCAGTAAC
hp_ATG4_R	ACCAGGTCTCATCGTTACTTTTGGTCATGCGGCTG
hp_GUS_F	ACCAGGTCTCAGGAGTAAAGAGCTGATAGCGCGTGAC
hp_GUS_R	ACCAGGTCTCATCGTTGTCGGTGTACATTGAGTGCAG
hp_PDX1_F	ACCAGGTCTCAGGAGGCCCGTATAGCTGAGGAGG
hp_PDX1_R	ACCAGGTCTCATCGTCCTTGGTGCGTATCATGGC
hp_PAL_F	ACCAGGTCTCAGGAGAGCCGTGGACATCTTAAAGC
hp_PAL_R	ACCAGGTCTCATCGTGCTGTTTGCGTCCTTCTCA
hp_MAPK3_F	ACCAGGTCTCAGGAGATCACTACCAAGTATCGTCCTCC
hp_MAPK3_R	ACCAGGTCTCATCGTCCTCTGATAAACCTTGGTTGGATC
hp_MAPK6_F	ACCAGGTCTCAGGAGCCTGGTAGAGATCACGTACACC
hp_MAPK6_R	ACCAGGTCTCATCGTGGATTAAATGCAAGCGACTCCC
hp_MAPK9_F	ACCAGGTCTCAGGAGGTGTTCTTCGCTGGTTTCAAC
hp_MAPK9_R	ACCAGGTCTCATCGTCAGATCCCACGACTCCATAAC
RT_NbMAPK3_F	TCATGTATCAGCTCCTCCGTG
RT_NbMAPK3_R	CGAGGATGTTGTGGGAGTTG
RT_NbMAPK6_F	ATGGATGGTTCTGGTCAGCA
RT_NbMAPK6_R	AAGGCTTCTCTCTGTGGTGG
RT_NbJoka2_A_Fr	GATTCCCGTAATGCAGATTTCA
RT_NbJoka2_A_R	CATGTAAACCCTTGAAAGACCA
RT_NbJoka2_B_Fr	GTGCGGTGCCATCAATAAAG

RT_NbJoka2_B_R	ATCTTGATAGAACTGCCACCAG
RT_NbJoka2_C_F	CCAAATCTCTCTCGGCGATT
RT_NbJoka2_C_R	GCTTAGGATCTTTGGATAACGAAC
RT_NbJoka2_D_F	TTGGTTGTGCCAGTGGATGTC
RT_NbJoka2_D_R	CTTCCAGCAACCACTGGCA
RT_NbPAL_A_F	GGCTCAGAAGCTTCACGAAAC
RT_NbPAL_A_R	TCCAAGCTTGGATTCCTTCCT
RT_NbATG4_F	CGTTGGTTCTTGGACTTGAC
RT_NbATG4_R	TTATCGTAAACAAAGGAGCACC
RT_NbATG9A_F	CCCAATGGAGTGCGCAT
RT_NbATG9A_R	ACGAAATAAACTTTGCGACGAC
RT_NbATG9B_F	GGCCCTAATGGAGTGCATAG
RT_NbATG9B_R	CAAAAGAAATGAACTTGCGATGAT
MAPK3_pOPINb_F	AAGTTCTGTTTCAGGGCCCGATGGCTGATGCAAATATGGG
MAPK3_pOPINb_R	ATGGTCTAGAAAGCTTTAAACATATTCAGGATTCAGTGACAAA
NBR1_pOPINb_F	AAGTTCTGTTTCAGGGCCCGATGCCGAAGCTGGACAGTCG
NBR1_pOPINb_R	ATGGTCTAGAAAGCTTTAGACCTGGATAAGCACCCATACACG
GA_35s_F	CGTTCCAACCACGTCTTCAAAGCAAG
GA_TERM_R2	GCAGGTCACTGGATTTTGGT
TRV2gg_cPCR-F	ACTCAAGGAAGCACGATG
TRV2gg_cPCR-R	TAATGTCTTCGGGACATGC
P21	ACCATTTACGAACGATAGCC
P22	GTAAAACGACGGCCAGTG
P23	CGAATCTCAAGCAATCAAGC
P24	CATTTTAGCTTCCTTAGCTCC
P25	CATTTGGATTGATTACAGTTGG

2.3 Agroinfiltration and Transient gene-expression assays in *N. benthamiana*

A. tumefaciens GV3101 strain carrying cloned constructs were grown on appropriate antibiotics. Bacteria lawn was scraped and resuspended in distilled water for washing. The suspension was centrifuged at 1500 g for 5 minutes. Washing was repeated twice and lastly bacteria were resuspended in agroinfiltration buffer (10 mM MgCl2, 5 mM 2-(N-morpholino)-ethanesulfonic acid (MES), pH 5.6) with a final OD600 of 0.2 unless it is stated otherwise. The suspension was gently infiltrated to the abaxial side of the leaves of 4-5-week-old *N. benthamiana* by 1 mL syringe. Depending on the experiment the infiltration zone can vary from a coin sized area (e.g. cell death experiments) to the half of the leaf (e.g. infection assays and protein level comparisons) or even the whole leaf (Co-IP) can be infiltrated to get enough protein amount.

2.4 Confocal Microscopy

Imaging of the abaxial epidermal cells of live leaves was performed using a Leica SP5 resonant inverted confocal microscope (Leica Microsystems) using 63x water immersion objective or a Leica SP8 with 40x water immersion objective. Leaf discs collected from *N. benthamiana* leaves using a cork borer size 3-4 and were mounted by Carolina observation gel (Carolina Biological Supply Company). BFP, GFP and RFP fluorophores were excited using 405, 488 and 561 nm laser diodes and their fluorescent emissions detected sequentially at 450-480, 495-550 and 570-620 nm, respectively. The images shown in each figure were maximum intensity projections of Z-stack of confocal images. Image analyses were performed using ImageJ (FIJI), Inkscape, Adobe Illustrator CS6 and Adobe Photoshop CS6.

2.5 Infection Assays

Zoospores were released from sporangia of *P. infestans* by adding cold water and incubating the culture at 4°C for 1-2 hours. Zoospore number was counted under microscope using a haemocytometer and the concentration was adjusted to 50,000 spores per mL. Infection of agroinfiltrated leaves was carried out by carefully adding 10

µL droplets containing zoospore onto abaxial surface of detached leaves, which had been agroinfiltrated by the target and control constructs. Leaves then incubated in a humid chamber with previously mentioned day-light conditions at 18°C. 10-12 days after infections, leaves were imaged by camera and the area of necrotic lesion was measured using ImageJ. Biotrophic growth of late blight pathogen was done by using *P. infestans 88069* isolate which expressed tdTomato fluorescent protein and can be visualized under fluorescence microscope at 5-7 days after infection. In order to visualize infection under confocal microscope, leaves were inoculated with zoospores on the adaxial surface of leaves which were then incubated in humid growth chambers for 2-3 days. In order to visualize haustoria of *P. infestans*, RFP:REM1.3 was coexpressed with other proteins due to its accumulation at EHM which enables us to spot infection sites (and haustoria).

2.6 Co-immunoprecipitations

Leaves agroinfiltrated 2 days prior to collection were weighed (around 3 g) and placed in 50 mL centrifuge tubes. The sample weights were equalized for easy handling for further processes and immediately dipped in liquid nitrogen to flash freeze the leaf tissues. For long term storage, they were placed in -80 until processing for protein extraction.

The extraction was performed by grinding 3 grams of leaf tissue using chilled mortar and pestle. Grinded tissue was collected back into 50 mL centrifuge tubes and 6 mL of GTEN (10% glycerol, 25 mM Tris-HCl pH 8.3, 1 mM EDTA, and 150 mM NaCl) containing 10 mM DTT, 0.5% protease inhibitor cocktail (Sigma-Aldrich), 2% w/v polyvinylpolypyrrolidone (PVPP) and 0.1% v/v IGEPAL was added on top of the samples. Each extract was vortexed vigorously for 1 minute and placed in ice when not handled. Afterwards the extracts were spun at 3,500 g at 4°C for 15 min to remove crude pellet and 5.5 mL of supernatant was passed through miracloth (22-25 µm pore size, Merck Millipore). Filtrate was centrifuged a second time with the same conditions and 5 mL of the supernatant was transferred into 5 mL centrifuge tubes in order to incubate with GFP or RFP trap agarose beads (Chromotek) on a rotator for an hour at 4°C. From remaining supernatant, 100 µL of extract was kept to run as an “input” for each sample. After incubation, the beads

were spun at 800g for a minute at 4°C and the supernatant was collected without disturbing the beads. IP (immunoprecipitation) buffer (GTEN with 0.1% v/v IGEPAL) was added on top of the beads. The beads were resuspended by tapping the side of the tubes and the suspension was transferred to 1.5 mL centrifuge tubes. After centrifugation for 30 s at 800g, the supernatant was replaced by fresh IP buffer. The beads were resuspended, and this washing process was repeated for three times in total. Lastly all the wash buffer was removed from the beads by using the edge of a needle of a 1 mL syringe and processed as a protein sample for western blot as described.

In order to release the proteins from the beads, 25 µL of Laemmli loading buffer (2% (w/v) SDS, 10 mM DTT, 10% (v/v) glycerol, 60 mM Tris and 0.01 % (w/v) bromophenol blue) was added on top of the beads. Input samples were diluted with 4X Laemmli buffer. All the samples then placed in heating block for 10 min at 70°C and the process was followed by running 10-20 µL of samples on SDS-PAGE.

2.7 Crude protein extraction

Depending on the protein levels of individual constructs and the time points for protein detection, leaf samples were collected from the plants at 2-3 dpai. The samples were sectioned using a cork borer size 4 and frozen immediately in liquid nitrogen to store later in ultra-low temperature freezer (-80°C). Leaf tissues were homogenized in 1.5 mL microcentrifuge tubes with a micropestle and protein extraction buffer (5:2:3 ratio mixture of Laemmli buffer (Bio-Rad): DTT (dithiothreitol): nuclease free dH2O) was added. Samples were centrifuged at 17000 g for 10 minutes after incubation at 70°C for 5-10 minutes. The supernatant was kept for SDS-PAGE.

2.8 SDS-PAGE, Transferring of proteins and Western blot

The supernatant of the crude extract, input or immunoprecipitated proteins are spun at 17 000 g for 5 min to remove pellets or beads. 10-20 µL supernatant was run on using SDS polyacrylamide gel electrophoresis (SDS-PAGE). The discontinuous gels with appropriate percentages were handmade consisting of stacking and separating phases. 10% separating gel was made by adding 1.25 mL 1.5 M Tris buffer (pH 8.3), 1.25 mL 40%

acrylamide:bis acrylamide solution (37.5:1; Bio-Rad), 50 µL 10% SDS, 50 µL ml 10% (w/v) APS (ammonium persulfate), 5 µL TEMED (N,N,N',N'-tetramethylethylene-diamine (Bio-Rad) and enough water to top-up to 5 mL total volume. Stacking gel was prepared by adding 1.25 mL 0.5 M Tris buffer (pH 6.8), 0.375 mL 40% acrylamide:bis acrylamide solution (37.5:1; Bio-Rad), 50 µL 10% SDS, 50 µL ml 10% (w/v) APS, 5 µL TEMED and enough water to complete the final volume to 5 mL. The run was done by using SDS-PAGE running buffer (25 mM Tris,192 mM glycine and 0.1% SDS) starting with constant 80 volts. The voltage was increased to 150 volts after proteins reached to the bottom of the stacking phase.

The separated proteins after SDS-PAGE were transferred to polyvinylidene difluoride (PVDF) membrane by using standard semi-dry Trans-Blot Turbo transfer system (Bio-Rad) using Bjerrum Schafer-Nielsen Buffer (48 mM Tris, 39 mM glycine, 1.3 mM SDS (0.00375% w/v) and 10% v/v ethanol (or methanol)). The PVDF membrane was wetted in absolute methanol to activate it and then placed in Transfer buffer for 5 min. The gel was also placed in transfer buffer for 5 min for exchange of running buffer with transfer buffer. The transfer time was adjusted depending on the size of the proteins but in general Transfer-Blot Turbo (Bio-Rad) standard transfer protocol was utilized (constant 25 volts, 1.0 A limited current for 30 min).

Following the transfer of proteins from SDS gel to PVDF membrane, blocking was employed by placing the membrane into blocking solution (3% bovine serum albumin (BSA) in Tris Buffered Saline (TBS, 20 mM Tris and 150 mM NaCl, pH 7.6)) for one hour. The gel was stained with Coomassie Brilliant Blue dye to check the remaining proteins and visualize RuBisCo amounts. The membrane was incubated with appropriate primary antibodies (ChromoTek) in antibody solution (3% w/v BSA in TBS with 0.1% w/v Tween-20) overnight at 4°C or 1 hour at room temperature (Table 2.2). Afterwards, the membrane was washed five times with TBS-T (0.1% w/v Tween-20 (Sigma-Aldrich) in TBS) for 5 min between changing wash buffer, and placed into antibody solution with proper horse radish peroxidase (HRP) or alkaline phosphatase (AP) conjugated secondary antibodies for 1 hour at room temperature (Table 2.2). After the incubation, excess secondary antibodies were washed off from the membrane using TBS-T wash

buffer five times at least 30 min in total. The detection was done by using Luminol for HRP-conjugated secondary antibodies (chemiluminescence (ThermoFisher)), or 5-bromo-4-chloro-3-indolyl phosphate (BCIP) and nitroblue tetrazolium (NBT) (Bio-Rad) for colorimetric detection according to the protocol provided by the manufacturer. Chemiluminescence was recorded by LI-COR Odyssey Fc Imaging System and color was imaged with a scanner. The membrane was stripped from antibodies by using mild stripping buffer (1.5% w/v glycine, 0.1% w/v SDS and 0.1% w/v Tween-20) and reblotted starting from blocking to detection as mentioned above. Colorimetric detection was utilized at the end of the detection procedure as the stained membrane cannot be reblotted. Membrane was stained with Ponceau S in order to show total protein as an indicator of equal loading. Image of the membrane was acquired by a digital camera or a scanner.

Table 2.2. Antibodies used for western blotting

Type of the antibody	**Dilutions**
Primary antibodies	
Rabbit anti-GFP (polyclonal, Chromotek)	1:3000
Rabbit anti-BFP (polyclonal)	1:5000
Rat anti-GFP (monoclonal, Chromatek)	1:2000
Mouse anti-RFP (monoclonal, Chromatek)	1:2000
Rat anti-HA (monoclonal, Chromatek)	1:2000
Mouse anti-FLAG (monoclonal)	1:3000
Rat anti-Myc (monoclonal, Chromatek)	1:2000
Rabbit anti-pMAPK (polyclonal)	1:2000
(anti-phospho-p44/42-ERK1/2, Cell Signalling)	
Rabbit anti-NBR1 (polyclonal)	1:5000
(anti-Joka2, Agrisera)	
Rabbit anti-ubiquitin (polyclonal, Agrisera)	1:10000
Rabbit anti-Actin (polyclonal, Abcam)	1:2000
Mouse anti-His-Tag (monoclonal, Agrisera)	

Secondary antibodies (HRP conjugated)	
Goat anti-rabbit (Sigma-Aldrich)	1 µL /10 mL
Goat anti-rat (Sigma-Aldrich)	4 µL /15 mL
Goat anti-mouse (Sigma-Aldrich)	1 µL /10 mL

Secondary antibodies (AP conjugated)	
Goat anti-rabbit (Sigma-Aldrich)	1 µL /10 mL
Goat anti-rat (Sigma-Aldrich)	1 µL /10 mL

2.9 Hairpin gene silencing and Virus-induced gene silencing (VIGS)

Both hairpin silencing and VIGS were used to knock down the genes of interest. Hairpin silencing was implemented to transiently knock down genes without causing developmental artifacts. The procedure was performed as described by Pun *et al.* (Yan, P. *et al.*, 2012). I have performed virus-induced gene silencing as described by Liu *et al.* (2002) in order to systematically knock down the genes. The genes targeted for both types of silencing were analyzed via Solgenomics blast tool to avoid possible off-targets (Fernandez-Pozo, N. *et al.*, 2015b). I have designed primers (Table 2.1) to produce 300-600 base pair long amplicons depending on the homology of the targeted genes to knock down closely related homologs. These amplicons were suitable for cloning into both pRNAiGG and TRV2 vectors. TRV2 vector used for this purpose was designed by Duggan *et al.* (unpublished) from original TRV2 vector so that those amplicons generated for hairpin silencing (pRNAiGG plasmid) can be inserted by using Golden gate cloning. RNA interference in plants was caused by *Agrobacteria* carrying hpMAPK3/6/9, hpPAL, or hpPDX by infiltrating them with OD of 0.3. hpGUS was utilized as a control due to undetectable GUS activity in most of the plants. The TRV2:MAPK3/6 construct was designed to target both *N. benthamiana MAPK3* and *MAPK6* mRNAs. TRV2:Joka2 was designed to silence all 4 homologs of *N. benthamiana Joka2*.

VIGS is established by using binary vector system where TRV1 and TRV2 (carrier of the targeted region) are agroinfiltrated separately. TRV1 carries general viral genes and

TRV2 can be used to carry the targeted region to be silenced. Agroinfiltration is employed as described before, however, after the last wash, agrobacteria are left in the dark in agroinfiltration buffer with 100 µM acetosyringone for 2 hours to increase the virulence of *A. tumefaciens*. TRV1 and TRV2 were prepared to be final OD of 0.4 and 0.2, respectively. The mixture is infiltrated into cotyledons of 10-days-old seedlings with 1 mL syringes. If there were true leaves, they were also agroinfiltrated. Plants were left under growth conditions for 4-5 weeks until they were ready for the experiments.

2.10 Reverse transcription PCR (RT-PCR)

After transient or systemic silencing of targeted genes and infection assays, total RNA was extracted from 6-8 leaf discs of plant tissue using Agilent Plant RNA isolation Mini Kit according to the protocol of the manufacturers. hpGUS, TRV2:EV and water treatment were used as control groups of transient silencing, systemic knocking down and *P. infection* experiments. Complimentary DNA was produced by reverse transcribing 2 µg of extracted total RNA using SuperScript IV reverse transcriptase (Thermo Fisher Scientific). In order to normalise the gene expressions, housekeeping gene GAPDH was used. RT primers in the Table 2.1 were used for the PCR and resulting DNA was run on 1% agarose gel with Tris-borate buffer (TBE, 89mM Tris, 89mM borate and 2mM EDTA, pH 8.3).

2.11 Recombinant protein expression

Plasmids for expression of NBR1 or MAPK3 with a N-terminal 6x-His tag were generated by cloning the corresponding DNA into a pOPIN vector for expression in E. coli. BL21(DE3) competent cells were transformed via heatshock with either the NBR1 or MAPK3 plasmid and grown on Luria–Bertani (LB) agar plates containing 100 µg/mL ampicillin at 37 °C overnight. A single colony from each was selected and used to inoculate 10 mL of LB containing 100 µg/mL ampicillin which was grown overnight at 37 °C with shaking at 200 rpm at bench top shaker.

The following day, 1 mL of the overnight culture was used to inoculate 1 L of LB containing 100 µg/mL ampicillin in 5 L flask which was grown at 37 °C with shaking at

200 rpm. When the culture reached an OD_{600} of 0.8 (typically 5-6 h), the culture was induced by the addition of IPTG to a final concentration of 0.5 mM. The induced culture was grown overnight at 18 °C with shaking at 200 rpm on bench top shaker. Cells were harvested by centrifugation for 20 mins at 4 °C. Samples for analysis by SDS-PAGE were taken pre and post induction.

2.12 Recombinant protein purification

The cell pellet (from 1 L of culture) was resuspended in 20 mL of buffer A (20 mM Tris-HCl, pH 7.5, 200 mM NaCl) containing a cOmplete protease inhibitor tablet and 10 µL of DNAse I. Cells were lysed by sonication and the cell debris pelleted by centrifugation at 15000 rpm for 45 min at 4°C.

Initial affinity purification made use of the N-terminal 6x-His tag and used 2 mL of Talon cobalt resin, which had been washed with 2 mL MilliQ water and equilibrated with 4 mL of buffer A. The resin and supernatant were combined and mixed at 4 °C for 2h to allow binding of the 6xHis-tagged protein to the resin. The resin was applied to a gravity flow column and the flow through collected. The resin was washed with 30 mL of buffer A and eluted using an imidazole step gradient prepared in buffer A as follows: 10 mL of 10 mM imidazole, 2x4 mL of 100 mM imidazole and 4 mL of 500 mM imidazole.

Samples of the cell debris pellet, the supernatant, and the Talon cobalt resin flowthrough, wash, and elutions were taken. All samples were analysed by SDS-PAGE using a 4-12% Bis-Tris gel. Fractions containing the protein of interest were combined and concentrated to 500 µL using a spin concentrator.

Following affinity purification, the protein of interest was further purified by means of size exclusion chromatography. A GE Superdex 200 10/30 column was washed with 35 mL of degassed MilliQ water and equilibrated in 35 mL of degassed and filtered buffer A at a flow rate of 0.5 mL/min. 500 µL of sample was injected onto the column and eluted in buffer A collecting 0.5 mL fractions. The fractions were analysed by SDS-PAGE. Fractions containing the protein of interest were combined.

2.13 *P. infestans* extract preparation and PAMP treatment

P. infestans hyphae were collected with a scalpel from an RSA plate to 1 mL water. The mixture was vortexed for 20 s and incubated at 90°C for 10 min. Afterwards, the solution was filtered using miracloth and and the filtrate was centrifuged for 30 min at highest speed at 4 °C. The supernatant was transferred into a new centrifuge tube without disturbing the pellet and passed through syringe filter with pore size of 0.45 µm. The obtained solution was aliquoted and stored in -20°C until infiltrating into plants. The extract was infiltrated into the leaves of *N. benthamiana* plants to induce PTI as the extract contains pathogen-associated molecular patterns (PAMPs). The effect of PAMP treatment on protein levels or gene expression was done using Wester blotting and RT-PCR.

2.14 Measurement and analysis of cell death

Autoactive MEK2 ($MEK2^{DD}$) was used to induce cell death on *N. benthamiana* leaves. Because autoactive MEK2 causes rapid cell death and collapse of the leaf tissue within a day with regular optical density of 0.2 that I used for other experiments, I have decreased optical density of agrobacterium carrying the construct ten times (OD: 0.02) to enable a reasonable time point to measure cell death. An observable cell/tissue death developed within 2-3 days with OD of 0.02 of $MEK2^{DD}$. A dying tissue on the leaf fluoresces at 800 nm channel of LI-COR Odyssey Fc Imaging System which can be later measured with the software Image Studio Lite.

CHAPTER 3 - HOST AUTOPHAGY MACHINERY ENHANCES FOCAL DEFENCE RESPONSES

This chapter of thesis is partially published in the following article (Dagdas, Y. F., Pandey, P., Tumtas, Y., Sanguankiattichai, N., Belhaj, K., Duggan, C., . . . Bozkurt, T. O. (2018). *Host autophagy machinery is diverted to the pathogen interface to mediate focal defence responses against the Irish potato famine pathogen*. eLife, 7. doi:10.7554/eLife.37476

3.1 INTRODUCTION

Plants are exposed to many destructive pathogens some of which intimately interact with their hosts through special infection structure. For instance, filamentous pathogens colonize their hosts through invasive hyphae that spread across the plant tissue. Some fungi and oomycete pathogens also form specialized infection structures called haustoria that are accommodated within the host cells (Panstruga, R. *et al.*, 2009), (described in more detail in the first chapter). Haustoria, however, do not directly face the intracellular environment as they are enveloped by a plant-derived membrane called the extrahaustorial membrane (EHM) (Bozkurt, Tolga O. *et al.*, 2015; Bozkurt, T. O. *et al.*, 2011; Whisson, S. C. *et al.*, 2016). As previously discussed in Chapter 1, EHM is crucial for host-pathogen interactions, and remains as the ultimate barrier preventing pathogens access to cellular resources (Dagdas, Y. F. *et al.*, 2016; Gutjahr, C. *et al.*, 2013; Koh, S. *et al.*, 2005; Le Fevre, R. *et al.*, 2015; Micali, C. O. *et al.*, 2011; Pumplin, N. *et al.*, 2012; Wang, S. *et al.*, 2017). However, the membrane source of the EHM and its biogenesis is still unclear.

The filamentous pathogen that is the focus of this thesis, *P. infestans*, is an oomycete that can produce multiple haustoria to infect plant cells (Whisson, S. C. *et al.*, 2016) Intriguingly, the composition of this special membrane around the haustoria, EHM, is different from that of the plasma membrane of the plant cell in terms of both protein and phospholipid content (Bozkurt, Tolga O. *et al.*, 2014; Lu, Y. J. *et al.*, 2012; Schornack, S. *et al.*, 2009). Therefore, multiple membrane sources have been proposed as a source for this non-uniform composition of the EHM (Bozkurt, Tolga O. *et al.*, 2014). It has been speculated that multiple trafficking pathways could be diverted to haustoria to contribute to EHM biogenesis.

Autophagy (macroautophagy) has been described in more detail in the previous section (Chapter 1). In short, it is a ubiquitous vesicle trafficking pathway that mediates removal of dysfunctional organelles, misfolded proteins, recycling cytoplasmic component and so forth (Stolz, A. *et al.*, 2014). Bulk autophagy is required for general homeostasis and is triggered by starvation to engulf and non-selectively recycle cytoplasmic content. Pre-lysosomal double membraned vesicles that are used to engulf the cargo to be degraded

are called autophagosomes. In contrast, selective autophagy utilizes various autophagy cargo receptors and ATG8 isoforms as an adaptor to recruit specific cargoes to the autophagosomes (Lamb, C. A. *et al.*, 2013). For example, a plant autophagy cargo receptor, Joka2, which has a higher affinity to Clade-I ATG8s, can mediate degradation of viral particles by inducing antibacterial autophagy which is specifically called xenophagy (Hafren, Anders *et al.*, 2017). Likewise limiting viral spread *in planta*, Dagdas *et al.* showed that Joka2 also activates selective autophagy during *P. infestans* infection and contributes to plant immunity (Dagdas, Y. F. *et al.*, 2016). In the same study, the authors also demonstrated how the pathogen evolved to redirect antimicrobial autophagy by secreting an RXLR-WY type virulence effector, PexRD54. Similar to Joka2, PexRD54 has an ATG8-interacting motif (AIM), with an even higher affinity to ATG8CL than ATG8IL, and restricts autophagy-mediated immunity by competing with Joka2 to form autophagosomes. Both Joka2 and PexRD54 trigger the formation of autophagosomes which are marked by mostly ATG8CL(Clade-I), and less frequently by ATG8IL (Clade-II). This tendency emphasizes the selectivity of antimicrobial autophagy against *P. infestans*. However, the subcellular fate of PexRD54 and Joka2 triggered autophagosomes during infection needs to be illuminated.

3.2 AIM

The goal of the chapter is to characterize the autophagy-related processes implicated in accommodation of filamentous plant pathogens inside the plant cells. To this end, defence-related autophagy targeted by *P. infestans,* will be the main focus of this project. As a model pathosystem, I use the solanaceous model plant *Nicotiana benthamiana* and the oomycete pathogen *P. infestans.* In this chapter, I will focus on the experiments carried out to determine the subcellular dynamics of Joka2-mediated selective autophagy during infection. In the beginning, I showed ATG8CL/Joka2 labelled autophagosomes accumulate around the haustoria. I have gone into more detail to determine the extent to which defence-related autophagy is diverted to the pathogen interface and dissected the autophagy components involved in this process.

3.3 RESULTS

3.3.1 Defence-related selective autophagy mediated by Joka2 is diverted towards haustoria

Although autophagy is widely known to facilitate lysosomal degradation of autophagosomal cargo, secretory autophagy can mediate relocation and secretion of specific cargo molecules (Bozkurt, T. O. *et al.*). To study the positive role of Joka2-mediated autophagy in plant immunity, first, I devised experiments to investigate the subcellular localization of Joka2 and its truncated versions during *P. infestans* infection.

3.3.1.1 ATG8CL-autophagosomes accumulate around the haustoria

In order to depict the full picture of what is happening to autophagy during the infection, I have to mention related work which our group has published. To this published work I contributed experiments regarding Joka2 and ATG9. Parts of this story which I have not directly contributed to are not included as figures in the "Results" part of my thesis but have been added to the "Appendix" so that I can deliver the message easily to help fully grasp the story.

At first, during pathogen infection functional ATG8CL positive autophagosomes were observed to selectively accumulate around the host-pathogen interface, and this accumulation is mostly true for ATG8CL autophagosomes, which Joka2 interacts, compared to ATGIL ones that Joka2 do not colocalise frequently (Dagdas, Y. F. *et al.*, 2018).

3.3.1.2 Joka2-labelled autophagosomes are directed towards the pathogen interface

The finding that autophagosomes accumulate around haustoria prompted us to further investigate the function of autophagy during infection. I focused on the autophagy cargo receptor as it has been shown to enhance plant immunity not only against *P. infestans* but also against bacterial pathogens (Hafren, Anders *et al.*, 2017). To better understand the mechanisms of Joka2 mediated autophagy in defence and to determine the subcellular dynamics of Joka2-autophagosomes during infection, a transiently expressed carboxyl-terminal blue fluorescence protein (BFP) fusion of Joka2 (Joka2:BFP) has been

monitored in *N. benthamiana* leaves infected with *P. infestans*. In order to further investigate the importance domains of Joka2 which might be crucial for trafficking those autophagosomes, I utilised mutants of Joka2 lacking the PB1-ZZ domains and a functional AIM region.

Autophagosomes labelled by the wild type Joka2 fused to BFP (Joka2:BFP) frequently accumulated around the haustoria (92%, N=50) and associated with the EHM, unlike the BFP vector control (Figure 3.1B). Intriguingly, a Joka2 mutant containing a non-functional ATG8 interacting motif (Joka2AIM:BFP) also labelled perihaustorial compartments, but with a lower frequency (74%, N=42) compared to wild type Joka2 (Figure 3.1C). Although, a Joka2 truncate lacking the PB1 domain (ΔPB1), which retains the ubiquitin binding and ATG8 interacting motifs, showed similar perihaustorial accumulation (96%, N=25, Figure 3.1D), the other truncate form of Joka2 without both PB1 and ZZ domains (ΔPZ) revealed distribution similar to the BFP vector control and failed to accumulate at the pathogen interface (1%, N=72) (Figure 3.1E-F). These findings suggest that the Joka2-ATG8CL interaction is not sufficient for recruitment of Joka2 to the puncta found around haustoria and that Joka2's oligomerisation and/or association with other proteins mediated by the PB1 and ZZ domains are critical for its haustorial accumulation.

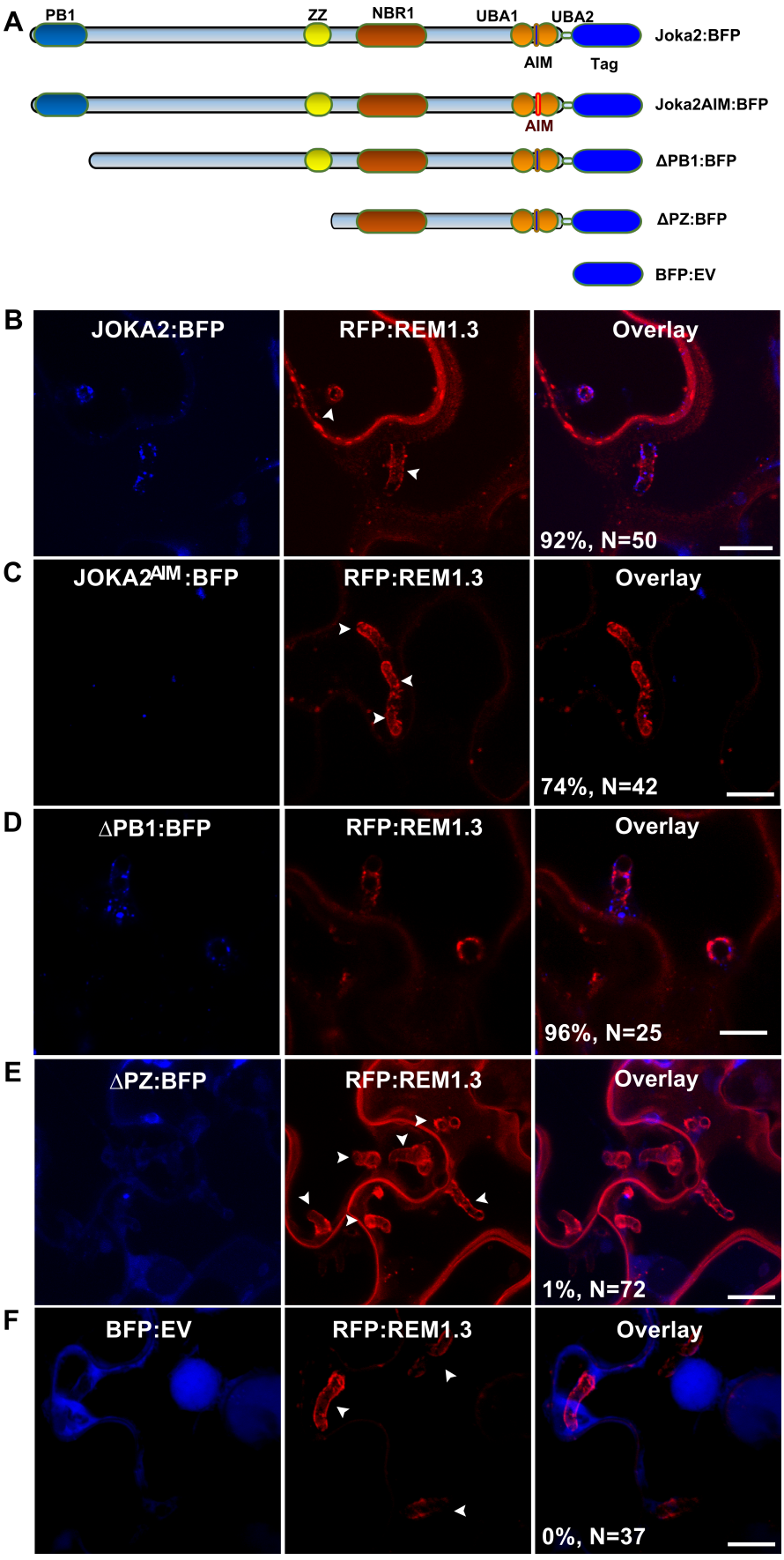

A
PB1
ZZ
NBR1
UBA1
UBA2
AIM
Tag
Joka2:BFP
Joka2AIM:BFP
ΔPB1:BFP
ΔPZ:BFP
BFP:EV
B
JOKA2:BFP
RFP:REM1.3
Overlay
92%, N=50
C
JOKA2AIM:BFP
RFP:REM1.3
Overlay
74%, N=42
D
ΔPB1:BFP
RFP:REM1.3
Overlay
96%, N=25
E
ΔPZ:BFP
RFP:REM1.3
Overlay
1%, N=72
F
BFP:EV
RFP:REM1.3
Overlay
0%, N=37

Figure 3.1. Joka2-mediated autophagy is directed towards the haustoria. (A) Schematic representation of blue fluorescent protein (BFP)-tagged Joka2 and its mutated and truncated versions lacking functional AIM region (Joka2^{AIM}), the PB1 domain(ΔPB1) or PB1-ZZ (ΔPZ) region. (B-F) Confocal microscopy of *P. infestans* infected *N. benthamiana* leaf epidermal cells expressing Joka2:BFP, Joka2^{AIM}:BFP, ΔPB1:BFP, ΔPZ:BFP or BFP:EV control. All Joka2 variants except ΔPZ:BFP displayed perihaustorial puncta although the frequency of finding haustorium with blue puncta was much lower in Joka2^{AIM}:BFP expression. Consistently, ΔPZ:BFP mainly showed cytoplasmic distribution similar to BFP:EV control and rarely marked puncta found around haustoria (1.3% of imaged haustoria) (C). Images shown are maximal projections of frames with 1 µm steps from top to bottom rows, respectively. Arrow heads mark haustoria. Scale bars represent 10 µm. Images were obtained at 3-4 dpi.

Finding that removal of first 487 N terminal amino acids (ΔPZ) aborts Joka2 diversion towards the infection sites led me to investigate the role of individual domains of Joka2 on localisation to the haustoria (Figure 3.1). As ΔPB1 did not hinder the perihaustorial accumulation of Joka2 (Figure 3.1D), to test whether the ZZ or the interdomain between PB1 and ZZ is responsible for the perihaustorial localisation phenotype of Joka2, I designed a Joka2 mutant with a deleted ZZ domain (ΔZZ) C-terminally conjugated to GFP (Figure 3.2A). Because the function of Joka2's NBR1 domain is not clear yet, a construct lacking the NBR1 domain was also generated for this purpose (Figure 3.2A) and for the future experiments which are discussed in the next chapter. ΔZZ and ΔNBR1 were transiently overexpressed as well as full length Joka2 and EV control. Infected pavement cells of *N. benthamiana* leaves were visualised by fluorescence confocal microscopy as described previously (Figure 3.2B-E) I included in the experiments the wildtype Joka2 fused with GFP as a positive control showing perihaustorial localisation. Empty vector (EV) consisting of only GFP protein was utilised as a negative control (Figure 3.2E). RFP:REM1.3 was co-infiltrated to mark both the plasma and extra-haustorial membranes. Similar to the previous figure, wildtype Joka2:GFP localisation was quite high in cells showing GFP signal and infected by *P. infestans* (97.0%, N=66) (Figure 3.2B). Similarly, removal of the ZZ domain did not disturb the localization of truncated Joka2 protein and ΔZZ:GFP showed high perihaustorial localisation- i.e., 93.3% (N=45). This finding indicates that the ZZ domain of Joka2 is not required for localisation (Figure 3.2C) to the infection site. Truncation of NBR1 lowered the frequency of GFP labelled puncta

around the haustoria (78.4%, N=144) (Figure 3.2D). However, this truncated version of Joka2 did not abort localisation altogether, instead, puncta formation was completely absent in some epithelial cells and that made the frequency much lower. This observation together with the findings which will be discussed in the next chapters made me hypothesised that NBR1 is not for localisation but mostly regulation of Joka2 function. Therefore, I narrowed down the region responsible for Joka2 localisation to the infection site in between PB1 and ZZ domains (Figure 3.2A). Unlike ΔPZ, both of the truncated versions of Joka2, ΔZZ and ΔNBR1, formed distinct puncta *in planta* (Figure 3.2C-D). I have utilised disorder prediction tool (Figure 3.3) in order to find an ordered structure between PB1 and ZZ domain (Ishida, T. *et al.*, 2007). In summary, truncation of individual domains of neither ZZ nor NBR1 completely disrupted EHM localisation of Joka2.

Figure 3.2. The ZZ and NBR1 domains are not essential for perihaustorial localization of Joka2. (A) Domain architecture of Joka2 and its truncated versions used in confocal microscopy experiments. ΔZZ and ΔNBR1 are truncated Joka2 proteins lacking ZZ and domains, respectively. Dotted red rectangle shows the hypothesized region responsible for Joka2 accumulation at perihaustorial region. (B-F) GFP-tagged Joka2, ΔZZ and ΔNBR1 are co-expressed with RFP:REM1.3, together with GFP empty vector control in infected *N. benthamiana* leaves. Whilst taking confocal images, multiple optical planes were obtained to cover visualized haustoria and puncta around them. White arrowheads point haustoria associated with puncta with GFP signal while yellow arrowheads label haustoria without them. Scale bars represent 10 μm.

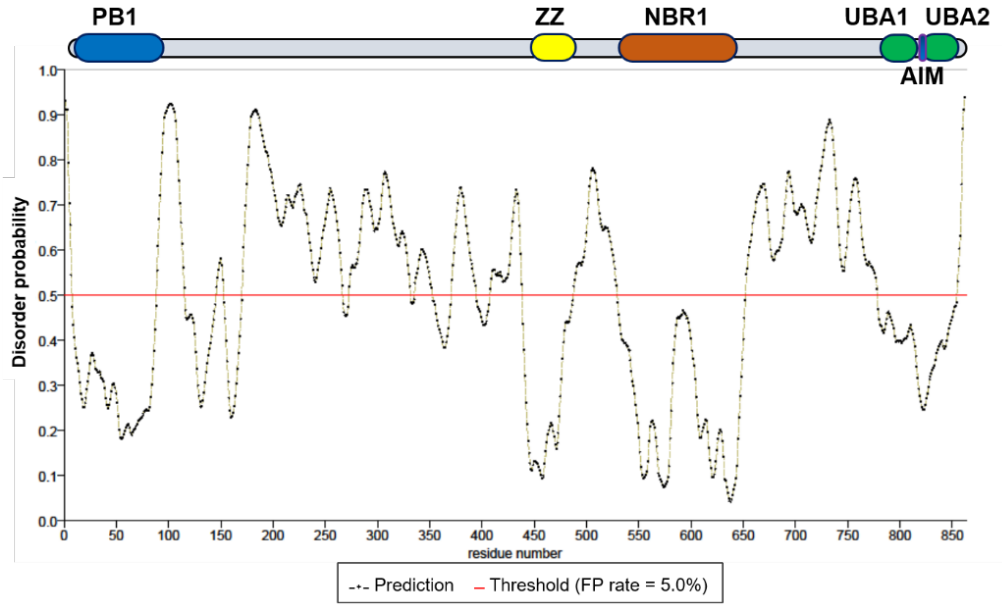


Figure 3.3. Ordered structure probability of Joka2. Online protein structure prediction tools reveal that only known domains of Joka2 are structured except one region just after PB1 domain.

3.3.1.3 Perihaustorial Joka2-autophagosomes contribute to plant focal immunity

Consistent with the positive role of Joka2 in immunity, knocking down *Joka2* renders plants more susceptible to *P. infestans* infection (Dagdas, Y. F. *et al.*, 2016). The observation that the truncated Joka2 construct ΔPZ fails to accumulate around haustoria, prompted me to investigate its role in plant immunity.

To test if focal accumulation of Joka2 is important for its antimicrobial function, Joka2:3xHA and ΔPZ:3xHA overexpressing leaves were infected with *P. infestans*. In contrast to leaf patches expressing the full length Joka2, which can accumulate at the perihaustorial autophagosomes (Figure 3.1B and Figure 3.2B), leaves expressing ΔPZ conferred only mild resistance (Figure 3.4A-B). Considering together with the cell biological analyses of Joka2 in haustoriated cells, infection assays suggest that diversion of plant antimicrobial autophagy towards the pathogen interface is required to limit *P. infestans* infection. Thus, the pathogen needs to subvert the biogenesis of antimicrobial Joka2/ATG8CLcompartments and/or neutralize their defence related function at the EHM via using the effector PexRD54.

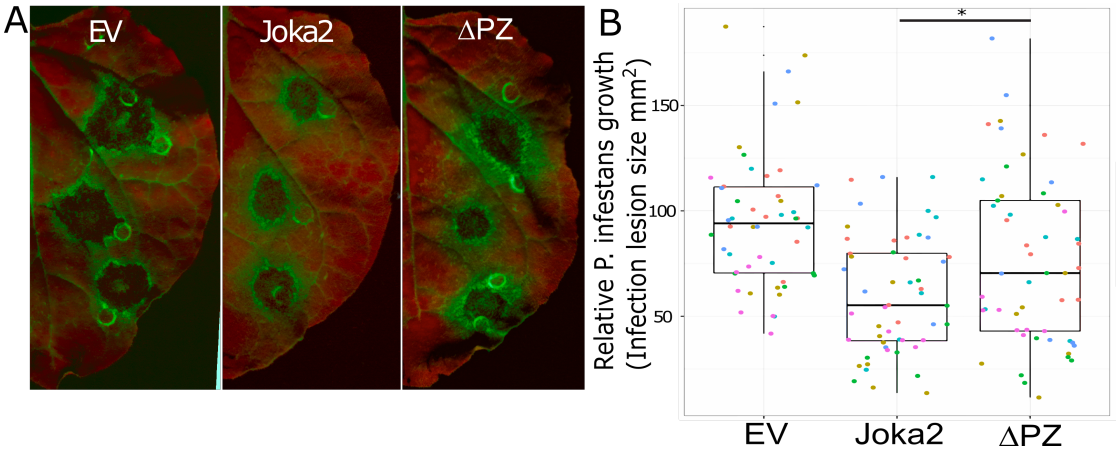


Figure 3.4. Joka2 lacking PB1-ZZ domains affect *P. infestans* growth. (A-B) Overexpression of full length Joka2 increases plant immunity against *P. infestans*, however, ΔPZ truncate, which does not localise to haustoria, only provides partial resistance. (B) *N. benthamiana* leaves expressing Joka2, ΔPZ and empty vector (EV) control were infected with *P. infestans*. Spread of necrotrophic pathogen growth was determined by measuring infection lesion size 8-9 days after infection. (C) Categorical scatter plots demonstrate the data obtained from infection assays. In each assay 8-10 leaves were infected, and six independent biological replicates were carried out (each colour represents a biological repeat). Welch's unequal variances t-test revealed a significant difference (P=0.013) in immunity provided by Joka2 compared to ΔPZ.

In order to confirm that perihaustorial puncta labelled by Joka2:BFP represent the presumed autophagosomes, I investigated the degree of co-localisation of Joka2:BFP, Joka2^{AIM}:BFP or BFP:EV with the autophagosome marker GFP:ATG8CL was investigated in infected plant cells. Haustoria were identified with the marker RFP:REM1.3. Joka2:BFP-labelled vesicles were fully marked with GFP:ATG8CL (100%, N=140) (Figure 3.5A). In contrast, the negative control, EV:BFP (Figure 3.5C), does not colocalise with GFP:ATG8CL (0%, N=20). This validates that perihaustorial puncta labelled by Joka2 are indeed ATG8CL-autophagosomes.

Intriguingly, Joka2:BFP also labelled vesicles that are not marked by GFP:ATG8CL, which indicates that Joka2 can localise to other compartments (Figure 3.5A) such as different ATG8 autophagosomes. Consistent with this observation, Joka2^{AIM}:BFP, which lacks the binding ability to ATG8CL, localised to puncta that were minimally overlapped with ATG8CL-autophagosomes around the haustoria (19%, N=37) (Figure 3.5B). Like

mammalian autophagy cargo receptors, Joka2 forms oligomers (Zientara-Rytter, Katarzyna *et al.*, 2014), therefore, this most likely accounts for the recruitment of Joka2^{AIM}:BFP to ATG8CL-autophagosomes.

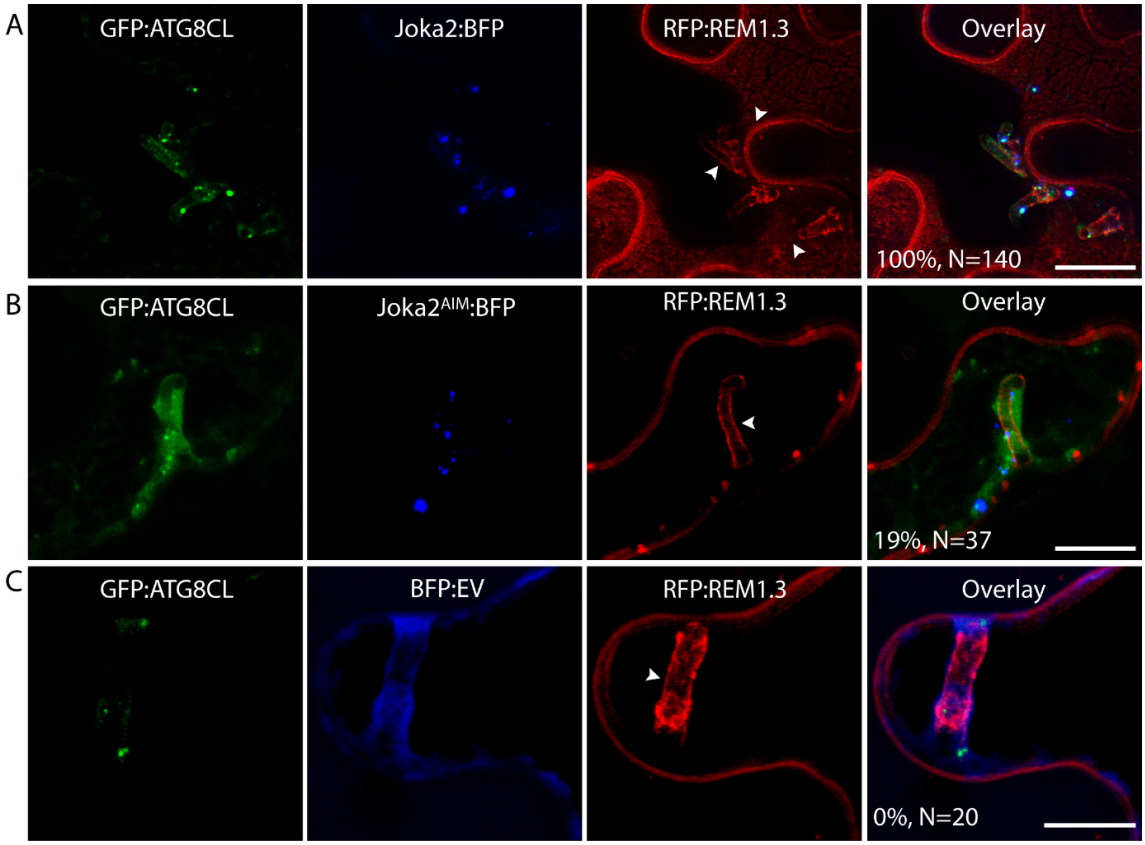


Figure 3.5. Joka2 localizes to ATG8c-autophagosomes found at perihaustorial region via its AIM domain. (A) Autophagosomes containing GFP:ATG8CL fully overlapped with the Joka2:BFP labelled puncta (100%) around haustoria. On the other hand, Joka2 mutant that cannot bind ATG8CL, Joka2^{AIM}:BFP, generally did not colocalise with autophagosomes showing GFP:ATG8c signal (19%) at infection site (B) similar to BFP:EV control (C). Images shown are maximal projections of 11, 10 and 8, frames with 1µm intervals from top to bottom rows, respectively. Arrowheads point to *P. infestans* haustoria. Scale bars represent 10 µm. Images are obtained at 3 dpi.

These results indicate that Joka2 localises to at least two distinct perihaustorial puncta; ATG8c-autophagosomes that requires a functional Joka2-AIM, and an unknown compartment in which the ATG8-binding is unnecessary. These results therefore demonstrate that Joka2 mediated antimicrobial autophagy is diverted to the pathogen interface (Chen, J. S. *et al.*, 2017).

3.3.1.4 ATG8CL and Joka2 protein levels are stabilised upon detection of pathogen

Based on the finding that Joka2-autophagosomes are diverted towards haustoria, I hypothesized that vacuolar degradation of Joka2 should be reduced. *Dagdas et al.* has already shown that degradation of ATG8CL slowed down upon *P. infestans* infection (2018). Supporting these findings, I have also shown that mRNA levels of Joka2 are upregulated after pathogen attack by using semiquantitative RT-PCR (Figure 7.3).

To test protein stability upon infection, Joka2 protein stability was measured in healthy and infected leaf tissues (Figure 3.6). Both ATG8CL and Joka2 protein levels were found to be higher in infected leaves compared to mock infected leaves (Figure 3.6). Similarly, when I infiltrated an extract from *P. infestans* which is composed of various PAMPs, even after 8 hours, ATG8CL and Joka2 levels were stabilised (Figure 3.6B). Since these protein levels were not affected by transcriptional regulation (due to constant expression by a viral promoter), the protein levels must be altered by posttranslational protein stability or degradation processes. These results may suggest that autophagy components diverted to host-pathogen interface are stabilised as ATG8CL/Joka2 mediated antimicrobial autophagy is activated and regular degradatory autophagy is slowed down.

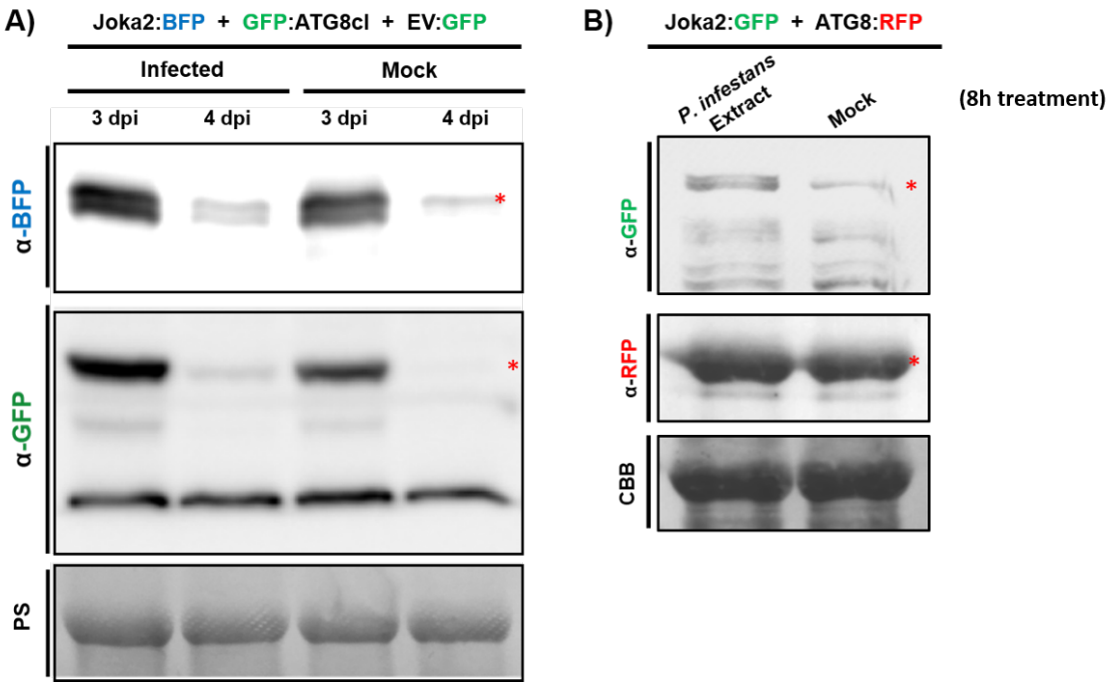


Figure 3.6. Joka2 and ATG8CL degradation slows down during *P. infestans* infection or after PAMP treatment. Transiently expressed Joka2:BFP and GFP:ATG8c protein levels were higher in leaf patches that were infected compared to mock-infected leaves at both 3 and 4 days post infection (dpi) (A). However, no such difference was detected in GFP:EV control in infected versus mock-infected samples. Similarly, both GFP and RFP signals were higher in leaf tissue that was infiltrated with *P. infestans* extract 8 hours prior to tissue collection. BFP detection was done by using α-BFP antibody and GFP was detected by using a monoclonal α-GFP antibody. Joka2:BFP/GFP (120 kDa) and RFP/GFP:ATG8CL (42 kDa) bands are marked with red asterisks. Lover bands in GFP detection panel are EV:GFP (27kDa). Protein loading was determined by staining the larger subunit of RuBisCO with PS.

3.3.2 Accumulation of perihaustorial ATG8CL-autophagosomes is dependent on the core autophagy machinery

Previous sections clarified the localisation of ATG8C autophagosomes and Joka2 puncta. To determine the role of autophagic machinery in this perihaustorial localisation, RNA interference (RNAi) was employed to knockdown gene expression of the core ATG components, ATG4 or ATG9 (Lamb, C. A. *et al.*, 2013). ATG4 and ATG9 are two core autophagy proteins and are described in more detail in Chapter 1. Haustorium association with GFP:ATG8CL puncta was determined upon silencing of *ATG4* or *ATG9*, both of which mediate biogenesis and maturation of autophagosomes. A significant

reduction in the frequency of perihaustorial ATG8CL-autophagosomes was observed when ATG4 (31.6%, N=205) or ATG9 (39.3%, N=286) were silenced compared to the negative control (GUS gene silencing, 63%, N=175) (Figure 7.2). Keeping in mind the fact that ATG4 and ATG9 homologs are not completely silenced (Dagdas, Y. F. *et al.*, 2018), these results indicate that the core autophagy proteins, hence the machinery, is required for accumulation of ATG8CL-labelled autophagosomes around *P. infestans* haustoria.

3.3.3 Haustoria are hotspots for autophagosome biogenesis

After validating that Joka2-labelled perihaustorial compartments are autophagosomes by co-expressing Joka2 with ATG8CL, I decided to use another established autophagosome marker, ATG9, for co-localisation with Joka2. ATG9 is the only known multi-spanning trans-membrane protein among the other ATG proteins and resides in unilamellar small vesicles (diameter of 30-60 nm) with unknown origin (Yamamoto, H. *et al.*, 2012; Zhuang, X. *et al.*, 2017). ATG9 also transiently associates with autophagosomes and is swiftly recruited back to ATG9 vesicles when the autophagosomes fuse to other cellular compartments (lysosomes, vacuoles etc.) (Yamamoto, H. *et al.*, 2012). As such ATG9 is used as a early biogenesis marker of autophagosomes. First, I produced a c-terminal GFP fusion of *N. benthamiana* ATG9 (ATG9:GFP) to test colocalisation of ATG9 with Joka2 in uninfected cells. When co-expressed in uninfected cells, Joka2:BFP puncta fully overlapped with ATG9:GFP vesicles (Figure 3.7A). GFP-tagged ATG9 containing vesicles can be found in the cell with small diameters, distributed throughout the cytoplasm (Figure 3.7B). GFP and BFP empty vector controls did not show any fluorescence signal at ATG9:GFP or Joka2:BFP puncta (Figure 3.7C). These results demonstrate that punctate fluorescence produced by Joka2:BFP originate from autophagosomes but not autolysosomes.

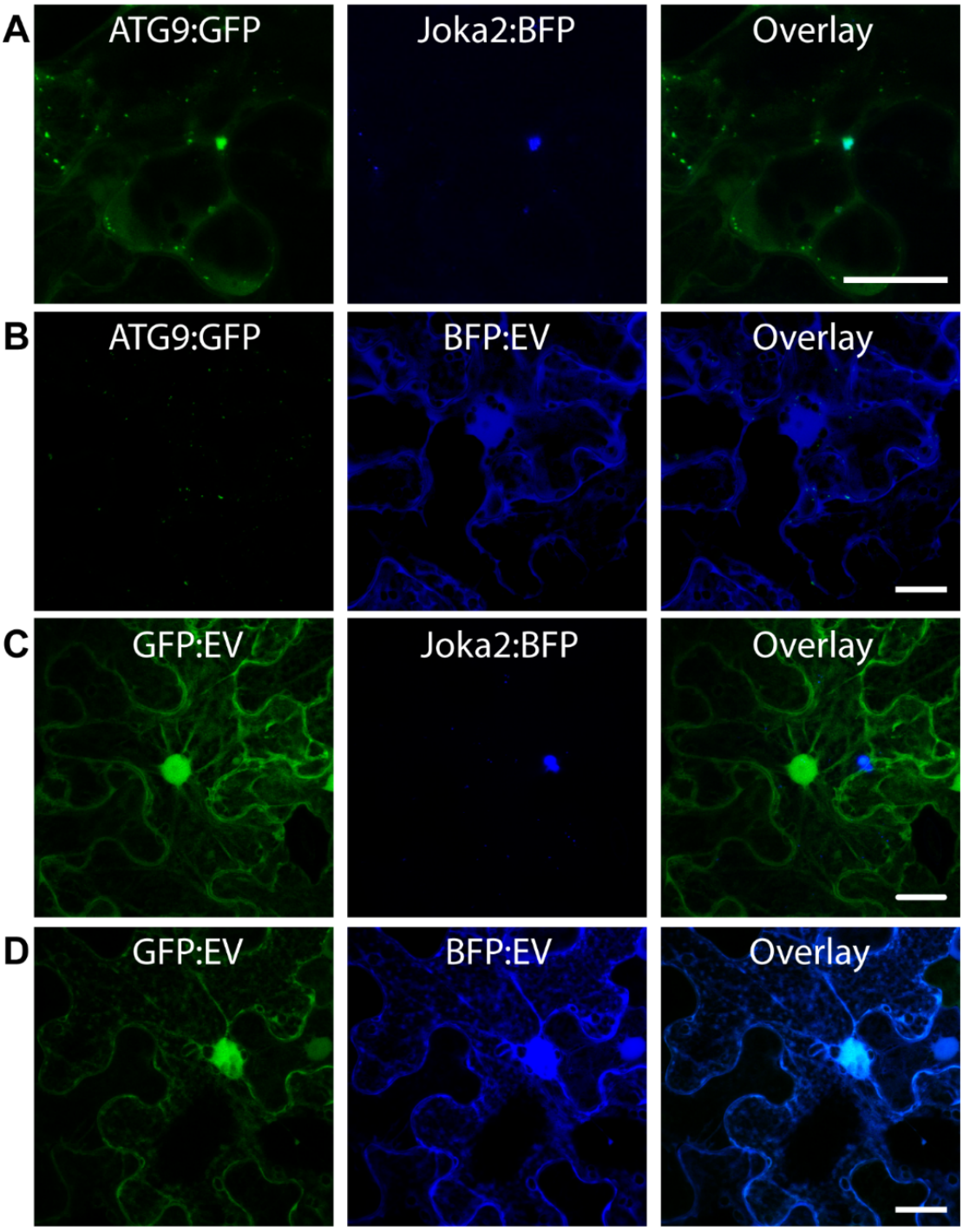


Figure 3.7. ATG9 colocalises with Joka2-autophagosomes/aggregates. Images of confocal microscopy of *N. benthamiana* leaf epidermal cells expressing ATG9:GFP, Joka2:BFP, EV:GFP or EV:BFP control. ATG9:GFP was found in numerous small sized puncta (A-B) and colocalised with Joka2:BFP autophagosomes and larger non-mobile aggregates (A) but not with EV:BFP control (B). EV:GFP control co-expressed with Joka2:BFP or EV:BFP, did not produce any punctate signal and did not label Joka2-autophagosomes. (C-D). Images were obtained at 3 dpi and scale bars represent 25 μm.

The confirmation that most of the Joka2-labbeled puncta are indeed autophagy-related, led us to further investigate the behaviour of puncta in infected cells. A recent study has shown that a plant ATG9 homolog in *Arabidopsis*, localises to the biogenesis sites of autophagosomes, moreover, mobile ATG9-positive vesicles remain adjacent to mature autophagosomes (Zhuang, X. *et al.*, 2017). Therefore, I decided to use fluorescently-tagged ATG9 as a marker for phagophore assembly sites (PAS) and monitored its localisation during *P. infestans* infection. Transient expression of ATG9:GFP in infected cells revealed that regardless whether there is ATG8c or Joka2 coexpression, ATG9 is present at the host-pathogen interface (>92%, Figure 3.8). BFP-tagged ATG8c and Joka2 puncta labelling perihaustorial autophagosomes, were partially overlapping with numerous ATG9 vesicles (Figure 3.8A-B). This finding suggests that in addition to accommodating mature ATG8CL autophagosomes, perihaustorial regions might be hotspots for autophagosome biogenesis. We also realised a considerable increase in the frequency of haustoria that associate with BFP:ATG8CL puncta when coexpressed with ATG9:GFP (Figure 7.4).

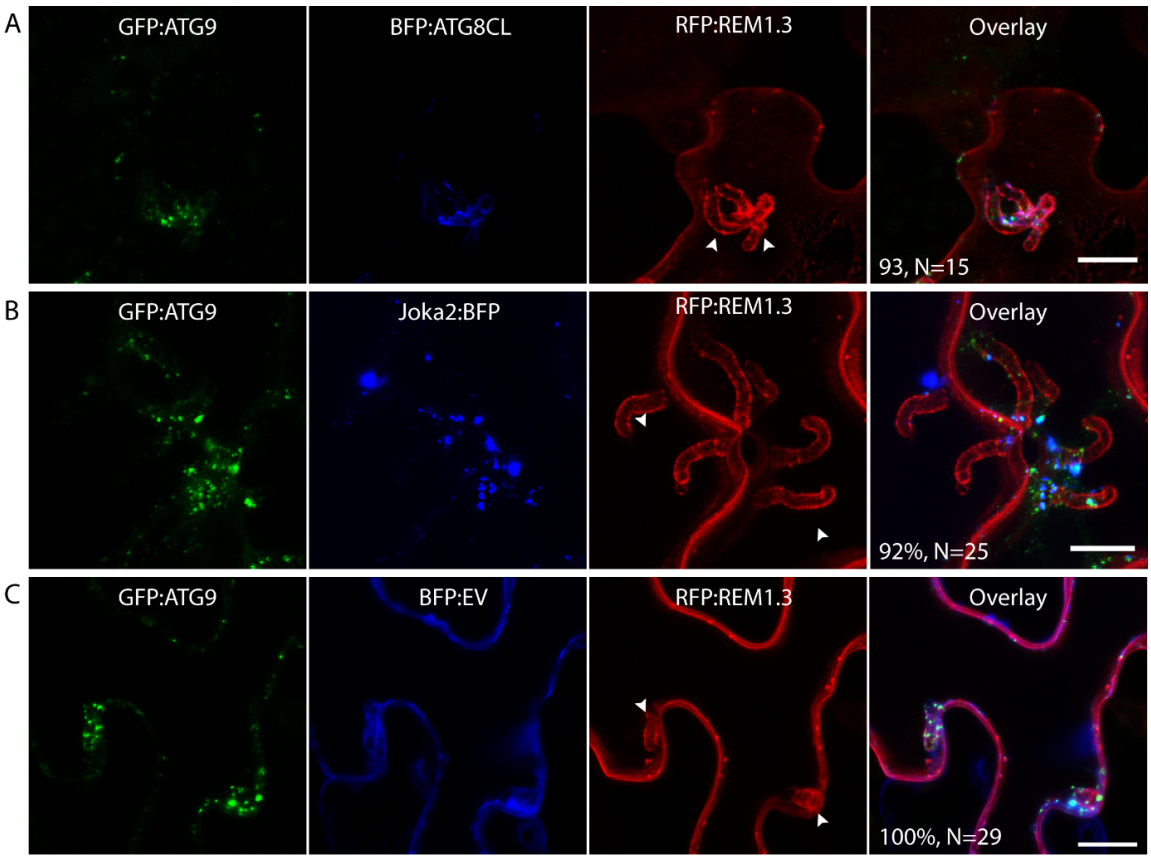


Figure 3.8. ATG9-labelled vesicles/autophagosomes accumulate around haustoria and Joka2 puncta colocalises with them. GFP:ATG9 was coexpressed with RFP:REM1.3 with BFP:ATG8CL, Joka2:BFP or BFP empty vector control. (A-C) Interestingly, ATG9:GFP labelled puncta were frequently observed around the haustoria (>%92). ATG9 puncta highly colocalised with the autophagosomes marked by BFP:ATG8c around haustoria (A). Joka2:BFP puncta overlapped significantly with ATG9:GFP labelled puncta (B). There was no BFP puncta in (C) therefore no overlap was observed between ATG9:GFP puncta and EV:BFP control. Images shown are maximal projections of frames with 1µm steps from top to bottom panels. Arrowheads label haustoria. Scale bars represents 10 µm. Images are taken at 3 days post infection.

Localisation of ATG9 vesicles at the perihaustorial region and its enhancing effect on the ATG8CL accumulation around haustoria led me to test its role in plant immunity. To do that, ATG9:GFP and GFP:EV were transiently expressed in the same leaves but at opposite sides, and the lesion size caused by *P. infestans* was measured 8 days post-inoculation (Figure 3.9). ATG9:GFP overexpression significantly decreased the spread of necrotrophic infection compared to GFP (p=0.0035, N=6). Overall, these results suggest that focally accumulating autophagy machinery operates against *P. infestans* to enhance plant immunity.

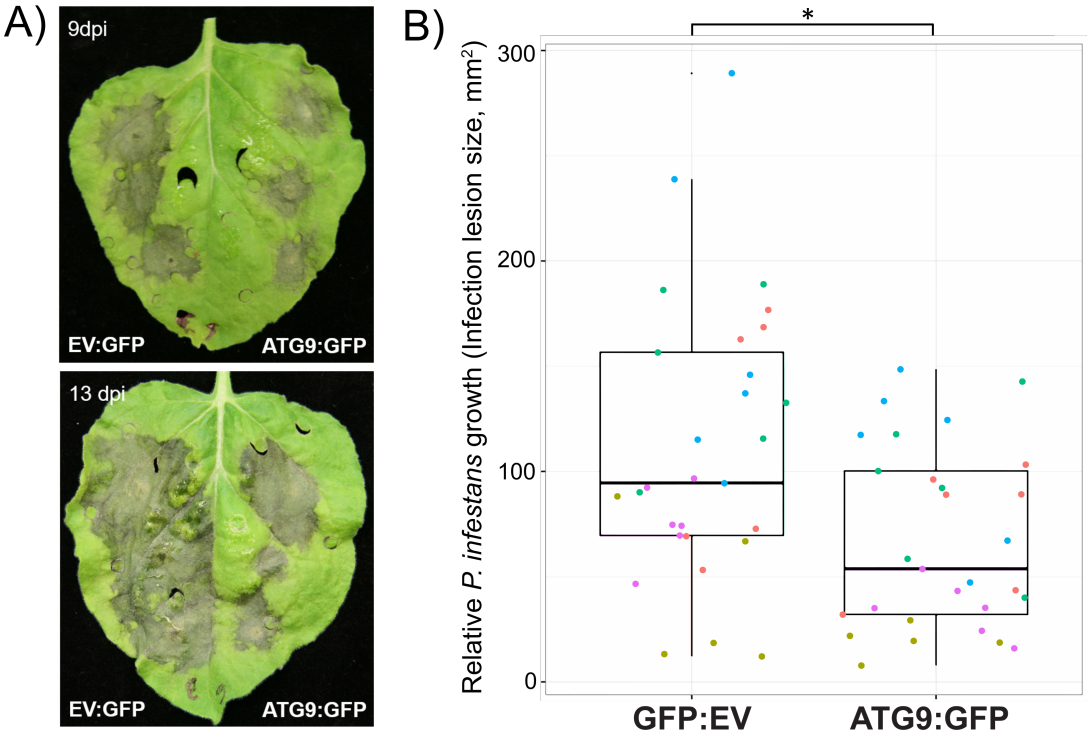


Figure 3.9. ATG9 contributes to plant immunity against *P. infestans*. (A) ATG9:GFP or GFP empty vector control were overexpressed on opposite sides of leaves which were infected with *P. infestans*. Necrotic infection area was measured to determine pathogen growth at 8-9 days post infection (B). Scatter plot graph shows 6 independent biological replicates (different colours) of infections. ATG9 overexpression significantly reduces (p<0.01) the necrotic lesion caused by the pathogen spread compared to the GFP control expression.

3.4 DISCUSSION

Induction of defence-related autophagy by plant autophagy cargo receptor Joka2 and subversion of this process by its antagonist, *P. infestans* effector PexRD54, prompted us to further investigate the role of autophagy in plant-microbe interactions. As with some other filamentous plant pathogens, *P. infestans* intimately interacts with the host cells by forming haustoria, which can be tracked to identify infected cells. In order to investigate the subcellular dynamics of antimicrobial autophagy, I utilised high-resolution microscopy to monitor and track Joka2-autophagosomes during *P. infestans* infection. Most of the work in this chapter was published as a part of Dagdas *et al.*, (2018).

Studying the autophagy machinery in plant resistance revealed that the core autophagy protein ATG8CL, the autophagy cargo receptor Joka2 and ATG9-vesicles accumulate at perihaustorial regions. In the study we published the results of this chapter, nature of subcellular localisation of effector PexRD54 was also investigated as well as Joka2 and core autophagy proteins ATG8 and ATG9 (Dagdas, Y. F. *et al.*, 2018). This investigation revealed that the pathogen effecter PexRD54 also accumulates and colocalises with ATG8 around haustoria. Overall, the findings suggest that the previously demonstrated antagonistic interactions of Joka2 and PexRD54 occur across the EHM, where PexRD54 outcompetes Joka2 and depletes it from ATG8CL autophagosomes to prevent antimicrobial autophagy. A similar mechanism has been reported in 2018 by Real *et al.*, where the group showed that plasmodium secretes an effector protein, UIS3, in infected hepatocytes. This effector sequesters the host ATG8 homolog in mammals, LC3, to prevent interactions of this ATG protein with its cargo receptors, so that the pathogen avoids elimination by autophagy (Real, E. *et al.*, 2018). Studies like these highlight the importance of conserved autophagy machinery against the invading pathogens in different eukaryotic systems.

Detailed confocal imaging with fluorescently labelled Joka2 and its truncated versions revealed that Joka2-autophagosomes are diverted to the pathogen interface with a high frequency. This finding indicates that not all Joka2-autophagosomes are transported to the central vacuole for degradation during pathogen attack (Figure 3.1 and Figure 3.2).

The Joka2^{AIM} mutant, which cannot bind ATG8CL, also showed perihaustorial distribution but mainly lost its ability to localize to ATG8CL autophagosomes (Figure 3.1C). Moreover, ΔPZ, fully lost its perihaustorial accumulation as well as abundant puncta formation (Figure 3.1E). Only ΔPB1 retained wild type Joka2 function in terms of haustorial accumulation (Figure 3.1D). This suggests that AIM motif is not crucial but can enhance directing Joka2 to pathogen site; and the region responsible for Joka2's trafficking to EHM must be between PB1-ZZ domains.

Joka2 is a modular protein with multiple domains including an N-terminal Phox and Bem1 (PB1) domain, central zinc finger (ZZ) and NBR1 domains followed by two C-terminal ubiquitin-associated domains (UBA) that flank an AIM (Zientara-Rytter, K. *et al.*, 2014). The PB1 and ZZ domains are implicated in self-oligomerisation and protein-protein interactions, whereas the UBA domains and the AIM act to bridge Joka2 to the autophagic machinery and the ubiquitinated cargo (Figure 3.1A). Recent findings suggest that the PB1 domain is crucial for the oligomerisation of NBR1 and p62 in mammals (Joka2 orthologs), a process which is required for its full function (Bjorkoy, G. *et al.*, 2006). The ZZ domain of p62 was also found to interact with non-linear ubiquitin chains (Zaffagnini, G. *et al.*, 2018). Insufficient oligomerisation as well as being deprived of binding to other unknown but critical proteins may explain the loss of perihaustorial localisation when both are truncated, and account for the decreased impact on plant immunity (Figure 3.4). However, individual removal of neither PB1 or ZZ domains hinders perihaustorial accumulation of Joka2, which suggests that there might be an undefined signal or domain in between PB1 and ZZ that diverts Joka2 puncta to the host-pathogen interface.

The autophagosomal identity of perihaustorial Joka2-compartments was validated by colocalisation assays using ATG8CL. As expected, wild type Joka2 revealed full colocalisation pattern with ATG8CL, unlike Joka2 with non-functional AIM. However, I still observed accumulation of Joka2^{AIM} puncta to a limited extent around haustoria which might be due to its ability to oligomerise with the endogenous Joka2 or be due to localization to a non-autophagic compartment. Plant cells appear to redirect Joka2

mediated autophagy towards the plant-pathogen interface instead of to the central vacuole, resulting in slower degradation of Joka2 (Figure 3.6).

Diversion of the autophagy machinery, particularly ATG9 vesicles, towards the cellular infection site suggests that the EHM serves as a cradle for autophagosome biogenesis and is critical for defence-related autophagic responses. Interestingly, ATG9 labelled smaller sized perihaustorial vesicle-like structures that are not marked by Joka2 were also abundant around haustoria. This might suggest that ATG9-labbeled vesicles can be a membrane source for the EHM, or a site for autophagosome production. Both in plants and animals, ATG9 marks an unknown type of vesicles, which are believed to supply the membrane source for autophagosome formation (Yamamoto, H. *et al.*, 2012). Hence, the increase in perihaustorial ATG9 vesicles could be due to the need for supplying more membranes for enhanced biogenesis of perihaustorial autophagosomes stimulated by Joka2 or a battlefield where plant and pathogen fight for control over autophagy related processes. Biogenesis of autophagosomes, whose membrane source is supported by ATG9, close to the pathogen entry site would eliminate the unnecessary energy spent to transport defence-related vesicles towards the infection site. In literature, similar studies showing defence-related autophagy against *Salmonella typhimurium* in mammalian cells can be encountered (Randow, F. *et al.*, 2013). It is possible that ATG9 vesicles can directly or indirectly supply the membranes for the EHM biogenesis via formation of autophagosomes that fuse with the EHM. However, further work is required to determine whether perihaustorial Joka2-autophagosomes fuse with the EHM and/or are secreted to the pathogen interface. Moreover, to investigate if ATG9 mediated increased plant immunity is dependent on other elements of autophagy, similar infection assay experiment can be conducted in the background of ATG8CL/Joka2 silencing. Overall, the emerging view is that the extrahaustorial membrane might be formed by steering different endomembrane trafficking pathways including autophagy to the host-pathogen interface.

CHAPTER 4 – VALIDATION OF JOKA2 INTERACTORS

4.1 INTRODUCTION

Perihaustorial accumulation of autophagy machinery, including the cargo receptor Joka2 and ATG8CL, as well as effector protein PexRD54, led me to reconsider the role of these proteins, especially Joka2, in immunity against pathogen infection. For example, which cargoes does Joka2 deploy around haustoria and how is this regulated? Could Joka2 deploy protein complexes or antimicrobial compounds to pathogen interface to fight against the filamentous pathogens? To address these questions, we decided to take advantage of a Joka2 proteomics screen, which revealed candidate Joka2 interactors in infected and uninfected plant tissue (Table 4.1)(Bozkurt *et al.*, unpublished). Thus, I have primarily selected to focus on candidate Joka2-interactors (listed below) based on their potential roles in plant immunity and their increased abundance in Joka2 protein complexes in infected versus uninfected plant samples. These include:

i) Mitogen-activated protein kinases 3, 6 and 9 like proteins (MAPK3, MAPK6 and MAPK9)
ii) Pyridoxal biosynthesis protein like (PDX)
iii) Phenylalanine ammonia-lyase like (PAL)

(In order to keep abbreviations short, the proteins in *N. benthamiana* will be called throughout the text as written above in parenthesis)

4.1.1 Mitogen-activated protein kinases in plant immunity

Mitogen-activated protein kinases (MAPKs, or MPKs) are serine-threonine kinase proteins which phosphorylate downstream elements after being activated by upstream kinases to mediate transduction of an environmental or developmental stimuli into intracellular response (Colcombet, J. *et al.*, 2008; Rodriguez, M. C. *et al.*, 2010).

MAPK signalling pathway is very essential for survival and adaptation of plants regarding plant-microbe interaction, because this signalling cascade is one of the earliest event when the cell senses an invading pathogen. MAPKs in plants have more similarity to

mammalian extracellular signal-regulated kinase (ERK) subfamily of MAPKs (Meng, X. *et al.*, 2013). *Arabidopsis* genome has about 90 genes encoding enzymes in MAPK pathway, which is comprised of 60 MAPK kinase kinases (MAPKKK, MAP3K or MEKK), 10 MAPK kinases (MAPKK, MAP2K, MKK or MEK), and 20 MAPKs (Meng, X. *et al.*, 2013; Pitzschke, A. *et al.*, 2009).

PTI involves MAP kinase signalling so that plants can alter gene-expression patterns/levels and enzymatic activities to hinder pathogen infection, e.g. by synthesizing anti-microbial reagents, ROS, or phytoalexins (low molecular mass secondary metabolites with antimicrobial activity), reprogramming transcriptional patterns or initiating HR via activation of R genes. Compared to the effector recognition studies, the downstream signalling events after NLR activation is still not well understood. Therefore, focusing on the underlying MAPK pathway and its relevance to autophagic components will broaden our understanding. Furthermore, although it is not so clear how *Agrobacterium tumefaciens* hijacks host resistance even though it intriguingly triggers activation of several defence-related MAPKs like MPK3, MPK4, and MPK6, in order to translocate its transfer DNA into host nucleus by VIP1 (substrate of MPK3) (Djamei, A. *et al.*, 2007; Pitzschke, A. *et al.*, 2009).

MAP3K are serine-threonine kinases capable of phosphorylating the S/T-X_{3-5}-S/T motives in activation loop of MAP2Ks, which activates MAPKs through phosphorylation of both threonine and tyrosine residues of the T-X-Y motif in MAP kinases' activation loop. MAPKs are serine-threonine kinases phosphorylating a broad range of substrates such as other kinases and/or transcription factors (Colcombet, J. *et al.*, 2008). MAPK cascade is regulated through other scaffolding proteins that are required for phosphorylation event of subsequent kinases or via MAPK phosphatases (MAKPs) (Colcombet, J. *et al.*, 2008). These enzymes required for phosphorylation events are quite conserved within higher plants, which are sub-divided to 4 groups (A-D) based on their sequence similarities, and they act mechanistically similar to their homologues in animals and yeast (Ichimura, K. *et al.*, 2002).

In a very short time after detecting PAMP or effectors, plants can alter gene-expression patterns/levels and enzymatic activities in order to hinder pathogen infection, e.g. by

synthesizing anti-microbial reagents, ROS, or phytoalexins (low molecular mass secondary metabolites with antimicrobial activity) or initiating HR via activation of R genes. The initiator of this event might be flagellin, harpin, lipopolysaccharides, chitin, ergosterol, or effector proteins (Rodriguez, M. C. *et al.*, 2010).

MAPK3 and MAPK6 are Group A (TEY) type MAPKs, over 80% sequence similarity makes them redundant for some of the cellular processes. For example, both MAPKs are phosphorylated by MKK4 and MKK5, orthologs of MEK2 in tobacco, to activate or deactivate cellular responses, such as phosphorylating WRKY transcription factors (Rodriguez, M. C. *et al.*, 2010). MKK4 and MKK5 are phosphorylated by the upstream MAPKKK3/5. Stimulation through this signalling cascade results is various immune responses in the plants such as stomatal immunity, indole glucosinolate biosynthesis, camalexin biosynthesis and ethylene biosynthesis (Devendrakumar, K. T. *et al.*, 2018). Due to the importance in plant immunity, the MKK4/5-MAPK3/6 signalling pathway, is targeted by some of the pathogens such as *Pseudomonas*. It has been reported that HopF2 inhibits flg22-induced MAP kinase activation by targeting MKKs. Likewise, HopAI1, directly de-phosphorylases MAPK3/6, inactivating PAMP-triggered gene expression (Zhang, J. *et al.*, 2007).

MAPK9 has been showed in recent studies that, together with MAPK12, they are playing role in ROS-mediated ABA (abscisic acid) signalling in guard cells (Jammes, F. *et al.*, 2009). When the genes of those MAPKs are silenced together, plants become unresponsive to ABA and/or H_2O_2, and ABA-mediated stomatal closure is impaired resulting in excess water loss in plants. That bring the authors to the conclusion, with other findings from further studies, that MAPK9 and MAPK12 as a downstream element of ROS and Ca^{2+}, and upstream of anion channels regulate ROS-mediated ABA and methyl jasmonate (MeJA) signalling cascades in guard cells (Jammes, F. *et al.*, 2011; Khokon, M. A. *et al.*, 2015). As stomatal opening/closing mechanism is one of the first line of host defence against pathogens, this finding led the authors to carry out experiments regarding pathogen susceptibility and they found increased infection after silencing of MAPK9 and MAPK12 (Jammes, F. *et al.*, 2011).

4.1.2 Phenylalanine ammonia-lyase and its role in plant defence

Phenylalanine ammonia-lyase (PAL) is an enzyme catalysing formation of ammonium ion and cinnamic acid from phenylalanine by non-oxidative deamination reaction (Hyun, M. W. *et al.*, 2011). It is responsible for the first step of synthesis of phenylpropanoids derivatives which are precursors of products including lignins (and other phenolic esters of cell wall), flavonoids and cumarins (phytoalexins) and stilbenes, and PAL also participates in the production of precursors for salicylic acid synthesis along with isochorismate synthase (Huang, J. *et al.*, 2010; Wanner, L. A. *et al.*, 1995; Wildermuth, M. C. *et al.*, 2001). Therefore, PAL activity resides at the initial step of production of primary metabolites for major secondary metabolic pathways. PAL has been extensively studied because of its importance in normal plant development and environmental stress.

The *ospal4* mutant (heterozygous) line, deficient of one PAL homolog in *Oryza sativa*, becomes prone to different diseases including bacterial blight, rice blight and sheath blight (Tonnessen, B. W. *et al.*, 2015). Similarly, *Arabidopsis* lack of PAL activity and tobacco lines epigenetically suppressed for *PAL* exhibited susceptibility to phytopathogens (Maher, E. A. *et al.*, 1994; Somssich, I. E. *et al.*, 1998). Treatment of *Arabidopsis* with PAL inhibitor, 2-aminoindan-2-phosphonic acid, made plants totally susceptible to downy mildew oomycete *Hyaloperonospora parasitica*, which could be reversed by salicylic acid treatment (Mauch-Mani, B. *et al.*, 1996).

Salicylic acid (SA) is a plant hormone regulating many processes from systemic to cellular level, including seed germination, respiration, and thermogenesis. It has been mostly studied, however, for its involvement in plant defence system upon pathogen attack (Loake, G. *et al.*, 2007). SA signalling is considered to play role in biotrophic pathogen defence while Jasmonic acid (JA) and ethylene (ETH) signalling pathway functions in resistance against necrotrophic pathogens (Loake, G. *et al.*, 2007). SA synthesis initiates with shikimic acid pathway in which the precursor, chorismic acid, is converted to SA, and the synthesis is mediated by two enzymatic pathways; via phenylalanine ammonia-lyase and isochorismate synthase (ICS1) (Mauch-Mani, B. *et al.*, 1996; Wildermuth, M. C. *et al.*, 2001). Although, some analyses showed that the majority of SA is produced by

isochorismate pathway, tobacco plants mutant for all *PAL* genes reduced basal and pathogen induced SA accumulation (Huang, J. *et al.*, 2010). In summary, whether PAL contributes to plant immunity via producing precursors for secondary metabolites or functioning in SA synthesis has not yet been totally resolved.

4.1.3 Vitamin B6 synthesizing enzyme in plant stress tolerance

Vitamin B6 is a collective name of molecules pyridoxine, pyridoxal, pyridoxamine and their phosphorylated derivatives, which are utilized as co-factors in various biochemical reactions in all cells from bacteria to eukaryotes. Their synthesis has been generally studied due to their importance in our daily diet as a phytonutrient. The synthesis of Vitamin B6 requires multimeric complex of pyridoxal biosynthesis 1 (PDX1) and PDX2 proteins. Three homologs of genes for PDX1 (*AtPDX1.1*, *AtPDX1.2* and *AtPDX1.3*) and one for PDX2 (*AtPDX2*) were identified in *Arabidopsis*, which are involved in synthesis pathway of vitamin B6 (Tambasco-Studart, M. *et al.*, 2007). Those enzymes have been implicated in stress tolerance and photo protection by functioning as an antioxidant producer (Havaux, M. *et al.*, 2009; Titiz, O. *et al.*, 2006; Vanderschuren, H. *et al.*, 2013). Due to their function as co-factor for enzymes universal (such as amino acid metabolism) and plant specific pathways (such as starch, ethylene and auxin metabolisms), plants lack of genes for one or two vitamin B6 biosynthesis enzymes, shows aberrant growth and seed production (Vanderschuren, H. *et al.*, 2013). In recent decades, it has been recognised that besides essential role in biochemical reactions, vitamin B6 molecules bear antioxidant activity in the cells even greater potential than of vitamin C and vitamin E (Mooney, S. *et al.*, 2009).

PDX homologs are shown to be involved in stress tolerance and protection against the radiation via production of vitamin B6 which reduces oxidation capacity *Arabidopsis thaliana* (Havaux, M. *et al.*, 2009; Titiz, O. *et al.*, 2006; Vanderschuren, H. *et al.*, 2013). For example, mutant *Arabidopsis* plants for PDX displayed sensitivity to high light and photo-oxidative stress (Havaux, M. *et al.*, 2009), while mutants capable of over-expressing high levels of PDX became more tolerant to high oxidative stress (Titiz, O. *et al.*, 2006; Vanderschuren, H. *et al.*, 2013). These findings in general give an idea that

vitamin B6 derivatives and enzymes responsible for their *de novo* synthesis (or conversion) are functioning as one of the mechanisms against abiotic stress.

Regarding biotic stress, there are two studies on *Arabidopsis* and tomato in which plants were infected by necrotrophic fungus, *Botrytis cinerea* (Zhang, Y. *et al.*, 2015; Zhang, Y. *et al.*, 2014). In these studies, authors mutated the several genes functioning in *de novo* or salvage pathways of vitamin B6 synthesis, and monitored the spread of pathogen infection. Although the studies are lack of sufficient evidence to show the molecular pathway underlying in increase in pathogen resistance, they concluded that vitamin B6 and its biosynthesis pathway is important in regulating immunity against *B*. *cinerea* by altering antioxidant capacity (Zhang, Y. *et al.*, 2014).

4.2 AIM

In the previous chapter, I discussed how Joka2 was recruited to the host-pathogens site and to which extent Joka2-mediated immunity dependent on this trafficking. In this chapter, my goal was to address the questions: what content do Joka2 puncta/autophagosomes hold so that it contributes to boost plant immunity? As I mentioned, I decided several candidate interactors from a proteomics screen of Joka2 pull-downs under normal and infection conditions. I chose the ones which has already been implicated in plant abiotic/biotic stress conditions. Through the thesis I focus on characterizing the effect of candidate interactors on Joka2 immunity, validation of their interaction with Joka2, and the outcome of this interaction in terms of the nature of the association of these protein with Joka2.

4.3 RESULTS

4.3.1 Identification of Joka2 targets

A proteomics screen identifying a list of candidate Joka2-interactors has already been performed under normal and infection conditions (Table 1). This screen was performed by pulling down control, ATG8c or Joka2 proteins. The first elimination of unwanted proteins was done by removing the proteins pulled-down by control flag-tag protein (not shown in the table). Secondly, I moved on ATG8c pull-down results. I selected the proteins predominantly coming together with Joka2 but not ATG8c. Thus, I discarded the proteins which had seemingly more affinity towards ATG8c. I still kept some as the potential interactor might form a protein complex with multiple proteins. Thirdly, and maybe the most importantly, I have included the proteins to be investigated in the list which had showed either higher or lower protein hit during the infection when Joka2 was pulled-down. Differential binding to Joka2 upon infection was a hint for a potential interactor that might be related to plant immunity by. This increased or decreased affinity can lead to selective degradation or differential regulation of a protein by Joka2. Lastly, among the proteins filtered in the first three steps, I have chosen the ones which have already been implicated in biotic or abiotic stress conditions. Therefore, I ended up with five potential interactors of Joka2 (PDX, PAL, MAPK3, MAPK6 and MAPK9) which are worth to validate for their associations with Joka2.

NAME OF THE PROTEIN	Protein hit frequency			
	ATG8c-Mock	ATG8c-Infected	Joka2-Mock	Joka2-Infected
Pyridoxal biosynthesis protein (PDX)	10	12	99	247
Phenylalanine ammonia-lyase (PAL)	0	0	2	20
Mitogen activated protein kinase 3 (MAPK3)	0	0	0	5
Mitogen activated protein kinase 6 (MAPK6)	3	3	0	4
Mitogen activated protein kinase 9 (MAPK9)	0	0	49	18

Table 4.1. Peptide hit counts from Mass Spectroscopy after EV, ATG8c and Joka2 co-immunoprecipitations in uninfected (mock) and infected conditions. The proteins named in this table are the candidate interactors of Joka2 which were chosen to be tested. Silencing and cloning constructs were generated for all of the potential interactors of Joka2 except silencing constructs of MAPK3 and MAPK6. These results represent the average of 3 independent repeats of IP/MS experiments.

4.3.2 Silencing of MAPK3 and PAL weakens plant immunity against P. infestans

Firstly, to investigate whether these potential Joka2-interactors have an impact on plant immunity, infection assays were performed for individual candidates using transgenic *P. infestans* that express RFP in the cytoplasm, referred to as the TD tomato strain. RNAi hairpin constructs of PDX, PAL, MAPK3, MAPK6, or MAPK9 were infiltrated into one side of the leaf, while the other side was infiltrated with a GUS silencing control. Pathogen growth was observed 8-9 days after inoculation with the zoospores of tdTomato *P. infestans* strain, which is not as virulent as wild type pathogen. Pathogen hyphal growth was imaged by fluorescence microscopy. The circular area covered by the hyphal growth was measured using ImageJ. Three assays were carried out for each candidate Joka2-interactor. Among the tested MAP kinases only silencing of MAPK3 mRNA showed significant reduction in pathogen spread on the infected *N. benthamiana* leaves (Figure 4.1A). A stronger effect was observed after silencing *PAL* mRNA in terms of increasing biotrophic growth of the pathogen (Figure 4.1E). However, PAL among the other potential interactors displayed a different pattern when its mRNA was silenced: pathogen became more biotrophic and reduced its necrotic spread (Figure 4.2). The necrotrophic growth was imaged by a camera and the area of the brownish dead leaf tissue was analysed using ImageJ.

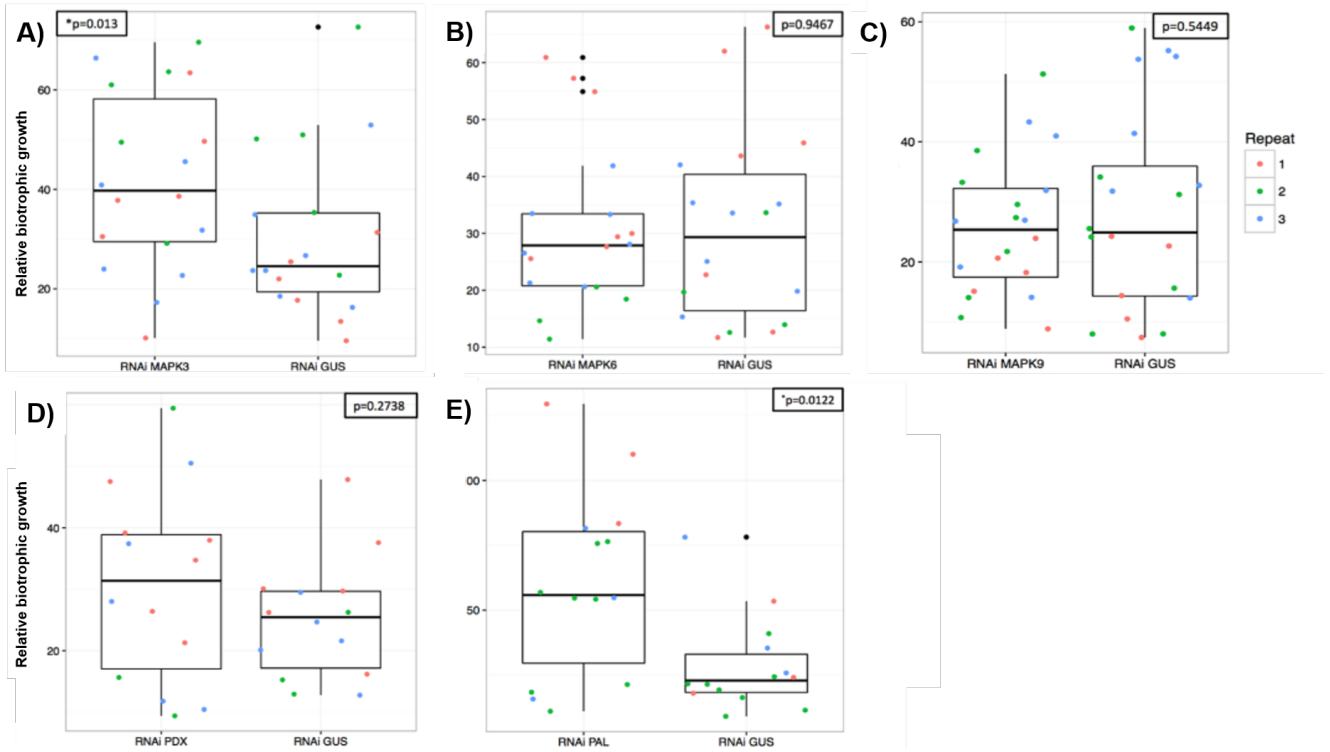


Figure 4.1. Silencing *MAPK3* and *PAL* in *N. benthamiana* leaves leads to augmented pathogen growth. (**a-e**) Categorical scatter plots show lesion diameters of infections sites from three independent biological replicates indicated by three different colors. Interference of *MAPK3* and *PAL* RNA showed a significant amount of change in pathogen growth. Each point represents the average area of biotrophic growth at three infection sites on the half of a leaf. Three independent biological replicates were used to generate the categorical scatter plots, indicated by three different colours. Student t-test was carried out to compare the difference.

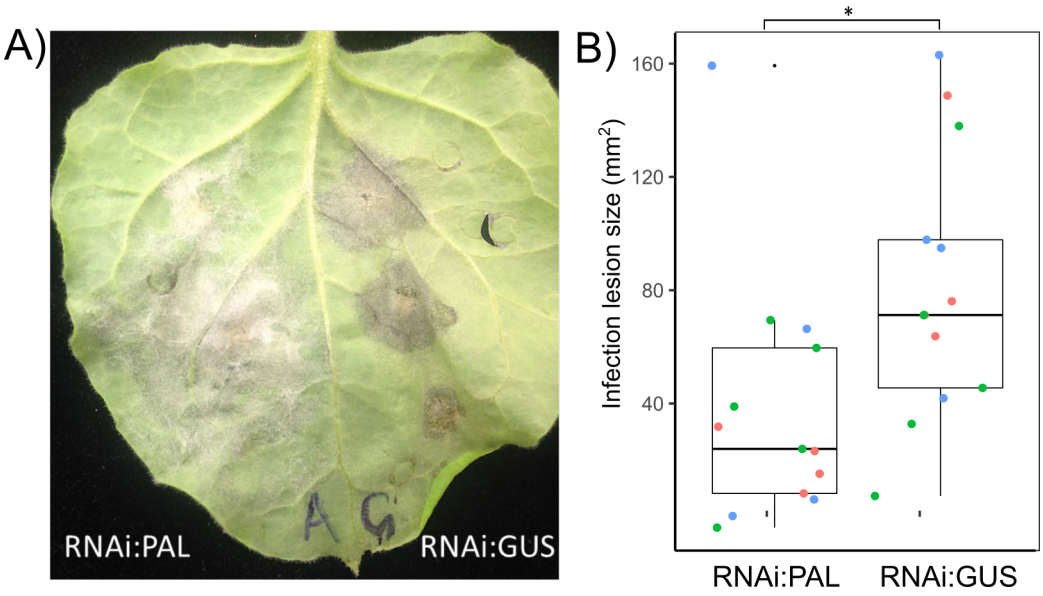


Figure 4.2. Silencing *PAL* in *N. benthamiana* causes *P. infestans* to cause less necrosis. A) *N. benthamiana* leaves silenced on each half either for *PAL* or *GUS* were infected with *P. infestans* and pathogen growth was determined by measuring infection lesion size eight days post-inoculation. (B) Categorical scatter plot illustrates infection lesion size of three infections sites from three independent biological replicates. Knocking down *PAL* significantly ($p<0.01$) reduces necrotic nature of *P. infestans*, but not biotrophic spread.

4.3.3 MAP3, MAPK6 and MAPK9 colocalise with Joka2 but not PDX or PAL

Candidate Joka2 interactors were firstly tested for colocalisation with Joka2 puncta. GFP fusions of the potential interactors were cloned from *N. benthamiana* cDNA and investigated their degree of colocalisation by transiently coexpressing them with Joka2:BFP in *N. benthamiana* epidermal cells (Figure 4.3). Preliminary screening revealed that N-terminally GFP-tagged PDX predominantly localised to the nucleus, produced faint signal at chloroplasts and did not show any colocalisation pattern with Joka2:BFP (Figure 4.3A). Interestingly, Joka2:BFP showed enhanced vacuolar signal and did not show many punctate signal when coexpressed with GFP:PDX compared to the previous observations where Joka2 was expressed by itself or coexpressed with ATG8 or ATG9 (Chapter 3). This suggests that PDX might regulate transport of Joka2 to the central vacuole, perhaps by activation of autophagy. However, to conclude this, further

repeats and additional experiments including controls such as autophagy-deficient plants are required.

Similarly, preliminary results did not show any indication for colocalisation of PAL:GFP with Joka2:BFP when they were coexpressed in the leaf tissue (Figure 4.3B). PAL:GFP showed cytoplasmic accumulation and was excluded from the nucleus. As PAL has been associated with plant immunity and has an increased peptide hit count upon infection (Table 1), further experiments were carried out to investigate subcellular localisation and protein-protein interactions of PAL and Joka2 upon infection.

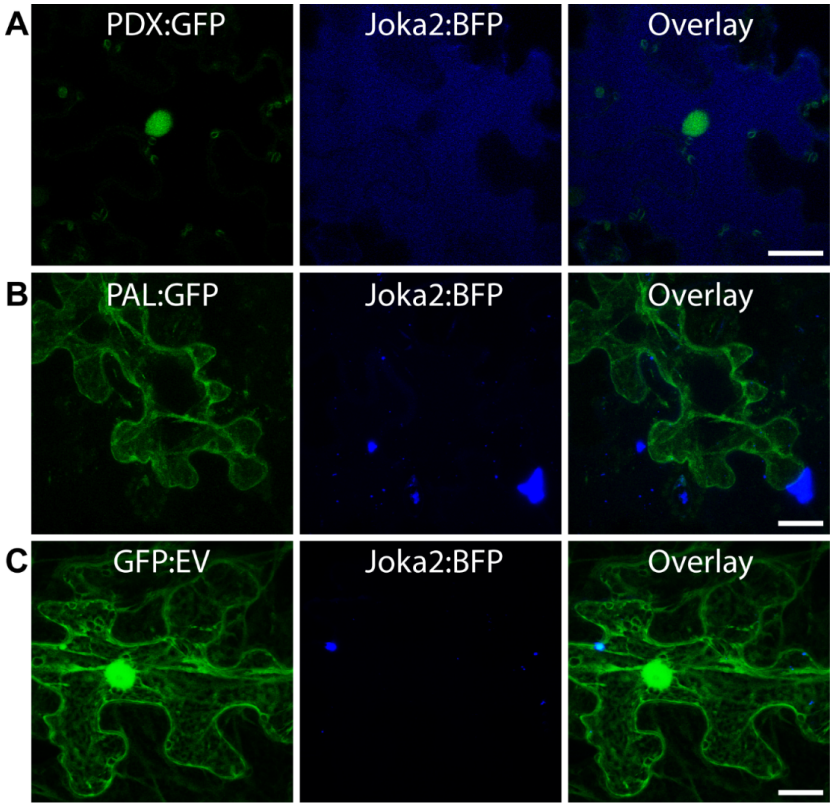
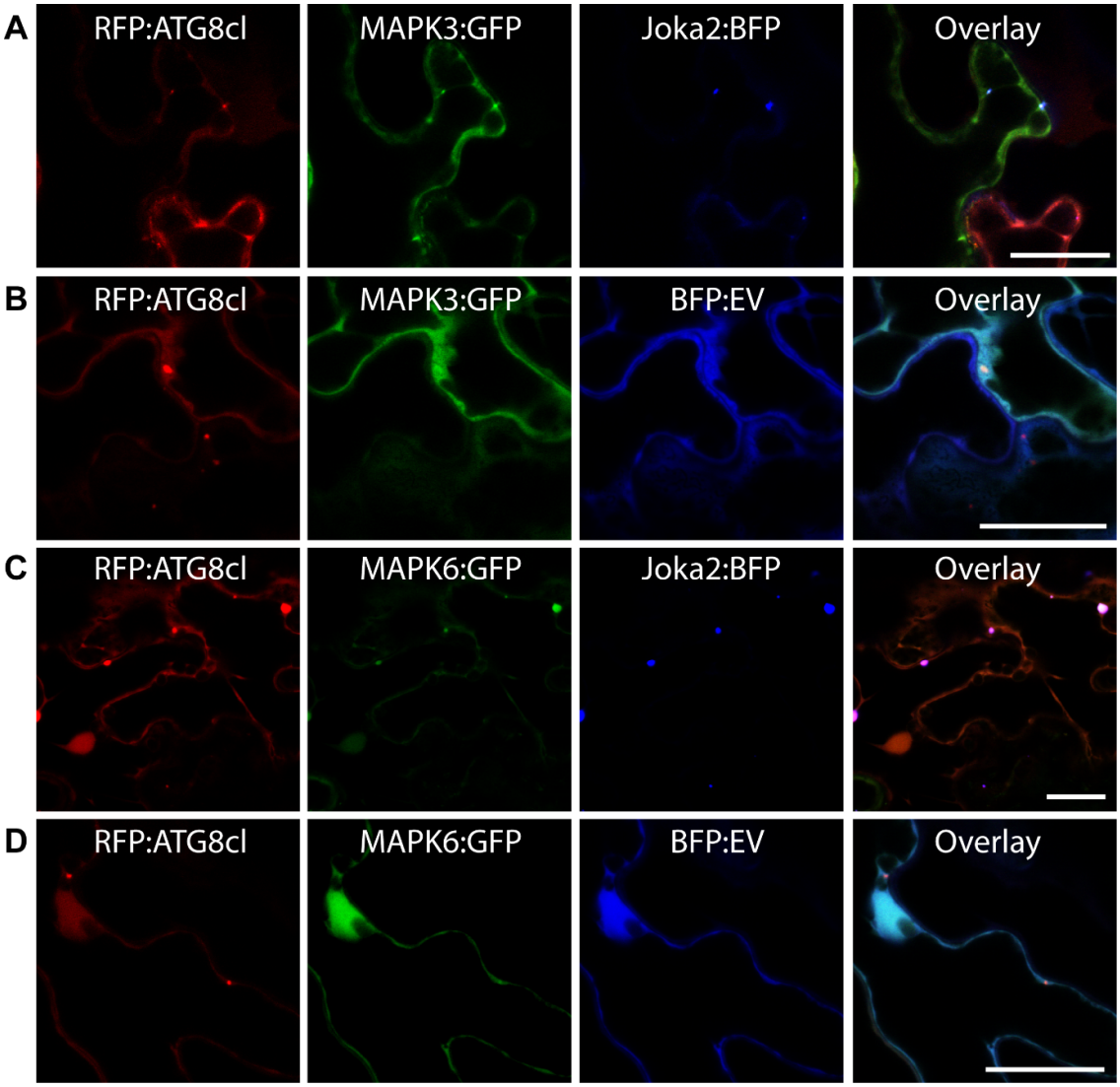


Figure 4.3. **Joka2 does not co-localise with PAL or PDX *in planta*.** Confocal microscopy images of epidermal cells of N. *benthamiana* co-infiltrated with agrobacteria carrying vectors for Joka2:BFP and GFP:PDX, PAL:GFP or EV:GFP. A) GFP:PDX labelled nucleus and in chloroplasts but not Joka2 compartments. PDX:GFP overexpression seemed to alter Joka2:BFP localisation towards central vacuole. B) PAL:GFP displayed cytoplasmic distribution and did not localise to Joka2:BFP-labelled puncta. C) EV:GFP control showed even distribution in cytoplasm and nucleus, and did not label any Joka2:BFP puncta. Images were obtained at 3 dpai and scale bars represent 25 µm.

Although there was no detectable Joka2-PDX or -PAL colocalisation, we observed significant overlap of MAPK3:GFP, MAPK6:GFP and MAPK9:GFP-labelled vesicle-like structures with Joka2:GFP puncta in preliminary experiments. In order to validate that colocalisation of selected MAPKs and autophagy cargo receptor Joka2 is related to autophagosomes, coexpression of ATG8CL-Joka2-MAPK with different fluorescent tags was performed (Figure 4.4). Unlike the GFP and BFP controls, all of the GFP tagged MAPKs colocalised with Joka2:BFP and RFP:ATG8CL (Figure 4.4). Interestingly, when there is no over-expressed Joka2, MAPKs do not form distinct puncta (Figure 4.4). This may indicate that recruitment of MAPKs from cytoplasm to puncta requires specific cargo receptor Joka2. In summary, these results demonstrate that, in uninfected plant cells, MAPK3, MAPK6 and MAPK9 colocalise with Joka2:BFP whereas PAL and PDX do not.

Having tested the subcellular localization of candidate interactors with Joka2 puncta under normal conditions and found out PAL and PDX did not colocalise with Joka2, I have exposed the agroinfiltrated plants (similar setup to the previous experiment) to infection by *P. infestans*. Because IP/MS data suggested that both PAL and PDX proteins associate with Joka2 more effectively during infection, it was possible that PDX and PAL might colocalise with Joka2 only during infection. GFP-tagged Joka2 candidates were co-expressed with Joka2:BFP and RFP:REM1.3 (cell membrane marker, red channel in the overlaid images). Similar to the previous observation, there was no significant colocalisation signal from Joka2 puncta belonging to PAL:GFP or GFP:PDX (Figure 4.5A and B), whereas MAPK3, MAPK6 and MAPK9 were accumulating in Joka2 puncta (Figure 4.5C-E). These experiments show that even under infection conditions of PAL and PDX do not have an association with Joka2 compartments.



(*Figure caption is on the next page*)

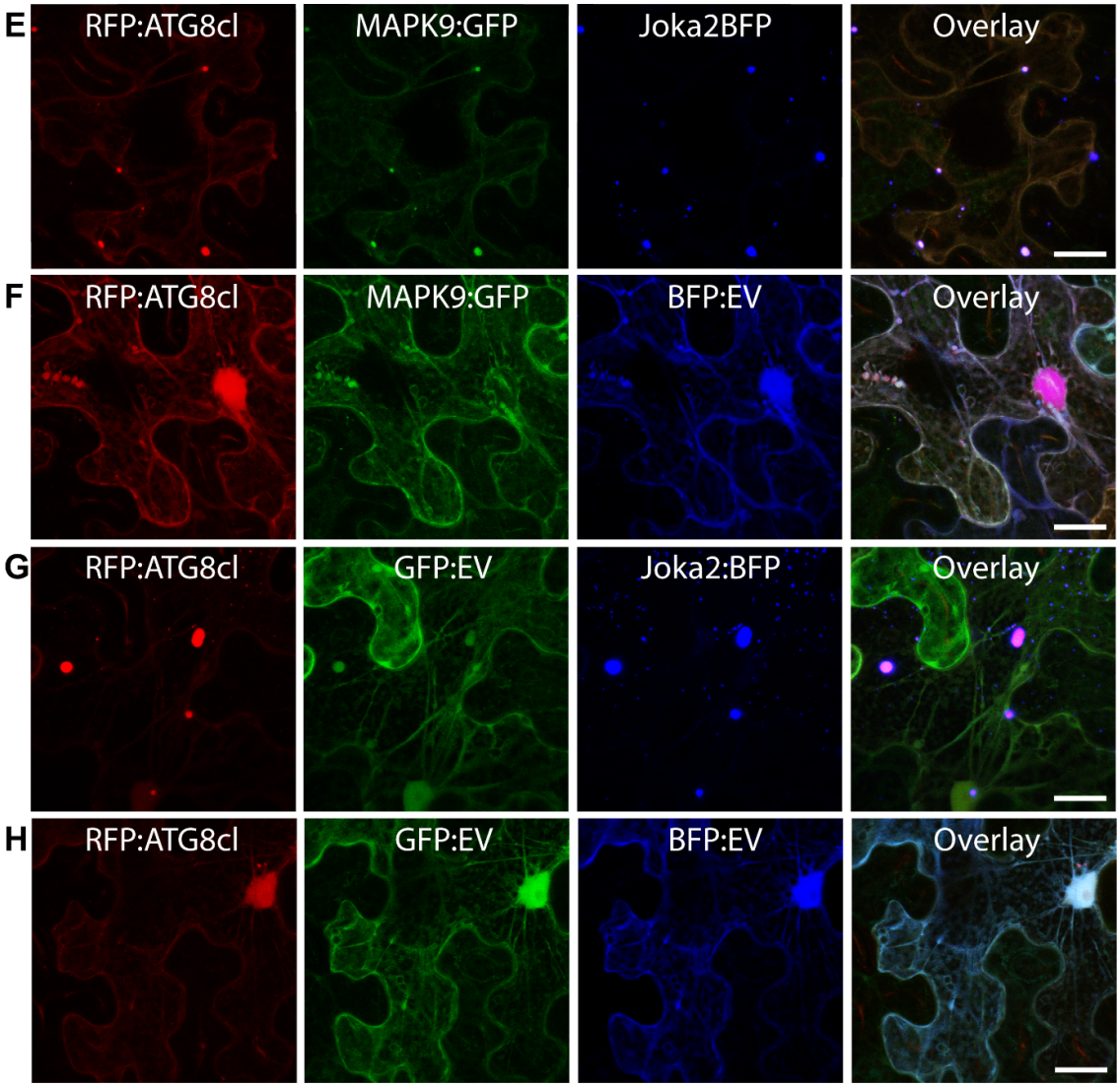


Figure 4.4. Colocalisation of Joka2 puncta with its candidate MAPK interactors in presence of ATG8CL-autophagosomes. Confocal microscopy images of epidermal cells of *N. benthamiana* co-infiltrated with agrobacteria carrying vectors for MAPK3:GFP, MAPK6:GFP, MAPK9:GFP, or GFP:EV with RFP:ATG8c and Joka2:BFP or BFP:EV. (A) MAPK3:GFP, (C) MAPK6:GFP and (E) MAPK9:GFP produced bright fluorescent signal that colocalised with Joka2:BFP-labelled ATG8c autophagosomes in addition to diffused cytoplasmic signal. (B, D and F) MAPKs did not exhibit detectable accumulation in conditions where Joka2 was not overexpressed. (G-H) GFP:EV control showed even distribution in cytoplasm and nucleus, and did not label any Joka2:BFP puncta. As previously reported, Joka2 overexpression increased the number of ATG8c autophagosomes (G), in contrast to BFP:EV (H). Images were obtained at 3 dpai and scale bars represent 25 µm.

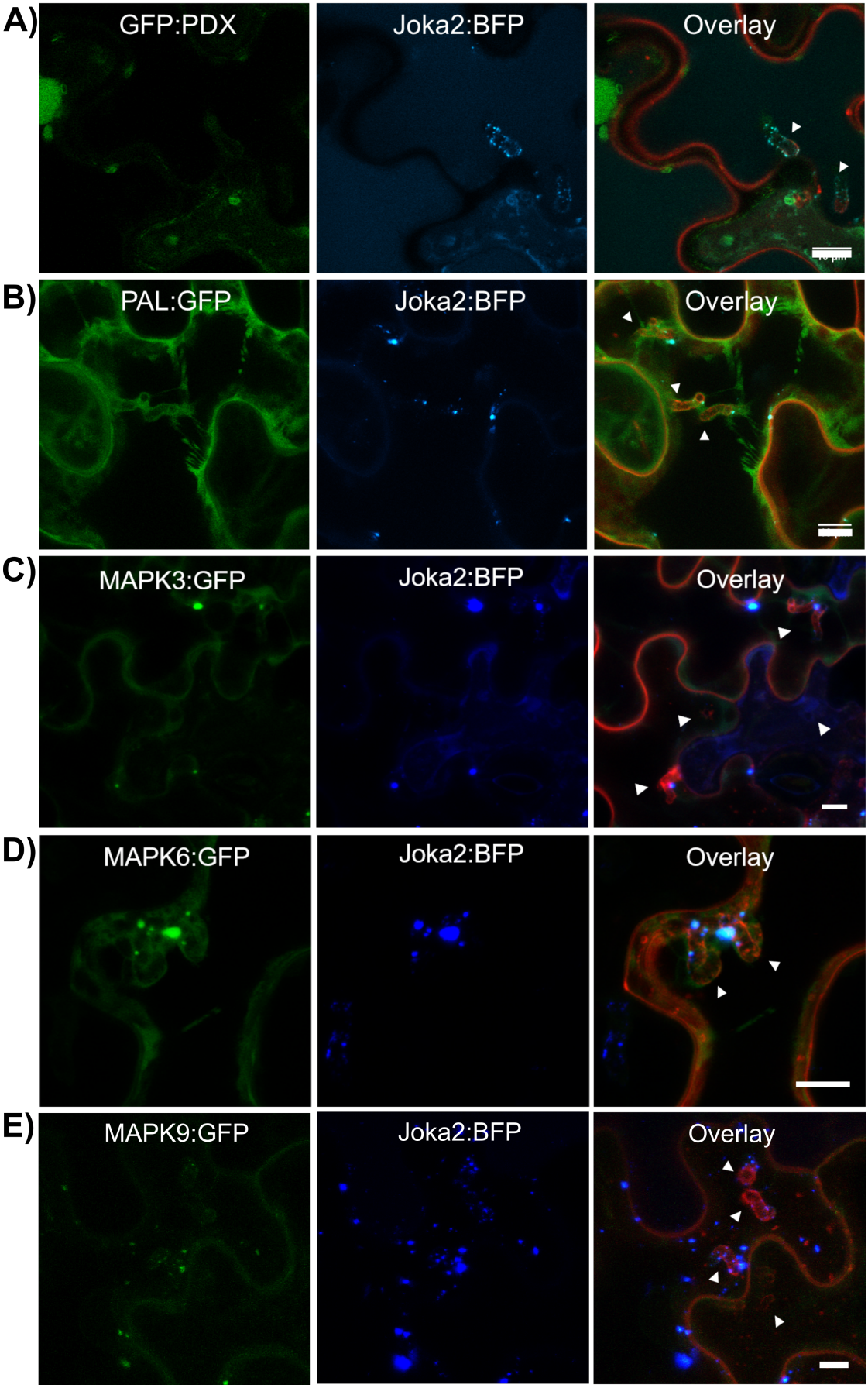


Figure caption is on the next page

Figure 4.5. Colocalisation of Joka2 puncta with its candidate MAPK interactors during infection. Confocal microscopy images of epidermal cells of *N. benthamiana* co-infiltrated with agrobacteria carrying vectors for GFP:PDX, PAL:GFP, MAPK3:GFP, MAPK6:GFP, MAPK9:GFP, or GFP:EV with Joka2:BFP and REM:1.3 (not shown separately) 2-3 days post infection with *P. infestans*. (A-B) Similar to un-infected cells, neither PDX nor PAL signal was detected from the Joka2 puncta. However, MAPK3:GFP (C), MAPK6:GFP (D) and MAPK9:GFP (E) produced distinct fluorescent signal that colocalised with Joka2:BFP puncta in addition to diffused cytoplasmic signal. Images were obtained at 3 dpai and scale bars represent 10 μm.

4.3.4 MAP kinase 3, 6, and 9 interact with Joka2

As Joka2-labelled puncta were confirmed to colocalise with the tested MAPKs and because MAPK3 silencing revealed a promising effect on plant resistance, we further investigated the association of the potential interactors and the autophagy cargo receptor. In order to test the binding of the MAP kinases 3, 6 and 9, we utilized immunoprecipitation of Joka2:RFP by using RFP trap beads. The presence of triple HA-tagged MAPKs was tested after running the extracts obtained from the beads on SDS-PAGE. All the tested MAP kinases were detected in IP after HA detection, confirming their association with Joka2 (Figure 4.6). MAPK3:3xHA and MAPK9:3xHA showed strong affinity binding in the IP whereas MAPK6:3xHA affinity signal was lower in both IP and input. In summary, co-immunoprecipitation of MAP kinases co-expressed with Joka2:RFP revealed the direct association of the MAP kinases, validating the findings obtained from confocal microscopy.

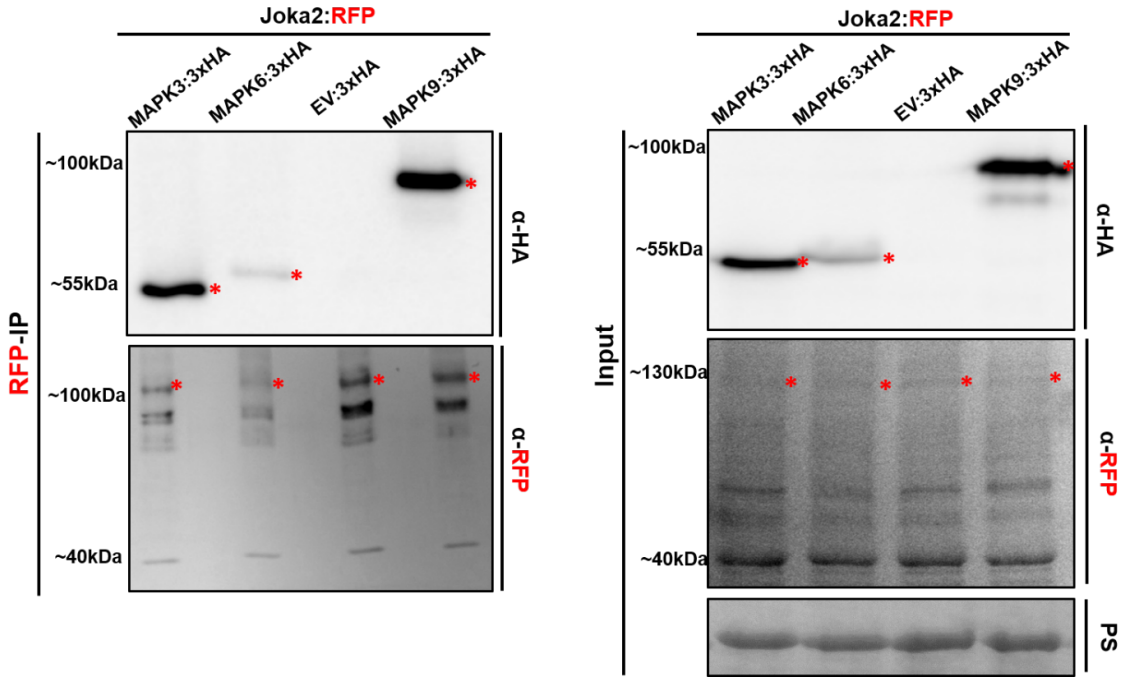


Figure 4.6 Validation of MAPK3, MAPK6, and MAPK9-Joka2 association *in planta*. 3xHA-taged MAPKs or EV:3xHA were transiently coexpressed with Joka2:RFP in *N. benthamiana* leaves. Immunoprecipitation (IP) was obtained by using anti-RFP antiserum and total protein extracts were immunoblotted with appropriate antisera. All the tested MAPKs were detected in Joka2:RFP pulldown, which indicates physical Joka2-MAPK association. Red asterisks indicate the protein bands with expected molecular weight.

Most of the Joka2 mutants were cloned into C-terminal GFP vectors that I use for co-IP experiments in this chapter, as I have used in previous work (such as ΔPB1 and ΔPZ, Chapter 3). Therefore I repeated the co-IP experiment to test if GFP-tagged Joka2 interacted with MAPK3 and MAPK6 the same way Joka2:RFP did. By doing so the MAPK-Joka2 interaction was shown to be not dependent on the type of the tag of Joka2, and GFP tag itself was not binding to either to MAPK3:3HA or MAPK6:3HA. Similar to the results I got in (Figure 4.7), MAPK3:3HA was co-immunoprecipitated with Joka2 in higher levels compared to MAPK6:3HA.

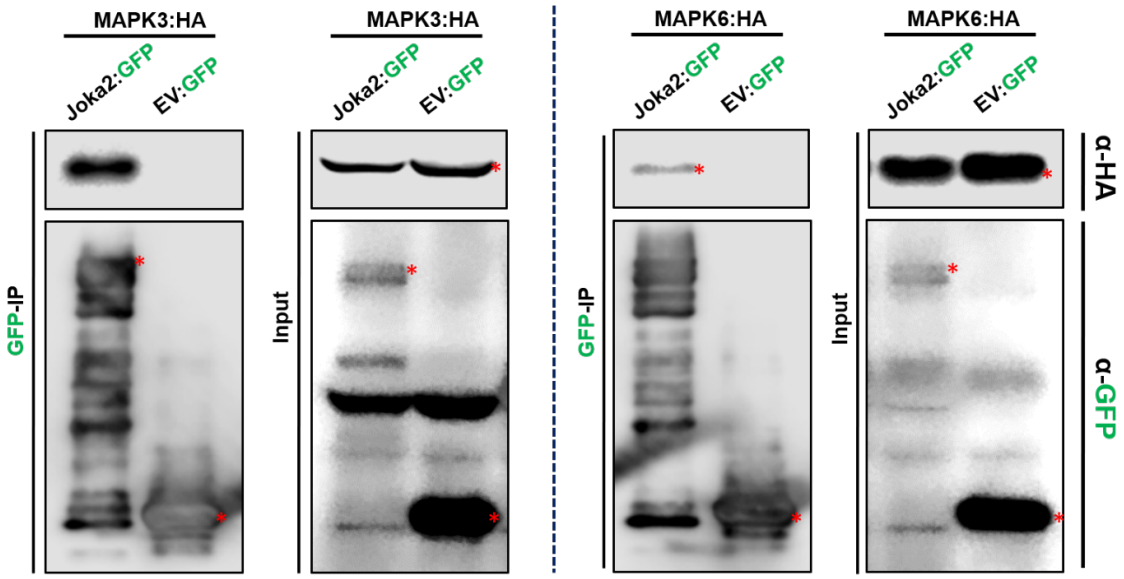


Figure 4.7. MAPK3 and MAPK6 interact with Joka2 regardless of the tag used to pulldown. MAPK3:HA or MAPK6:HA were transiently co-expressed with Joka2:GFP or EV:GFP in 4 weeks old *N. benthamiana* leaves and proteins were extracted 2 days after agroinfiltration. Immunoprecipitations (IPs) were obtained by using anti-GFP antiserum and total protein extracts were immunoblotted with appropriate anti-HA and anti-GFP antisera. HA-tagged MAPK3 and MAPK6 were detected in Joka2:GFP pulldown, which indicates physical Joka2-MAPK association regardless the tag of Joka2. Red asterisks indicate the protein bands with expected molecular weight.

4.3.5 Exploring Joka2 domains that are responsible for MAPKs and PAL interaction

4.3.5.1 MAPK3 affinity of Joka2 is not affected by mutating UBA domains

Having confirmed that MAPKs colocalize and interact with Joka2 autophagosomes, one possibility is that MAPKs are degraded by autophagy to regulate PTI signalling. In order to investigate this hypothesis, I employed full length Joka2 and its mutated version with non-functional UBA domain, (Joka2^{UBA1,2}) as autophagy cargo receptors typically recruit ubiquitinated cargoes. To address this, GFP-tagged Joka2 or Joka2^{UBA1,2} were transiently co-expressed with MAPK3:3HA in *N. benthamiana* leaves. Optical density of the agrobacteria carrying Joka2^{UBA1,2}:GFP vector was infiltrated one third of Joka2:GFP's as turnover of Joka2 is normally higher than the mutant with unfunctional UBA domains (Figure 4.8). EV control was used to make sure GFP did not come along with MAPK3 or

HA tag. WB showed that MAPK3:HA came along with both functional and unfunctional Joka2. Joka2^{UBA1,2}:GFP was more stable than wild type Joka2:GFP (input, Figure 4.8), however their protein levels were similar in IP, which indicates potential loss of Joka2^{UBA1,2}:GFP coated beads during IP washes. Consistently, there was a slight signal reduction in MAPK3:3HA in Joka2^{UBA1,2}:GFP pull downs compared to wild type Joka2.

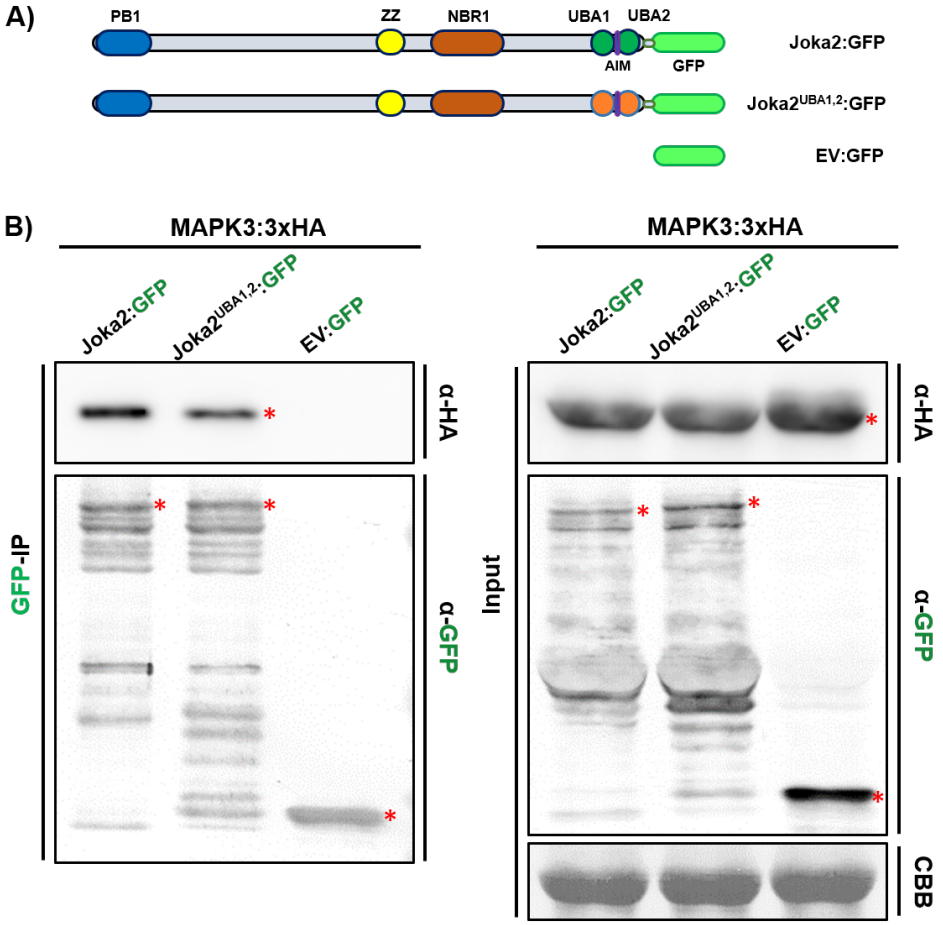


Figure 4.8. MAPK3 interacts with Joka2 regardless of Joka2's polyubiquitin binding ability. (A) Schematic domain organisation of GFP-tagged Joka2, Joka2UBA1,2 and EV that are used to pulldown HA-tagged MAPK3. (B) Co-immunoprecipitation of MAPK3 with Joka2 and its mutant version *in planta*. UBA1,2 lacks binding ability to polyubiquitin chains. MAPK3 was transiently co-expressed with tagged Joka2:GFP, Joka2UBA1,2:GFP or EV:GFP in 4 weeks old *N. benthamiana* leaves and proteins were extracted 2 days after agroinfiltration. Immunoprecipitation (IP) was obtained by using anti-GFP antiserum and total protein extracts were immunoblotted with appropriate anti-HA and anti-GFP antisera. MAPK3 signal was detected even when Joka2 mutant lacking ability to bind to polyubiquitin chains is pulled down. Red asterisks indicate the protein bands with expected molecular weight.

I then set out to reproduce these results. A lower OD for Joka2^{UBA1,2}:GFP was preferred as it has higher protein stability than Joka2. In the earlier repetition of the same experiment (Figure 4.9), I used the same optical density of agrobacteria carrying the constructs. Since the stability of Joka2^{UBA1,2}:GFP is higher than wild type Joka2, I detected higher levels of Joka2^{UBA1,2}:GFP in both input and IP (Figure 4.9B). MAPK3:3HA signal was also much higher when it was co-immunoprecipitated with abundant Joka2^{UBA1,2}:GFP. From this result, I could not deduce if MAK3 association decreased or increased as pulled down Joka2 and Joka2^{UBA1,2}:GFP levels were different. The most interesting result of this semi-failed experiment (due to not equal amounts of proteins), was that in both HA and GFP detection, there was a signal from a region where higher molecular weight proteins reside. Together with some more supporting experiments, this observation will be discussed in the next chapter in more detail. In summary, these results suggest that MAPK3 associates with a different domain of Joka2 other than the UBA domains and MAPK3 may not be an autophagic substrate of Joka2, on the contrary, MAPK3 might form complexes with Joka2.

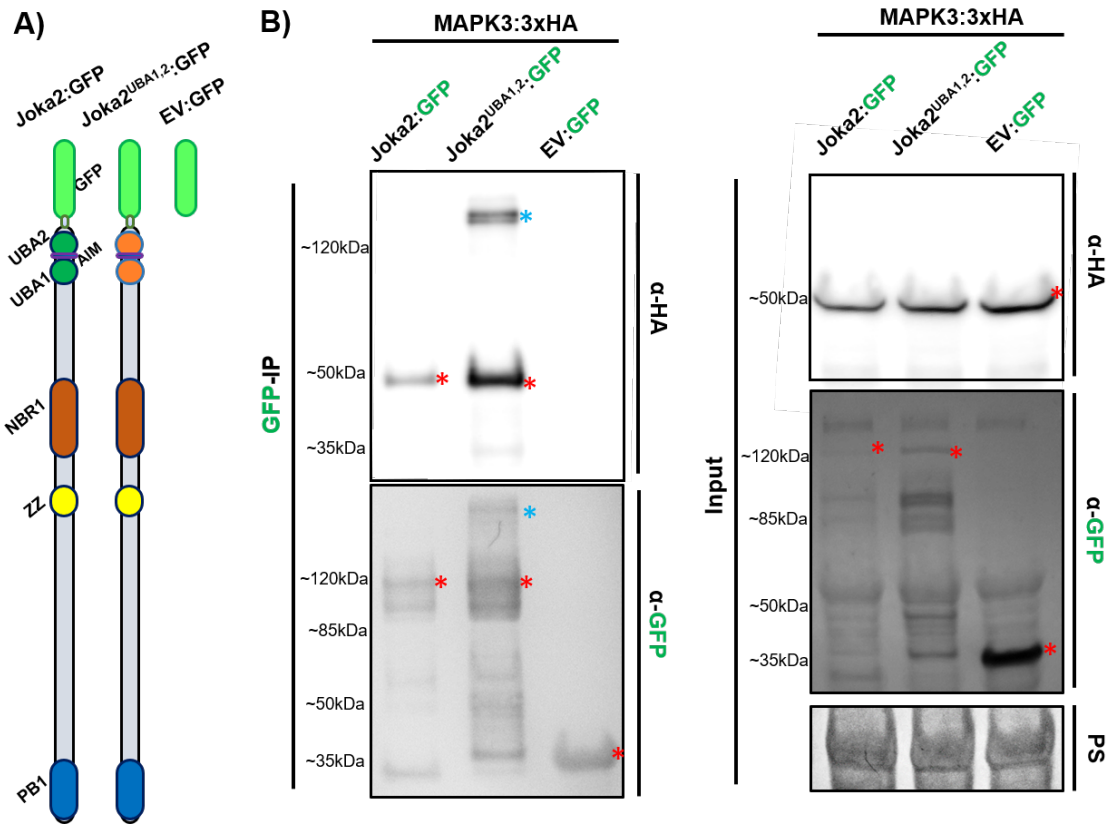


Figure 4.9. MAPK3 interacts with Joka2UBA1,2 and reveals a high molecular weight band. (A) Schematic domain organisation of GFP-tagged Joka2, Joka2UBAs1,2 and EV that are used to pulldown HA-tagged MAPK3. (B) Co-immunoprecipitation of MAPK3 with Joka2 and its mutant version *in planta*. UBA1,2 lacks binding ability polyubiquitin chain. MAPK3 was transiently co-expressed with tagged Joka2:GFP, Joka2UBAs1,2:GFP or EV:GFP in 4 weeks old *N. benthamiana* leaves and proteins were extracted 2 days after agroinfiltration. Immunoprecipitation (IP) was obtained by using anti-GFP antiserum and total protein extracts were immunoblotted with appropriate anti-HA and anti-GFP antisera. MAPK3 signal was significantly high when it was pulled down with abundant Joka2UBA1,2 mutant. An unexpected band of a protein or a protein complex was detected when both MAPK3:3HA and Joka2UBA1,2:GFP protein levels were high (turquoise asterisk). Red asterisks indicate the protein bands with expected molecular weight.

I next validated the functionality of Joka2 UBA mutants. Although the ubiquitin binding properties of UBA domains is well-known, the construct containing UBA domains generated from Joka2 and fluorescent tag were tested with a co-IP by co-expressing UBAs:GFP, UBAs^{1,2}:GFP or EV:GFP with UBQ:HA and pulling down GFP to detect ubiquitin. Only functional UBAs:GFP construct was positive for a strong signal in IP panel when western blotted with an antibody raised against ubiquitin (α-UBQ) (Figure 4.10).

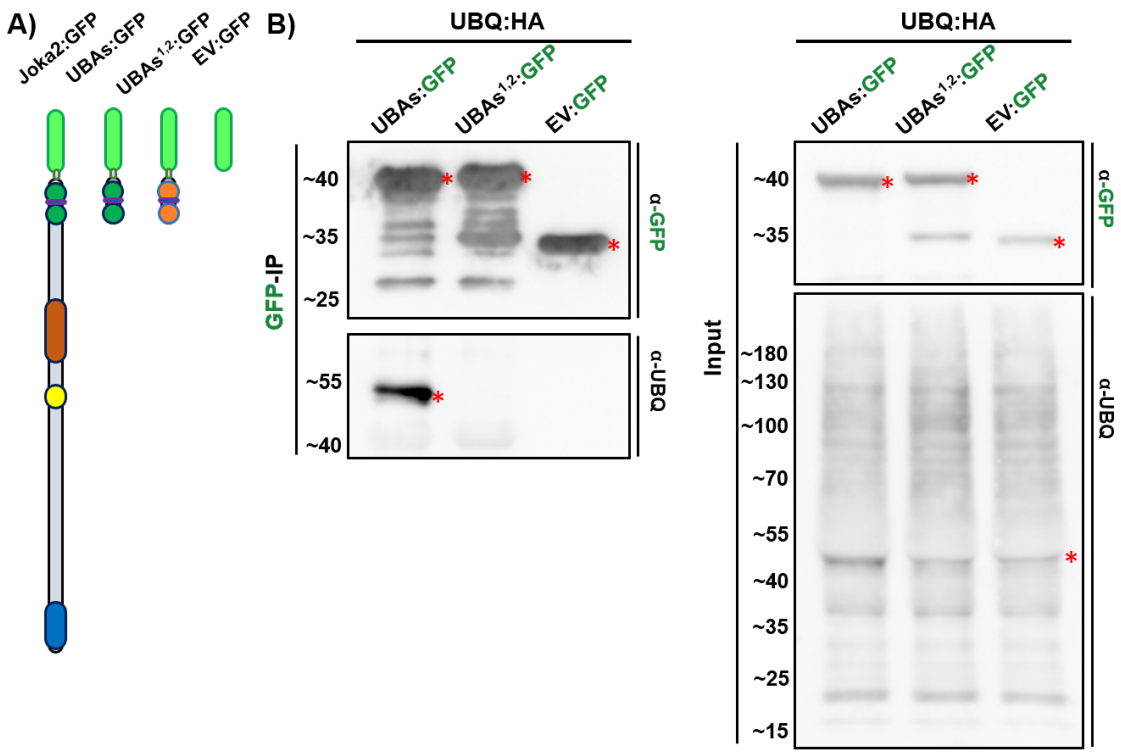


Figure 4.10. Only functional UBA domains pull down polyubiquitin. (A) Schematic domain organisation of GFP-tagged UBAs, UBAs^{1,2} and EV that are used to pulldown HA-tagged ubiquitin (UBQ). (B) Co-immunoprecipitation of UBQ with UBA domains and its mutant version *in planta*. UBQ:HA was transiently co-expressed with tagged UBAs:GFP, UBAs^{1,2}:GFP or EV:GFP in 4 weeks old *N. benthamiana* leaves and proteins were extracted 2 days after agroinfiltration. Immunoprecipitation (IP) was obtained by using anti-GFP antiserum and total protein extracts were immunoblotted with appropriate anti-HA and anti-GFP antisera. HA signal of UBQ was only detected when functional UBA domains were pulled down. That further proves that the clone generated in our laboratory was functional. Red asterisks indicate the protein bands with expected molecular weight.

4.3.5.2 MAPK3 has an affinity to Joka2 region after ZZ domain

Having shown by both microscopy and co-immunoprecipitation that there is an interaction between Joka2 and MAP kinases, I went on to investigating which region of Joka2 is responsible for this interaction. In Figure 4.8, I have shown that ubiquitin binding ability of Joka2 was not essential for MAPK3-Joka2 interaction; therefor, other domains of Joka2 must be responsible for this association. Joka2 truncates (missing either the PB1 domain (ΔPB1) or PB1 and ZZ domains (ΔPZ)) were already available from

the experimental setup explained in Chapter 2 to monitor localisation of Joka2, therefore, these constructs were utilised again to narrow down the regions required for the interactions. GFP-tagged wild type potato Joka2, ΔPB1, ΔPZ or control was transiently co-expressed with triple HA-tagged MAPK3 in *N. benthamiana* leaves. Expression levels were kept similar by infiltrating 3-4 leaves for each construct. Intriguingly, MAPK3 was detected with all the constructs containing Joka2 or its truncates unlike EV:GFP control. Although there was not much difference in protein levels of Joka2 and its truncate mutants in GFP-IP (Figure 4.11), ΔPB1 showed stronger binding to MAPK3. MAPK3:3xHA levels were also similar on all constructs except EV:GFP control which showed more MAPK3 protein levels in the input. This finding suggests that Joka2 is binding to MAPK3 through other known or uncharacterized domains present on Joka2.

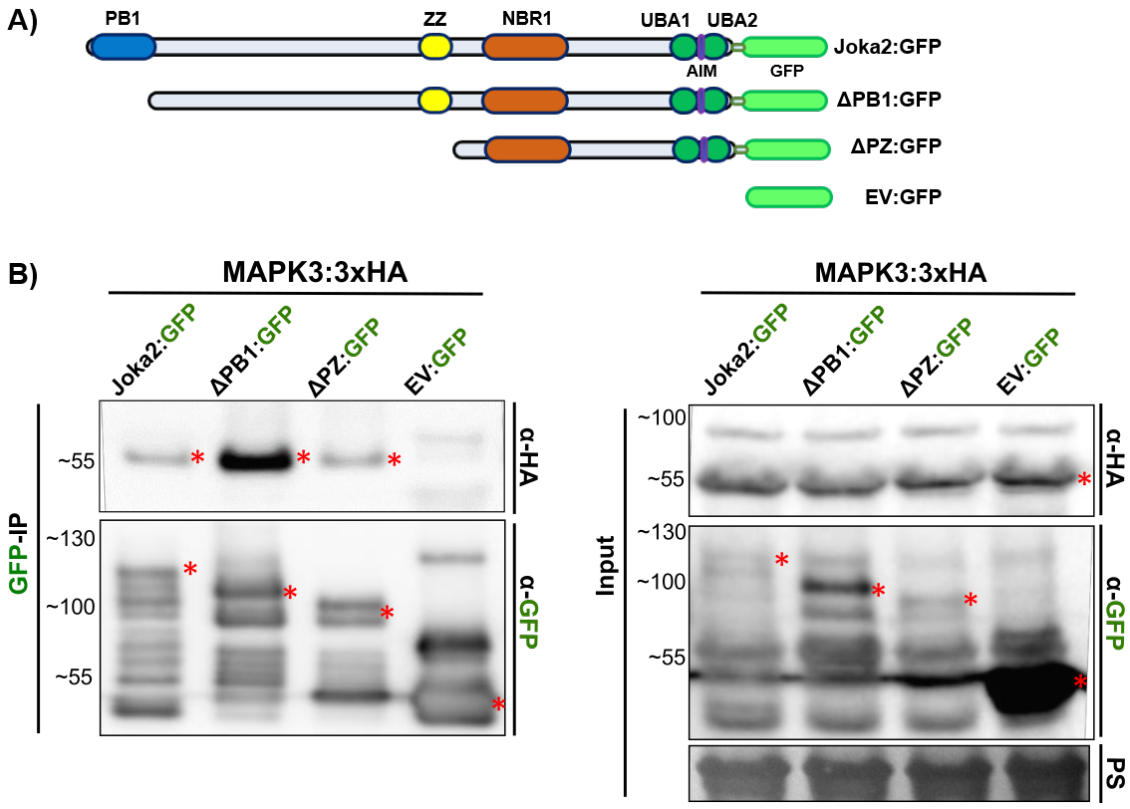


Figure 4.11. MAPK3 does not interact with Joka2 via PB1 or ZZ domains. (A) Schematic domain organisation of GFP-tagged Joka2, ΔPB1, ΔPZ and EV are used to pulldown HA-tagged MAPK3. (B) Co-immunoprecipitation of MAPK3 with Joka2 and its truncated versions *in planta*. MAPK3:3xHA was transiently co-expressed with GFP-tagged Joka2 variants and GFP:EV in 4 weeks old *N. benthamiana* leaves and proteins were extracted 2 days after agroinfiltration. MAPK3:3xHA was detected after Co-IP

even with Joka2 mutants lacking either the PB1 or PB1-ZZ domains. Immunoprecipitation (IP) was obtained by using anti-GFP antiserum and total protein extracts were immunoblotted with appropriate anti-HA and anti-GFP antisera. Red asterisks indicate the protein bands with expected molecular weight.

4.3.5.3 Removal of three main domains, PB1, ZZ and NBR1, diminishes the interaction between MAPK3 and Joka2

After concluding that the interaction of Joka2 with MAPK3 might be through the regions after ZZ domain, I generated constructs lacking only ZZ or NBR1 domains (ΔZZ and ΔNBR1), and constructs without N-terminal regions of Joka2 just after NBR1 domain and just before UBA domains (ΔPZN and UBAs). They are all cloned into C-terminal GFP vectors and transiently co-expressed with MAPK3 which is tagged with HA (3x). The most remarkable observation was that even though the expression levels or protein stability of ΔPZN:GFP and UBAs:GFP were the highest by far, those truncated proteins pulled down very little MAPK3. In contrast, ΔZZ had the highest interaction with MAPK3 considering its protein level both in input and IP (Figure 4.12) was the lowest, which suggests that ZZ domain is not required for stable MAPK3-Joka2 interaction. Although ΔNBR1 protein level was higher than ΔZZ, substantial loss of affinity was observed after removing only NBR1 domain. That hints that either NBR1 domain or a region covering NBR1 is responsible for Joka2-interaction.

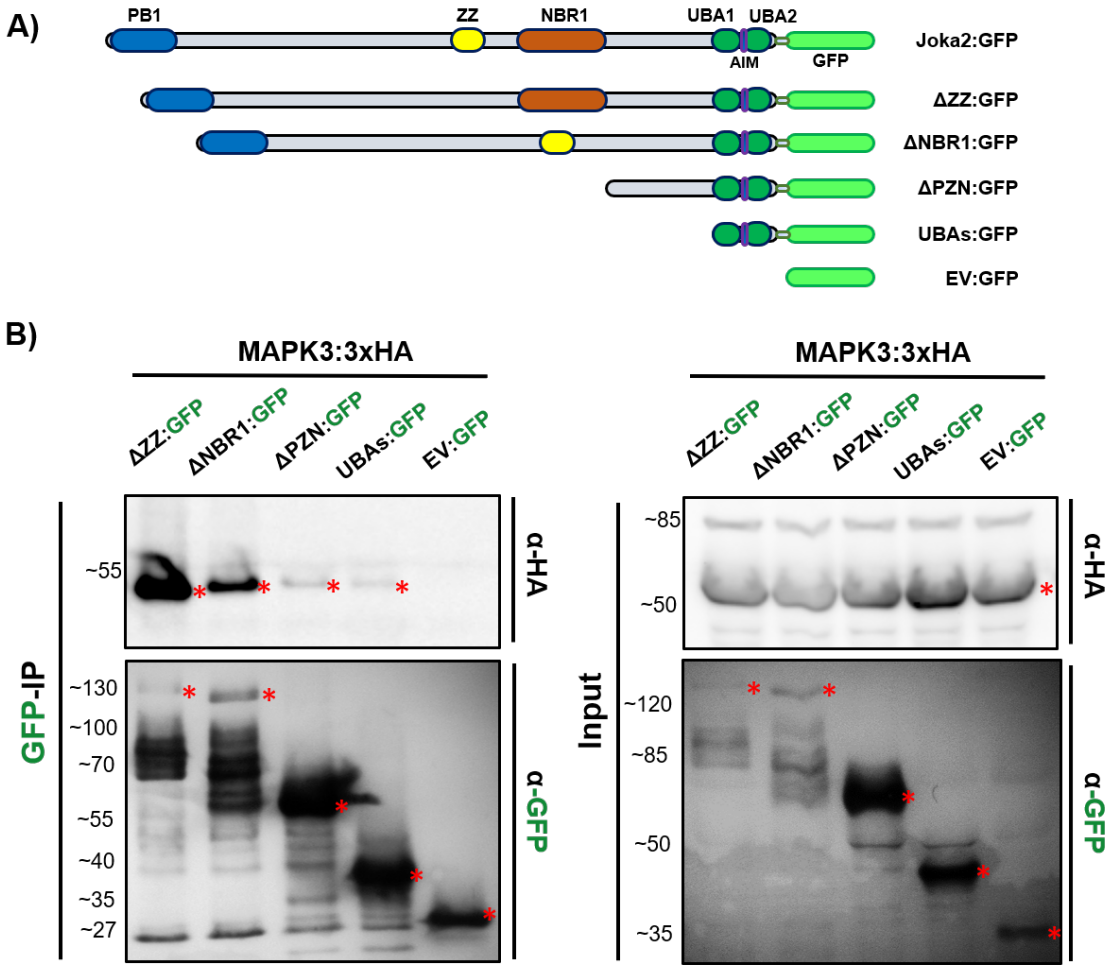


Figure 4.12. MAPK3-Joka2 interaction is diminished upon removal of PB1, ZZ and NBR1 domains. (A) Schematic domain organisation of GFP-tagged Joka2, ΔZZ, ΔNBR1, ΔPZN, UBAs and EV that are used to pulldown HA-tagged MAPK3 (except wild type Joka2). (B) Co-immunoprecipitation of MAPK3 with Joka2 and its truncated versions *in planta*. MAPK3:3xHA was transiently co-expressed with ΔZZ:GFP, ΔNBR1:GFP, ΔPZN:GFP, UBAs:GFP or EV:GFP in 4 weeks old *N. benthamiana* leaves and proteins were extracted 2 days after agroinfiltration. Immunoprecipitation (IP) was obtained by using anti-GFP antiserum and total protein extracts were immunoblotted with appropriate anti-HA and anti-GFP antisera. Joka2-MAPK3 interaction was diminished upon truncation of three N-terminal domains **P**B1, **Z**Z and **N**BR1 (ΔPZN). Removal of NBR1 also reduced the interaction of Joka2 and MAPK3 significantly compared to removal of ZZ domain. Red asterisks indicate the protein bands with expected molecular weight.

4.3.5.4 Region containing NBR1 domain might be the docking site of MAPK3 to Joka2

The observation of weak MAPK3-Joka2 interaction even after losing a big chunk of N-terminal region of Joka2, which results in constructs with mainly UBA domains, prompted me to clarify the involvement of UBA domains on this interaction. I would like to keep wildtype Joka2 as a control and ΔNBR1 to monitor if I could find the same reduction of interaction. ΔPB1 was also included as it has an important role in Joka2 dimerization, cargo binding, and therefore, autophagic flux induction. In addition, a construct with only UBA domains but containing mutations in the region for ubiquitin binding was generated to probe the nature of the interaction. Those constructs were transiently co-expressed with MAPK3:3HA in *N. benthamiana*. GFP tagged Joka2, its truncated version and control group was pulled down and MAPK3:3HA presence was determined via western blotting (Figure 4.13). This WB further validated the previous observation: (i) NBR1 removal reduces Joka2-MAPK3 interaction, (ii) PB1 domain is required for the function of Joka2 and its absence does not omit the interaction pattern, (iii) UBA domain is not the sole region for the interaction. Additionally, UBAs-MAPK3 interaction is not directly related to ubiquitin binding affinity of UBA domains, as $UBAs^{1,2}$:GFP still managed to pull down MAPK3 similar to UBAs:GFP. These results further support the idea that MAPK3 interaction might be established through the region covering NBR1 domain or the domain itself.

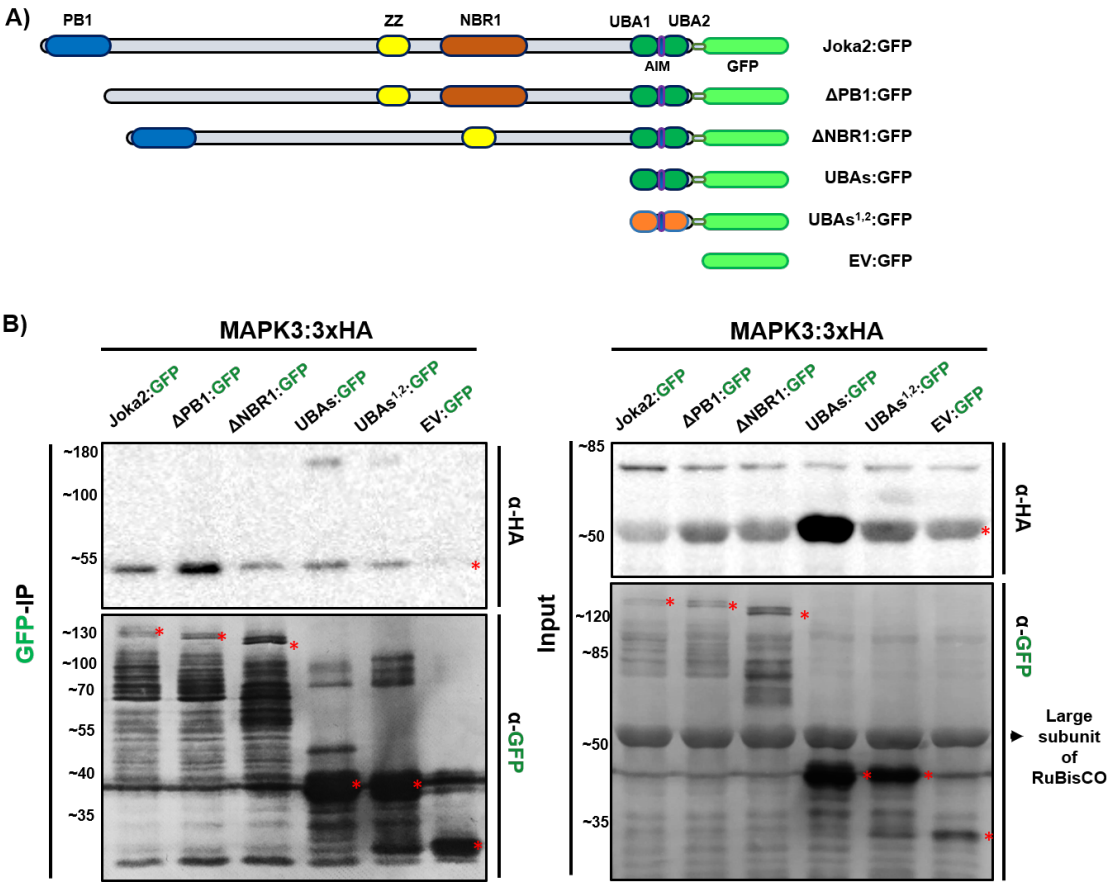


Figure 4.13. Removal of only NBR1 domain significantly reduces Joka2-MAPK3 interaction. (A) Schematic domain organisation of GFP-tagged Joka2, ΔPB1, ΔNBR1, only UBA domains (UBAs), unfunctional UBA domains (UBAs^{1,2}) and EV that are used to pulldown HA-tagged MAPK3. (B) Co-immunoprecipitation of MAPK3 with Joka2 and its truncated versions *in planta*. HA-tagged MAPK3 was transiently co-expressed with Joka2:GFP, ΔPB1:GFP, ΔNBR1:GFP, UBAs:GFP, UBAs^{1,2}:GFP or EV:GFP in 4 weeks old *N. benthamiana* leaves and proteins were extracted 2 days after agroinfiltration. Immunoprecipitation (IP) was obtained by using anti-GFP antiserum and total protein extracts were immunoblotted with appropriate anti-HA and anti-GFP antisera. MAPK3:3xHA was detected when Joka2 or its truncated versions were pulled down, however, removal of only NBR1 domain caused the most significant interaction loss compared to other Joka2 mutants considering the signal levels of pulled down proteins. Red asterisks indicate the protein bands with expected molecular weight.

For a final comparison, I carried out a co-IP with all truncated Joka2 constructs and controls (Joka2 and EV). The constructs were co-expressed and processed similar to the previous co-IPs, with an exception of adjustment of OD levels of agrobacteria carrying GFP tagged proteins. This attempt was mostly successful except the levels of ΔZZ:GFP in

input and IP. In that WB of co-IP, it was clearer that removal of the main domains (ΔPZN) caused loss of MAPK3 interaction with Joka2 (Figure 4.13). Truncating ZZ domain appeared to diminish MAPK3:3HA affinity, however, GFP signal was also significantly lower in the GFP detection panel. Pulling down ΔNBR1 resulted in a similar outcome to the previous IPs (Figure 4.12 and Figure 4.13), and this time more clearly; subsequent interaction loss despite a high GFP signal from ΔNBR1. The contribution of the NBR1 domain and the link between MAPK3 and autophagy is further investigated in Chapter 5.

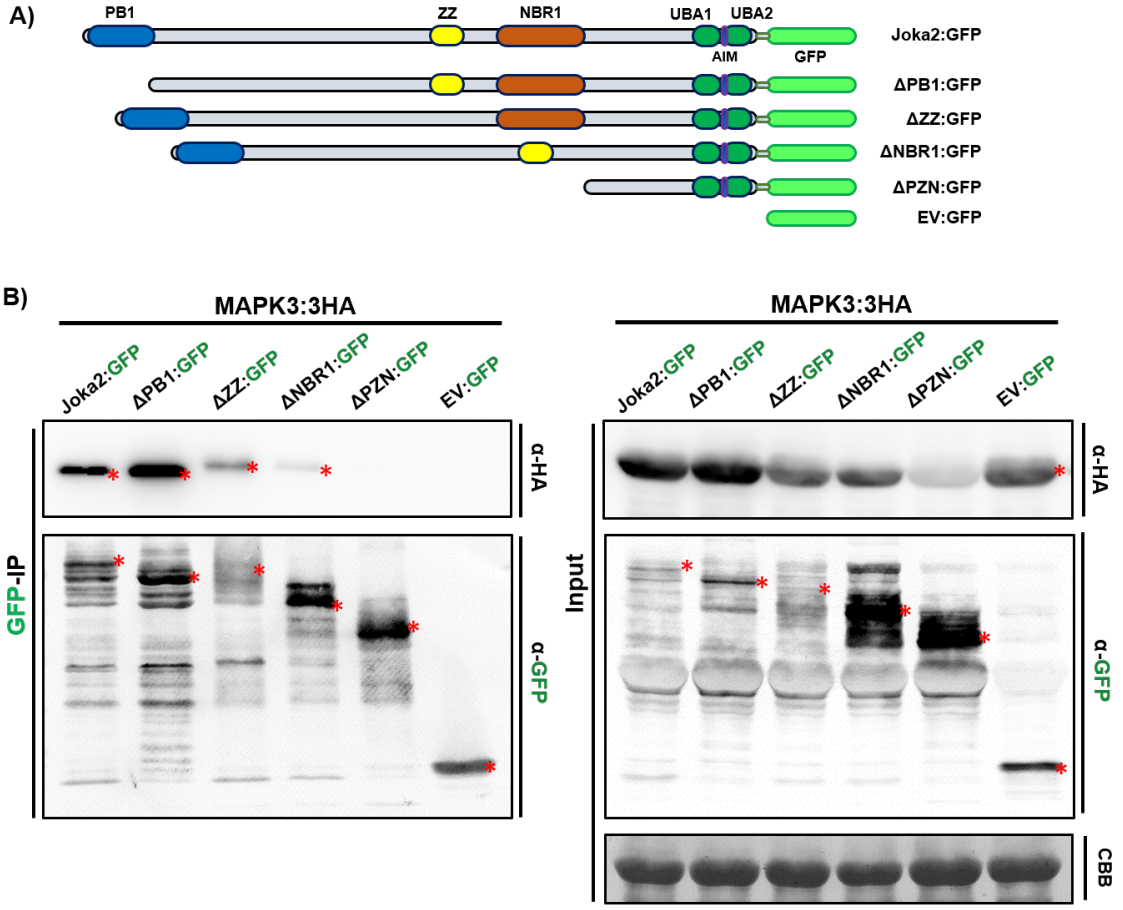


Figure 4.14. Removal of only NBR1 domain significantly reduces Joka2-MAPK3 interaction. (A) Schematic domain organisation of GFP-tagged Joka2, ΔPB1, ΔZZ, ΔNBR1, ΔPZN and EV that are used to pulldown HA-tagged MAPK3. (B) Further validation of losing interaction after removal of NBR1 domain. MAPK3:3xHA was transiently co-expressed with Joka2:GFP, ΔPB1:GFP, ΔZZ:GFP, ΔNBR1:GFP, ΔPZN:GFP or EV:GFP in 4 weeks old N. *benthamiana* leaves and proteins were extracted 2 days after agroinfiltration. Immunoprecipitation (IP) was obtained by using anti-GFP antiserum and total protein extracts were immunoblotted with appropriate anti-HA

and anti-GFP antisera. Compared to the pulled down Joka2 and mutant Joka2 levels, truncating NBR1 had the strongest effect on MAPK3-Joka2 interaction. Removal of ZZ domain also showed significant decrease of interacted MAPK3 levels, however, protein level of ΔZZ was the lowest compared to other pulled down proteins. Red asterisks indicate the protein bands with expected molecular weight.

4.3.5.5 MAPK6 shows similar interaction pattern with Joka2

The fact that MAPK3 and MAPK6 are homologous proteins in the Group-A subfamily of MAP kinases directed me to speculate that those kinases might be interacting through the same region of Joka2 even though MAPK3 and MAPK6 have different affinities *in vivo* (Figure 4.15). In order to investigate the region of the autophagy cargo receptor for its binding to MAPK6, I used the same approach that I used for MAPK3, that is, to utilise truncated Joka2 constructs to pull down MAPK6. GFP tagged Joka2, ΔZZ, ΔNBR1, or empty vector control were transiently co-expressed together with HA-tagged MAPK6 in N. *benthamiana* leaves and analysed by western blot. Figure 4.15 shows that MAPK6 behaves similar to MAPK3 in terms of its affinity to domains of Joka2, but with subtle differences. Removal of NBR1 reduced the interaction of MAPK6 notably (Figure 4.15). Taking account of the data obtained from MAPK3-Joka2 interaction study, observing a similar reduction in MAPK6-Joka2 affinity upon NBR1 removal led me to focus on the NBR1 domain (Chapter 5).

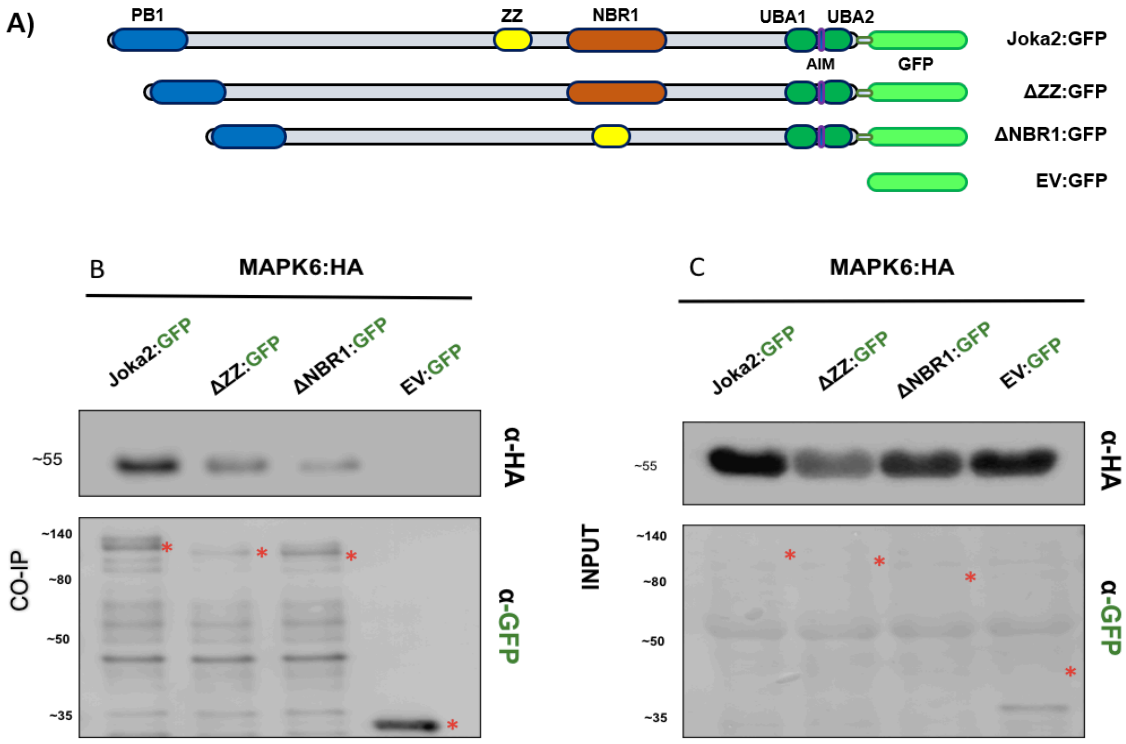


Figure 4.15. MAPK6 interacts with Joka2 and mutants lacking ZZ and NBR1 domains. (A) Schematic domain organisation of GFP-tagged Joka2, ΔZZ, NBR1 and EV that are used to pulldown HA-tagged MAPK6. (B) Co-immunoprecipitation of MAPK6 with Joka2 and its truncated versions *in planta*. MAPK6:3xHA was transiently co-expressed with Joka2:GFP, ΔZZ:GFP, NBR1:GFP and EV:GFP in 4 weeks old *N. benthamiana* leaves and proteins were extracted 2 days after agroinfiltration. Immunoprecipitation (IP) was obtained by using anti-GFP antiserum and total protein extracts were immunoblotted with appropriate anti-HA and anti-GFP antisera. MAPK6 was detected in pull-downs of Joka2 and its mutants lacking ZZ and NBR1 domains. Red asterisks indicate the protein bands with expected molecular weight.

4.3.5.6 PAL interacts with Joka2 despite of no obvious subcellular colocalisation with Joka2 puncta

PAL is an important enzyme in the process of producing the plant hormone salicylic acid (SA). This hormone has been studied and is known for its role in plant immunity. The previous data (Figure 4.16) showing that silencing *PAL* led me to continue working with PAL, even though there was no distinctive accumulation of PAL signal with Joka2 puncta (Figure 4.16). Concentrating GFP-tagged Joka2 and its truncated versions (ΔPB1, ΔZZ, ΔNBR1 and ΔPZN) with GFP-trap beads together with co-expressed HA-tagged PAL

revealed that PAL had affinity to all those proteins except the control EV:GFP. This finding depicts a different picture compared with the Joka2 MAPK3/6 interaction; PAL might be binding through UBA domains in a ubiquitin dependent manner.

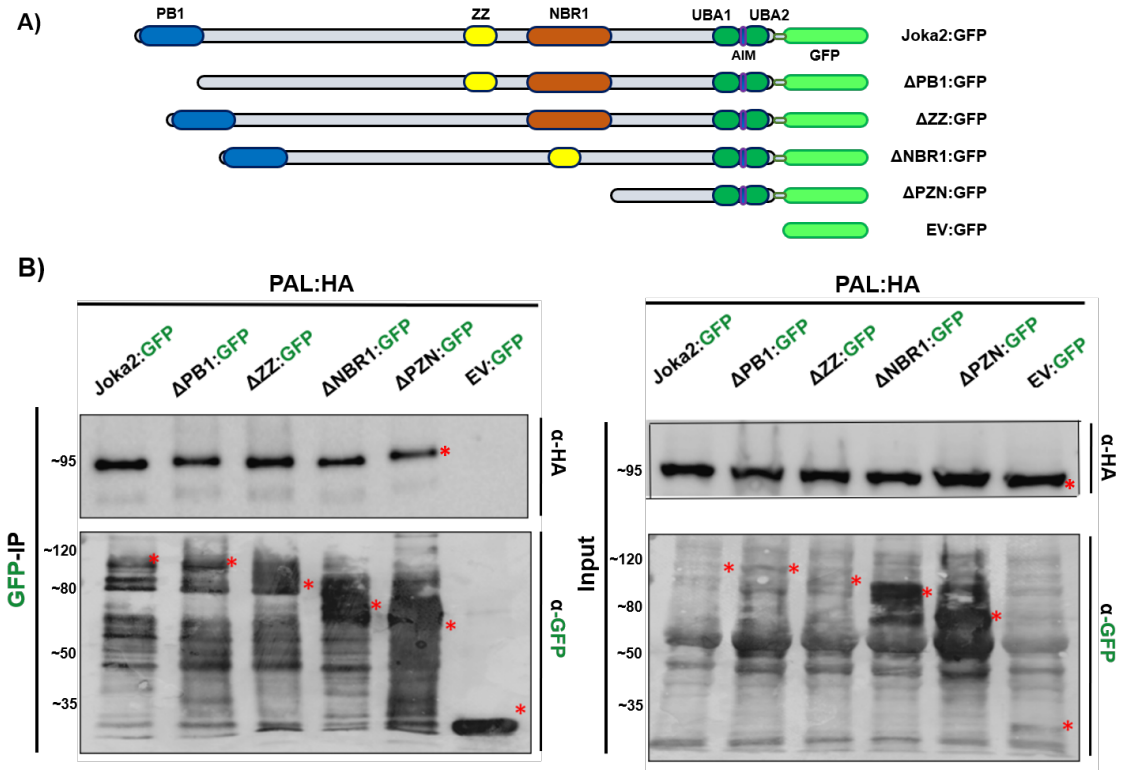


Figure 4.16. PAL interacts with both wild type Joka2 and all truncated mutants. Schematic domain organisation of GFP-tagged Joka2, ΔPB1, ΔZZ, ΔNBR1, ΔPZN and EV that are used to pulldown HA-tagged PAL. (B) Co-immunoprecipitation of PAL with Joka2 and its truncated versions *in planta*. PAL:HA was transiently co-expressed with Joka2:GFP, ΔPB1:GFP, ΔZZ:GFP, ΔNBR1:GFP, ΔPZN:GFP or EV:GFP in 4 weeks old *N. benthamiana* leaves and proteins were extracted 2 days after agroinfiltration. Immunoprecipitation (IP) was obtained by using anti-GFP antiserum and total protein extracts were immunoblotted with appropriate anti-HA and anti-GFP antisera. PAL not only interacts with Joka2 but also with all truncated versions of it. Red asterisks indicate the protein bands with expected molecular weight.

4.3.5.7 PAL associates with Joka2 in a UBA depended manner

In order to test that notion of PAL-Joka2 interaction through UBA domains, I utilized the truncated Joka2 which lacks all the domains but UBA domains, and a Joka2 mutant which is non-functional at its UBA domains. Wild type Joka2 and EV control were also used as positive and negative controls, respectively (Figure 4.17). The data suggested that UBA domains by themselves were enough to interact with PAL, even though the affinity to UBAs was not as strong as to the full length Joka2 (Figure 4.17). Supporting this, Joka2 with mutated UBA domains lost its affinity significantly to PAL. These results suggest that PAL is binding to UBA domains of Joka2.

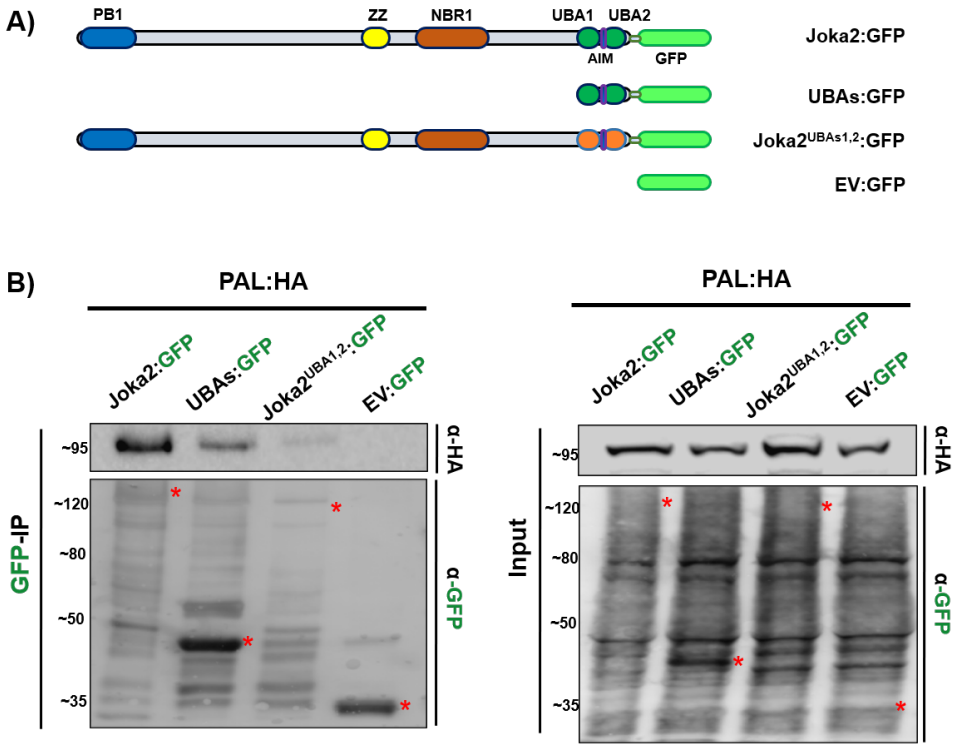


Figure 4.17. PAL interacts with both wild type Joka2 and its UBA domains regardless of their polyubiquitin binding abilities. (A) Schematic domain organisation of GFP-tagged Joka2, UBAs, UBAs^{1,2} and EV that are used to pulldown HA-tagged PAL. (B) Co-immunoprecipitation of PAL with Joka2 and its truncated versions *in planta*. UBA^{1,2} lacks binding ability polyubiquitin chain. PAL:HA was transiently co-expressed with tagged Joka2:GFP, UBAs:GFP, UBAs^{1,2}:GFP or EV:GFP in 4 weeks old *N. benthamiana* leaves and proteins were extracted 2 days after agroinfiltration. Immunoprecipitation (IP) was obtained by using anti-GFP antiserum and total protein extracts were immunoblotted with appropriate anti-HA and anti-GFP antisera. PAL can interact with UBA domain even though UBA domain does not bind to polyubiquitin chain. Red asterisks indicate the protein bands with expected molecular weight.

4.3.5.8 PAL is heavily ubiquitinated in the cells

In order to investigate the nature of PAL-UBA interaction, I designed an experiment in which I used only UBA domains (functional and unfunctional) to avoid the interference of other Joka2 domains (Figure 4.18). Joka2:GFP and EV:GFP were used as controls. PAL:HA was transiently co-expressed with those GFP tagged constructs *in planta*. WB was carried out with appropriate antibodies. This time an antibody against ubiquitin was used to determine if the co-immunoprecipitated PAL was ubiquitinated. Harsh stripping conditions were provided to make sure detachment of antibodies before proceeding to detect with the next antibody. The figure below showed that the pulled down PAL together with Joka2 or its mutants were mostly ubiquitinated. The ubiquitination level of PAL was slightly higher with UBAs compared to UBAs^{1,2}. Even the protein detection for the total protein extract showed that PAL is highly ubiquitinated *in vivo* (Figure 4.18B). In conclusion, PAL appears to be ubiquitinated regularly in the cells and that the UBA domains, functional or not, interact with PAL and can be pulled down in co-IP.

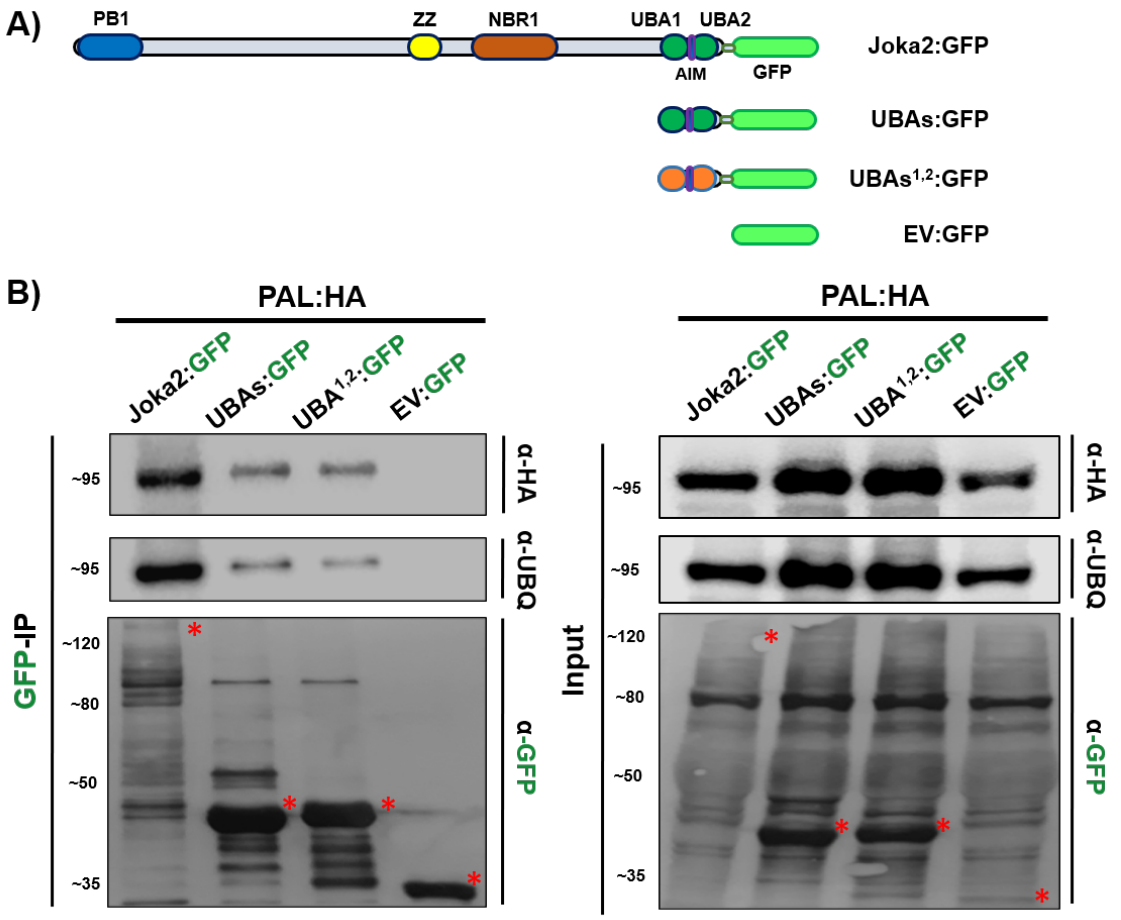


Figure 4.18. PAL interacts with both wild type Joka2 and its UBA domains regardless of their polyubiquitin binding abilities. (A) Schematic domain organisation of GFP-tagged Joka2, UBAs, UBAs^{1,2} and EV that are used to pulldown HA-tagged PAL. (B) Co-immunoprecipitation of PAL with Joka2 and its truncated versions *in planta*. UBA^{1,2} lacks binding ability to polyubiquitin chain. PAL:HA was transiently co-expressed with tagged Joka2:GFP, UBAs:GFP, UBAs^{1,2}:GFP or EV:GFP in 4 weeks old *N. benthamiana* leaves and proteins were extracted 2 days after agroinfiltration. Immunoprecipitation (IP) was obtained by using anti-GFP antiserum and total protein extracts were immunoblotted with appropriate anti-HA and anti-GFP antisera. PAL can interact with UBA domain even though UBA domain does not bind to polyubiquitin chain. Red asterisks indicate the protein bands with expected molecular weight.

4.3.6 Impact of Joka2 on regulating MAPK3 and MAPK6 protein stability

4.3.6.1 Overexpression of Joka2 does not substantially affect MAPK protein levels

Validation of MAP kinase-Joka2 binding led me to investigate the protein stability of MAP kinases upon overexpression or silencing of Joka2, as Joka2 is required for selective clearance of autophagy substrates that are to be degraded. MAP kinases 3 and 6 stability might not be significantly affected by Joka2 abundance, as I found that MAPK3 did not have a high affinity to UBA domain region of Joka2 *in planta* (Figures 4.8 and 4.9). To determine the effect of Joka2 abundance on MAP kinases, Joka2:RFP or GUS:RFP were transiently co-expressed on the opposite sides of a leaf together with GFP-tagged MAPK3, MAPK6 or control in *N. benthamiana*. After crude extraction of the proteins at 3 dpi, the samples were run on an SDS gel and detected by WB. It has been observed that both of the MAPKs were reduced upon Joka2:RFP overexpression (Figure 4.19). However, the control, a free GFP tag, was also stabilized by Joka2 abundance. Due to technical issues, such as the age of the antibodies used, or the abundance of Joka2:RFP, Joka2 protein levels could not be detected with α-RFP antibody. To circumvent this, an antibody against plant NBR1 was utilized to detect both the RFP tagged Joka2 and endogenous Joka2 (NBR1). This NBR1 antibody revealed that Joka2:RFP was indeed expressed and that it was more abundant than the endogenous Joka2. Actin levels were also detected to make sure the loading was equal. This WB result suggested that Joka2 overexpression can potentially increase MAPK3/6 levels.

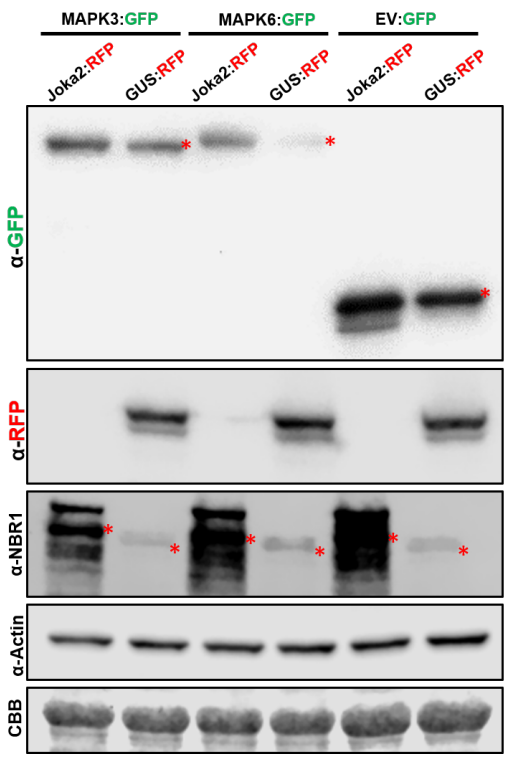


Figure 4.19. MAPK levels might be affected by Joka2 overexpression. MAPK3:GFP, MAPK6:GFP or EV:GFP was co-expressed with Joka2:RFP or GUS:RFP in 3-4 weeks old *N. benthamiana* leaves and protein levels in total extracts were determined three days post agroinfiltration. Protein levels of overexpressed MAPK3, MAPK6 and EV:GFP levels were elevated by overexpression of Joka2. Total protein extracts were immunoblotted with appropriate antisera. Overexpression of Joka2 was shown by using antibody against native Joka2. Gels were stained with coomassie brilliant blue (CBB) and actin levels were detected to show equal loading. Red asterisks indicate the protein bands with expected molecular weights.

Since the previous experiment was not conclusive without a stable control group, I increased the sample number and focussed on one protein at a time for WB. Therefore, MAPK3:GFP or EV:GFP was co-expressed with RFP-tagged Joka2 or GUS in three separate plants. After detection with proper antibodies, MAPK3:GFP and EV:GFP this time showed no noticeable change in protein levels. This supports the idea that overexpression of Joka2 does not lead to degradation or destabilisation of MAPK3 (Figure 4.20).

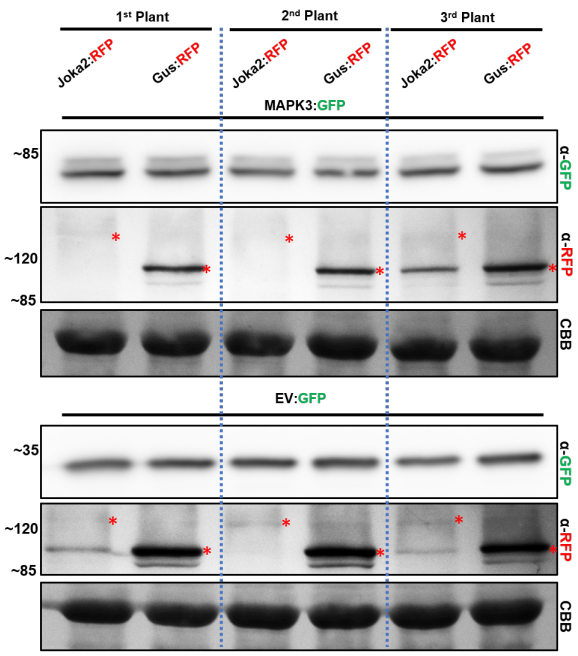


Figure 4.20. Joka2 overexpression does not affect MAPK3 protein levels *in planta*. MAPK3:GFP or EV:GFP was co-expressed with Joka2:RFP or Gus:RFP in 3-4 weeks old *N. benthamiana* leaves and protein levels in total extracts were determined three days post agroinfiltration. MAPK3:GFP and EV:GFP levels did not change when Joka2:RFP or EV:RFP were overexpressed in three different plant leaves. Total protein extracts were and immunoblotted with appropriate antisera. Gels were stained with coomassie brilliant blue (CBB) to show equal loading. Red asterisks indicate the protein bands with expected molecular weights.

In order to further investigate if the protein stability of MAPK3 was regulated by the autophagy degradation process, TAIL:RFP, TAIL^{AIM}:RFP and EV:RFP were co-expressed with MAPK3:3HA and a BFP control (BFP:3HA). TAIL is a small peptide containing the AIM motif of the *P. infestans* effector, *PexRD54*, and this effector blocks autophagy (Pandey, P. *et al.*, 2020). Therefore, degradation of proteins cleared by autophagic flux can be interfered by overexpressing TAIL:RFP . This peptide strongly binds ATG8 so that it blocks the docking site for ATG8-interacting proteins. Hence, this physical intervention by TAIL does not allow ATG8 and autophagy cargo receptors to interact and therefore degradation by autophagy is diminished. As TAIL^{AIM} is mutated at the AIM region and has lost its affinity to ATG8, it is used as a control along with a control for the vector and fluorescent protein, EV:RFP (Figure 4.21). The results support the idea that MAPK3 levels are not affected by autophagy. Even though endogenous ATG8s were overly occupied by TAIL:RFP, i.e. autophagic flux was sabotaged, MAPK3:3HA levels and BFP:3HA levels vary with similar levels to the control groups (Figure 4.21).

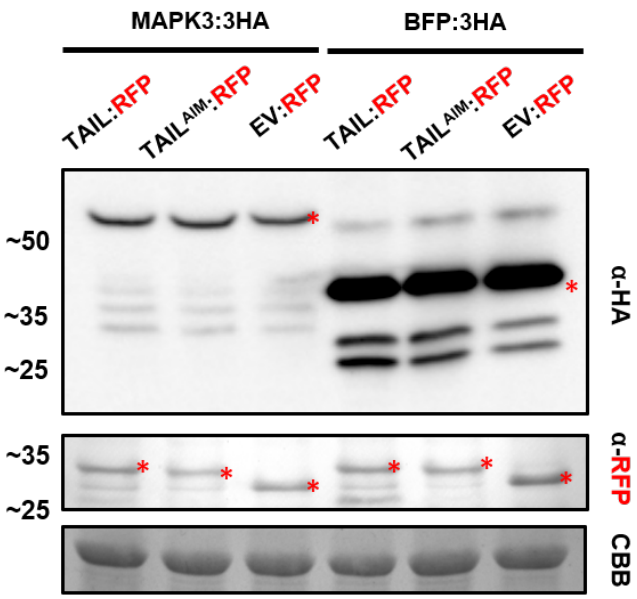


Figure 4.21. Inhibition of autophagy seems to not alter MAPK stability. MAPK3:3HA or BFP:3HA was transiently co-expressed with TAIL:RFP, TAIL^{AIM}:RFP or EV:RFP in 3-4 weeks old *N. benthamiana* leaves and protein levels in total extracts were determined three days post agroinfiltration. Neither MAPK3:3HA nor control BFP:3HA showed significant protein intensity change when they were co-expressed with tagged autophagy inhibitor peptide obtained from PexRD54, TAIL, its non-functional version, TAIL^{AIM}, or EV:GFP control. Total protein extracts were immunoblotted with appropriate antisera. Gels were stained with Coomassie brilliant blue (CBB) to show equal loading. Red asterisks indicate the protein bands with expected molecular weights.

4.3.6.2 Silencing of Joka2 may to slightly stabilize MAPK3 protein level in N. benthamiana

Having checked the protein stability upon overexpression of Joka2, the next step would be to test the protein levels of MAPKs when endogenous Joka2 was silenced. TRV vectors were used to silence all four *Joka2* homologues in *N. benthamiana* seedlings. Grown plants were silenced for the targeted genes and they were ready for agroinfiltration in 3-4 weeks. TRV2:EV was used as control. Since there was no possibility of comparing MAPK protein levels in the same plant because of the systemic silencing by VIGS, several plants were used to average the protein levels in each group. I made a few attempts with GFP tagged proteins (Figure 4.19 and 4.20), however I decided to use HA tagged versions of proteins as they are much smaller so that structurally closer to their native versions.

MAPK3:3HA, MAPK6:3HA or BFP:3HA were transiently expressed in plants carrying TRV2:Joka2 or TRV2:EV. Since the control group, HA-tagged blue fluorescent protein (BFP:3HA) was abundantly expressed, I had to lower the OD_{600} of agrobacteria for this

construct. Samples collected from four plants were processed in the same tube to obtain total protein extract, which was run on SDS-gel. HA detection revealed that BFP:3HA control signal was similar in both Joka2 silenced and mock silenced lanes (Figure 4.22). In contrast with the previous finding where MAPK6 protein level was enhanced, HA tagged MAPK6 did not show noticeable difference between Joka2 silenced and non-silenced plants. Unlike MAPK6, MAPK3 showed a similar pattern with the previous finding and had higher protein stability when Joka2 was silenced (Figure 7.7). This result suggests that Joka2 might have a preferential regulatory function towards MAPK3 protein stability.

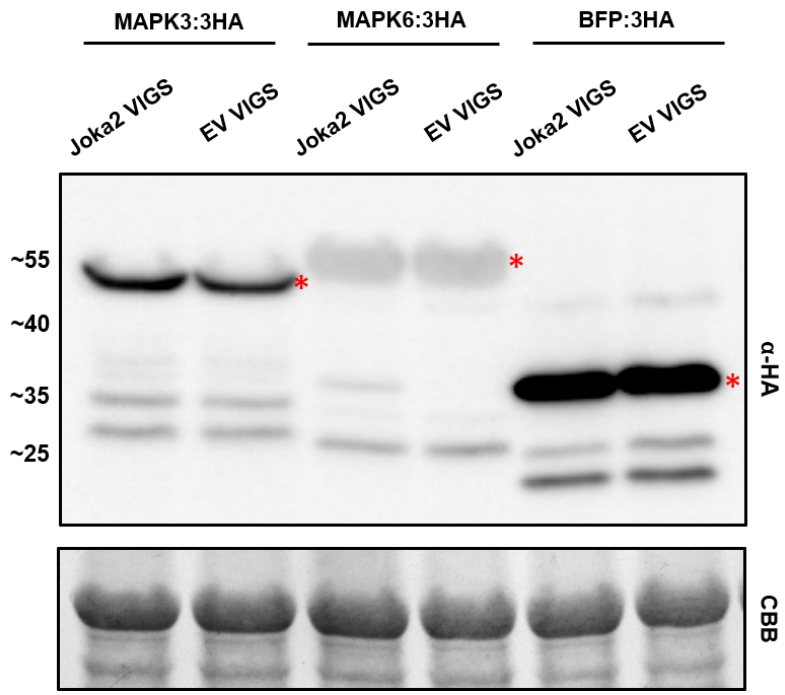


Figure 4.22. Silencing Joka2 in plants may cause protein stability of MAPK3. MAPK3:3HA, MAPK6:3HA or BFP:3HA was transiently overexpressed in plants knocked down for Joka2 or EV (mock silencing). 3-4 weeks old *N. benthamiana* leaves were agroinfiltrated and protein levels in total extracts were determined two days post agroinfiltration. MAPK3:3HA seems to be stabilized upon Joka2 knock down unlike unchanged levels of MAPK6:HA and control BFP:HA. Leaf tissues from four individual plants were used per sample to get average protein levels. Total protein extracts were immunoblotted with appropriate antisera. Gels were stained with Coomassie brilliant blue (CBB) to show equal loading. Red asterisks indicate the protein bands with expected molecular weights.

In order to make sure *Joka2* was silenced in the plants that were used in the second experiment to test protein stability of MAPKs, Joka2 protein levels was determined by using an α-NBR1 antibody. Total protein extracts from four plants were processed to determine if Joka2 was silenced *in planta*. This antibody is raised against the UBA domains of *Arabidopsis* NBR1 (Joka2), therefore it can bind with other UBA domain containing proteins. This presents a problem as a smear on the lanes is produced because the antibody binds to many proteins and degraded Joka2 products on the membrane (Figure 4.23). Thanks to Joka2's high molecular weight, it can be detected individually on the membrane (red asterisks). Silencing Joka2 by VIGS results in this high molecular weight band not being present (Figure 4.23). This WB result showed that the silencing by TRV2:Joka2 generated by me was functional at eliminating translation of Joka2.

As a complementary experiment to show the silencing capacity of TRV2:Joka2, I have overexpressed potato Joka2, tagged with RFP, on *Joka2* silenced or mock silenced plants. Luckily, the nucleotide sequence of potato Joka2 is close enough to *N. benthamiana*'s, as when the samples were processed to be detected for RFP signal, Joka2:RFP was either not detectable or significantly reduced in Joka2 silenced plants (Figure 4.24). That result demonstrates that VIGS construct TRV2:Joka2 is strong enough to silence even overexpressed protein Joka2:RFP.

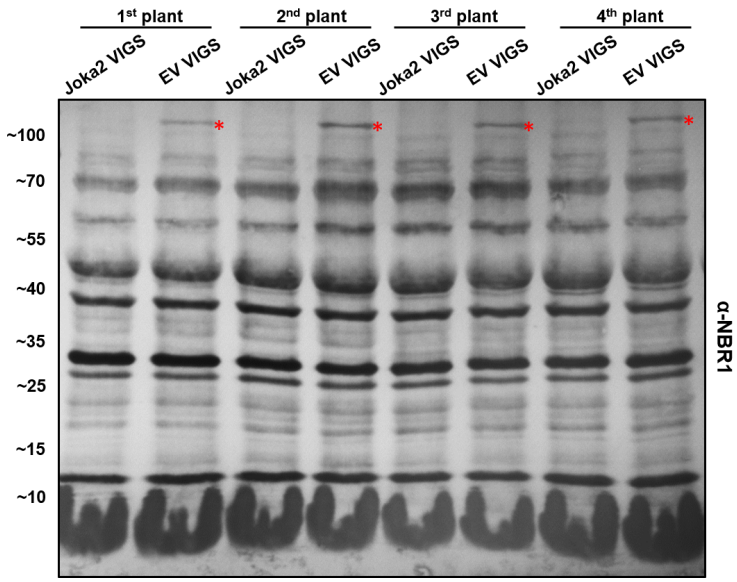


Figure 4.23. Validation of silencing of Joka2 in *N. benthamiana* by using VIGS. Total protein extracts from four plants expressing either TRV2:Joka2 or TRV2:EV were immunoblotted with anti-NBR1 antiserum from 3-4 weeks old *N. benthamiana*. The polyclonal antibody against plant NBR1 (Joka2) is raised to recognize UBA domains of Joka2, therefore, it produces multiple bands on western blot by detecting various proteins baring UBA domains and the degradation product of Joka2. Red asterisks indicate the protein bands with expected molecular weights.

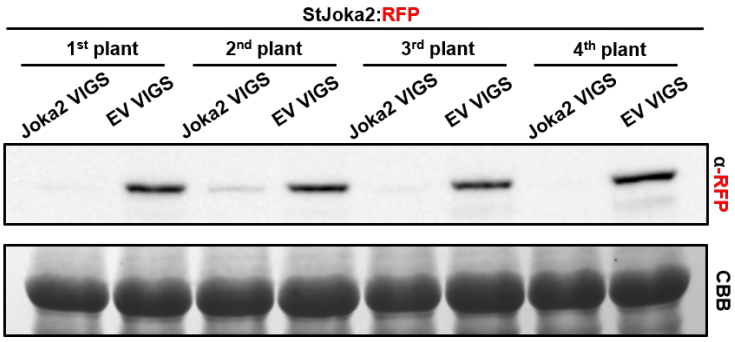


Figure 4.24. VIGS of *StJoka2* also knocks down *NbJoka2*. StJoka2:RFP was transiently expressed in 3-4 weeks old *N. benthamiana* leaves which were silenced for Joka2 or EV (mock). Protein levels in total extracts of four plants per silencing construct were determined three days post agroinfiltration. Overexpression of StJoka2:RFP was suppressed by TRV2:Joka2 plants, however, mock silenced plants kept expressing StJoka2:RFP. Total protein extracts were immunoblotted with appropriate antisera. Gels were stained with coomassie brilliant blue (CBB) to show equal loading. Red asterisks indicate the protein bands with expected molecular weights.

4.4 DISCUSSION

Autophagy is, as the name implies, a degradation process. However, the mechanism itself and the components individually can play different roles in the cell. I and my colleagues have been observing autophagic vesicles and their related proteins regulating immune-related responses negatively or positively against the pathogens, specifically against *P. infestans* (Dagdas, Y. F. *et al.*, 2016). One of those components of autophagy, Joka2, is a well-known cargo receptor in this machinery, and has been reported to reduce filamentous pathogen growth (Dagdas, Y. F. *et al.*, 2016). However, how Joka2 manages to enhance immunity in plants is not documented.

The work of Dagdas *et al.* suggested that Joka2 could mediate selective degradation of some negative regulators of immunity by autophagy, which in turn enhances plant immunity (Dagdas, Y. F. *et al.*, 2016). In addition to this, subcellular localisation of Joka2 was investigated in detail under infection conditions and it has been shown that Joka2-autophagosomes are diverted to pathogen interface (Chapter 3). Localisation of Joka2 puncta towards the haustoria of the pathogen has been shown to be needed to suppress the pathogen invasion (Chapter 3)(Dagdas, Y. F. *et al.*, 2018). But, why are Joka2 autophagosomes diverted towards the haustoria? One possibility could be that recruitment of Joka2-autophagosomes towards haustoria could be a plant strategy to deploy defence related signalling complexes and/or antimicrobial components to the pathogen interface. For instance, some autophagy and defence signalling components are targeted to the pathogen interface in intracellular pathogenic salmonella infected mouse cells (Tattoli, I. *et al.*, 2012). To address this question, one of the goals of this chapter was to identify the components of the perihaustorial Joka2-autophagosomes.

Joka2 was found to pull down various proteins implicated in immune signalling and stress responses (Table 4.1). In order to investigate their impact on resistance *to P. infestans*, I employed RNAi mediated gene silencing of *PDX*, *PAL*, *MAPK3*, *MAPK6*, and *MAPK9* and measured biotrophic pathogen growth (Figure 4.1). Data revealed that silencing of *PDX*, *MAPK6* or *MAPK9* did not profoundly alter the spread of the infection. This could be due to genetic redundancy, insufficient knocking down of the genes or presence of *P. infestans* effectors that already effectively supress PDX, MAPK6 and

MAPK9 activities against biotrophic growth of the pathogen. Because *N. benthamiana* is an allotetraploid plant, i.e. a hybrid with four sets of haploid genes, the mRNA sets are not completely conserved. This situation causes the risk of not knocking down the target genes.I have shown that the primary mRNA levels of PAL, MAPK3, MAPK6 and MAPK9 were decreased in those silenced plants, however, I do not have an evedince to show the same result with PDX (appendix Figure 7.8). Simultaneous silencing of other MAPKs that interact with Joka2 could help clarify the issues with genetic redundancy of MAPK6 and MAPK9. In contrast to silencing of *MAPK6/9* or *PDX*, I have observed significant susceptibility towards *P. infestans* when *MAPK3* or *PAL* is knocked down (Figure 4.1). The necrotrophic growth of the pathogen could be imaged by using a UV light source as the dead tissue fluoresces under UV light. That would prevent any mistake made by eye comparison of the dead tissue. However, for this imaging uniform illumination was required, which was not available to me. In order to detect more natural biotrophic growth, the wild type pathogen hyphae could be stained with trypan blue, the spore number would be counted per area of infection or some house-keeping gene from the pathogen could be quantified on infection sites.

Among the interactors of Joka2, PDX and PAL are enzymes involved in pathways producing metabolites and compounds in response to biotic and abiotic stress. The role of PDX in abiotic stress conditions is well documented. Since the final products produced by PDX and its homologs, (which are mainly vitamin B6 derivatives) possess antioxidant properties, PDX to contributes to resilience against the stress conditions via scavenging reactive oxygen species. In *Arabidopsis*, for instance, mutants deficient for PDX were sensitive to high light intensity because of photo-oxidative stress (Havaux, M. *et al.*, 2009), whereas PDX over-expressing lines were more tolerant to high oxidative stress due to its capacity produce more vitamin B6 in the plant (Titiz, O. *et al.*, 2006; Vanderschuren, H. *et al.*, 2013). Furthermore, in *Arabidopsis* and *S. Lycopersicum*, by altering host cell antioxidant capacity, PDX contributed to defence against the necrotrophic fungus *Botrytis cinerea* (Zhang, Y. *et al.*, 2015; Zhang, Y. *et al.*, 2014). Primary infection assays did not show a significant difference in the spread of the pathogen when PDX is silenced via RNA interference in *N. benthamiana* leaves (Figure 4.1). For future experiments, infection assays should be repeated in Joka2-

overexpression/silencing /knockout background to monitor for potential perturbation in Joka2-mediated immunity.

Transient overexpression of GFP:PDX did not show any colocalisation with Joka2 puncta. This finding along with the fact that silencing of PDX does not affect pathogen growth led me to not continue with PDX for subsequent experiments. Intriguingly, GFP:PDX altered the subcellular distribution of Joka2 (Figure 4.3). Even though Joka2 can be observed as puncta at 3 dpi in the cells, based on the personal and collective experience in the laboratory, overexpression of PDX resulted in most of the Joka2:BFP localising to the central vacuole of the cells. It is possible that PDX stimulates autophagy resulting in enhanced uptake of Joka2 and associated cargoes in autophagosomes. As the central vacuole of epidermal cells is responsible for both storage and/or degradation of its content, the stability of Joka2 should be measured via a time course protein blotting assays. Vacuolar GFP signal was not detectable, unlike BFP, when GFP:PDX is overexpressed with Joka2:BFP. However, GFP is a pH sensitive probe and it does not produce fluorescence signal in acidic compartments such as vacuoles or apoplasts. To eliminate loss of signal from PDX, if it is also directed to the vacuole, a construct with a pH stable tag (such as RFP) should be used. Furthermore, the colocalisation experiments can be repeated in infected tissue to monitor for disturbance in the perihaustorial distribution of Joka2 puncta as a result of PDX overexpression or silencing. In summary, although the direct relationship between Joka2 and PDX is not yet clear, there could be crosstalk between the two proteins, where PDX could have a regulatory role in Joka2-mediated plant resistance.

In order to validate association of Joka2 to PDX, other potential protein-protein interaction methods can be utilised. Instead of co-IP, relatively easier methods such as bimolecular fluorescence complementation (BiFC) and yeast two-hybrid (Y2H) systems can be implemented. In BiFC Joka2 and the target protein carries a tag which can only emits a signal only if Joka2 and PDX comes close in the cell. The signal is detected by fluorescence microscopy (Kerppola, T. K., 2008). Y2H is also relatively an easy method. This method avoids using plant system and based on expressing proteins in yeast cells and only the transfected yeast cells survive with interacting proteins. Another method

utilizing *in-vivo* crosslinking of protein complexes using photo-reactive amino acid analogs can be used to link the proteins near Joka2. Then, tagged PAL or PDX can be detected using western blot or mass spectroscopy (Suchanek, M. *et al.*, 2005). More specific methods can also be considered such as ITC (isothermal titration calorimetry) to find if proteins are interacting *in vitro* conditions. The purified proteins either from bacteria, yeast or plant cells are mixed in a well isolated chamber of the instrument so that even the tiniest thermal change caused by an interaction of two proteins can be detected (Dagdas, Y. F. *et al.*, 2016).

Phenylalanine ammonium lyase (PAL) appeared as an interesting potential interactor of Joka2, because of its well-documented role in the production of precursors of cell wall component such as lignin, antimicrobial phytoalexins and salicylic acid (Huang, J. *et al.*, 2010; Wildermuth, M. C. *et al.*, 2001). In uninfected *N. benthamiana* epidermal leaf cells, PAL did not co-localise with Joka2 puncta (Figure 4.3). These results indicated that PAL may not be a cargo target of Joka2 or that it does not have a regulatory role of Joka2 function in uninfected cells. Confocal microscopy of fluorescently tagged PAL can be carried out in infected leaf tissue for future experiments. As mentioned in the introduction, *P. infestans* is a hemibiotrophic pathogen that requires living cells to colonize in the early stages of its infection cycle, then switching to a necrotrophic lifestyle at later stages. Our analyses show that although the necrotrophic pathogen growth is reduced when *PAL* is silenced, biotrophic pathogen growth is enhanced, evidenced by increased sporulation (Figure 4.2). To support these findings, we documented the hyphal growth of the pathogen by using a fluorescently labelled *P. infestans* strain. Similarly, in rice, a *PAL* mutant was more vulnerable to diseases including bacterial blight, rice blight and sheath blight (Tonnessen, B. W. *et al.*, 2015). In *Arabidopsis* and tobacco, lack of PAL activity led to increased susceptibility to phytopathogens (Maher, E. A. *et al.*, 1994; Somssich, I. E. *et al.*, 1998). But how can PAL determine the pathogen lifestyle during infection? As mentioned earlier, PAL is a key enzyme in SA biosynthesis that functions in defence against necrotrophic pathogens. Silencing of PAL can reduce SA production, which is sensed by the pathogen that then adopts a more biotrophic infection strategy. Interestingly, autophagy-deficient *Arabidopsis* mutant lines show enhanced accumulation of SA are more prone to

infection by necrotrophic pathogens suggesting that autophagy might regulate SA production (Yoshimoto, K. *et al.*, 2009). It would be interesting to investigate the roles of Joka2 and PAL in these processes.

PAL did not colocalise with Joka2 puncta in epidermal cells, however I have shown that PAL interacts with Joka2 by using co-IP (Figure 4.16), therefore confirming the proteomics screen of Joka2. In order to narrow down the region where PAL interacts with Joka2, I conducted multiple co-IPs with Joka2 mutants to pull down PAL. Unlike MAPK3/6, PAL did not lose its affinity to Joka2 when its main characterised domains (PB1, ZZ and NBR1) were truncated (Figure 4.16). N-terminal domains of Joka2 do not seem essential for PAL -Joka2 interaction, I designed an experimental setup using GFP tagged UBAs and Joka2^{UBA1,2} (Figure 4.17A). This co-IP showed a significant decrease of PAL-Joka2 interaction with the Joka2 mutants either lacking the N-terminal region up to UBA domains or functional UBA domains themselves. This suggests that PAL requires intact Joka2 to sustain stable binding affinity for Joka2 but interaction is not dependent on that region. Furthermore, ubiquitin binding ability of Joka2 seems to be important for PAL binding affinity to Joka2 as PAL signal drops substantially when the UBA domains are non functional.

Having found that UBA domains are important for Joka2-PAL interaction, I reasoned that it would be of interest to check ubiqutination of PAL. Ubiqutination of proteins occurs, in general, to direct the ubiquitinated protein towards the proteosome and/or autophagosomes for degradation. Therefore, PAL could pull-down with Joka2 because it is ubiquitinated for degradation. In order to investigate further, I used the smallest constructs of Joka2 with UBA domains, UBAs and UBAs^{1,2}, which eliminates any potential interaction with the other Joka2 domains (Figure 4.18). Co-IP revealed that ubiquitin signal was detected in all the lanes where PAL:HA was also present, which means some amount of PAL was ubiquitinated. It is impossible to determine the percentage of ubiquitinated PAL as there is no way to compare signals coming from two different antibodies in this experimental setup. Interaction of PAL with UBA domains in spite of mutating UBAs to prevent ubiquitin binding suggests that either PAL has an affinity to UBAs regardless of its binding affinity to ubiquitin or PAL was co-precipitated

with UBAs[1,2] because it bears a functional AIM motif which could enable formation of autophagic complexes that interact with PAL. This situatioin can be elucidated by expressing PAL and Joka2 (or UBA domains) separetaly *in planta* or in bacterial/mammalian cells, and test their affinity with *in vitro* assays such as gel filtration chromatography or isothermal titration calorimetry (ITC) before and after treatment with ubiquitinases. To conclude, it is possible that Joka2 regulates the function of PAL in producing precursors for vital elements of plant immunity via interaction with its UBA domains. In the future, an interesting avenue for further research would be to investigate the protein levels of PAL upon Joka2 silencing/overexpression, the effect of PAL on formation of Joka2 positive autophagosomes and how PAL contributes to immunity against *P. infestans*.

(Kerppola, T. K., 2008)The Joka2 interactor screen from infected and uninfected *N. benthamiana* leaves (Bozkurt *et al.*, unpublished) pointed towards some exciting candidate Joka2-interactors including proteins that play important roles in PTI signalling, such as mitogen activated kinases 3, 6 and 9 (MAPK3, 6, 9) (Jammes, F. *et al.*, 2009; Mao, G. *et al.*, 2011). MAPK3 and MAPK6 are activated through triggering of receptors on the PTI pathway by a bacterial flagellum peptide derivative (flg22) in *Arabidopsis* (Suarez-Rodriguez, M. C. *et al.*, 2007). Likewise, the hormone-regulated defence-related role of MAPK9 has been documented in plants in the literature (Jammes, F. *et al.*, 2009; Jammes, F. *et al.*, 2011; Khokon, M. A. *et al.*, 2015). Some adapted pathogens deploy effectors that target MAPK signalling cascades, counteracting PTI, to disarm host defence mechanisms and promote successful colonization (Boller, T. *et al.*, 2009). For example, HopAI1, an effector from *Pseudomonas syringae pv. tomato*, de-phosphorylates MAPK3 and MAPK6, which leads to prevention of host defence activation (Li, H. *et al.*, 2007; Rodriguez, M. C. *et al.*, 2010).

As the contribution of MAPKs to immunity is well documented, I prioritized MAPK3 (especially), MAPK6 and MAPK9 throughout my thesis to investigate any link between PTI signalling and Joka2-mediated autophagy. My hypothesis was that PTI signalling could activate defence related autophagy via MAPK-Joka2 interplay or Joka2-mediated autophagy regulates MAPK signalling cascades to enhance plant immunity. The first

thought after observing trafficking of Joka2 puncta towards the pathogen sites was that Joka2 might be regulating protein turnover of MAPKs via selective autophagy under normal physiological conditions. However, upon activation of PTI after pathogen recognition, Joka2 might mediate accumulation of MAPKs at the host-pathogen interface to enhance defence signalling. Consistent with this hypothesis, I have demonstrated that all the candidate MAPK interactors physically associate with Joka2 and Joka2 puncta in the cells via co-IP and confocal microscopy (Figure 4.4 and Figure 4.6).

Since these MAPKs colocalise with Joka2 under uninfected and infected conditions, and interact with Joka2 *in planta*, I hypothesised that MAPKs might be an autophagic cargo of Joka2, and that their degradation could help regulate PTI signalling. The reason that I have not detected MAPK puncta without overexpression of Joka2 would be due to the endogenous protein levels of Joka2 might not be enough to detect by the confocal microscopy detectors. The signal coming from cytoplasmic MAPKs would interfere with small sized Joka2-MAPK puncta formed by native Joka2. However, when both MAPKs and Joka2 are overexpressed together, then there are enough protein association to be spotted by the detectors.

The basic autophagy cargo receptor function of Joka2 is enabled by its UBA domain 2, which binds to ubiquitin chains of proteins targeted for degradation. Therefore, I designed an experiment to test whether Joka2 lacking functional UBA pulls-down with MAPK3. Although binding affinity was reduced, MAPK3 came together with mutant Joka2, Joka2^{UBA1,2} as well as with wild type Joka2. This suggested that MAPK3 might have an internal docking site of Joka2 rather than UBA domains and that MAPK3 is not a ubiquitinated cargo to be degraded. Figure 4.8 and Figure 4.9 revealed that MAPK3 was able to interact with Joka2^{UBA1,2} even though this mutant cannot bind ubiquitinated proteins. However due to protein stability difference in Joka2^{UBA1,2}, it was not possible to discard the prospect that MAPK3 might be still ubiquitinated. However, one important observation made the MAPK3-Joka2 interaction more interesting. I observed a higher protein band on top of Joka2 mutant and MAPK3 when the protein levels were abundant (Figure 4.9, cyan asterisk). This higher molecular weight band indicates that,

when Joka2 is stabilised through mutations on its UBA domains, it might be forming tighter interactions with MAPK3 to produce a higher molecular weight complex.

After confirmation of that MAPK3 was not affected strongly by mutating UBA domains of Joka2, I have focused on the other three main domains of Joka2. Since I generated truncated constructs of Joka2 (ΔPB1 and ΔPZ) in the previous chapter to follow Joka2 puncta in the infected cells, I started to dissect MAPK3's association with the different Joka2 domains. After a co-IP experiment with native Joka2, ΔPB1, ΔPZ and EV (Figure 4.11.), I observed that MAPK3-Joka2 interaction did not rely on the PB1 or ZZ domains of Joka2, therefore my interest moved to other domains like NBR1 or inter-domain regions.

In this co-IP, MAPK3:HA pulled down abundantly by Joka2 without a PB1 domain. The observation of higher protein levels with Joka2 lacking the PB1 domain needs more clarification (Figure 4.12). However, considering the stability patter of Joka2 upon removal of different domains, relative increase in Joka2-MAPK3 interaction in that co-IP result is mostly due to enhanced stability of ΔPB1:GFP compared to Joka2:GFP. Input levels of MAPK3 are not significantly different when it was co-expressed with wild type Joka2 or ΔPZ mutant (lacks PB1 and ZZ domains, Figure 4.11). Another reason might be that in the natural state of Joka2, the PB1 domain might physically interfere with the stable binding of MAPK3. Similar to Zaffagnini *et al.* who observed that removal of PB1 from p62 increased the affinity towards non-linear chains of ubiquitin (Zaffagnini, G. *et al.*, 2018), losing the PB1 domain might increase the binding affinity of Joka2 for MAPK3.

Considering the co-IP data shown in Figure 4.11 and Figure 4.12the potential interaction region of Joka2 and MAPK3 was limited to the NBR1 region of Joka2. UBAs could still bind to MAPK3 in low stringency conditions, however adjustment of OD of *Agrobacteri*um infiltration and stringency of the co-IP revealed that UBAs are not necessary for binding to MAPK3. MAPK6 has shown a very similar pattern when pulled down with Joka2 mutants. This result, combined with the amino acid sequence similarity between MAPK3/6, suggests that MAPK6 might have a similar docking site to Joka2, as MAPK3, which is around the NBR1 domain. MAPK3/6 affinity to the NBR1 domain will be explored in more detail in the following chapter.

Although MAPK9, like MAPK3/6, was also shown to be a potential interactor of Joka2 in the initial IP/MS screen, I focused mainly on the interaction between Joka2 and MAPK3/6. While a proper characterization of MAPK9 and Joka2 needs to be carried out, considering the sequence variation between these MAPKs, I would hypothesise that MAPK9 may interact with Joka2 through other domains. However, this hypothesis needs to be confirmed by protein interaction assays. Supporting the idea that Joka2 might regulate MAPK function, overexpression of Joka2 had an impact on MAPK protein stability (Figure 4.19). Preliminary observations showed that overexpression of Joka2 reduced MAPK9 protein stability. However, silencing of Joka2 on the plants showed a non-complimentary result on MAPK9 stability (Figure 7.5). These experiments should be repeated with higher number of plants, fresh antibodies, smaller construct tag, and confirmation of efficient Joka2 silencing by RNAi. Further assays are required to precisely determine the mechanism and impact of Joka2-MAPK deployment to pathogen interface on plant immunity.

Measuring MAPK3/6 protein levels upon overexpression and silencing of Joka2 somewhat supported that MAPK3 and MAPK6 are not primarily degraded by Joka2 (Figures 4.19 and 4.20). However, these results were more controversial than the co-IP results. Due to failed control groups of some western blotting experiments, MAPK3/6 protein levels in Joka2 overexpression or silencing samples were not convincingly different (Figure 4.20). When I used higher numbers of samples per group and properly expressed controls, the effect of Joka2 on MAPK3/6 stability reduced. One silver bullet experiment would be to exploit the AIM peptide of PexRD54 (TAIL) to test if MAPK3 is affected by overexpression of this construct (Figure 4.21). TAIL:RFP has been shown to inhibit autophagy as it blocks access to the binding pocket of ATG8 for cargo receptors, resulting in the stabilisation of proteins regularly degraded by this recycling process . Its mutated version lacks a functional ATG8-interacting motif (AIM), and therefore has no inhibitory effect on autophagic flux. I have shown that when autophagy was inhibited by TAIL:RFP, MAPK3:HA protein level was similar compared to the control levels at 3 dpi. It would be more rigorous to repeat this experiment at different time points to gain supporting evidence Figure 4.21.

In conclusion, this chapter explored interactions between Joka2 and several candidate interactors that were identified through an IP/MS screen. Interestingly, PDX did not show any co-localisation or interaction through the experiments I have conducted. This is particularly surprising given that PDX had the highest hit counts in the IP-MS Joka2 screen. However, I cannot unequivocally remove its candidacy as a Joka2 interactor due to the limitations of the techniques I used. In general, overexpression of proteins is not a desired condition for identifying the function of proteins or their interactions as abundant proteins might not behave in their natural state. Those overexpressed protein can also change the transcription, translation or past-translational modifications of off target, which can lead to unspecific results. In ideal conditions, it would be preferred to use proteins expressed with their natural promoter and without tags. However, this would not allow us to detect or follow the proteins in subsequent cellular or biochemical experiments. Therefore, I had to use the overexpressed proteins even though the possibility of obtaining risky results.

In contrast to PDX, PAL and MAPKs 3, 6, and 9, were confirmed to interact with Joka2 through subsequent confocal microscopy and co-IP experiments. PAL and MAPK3 showed a significant effect on plant immunity against *P. infestans*. Joka2 seems to interact with MAPK3 and MAPK6 through a region around the NBR1 domain, whereas PAL has affinity to the UBA domains. There is much left to ascertain with PAL regarding its protein stability under Joka2 silencing and overexpression. Moreover, Joka2's impact on SA or cell wall production could be tested to elucidate the importance of the PAL-Joka2 interaction in these processes. Joka2 seems to affect protein levels of MAPK9 however MAPK3/6 protein stability is not primarily regulated by Joka2. To support this conclusion, it would be interesting to replicate some of the work detailed in this chapter in cells where proteasome-mediated degradation is inhibited, as this would eliminate any crosstalk between autophagy and UPS.

CHAPTER 5 – CONTRIBUTION OF JOKA2 TO PLANT IMMUNITY BY STABILISING MAPK3/6 AND ENHANCING PROGRAMMED CELL DEATH

5.1 INTRODUCTION

As explained earlier, plants detect pathogens through surface PRRs and/or intracellular NLR receptors. PRRs transduce signal upon recognition of ligands and activate MAPK signalling cascades. Detection of pathogens activates PTI and leads to upregulated defence-gene expression, generation of reactive oxygen species ROS, and callose deposition at the pathogen interface.

Canonical MAPKs consist of three TEY-type kinases (from A to C) and TDY clade which is designated as group D (Doczi, R. *et al.*, 2012). Group A and B kinases are separated in land plants while group C and D can be found in both land plants and algal species (Kalapos, B. *et al.*, 2019). *N. benthamiana* MAPK3 and MAPK6 belongs to TEY A group kinases. The study published by Lu *et al.*, revealed the relationship between some mitogen-activated protein kinases among several model plants (Lu, K. *et al.*, 2015). Although, they did not include MAPKs from Australian tobacco *N. benthamiana*, the South American tobacco *N. tabacum* WIPK and SIPK (also NTF4) are involved in the study which are the closest orthologs of NbMAPK3 and NbMAPK6, respectively (Figure 5.1).

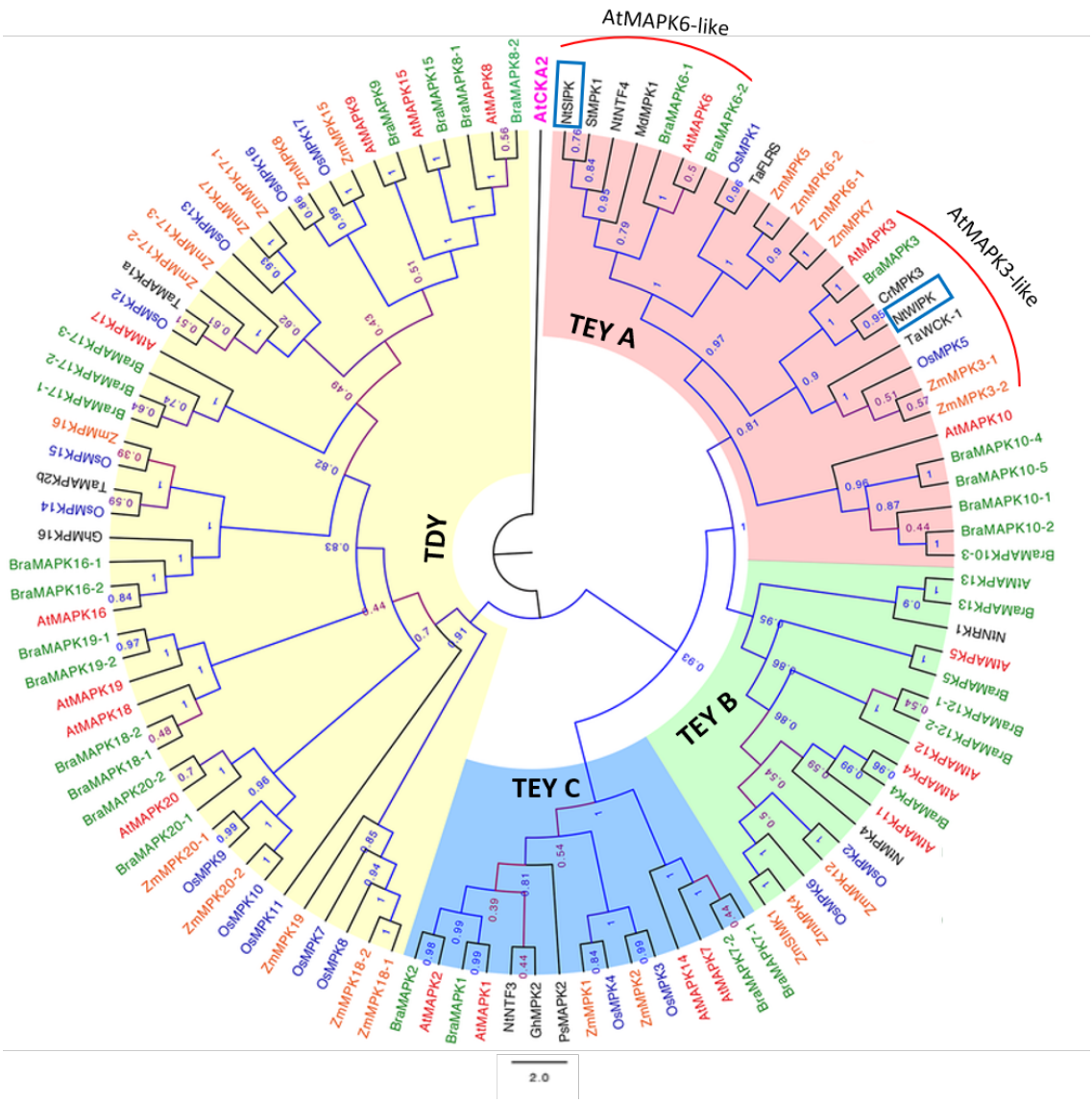


Figure 5.1 Phylogenetic tree of plant MAPKs. The analysis was done by Lu *et. al.*, to show relationship of *A. thaliana*, *B. rapa*, *O. sativa*, *Z. mays*, *C. roseus*, *G. hirsutum*, *M. domestica*, *N. tabacum, P. sativa*, *S. tuberosum* and *T. aestivum* MAPK proteins (Lu, K. *et al.*, 2015). Plant MAPKs cluster in four distinct groups which can be labelled as TEY A (group A), TEY B (group B), TEY C (group C) and TDY (group D) depending on the activation motifs. The tree was constructed by using NJ method with bootstrap analysis (1000 replicates). Adapted from the Figure 2 of research article by Lu *et al.* (2015).

Several studies strengthen the importance of MAPK cascade in plant immunity against pathogens (Cardinale, F. *et al.*, 2002; Meng, X. *et al.*, 2013; Rodriguez, M. C. *et al.*, 2010; Zhang, S. *et al.*, 2001). For example, one of the most well know PRR, FLS2, LRR-RK flg22 (peptide of flagellin) receptor in *Arabidopsis*, along with BRI1-associated kinase (BAK1),

triggers MAPK signalling cascade. Studies showed that MKK3/4-MPK3/4 cascade are involved in this signalling event (Asai, T. *et al.*, 2002; Ichimura, K. *et al.*, 2006; Qiu, J. L. *et al.*, 2008; Suarez-Rodriguez, M. C. *et al.*, 2007). Transcriptome and chromatin immuno-precipitation analyses exhibited that cascade induced by flg22 also controls gene expression of defence responses such as synthesis of camalexin, a phytoalexin in *Arabidopsis*. MAPK3 and MAPK6 are also shown to be activated in response to flg22 in *Arabidopsis* independently of MEKK1 (Suarez-Rodriguez, M. C. *et al.*, 2007). The tight regulation by positive (MPK3/6) and negative (MPK4) signalling cascades controls the fine-tune of the defence response to make decision on death vs. survival (Rodriguez, M. C. *et al.*, 2010).

MAPKs are also involved in ETI part of the plant immunity. In tobacco, for instance, silencing of genes expressing wound-induced protein kinase (WIPK), SA-induced protein kinase (SIPK) and their upstream element MEK2 revealed a vital role of those kinases as activation of them upon sensing of tobacco mosaic virus (TMV) leads to expression of N-resistance genes (Meng, X. *et al.*, 2013; Zhang, S. *et al.*, 1998). Two MAPK-MAPKK pairs in tomato, MEK1-NTF6 and MEK2-SIPK, have been shown to participate in expression of Pto resistance gene (Ekengren, S. K. *et al.*, 2003). It is also worth to mention that some pathogen effectors target MAPK signalling cascade to prevent host defence mechanism (Boller, T. *et al.*, 2009). As mentioned before, HopAI1 bacterial effector both infecting plants and animals, for instance, with its phosphothreonine lyase activity which de-phosphorylates MAPKs, MPK3 and MAPK6, to prevent host defence by inactivating PTI and callose deposition which fortify cell walls (Li, H. *et al.*, 2007; Rodriguez, M. C. *et al.*, 2010). There are hundreds of probable substrates of MAPK3 and MAPK6, which were in a proteomic assay by several groups (Hoehenwarter, W. *et al.*, 2013; Lassowskat, I. *et al.*, 2014) which shows the diverse signalling function of these to MAPKs.

One important aspects of MAPK proteins that they can interact with scaffold proteins to reach signalling specificity. Those proteins regulates activities of MAPKs by altering the subcellular localization of MAPKs, compartmentalizing positive and negative feedback loops, providing physical proximity to MAPKKs or phosphatases, and isolating

them from interacting with other MAPK substrates (Bequette, C. J. *et al.*, 2018). In recent years, RACK1 was reported to be the first scaffold protein for MAPKs in plants (Cheng, Z. *et al.*, 2015; Su, J. *et al.*, 2015). This protein can bind to bind to the MEKK1, the MKK4 and MKK5, and the MAPK3 and MAPK6.

5.2 AIM

In the previous chapter, I have shown that MAPKs are not the cargos of Joka2 to be degraded. Since they are associated to the internal structure of Joka2 and orthologs of Joka2, p62 and NBR1, are shown to be a scaffold proteins for some signalling pathways, I decided to investigate the possibility of Joka2-MAPKs in this extent. I aimed to focus on the region responsible for Joka2-MAPK3 interaction which can hint the outcome of this interaction. Moreover, I decided to investigate the possible regulatory effect of Joka2 on MAPK signalling by testing Joka2's impact on cell death caused by activated MAPKs. These approaches can unlock the functional principles of the MAPK signalling and its link to defence-related autophagy. Revealing the functional link or network between these processes would enhance our capacity to engineer plant immunity.

5.3 RESULTS

5.3.1 Impact of NBR1 domain on Joka2-MAPK association and plant immunity

I have left Chapter 4 without finalizing the story about domain(s) of Joka2 responsible for MAPK3/6 interactions. Therefore, here I focus on concluding the story and consequences of said interactions.

5.3.1.1 NBR1 domain is crucial for Joka2 to interact with MAPK3 but not with MAPK6

In Chapter 4, the region of Joka2 required for its interaction with MAPK3 was narrowed down to the NBR1 region. As no ordered protein structure around the NBR1 region is present, I decided on using the NBR1 domain in isolation, to check if it has affinity for MAPK3 by itself. To do this, I generated a GFP tagged construct of only NBR1 domain, and I included this construct in a co-IP experiment in which Joka2:GFP, mutated Joka2 version ΔNBR1:GFP and EV:GFP were used to pulldown HA-tagged *N. benthamiana* MAPK3 (Figure 5.2). Joka2 and its mutated version, ΔNBR1, pulled down MAPK3 as expected (in line with co-IPs presented in Chapter 4). The affinity of MAPK3 to ΔNBR1 was drastically reduced compared to wild type Joka2, when levels of input and IP of the GFP signals are considered. Intriguingly, NBR1 domain itself was enough to pulldown MAPK3 (Figure 5.2B). This suggests that a stable interaction between the two proteins requires full length Joka2, however, NBR1 is the main domain for the MAPK3-Joka2 interaction.

Confirming that MAPK3 had an affinity towards NBR1, prompted me to test if the same region is responsible for MAPK6-Joka2 interaction. The same setup as the previous co-IP (Figure 5.2B) was executed where MAPK3:3HA was switched with MAPK6:3HA (Figure 5.3B). The result, somewhat surprisingly considering the homology of MAPK3 to MAPK6, pointed out that MAPK6 was not behaving like MAPK3 in terms of its affinity to Joka2 (Figure 5.4).

Although ΔNBR1:GFP has less affinity to MAPK6, a reasonable amount of interaction remains compared to MAPK3, as shown in Figure 5.3B. Complementary to this, the NBR1 domain itself did not show any sign of an interaction with MAPK6:3HA (Figure 5.3B).

These suggest that MAPK6 might be binding somewhere close to NBR1 or that the interaction requires the intact 3D structure of Joka2 to have a strong affinity.

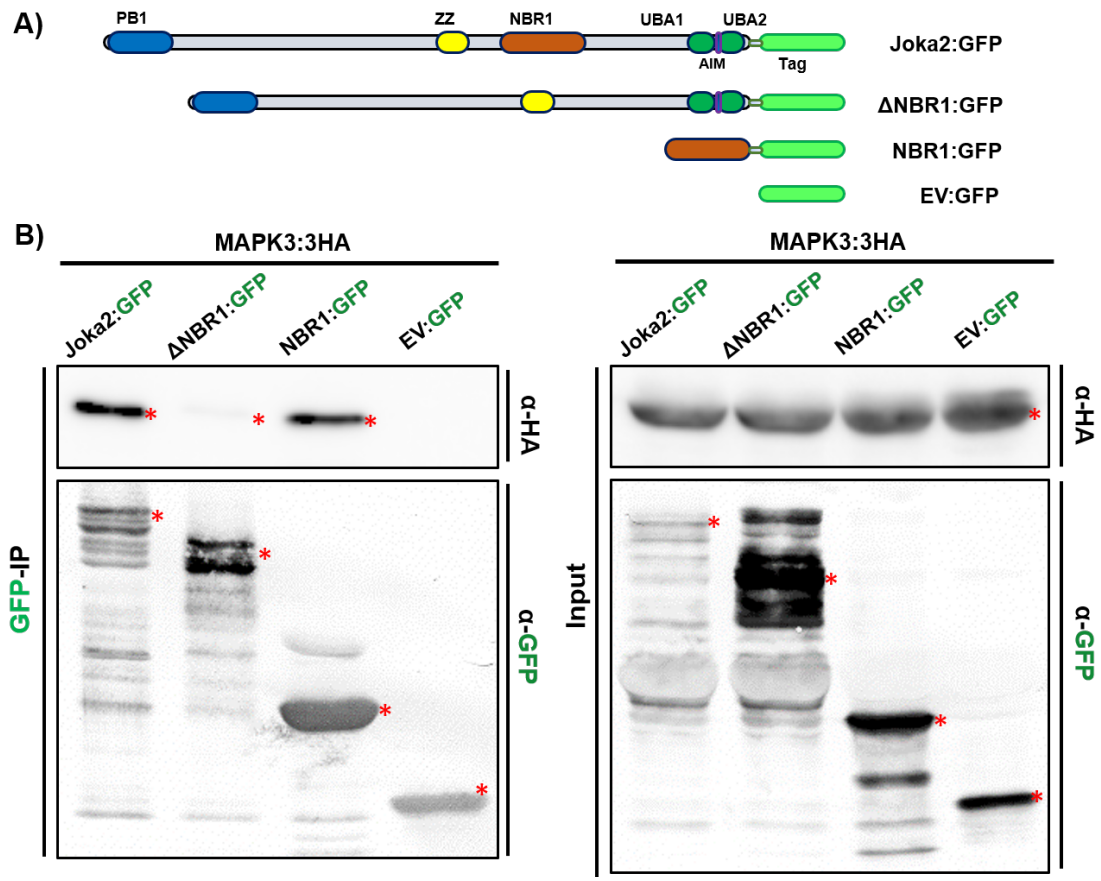


Figure 5.2. NBR1 domain of Joka2 is the site of MAPK3 interaction. (A) Schematic showing domain organisation of GFP-tagged Joka2, ΔNBR1, NBR1 and EV control used to pulldown HA-tagged MAPK3. (B) Validation of NBR1 domain and Joka2 association *in planta*. MAPK3:3HA was transiently co-expressed with Joka2:GFP, ΔNBR1:GFP, NBR:GFP or EV:GFP in 4 weeks old *N. benthamiana* leaves and proteins were extracted 2 days after agroinfiltration. Immunoprecipitation (IP) was obtained by using anti-GFP antiserum and total protein extracts were immunoblotted with appropriate anti-HA and anti-GFP antisera. Although it is not as strong as wild type Joka2, MAPK3 still shows affinity when only NBR1 domain of Joka2 is present. Red asterisks indicate the protein bands with expected molecular weight.

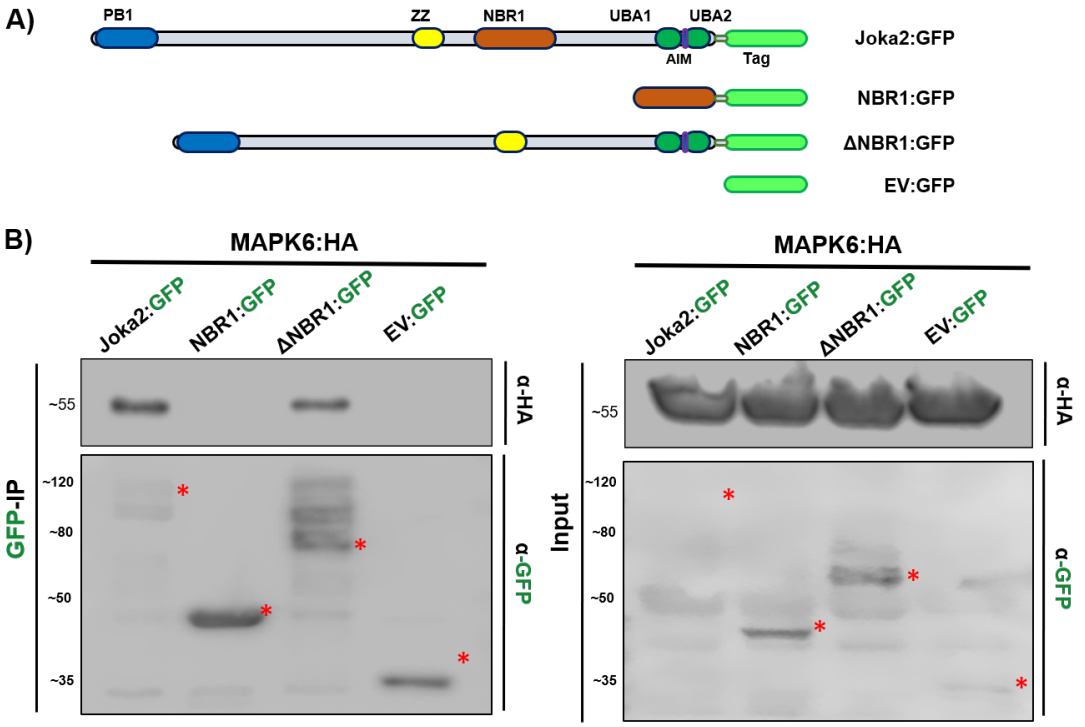


Figure 5.3. MAPK6 does not have an affinity to NBR1 domain. (A) Schematic domain organisation of GFP-tagged Joka2, NBR1, ΔNBR1 and EV control that are used to pulldown HA-tagged MAPK6. (B) Co-immunoprecipitation of MAPK6 with Joka2 and its truncated versions either lacking NBR1 domain or other domains except NBR1 domain. MAPK6:3HA was transiently co-expressed with Joka2:GFP, NBR:GFP, ΔNBR1:GFP or EV:GFP control in 4 weeks old *N. benthamiana* leaves and proteins were extracted 2 days after agroinfiltration. Immunoprecipitation (IP) was obtained by using anti-GFP antiserum and total protein extracts were immunoblotted with appropriate anti-HA and anti-GFP antisera. MAPK6 retained its affinity to ΔNBR1 and did not show detectable affinity to the NBR1 domain in isolation. Red asterisks indicate the protein bands with expected molecular weight.

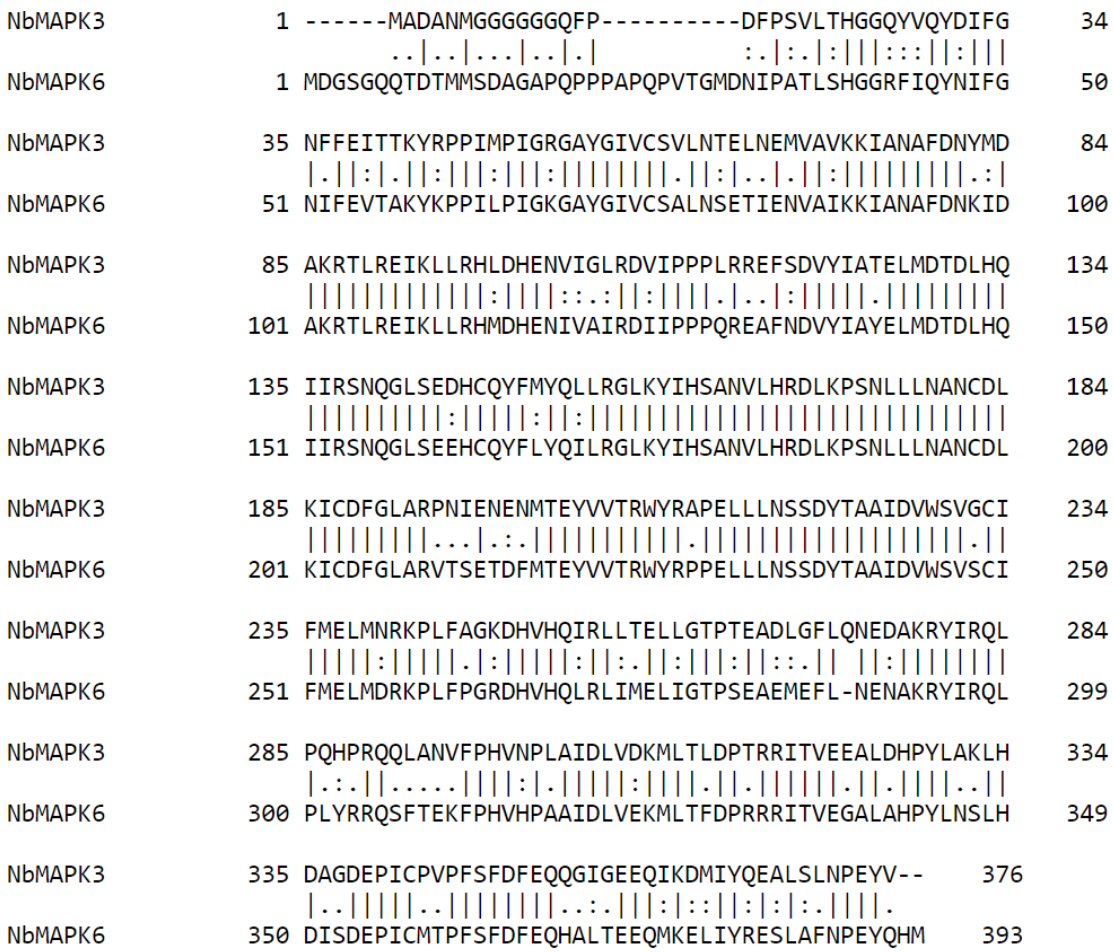


Figure 5.4. Pairwise comparison of *N. benthamiana* MAPK3 and MAPK6. The amino acid sequences of MAPK3 and MAPK6 are globally aligned using the Needleman-Wunsch algorithm (Sievers, F. *et al.*, 2011). Comparison of *N. benthamiana* MAPK3 and MAP6 revealed 80 % similarity (69.8% identity). Vertical lines (|) indicate identical amino acid match, colons (:) show amino acids with similar properties and single dots (.) are for any positive score for the compared amino acids. A space is used for a mismatch or a gap.

5.3.1.2 Truncation of NBR1 domain interferes with the enhanced immunity mediated by Joka2

To investigate if removal of NBR1 region, responsible for the Joka2-MAPK3 interaction, affects Joka2-mediated immunity, I measured the necrotic pathogen growth on plants transiently expressing control group and targeted proteins on opposite sides of the leaf. Joka2, ΔNBR1 and EV control groups were compared to each other. This infection assay demonstrated that Joka2 kept its immunity enhancing ability whereas the mutant lacking NBR1 domain, ΔNBR1, lost its ability to reduce pathogen spread on the leaf (Figure 5.5).

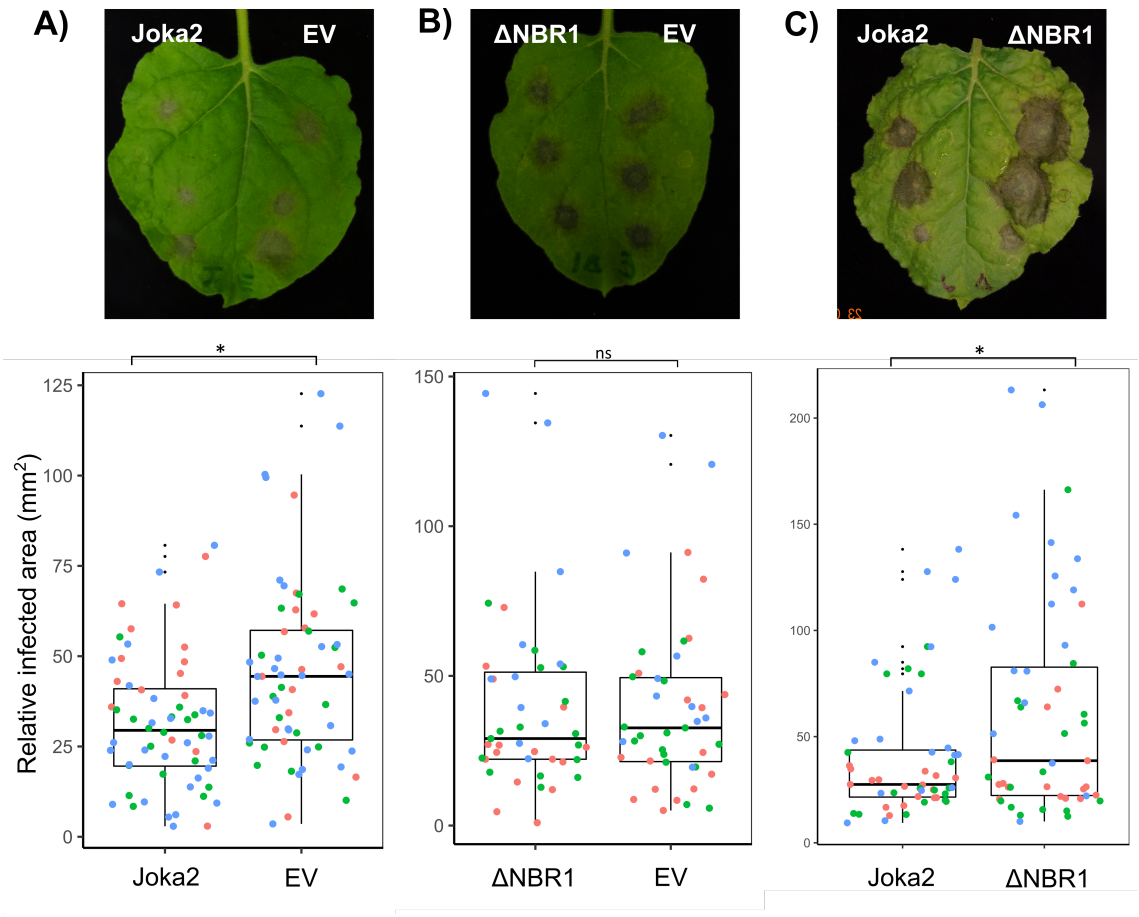


Figure 5.5. Removal of NBR1 abolishes Joka2-mediated plant immunity against *P. infestans*. A) The side of the leaf overexpressing of Joka2 is more resistant compared to the side expressing EV:HA control (A), whereas ΔNBR1 overexpression is unable to elevate resistance to *P. infestans* (B). This pattern was consistent when Joka2 and ΔNBR1 were overexpressed side by side (C). Images were obtained 7-8 days post infection. Boxplots represent quantification of the area of necrotic disease lesions obtained through three independent experiments. Overall, there is a significant difference with Joka2 overexpression but not with ΔNBR1 overexpression. The paired samples Wilcoxon test was used to test meaningful differences between means. Asterisks mean P<0.05 and ns is an acronym of "not significant".

5.3.1.3 Bacterial expression vectors were generated to test in vitro MAPK3-NBR1 binding

Having discovered the domain responsible for the MAPK3-Joka2 interaction, and also showing that loss of this interaction influences plant immunity, I started investigating if this interaction was direct, i.e. whether or not there is an additional protein acting as a bridge between MAPK3 and Joka2. Since the co-IP experiments I have been carrying out are all done from the crude extracts of plants, we cannot eliminate the involvement of

other proteins. Therefore, physical binding of MAPK3 and NBR1 should be confirmed through an *in vitro* binding approach.

In order to achieve this, I cloned MAPK3 and NBR1 in pOPIN vectors in order to express these proteins in *E. coli* B21(DE3) strain. Although there was no detectable sign of MAPK3 or NBR1 when I ran the samples from bacteria on an SDS polyacrylamide gel Figure 5.6A, upper panel), the proteins where detected upon western blotting against the N terminal His tag present on the proteins Figure 5.6A, lower panel). The protein levels were not as high as ATG8CL expressed in *E. coli*, which was used as a positive control. Regardless, the purification was continued utilizing a cobalt affinity resin (Figure 5.6B) to enrich the recombinant proteins. Although this enrichment was successful, it did not provide a pure/clean final product.

Size exclusion chromatography (SEC, or gel filtration chromatography) was implemented to further purify MAPK3 and NBR1 via size difference of the extracted proteins (Figure 5.7B). A relatively pure sample of NBR1 was achieved after size exclusion chromatography, as can be seen from the UV absorption graph and SDS gel (yellow and red dotted boxes, Figure 5.7A and B), however the concentration of the final product was low. MAPK3 purification, on the other hand, provided a higher concentration of MAPK3 (yellow dotted box) but lower protein purity (other proteins in the red dotted box, Figure 5.7C-D). Further experiments, such as ion exchange chromatography, need to be carried out to optimize the purification methods for MAPK3 and NBR1, and to prove the physical interaction of these two proteins *in vitro*.

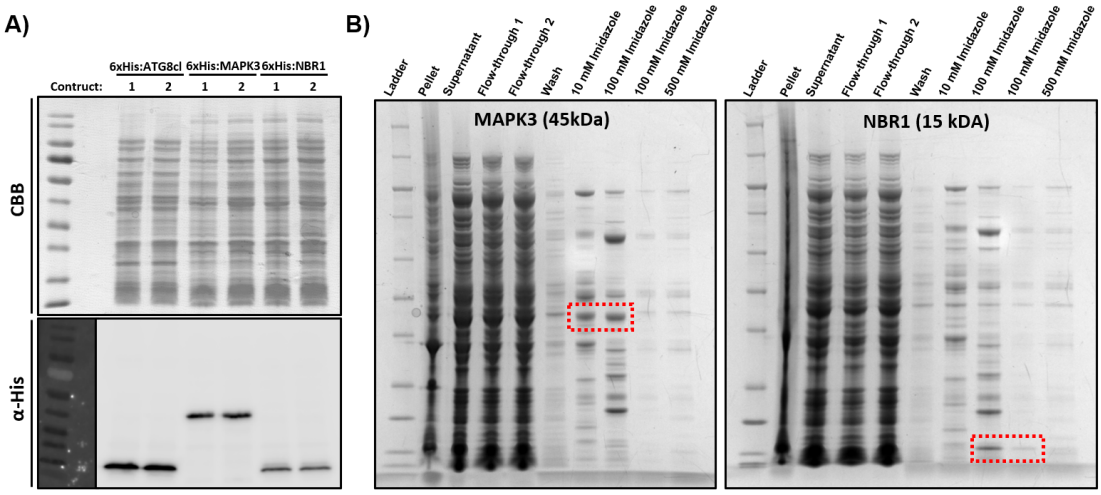


Figure 5.6. MAPK3 and NBR1 can be expressed in bacteria and purified with cobalt columns. A) E. coli BL21(DE3) was used for bacterial expression of 6xHis-tagged MAPK3 and NBR1. Two samples were started from two different stocks of E. coli (1, 2). CBB staining was not enough to reveal MAPK3 or NBR1 expression even post induction, unlike ATG8CL positive control. B) MAPK3 and NBR1 were pulled down by using Cobalt column. CBB staining of the gels show concentration of MAPK3 and NBR1 after purification step. Red dotted boxes are indicating the protein band corresponding to 6xHis tagged MAPK3 (B, left) and NBR1 (B, right).

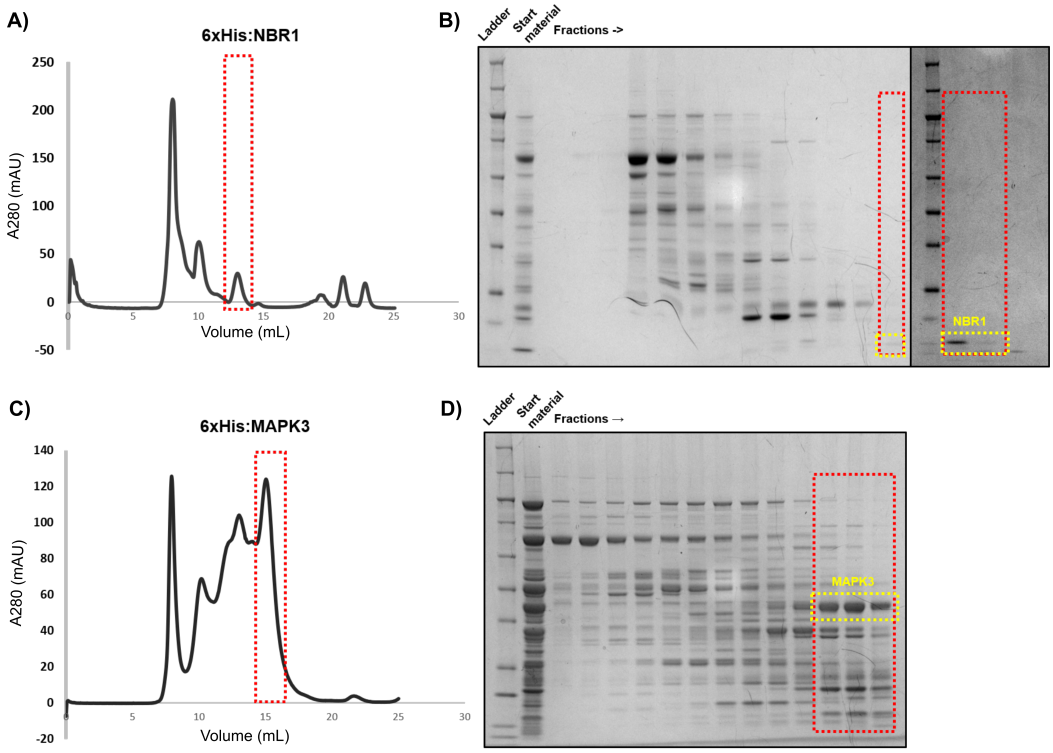


Figure 5.7. SDS-PAGE of fractions obtained after size exclusion chromatography of His-tagged NBR1 and MAPK3. NBR1 (A) and MAPK3 (C) were passed through a gel filtration chromatography column to separate them from other bacterial proteins after cobalt column, the graphs represent the elution profile at 280nm. SDS-PAGE of the fractions obtained from the chromatography showed that NBR1 (B, yellow dotted box) can be obtained almost pure (red dotted boxes), however, fractions containing MAPK3 (D, yellow dotted box) still retain other bacterial proteins (red dotted box).

5.3.2 Joka2 might serve as a scaffold for immune related proteins in MAPK signalling pathway

5.3.2.1 Co-expressing MAPK9 and MAPK3/6 enhances their interaction with Joka2

Throughout Chapter 4 and in the first section of this chapter, I have shown that MAPKs implemented in plant immunity interact with Joka2 and it seems like this interaction might link PTI signalling to Joka2-mediated plant immunity. While focusing on Joka2-MAPK protein interaction, I noticed from the IP/MS data that while protein hits of MAPK3 and MAPK6 were increasing upon infection (Table 4.1), MAPK9 was showing lower protein hits after infection. This led me to postulate that MAPK3/6 might be competing with MAPK9 to bind to Joka2, and infection by *P. infestans* might adjust

Joka2's binding profile to MAPKs associated with Joka2. To test this, I designed an experiment where I pull down GFP tagged Joka2 when MAPK9 and MAPK3/6 were expressed individually or together, such that I could observe lowered affinity of one of the MAPKs when the other one was binding to Joka2 (Figure 5.8).

To my surprise, when I conducted the co-IP experiments, I noticed that MAPK9 and MAPK3/6 levels were higher when they were co-expressed compared to their expression with EV control. These blots obtained from SDS-PAGE also revealed something unexpected; there were higher molecular weight bands and expression of MAPKs together with Joka2 was yielding a slightly stronger signal (Figure 5.8 A and B, blue asterisks). This data suggested that despite my previous hypothesis where MAPKs were competing to interact with Joka2, Joka2 might serve as a scaffold for different MAPKs to bind and form higher molecular weight multi-protein complexes.

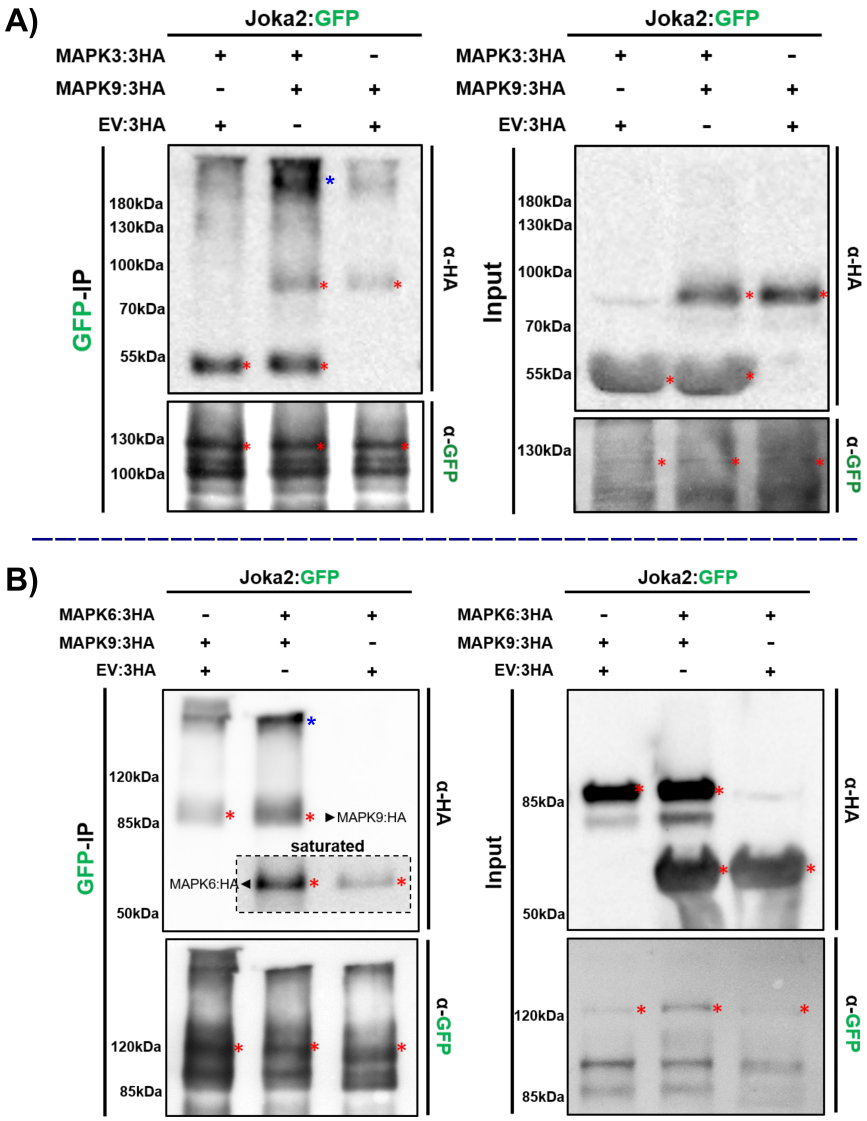


Figure 5.8. Joka2 might be serving as a scaffold protein for MAPK3 and MAPK6 to form high molecular weight multiprotein complexes with MAPK9. (A-B) Co-immunoprecipitation of MAPK9 - MAPK3/6 with Joka2 *in planta*. GFP-tagged Joka2 was transiently co-expressed with combinations of MAPK9:3HA, EV:3HA, and MAPK3:3HA or MAPK6:3HA in 4 weeks old *N. benthamiana* leaves and proteins were extracted 2 days after agroinfiltration. Immunoprecipitation (IP) was obtained by using anti-GFP antiserum and total protein extracts were immunoblotted with appropriate anti-HA and anti-GFP antisera. When MAPK3/6 were co-expressed with MAPK9, Joka2 seems to pull-down more MAPK3/6 and MAPK9 when they are expressed together in the plant cells. Red asterisks indicate the protein bands with expected molecular weight. Blue asterisks show unexpected high molecular weight bands.

5.3.2.2 Joka2 also pulls down MAPK-kinase that can phosphorylate MAPK3 and MAPK6

Since I suggest that MAPKs might be forming a complex together with Joka2, I speculated that the upstream elements of this MAPK signalling should be interacting with Joka2 as well. Therefore, I found the MAPK kinase that is reported to phosphorylate MAPK3/6 in tobacco and *Arabidopsis*. Arabidopsis has two MAPK kinases, MKK4 and MKK5, which are homologs of tobacco MEK2, and these kinases all activate MAPK3/6. I cloned *N. benthamiana* MEK2 into a vector carrying C-terminal multiple HA tag and utilised this to check if it was immunoprecipitated with Joka2 pull down (Figure 5.9). MAPK3 was used as a positive control, as it is known that MEK2 binds to MAPK3 to phosphorylate it. When GFP-tagged MAPK3, Joka2 and EV were immunoprecipitated, MEK2:HA came along with both MAPK3 and Joka2. That data suggests that Joka2 interacts with upstream MAPK signalling element, MEK2, as well as MAPK3 and MAPK6.

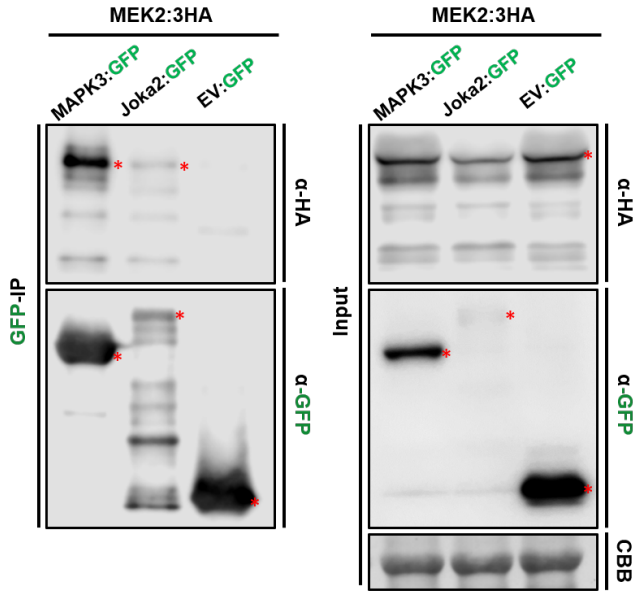


Figure 5.9. Validation of Joka2 and MEK2 association *in planta*. MEK2:3HA was transiently co-expressed with GFP-tagged MAPK3, Joka2 or empty vector control in 4 weeks old *N. benthamiana* leaves and proteins were extracted 2 days after agroinfiltration. Immunoprecipitation (IP) was obtained by using anti-GFP antiserum and total protein extracts were immunoblotted with appropriate anti-HA and anti-GFP antisera. MEK2, an upstream MKK in MAPK3/6 signalling pathway, associates with Joka2. Red asterisks indicate the protein bands with expected molecular weight.

5.3.3 Joka2 stabilises MAPK3/6 and enhances programmed cell death

Having shown that Joka2 interacts with multiple MAPK signalling proteins, potentially serving as a scaffold protein, I needed to demonstrate the outcome of these interactions. What does a multiprotein complex interacting with Joka2 do? Is Joka2 mediated immunity dependent on PTI signalling? These were the main questions to be answered.

5.3.3.1 MAPKs can be activated by treatment with P. infestans *extract or autoactive MEK2*

To be able to understand the link between Joka2 and MAPK signalling I had to find a way to detect the function of MAPKs. As MAPKs function through subsequent phosphorylation events, I used an antibody that detects phosphorylated forms of MAPK3 and MAPK6. To tests its binding ability towards *N. benthamiana* MAPKs, I utilised the *P. infestans* extract to mimic infection and trigger PTI. I infiltrated leaves with the extract and collected leaf tissues subsequently in different time points (Figure 5.10). After processing the leaf tissues and detecting the phosphorylated MAPKs, I found three things: i) the antibody was working on phosphorylated *N. benthamiana* MAPK3/6, ii) one hour after treatment with *P. infestans* extract was a good point to detect the phosphorylated enzymes and iii) either endogenous MAPK3 levels or the antibody's detection ability for phosphorylated MAPK3 was low.

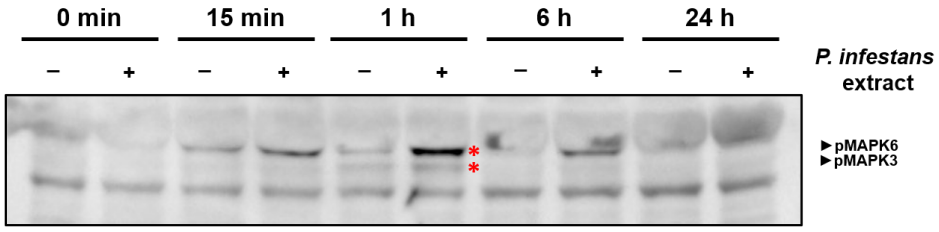


Figure 5.10. Phosphorylated MAPK3/6 levels are highest 1 hour after treatment with *P. infestans* extract. *P. infestans* extract or water was infiltrated on opposite sides of the leaves, and some leaf tissue was taken to be processed at the time points indicated in the figure. Leaf tissues from three individual plants were used per sample to get average protein levels and total protein extracts were immunoblotted with α-pMAPK antibody. The highest signal levels were obtained after an hour of the treatments, in particularly from MAPK6. Red asterisks indicate the protein bands for indigenous MAPK6 and MAPK3 from top to bottom.

Since *P. infestans* extract is full of PAMPs, potentially triggering multiple PTI pathways, to get specific signals from phosphorylated MAPKs (pMAPKs), I generated a MEK2 variant which is constantly active and capable of phosphorylating MAPK3/6, which is called MEK2^{DD} because two amino acids in its active site were replaced by Glu to mimic the negative charge provided by phosphate groups.

I also wanted to show that the constructs I have cloned from *N. benthamiana* cDNA were functional and phosphorylated by PAMP treatment and MEK2^{DD}. Therefore, I designed experiments in which I overexpressed MAPK3 and MAPK6 tagged with GFP (increasing their molecular weight to enable separation on SDS-PAGE from endogenous MAPKs), and activated PTI either by expressing MEK2^{DD} or by PAMP treatment (Figure 5.11A and B, respectively). EV:HA and water were used as. When MEK2^{DD} was expressed, both endogenous MAPK6 and MAPK6:GFP were heavily phosphorylated, whereas phosphorylation levels or detection of phosphorylation of endogenous MAPK3 and MAPK3:GFP were remarkably low (Figure 5.11A). Another important observation was that MEK2^{DD} was strongly triggering cell death which resulted in lower amounts of GFP tagged MAPKs, control group and even RuBisCO levels (PS staining). *P. infestans* extract was a better option to phosphorylate all MAPKs especially the endogenous ones. pMAPK6:GFP had again a stronger signal compared to pMAPK3:GFP, although MAPK6:GFP had lower protein levels than MAPK3:GFP (Figure 5.11B).

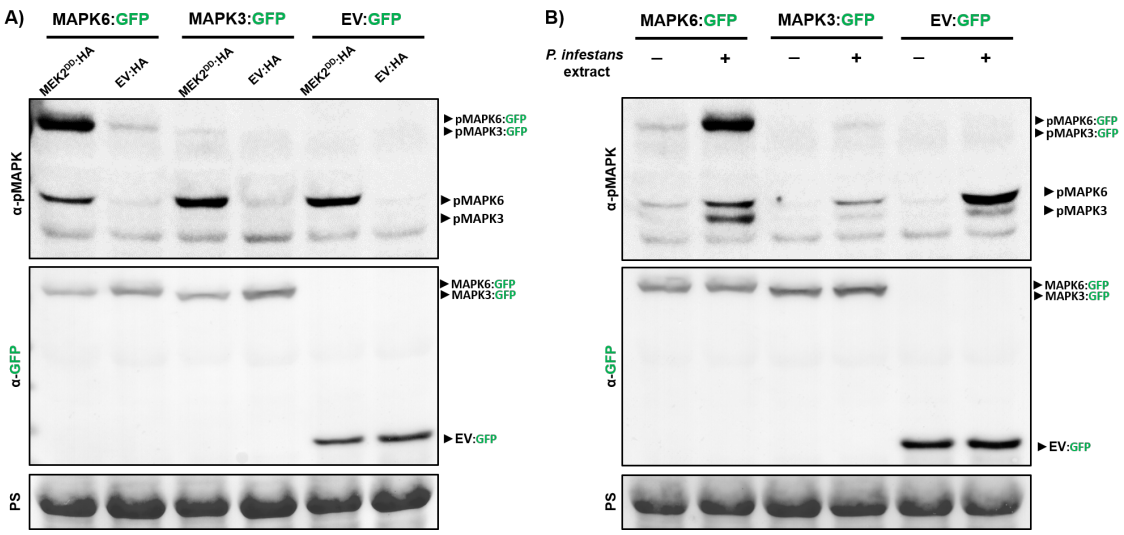


Figure 5.11. The tagged proteins generated from *N. benthamiana* MAPK3 and MAPK6 can be phosphorylated by autoactive MEK2 and PAMP treatment. A) MAPK6:GFP, MAPK3:GFP or EV:GFP control were transiently expressed in multiple leaves and expressed for 2 days in *N. benthamiana* leaves. A) At the opposite side of the leaves either MEK2^{DD}:HA or EV:HA were co-expressed with GFP tagged proteins simultaneously. B) The opposite sides of the leaves were infiltrated with water or *P. infestans* extract at 2 days post agroinfiltration and leaf tissue were collected after an hour of this treatment. Total protein extracts were immunoblotted with α-pMAPK and α-GFP antibodies. In both experiments, ectopically and indigenously expressed MAPK6 were heavily phosphorylated (A-B). Indigenous pMAPK3 could be detected in PAMP treatment only (B). pMAPK3:GFP signal was considerably faint but it could only be detected when either MEK2^{DD} was co-expressed or PAMP treatment was implemented. EV:GFP levels were lower when autoactive MEK2 was coexpressed compared to EV:HA control. Gels were stained with PS to show equal loading. RuBisCO amount was consistently lower in plants expressing MEK2^{DD}:HA. These data suggest MAPK3/6 constructs can be phosphorylated and α-pMAPK antibody might not be proper for detection of pMAPK3.

5.3.3.2 MAP kinases 3 and 6 are stabilised when Joka2 is overexpressed

Having confirmed that MAPK3/6 constructs can be used to show the phosphorylation levels and PAMP treatment is a viable approach to show short term signalling patterns, I used GFP tagged MAPKs and the PAMP treatment method to show the effect of Joka2 on PTI signalling. As Joka2 interacts with all abovementioned MAPKs and MEK2, I would expect to find that Joka2 would stabilise phosphorylated MAPK levels as it is a sign of pathogen attack. Thus, GFP-tagged MAPK3 or MAPK6 were transiently co-expressed with Joka2:HA or EV:HA, at 2 days post agroinfiltration PAMP treatment was employed for an hour to activate PTI signalling so that I could measure the levels of phosphorylated kinases (Figure 5.12). The tissues were collected 15 min and 60 min post infiltration to be processed and blotted. pMAPK detection of the experimental groups showed that phosphorylated protein levels were always higher in the groups where Joka2 was overexpressed. However, it is not clear if this is due to more protein levels of GFP-tagged MAPK3/6 or not. This finding might suggest that MAPKs are stabilised upon overexpression of Joka2 which leads to a higher PTI signalling activity.

In order to clarify if MAPK stabilisation was contributing to enhanced phosphorylated protein levels to support the findings in Figure 5.12, I conducted a similar experiment using MAPK6:GFP and $MEK2^{DD}$ as it is easier to detect pMAPK6 levels (compared to MAPK3), and $MEK2^{DD}$ acts specifically through both MAPK3 and MAPK6 (Figure 5.15), i.e. only MAPK3/6 levels would be affected by autoactive MEK2 (PAMP treatment can fire many other signalling cascades). I increased the number of biological repeats where MAPK6:GFP was co-expressed with $MEK2^{DD}$:HA and either Joka2:HA or EV:HA (Figure 5.13). After detection of MAPK:GFP and phosphorylated MAPK6s (overexpressed and endogenous), this figure suggests that Joka2 stabilises MAPK6 levels so that it enhances MAPK phosphorylation events.

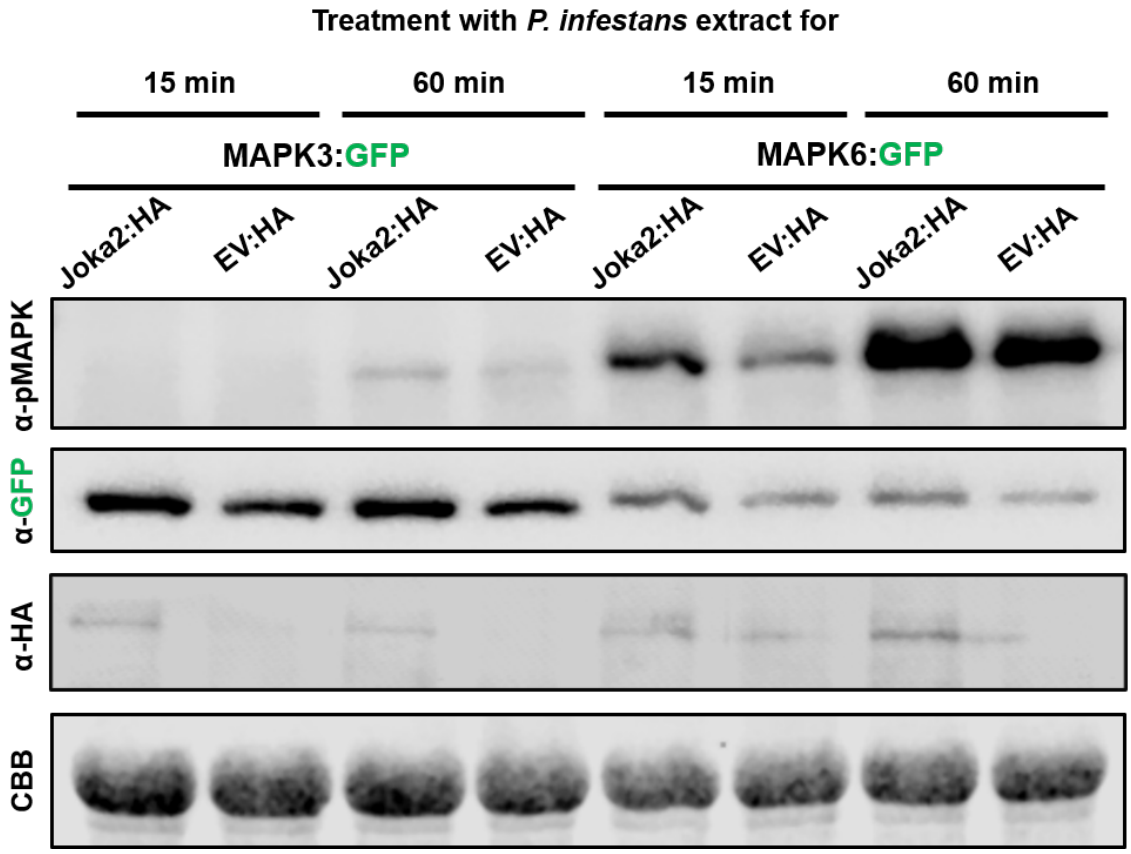


Figure 5.12. Joka2 enhances the protein stability of MAPK3/6 elevating phosphorylated MAPK levels. MAPK3:GFP or MAPK6:GFP was transiently co-expressed with either Joka2:HA or EV:HA in *N. benthamiana* leaves. The leaves were infiltrated with *P. infestans* extract and tissues were collected after 15 and 60 mins of the treatment. Total protein extracts were immunoblotted with α-pMAPK, α-GFP or α-HA antibodies. Joka2:HA stabilized the protein levels of MAPKs (GFP detection), and so that signal from phosphorylated proteins was higher in Joka2 expressing parts of the leaves (pMAPK detection). Joka2 overexpression was confirmed via HA detection. Leaf tissues from three individual plants were used per sample to get average protein levels. Gels were stained with CBB to show equal loading.

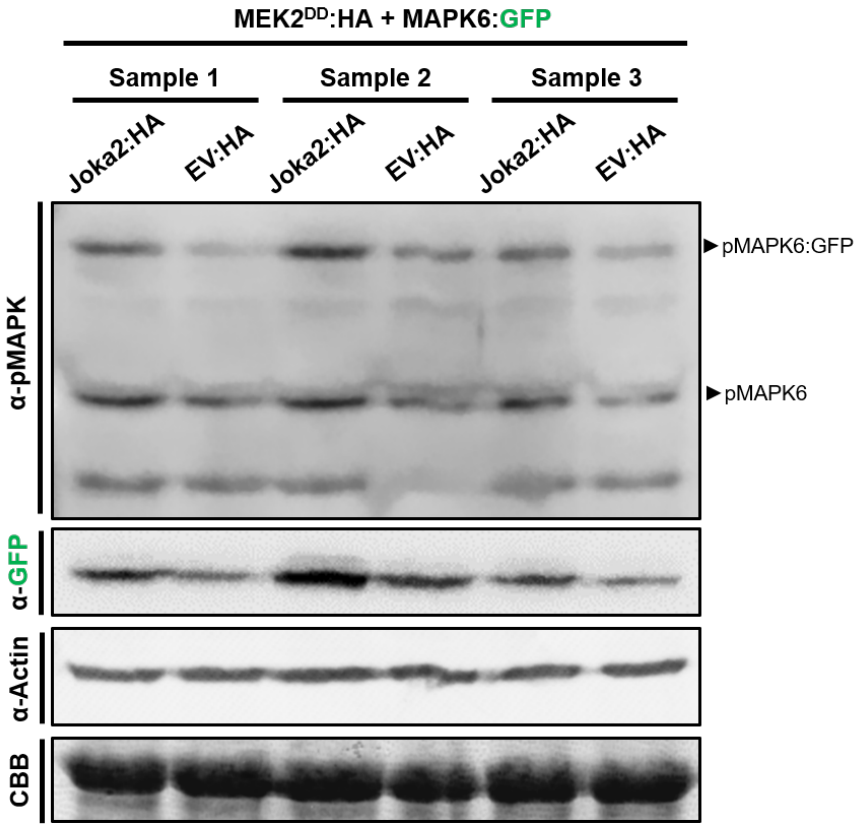


Figure 5.13. Joka2 enhances the protein stability of MAPK6 and increases MAPK6 phosphorylation by autoactive MEK2. MAPK6:GFP together with MEK2^{DD}:HA were transiently co-expressed with either Joka2:HA or EV:HA in *N. benthamiana* leaves. The leaf tissues were collected at 2 days post agroinfiltration. Total protein extracts were immunoblotted with α-pMAPK, α-GFP or α-Actin antibodies. Joka2:HA consistently stabilized the protein levels of MAPK6:GFP, and so that signals from phosphorylated indigenous and transiently expressed MAPK6 were higher in Joka2 overexpressing parts of the leaves (pMAPK detection). Tissues from multiple leaves per sample and three individual plants for repeats were used to get average protein levels. Gels were stained with CBB, and housekeeping protein, actin, was detected to show equal loading.

5.3.3.3 Joka2 increases cell death triggered by MEK2^{DD}

Whenever MAPK3/6 or MEK2 were overexpressed in the leaves of *N. benthamiana*, I observed cell death in subsequent days, this was dependent on how concentrated the Agrobacteria were and on MEK2's activation state. Together with this observation and the finding that Joka2 stabilizes MAPK levels, I tested if Joka2 was enhancing cell death induced by MAPK signalling. Autoactive MEK2 was an excellent protein to try this as it readily causes an intense cell death. However, autoactive MEK2 is like a wildfire to destroy anything it touches, normal amount of agrobacterium with OD 0.1-0.2 directly kills the tissue when it is transiently expressed within 1-2 days. That's why I tried several OD values and found out that 0.02 was ideal for observing HR in 2 days. I always used MEK2^{DD} with OD of 0.02 that leads to slower cell death, which opens a timeframe that I could use to detect both protein expression levels and cell death experiments. I expressed MEK2^{DD} with either Joka2:HA or EV:HA, I expected to see the impact of abundant Joka2 levels on the signalling capacity of MEK2 by analysing cell death (Figure 5.14). In general, autoactive MEK2 caused more necrotic tissue when Joka2 was overexpressed (Figure 5.14A). There are multiple ways to measure the necrosis/HR on leaves. We noticed in our lab that the machine used to detect to detect fluorescent signals from fluorescent antibodies on WB membranes, is also capable of detecting the fluorescence emitted from the dead tissue of the necrotic region (800nm channel of Odyssey Imaging Systems, Figure 5.14B). Since this machine is capable of detecting relative signal, it is straightforward to analyse and quantify the necrosis (Figure 5.14C). Paired t-test revelled a significant difference between the Joka2 and EV expressed experimental groups. Therefore, I concluded that Joka2 can enhance the PTI signal activated by MEK2, which is an upstream element of MAPK3 and MAPK6.

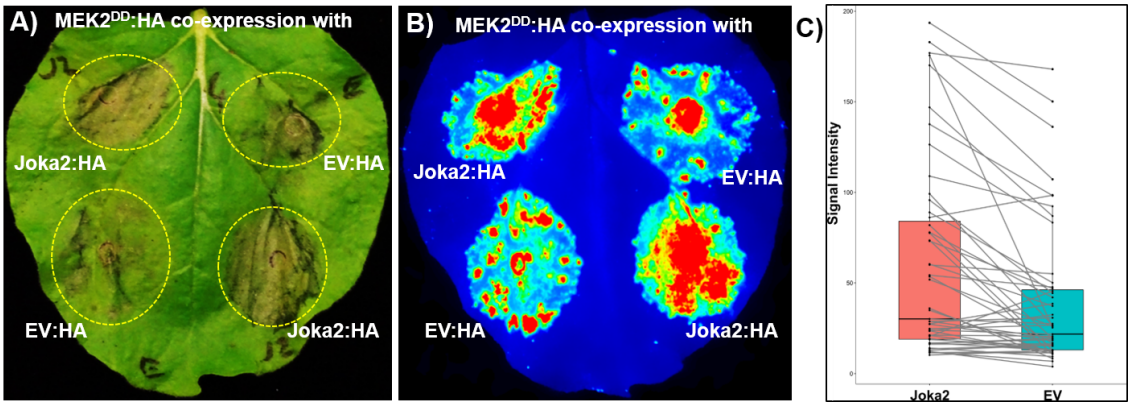


Figure 5.14. Joka2 enhances MEK2 mediated cell death. A) MEK2^{DD}:HA was transiently co-expressed with either Joka2:HA or EV:HA in *N. benthamiana* leaves. Day-light images of the leaves were taken at 2 days post agroinfiltration. MEK2^{DD}:HA co-expressed with Joka2:HA triggered more cell death compared to its co-expression with EV:HA. B) Fluorescent images of the leaves at 800 nm channel was taken to measure cell death. C) Relative signal from the dead tissue was plotted on a graph and showed significant difference (Paired t-test).

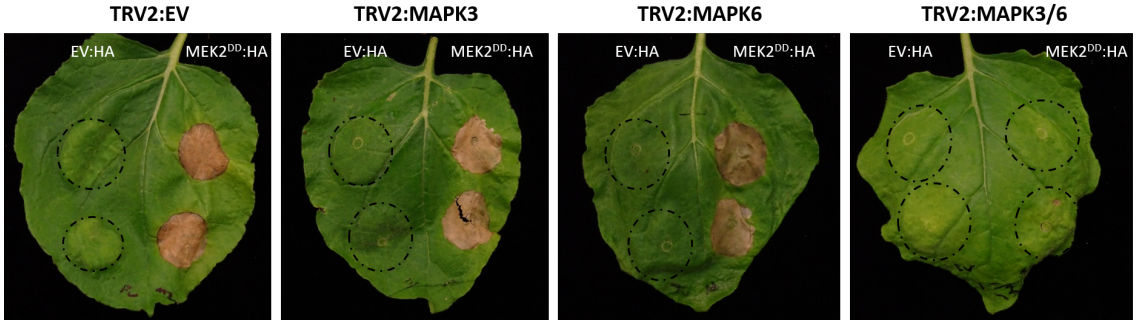


Figure 5.15. Validation of double silencing of MAPK3 and MAPK6 by the construct TRV2:MAPK3/6. The 4-5 weeks old plants, silenced for MAPK3, MAPK6, MAPK3/6 (double silencing) or mock (EV), were agroinfiltrated with constructs overexpressing either EV:HA or MEK2^{DD}:HA. The daylight images of the leave were taken 4 days post agroinfiltration. MEK2^{DD} triggered complete necrosis of the tissue in all leaves except the one knocked down for both MAPK3 and MAPK6. There is a partial cell death at the patches expressing MEK2^{DD}:HA but not EV:HA of TRV2:MAPK3/6. This confirms that virus induces gene silencing of both MAPK3 and MAPK6.

5.4 DISCUSSION

Throughout the work I have done for my thesis I have tested potential interactors of Joka2 to confirm their interaction, expecting to find their degradation by Joka2 to enhance plant resistance against *P. infestans*. I could not have been more wrong (or partially)! The experiments discussed in Chapter 4 encouraged me to focus on MAPKs and the signalling pathway they are involved in to induce plant immune responses. Chapter 3 also gave me a hint; Joka2 might not be a degradatory autophagy cargo receptor after all, at least for MAPKs that are involved in plant immunity.

After narrowing down the domains of Joka2 that provide interactions with MAPK3 and MAPK6 to a region around NBR1 domain, I have confirmed that NBR1 is indeed required for the interaction between Joka2 and MAPK3 but not MAPK6 (Figure 5.2 and Figure 5.3). I suspected MAPK3 and MAPK6 might be docking to the same region of Joka2 because of two reasons: i) MAPK3 and MAPK6 are homologous proteins and sometimes function redundantly for phosphorylating enzymes (>80% similarity in *N. benthamiana* between MAPK3 and MAPK6), and ii) MAPK6 looked like it might be interacting with Joka2 around the region where NBR1 is also present (Chapter 4).

No interaction between MAPK to NBR1 domain has been reported in plants or in other kingdoms to my knowledge. But what does that interaction mean? The function of the NBR1 domain is not clear, however prediction analysis suggests that it has an immunoglobin-like fold and it might be homologous to domains functioning in cell adhesion found in bacteria (Zientara-Rytter, K. *et al.*, 2011), which seems unrelated to the function of MAPK binding. Therefore, we do not have a starting point to predict the function of the NBR1-MAPK3 interaction. Finding a link, however, between members of PTI signalling in plant immunity and autophagy machinery, is an exciting result. In order to show the physical binding of NBR1 and MAPK3, protein purification steps must be optimised for *in vitro* binding assays (Figure 5.6 and Figure 5.7).

Supporting the idea that NBR1 domain of Joka2 is linking immunity related MAPK signalling, I have found that truncating the NBR1 region abolishes Joka2's contribution to resistance against *P. infestans*. This observation has broadened the knowledge about

the function of NBR1 domain and linked this domain to plant immunity. Whether it is MAPK signalling dependent or not requires more experiments such as repeating the experiments on plants with MAPKs silenced. However, this is not an ideal situation as MAPK3 and MAPK6 are also required for differentiation of healthy guard cells on the leaves (Larue, H. *et al.*, 2019).

MAPKs have been reported in many organisms, from many kingdoms, to interact with each other, their upstream elements, their target substrates and scaffold proteins such as RACK1 (Su, J. *et al.*, 2015). Even considering this, I was still surprised to find that MAPK9 was increasing the interaction between MAPK3/6 and Joka2 (Figure 5.8). This is because MAPK3/6 and MAPK9 showed a different pattern of interaction when Joka2 interactors were pulled down in normal and infected conditions (Bozkurt *et al.* unpublished, Table 4.1). This co-IP experiment can be repeated to test if there is a similar effect upon infection/PAMP treatment or MEK2 activity. Bequette *et al.* reported that various MAPK3 and MAPK6 homologs in *Arabidopsis*, tomato and tobacco (Bequette, C. J. *et al.*, 2018) form high molecular weight multiprotein complexes, which correlates with my observation with *N. benthamiana* MAPK3/6. In that report, the authors also showed that MEK2 homologs in *Arabidopsis*, *MKK4*, was present in the multiprotein complexes which further supports the finding that Joka2 was also interacting with MEK2 (Figure 5.9).

For the last few decades, we have known that autophagy is induced during different abiotic and biotic stresses (Dagdas, Y. F. *et al.*, 2016; Gaude, N. *et al.*, 2012). I found a similar case for Joka2 when plants sense infection (Figure 3.6). Similarly, triggering autophagy exogenously via chemical means or by overexpressing autophagy related proteins improves the plant immunity as our group and colleagues have reported (Hafren, Anders *et al.*, 2017). However, it has not been investigated how Joka2 affects the immune responses in plants. In order to achieve that I had to do some optimization such as finding ways to trigger immunity with oomycete PAMPs and detect PTI signalling. When I utilised *P. infestans* extract I showed that a proper time point to check MAPK3/6 phosphorylation was around one hour after the treatment (Figure 5.10). *P. infestans* treatment successfully triggers MAPK signalling cascade which can even be

detected for cloned MAPK3/6 which are tagged with GFP after an hour (Figure 5.11). This finding allowed me to continue experiments necessary for following MAPK protein stability experiments. Since I did not work with endogenous MAPK stability, I did not have to order an antibody raised against the native MAPKs, i.e. the constructs could be easily detected by relatively cheaper antibodies (such as α-GFP). Moreover, post-translational regulation is mostly ruled out as the clones were not dependent on their native promoter to be translated; a constitutive promoter provided steady protein expression.

In this chapter, I have concluded that protein levels of MAPK3 and MAPK6 were stabilised by overexpressed Joka2, which contradicted my initial thoughts about how Joka2 might be contributing to plant immunity (Figure 5.12 and Figure 5.13). As I mentioned, Joka2 was thought to carry its interactors such as MAPKs to autophagosomes (Figure from chapter 2) and in doing so regulate their functions by adjusting their availability to upstream elements and downstream target substrates. The results that I obtained regarding Joka2's effect on MAPK stability were not quite convincing for multiple reasons, but combined with the findings in this chapter, especially after observing that MAPK levels were higher on Joka2 expressing side when there is MEK2 signalling or PAMP treatment, I can conclude that Joka2 overexpression stabilises MAPK3/6 protein levels. This stabilisation event subsequentially leads to enhancement of the MAPK signalling cascade triggered by the pathway including MEK2-MAPK3/6 steps (Figure 5.14), and apparently MEK2 has its drastic effect on cell death only through MAPK3 and MAPK6 (Figure 5.15).

Due to $MEK2^{DD}$'s fast effect I had to monitor plants for HR regularly and take the images accordingly (Figure 5.14B). There was still a large variation in HR of the patches, however, the pattern was quite consistent: $MEK2^{DD}$ co-expressed with Joka2 was showing higher cell death compared to $MEK2^{DD}$ co-expressed with EV control (Figure 5.14C).

A study conducted by Mardakheh *et al.* showed that the mammalian NBR1 (homolog of plant Joka2) had a similar stabilisation effect on ERK1/2 (homologs of plant MAPK3/6) (Mardakheh, F. K. *et al.*, 2010). They claimed that NBR1 acts as "an inhibitor of ligand-

mediated receptor tyrosine kinase (RTK) degradation" and demonstrated how NBR1 contributed to the signalling cascade by interacting with ubiquitinated RTKs. By doing so, NBR1 inhibits internalization of ligand-mediated receptor from the cell surface. They, however, mostly focused on RTK-NBR1 interaction and found that C-terminal region (UBA domain) is responsible for this interaction. In the same study, the authors showed that this increased signalling was not because of the protein stability of MAPKs, but due to inhibition of RTK degradation (Mardakheh, F. K. *et al.*, 2010; Mardakheh, F. K. *et al.*, 2009). To my knowledge, the earliest MAPK-NBR1 interaction study comes from 2010 by Whitehouse *et al.*, who showed p38 was interacting with NBR1 (Whitehouse, C. A. *et al.*, 2013). However, the interaction was not shown to be provided by the NBR1 domain but with the C-terminal region of NBR1. This group reported that NBR1 was negatively regulating postnatal osteoblastic bone formation by modulating p38 MAPK signalling in osteoblasts and so that it acts as a regulator of osteoblast differentiation.

In addition to NBR1's contribution to signalling pathways which covers MAPK cascades, the other mammalian homolog of Joka2, p62/SQSTM1, had already been discovered first for its function as a signalling hub for multiple proteins before finding that it also functions in autophagy (Bjorkoy, G. *et al.*, 2006; Pankiv, S. *et al.*, 2007). The best known of these interactions is p62's binding ability to ubiquitin which regulates the nuclear factor kappa B (NF-κB) family of transcription factors (Long, J. *et al.*, 2010). I am not aware of any binding of p62 to MAPKs. In plants, RACK1 was reported to be a scaffold protein for interaction of kinases in MAPK signalling cascade (Su, J. *et al.*, 2015). The authors suggest that RACK1 "connects heterotrimeric G protein with a MAPK cascade to form a unique signalling pathway in plant immunity". Like RACK1, Joka2 might be acting as a scaffold and forming a bridge between receptors and accumulated MAPKs (Bequette, C. J. *et al.*, 2018) to enhance signalling cascade upon detection of pathogens (Figure 5.14). When double silencing MAPK3/6, one should be cautious as MAPK3 and MAP6 are involved in stomatal development of the epidermal cells (Wang, H. *et al.*, 2007). The plants silenced for MAPK3/6 phenotypically looked similar to EV silenced plants, though (Figure 5.15).

In conclusion, since the discovery that Joka2 was contributing to plant immunity against *P. infestans* as a selective cargo receptor, I have been working on how Joka2 might be managing this function (Dagdas, Y. F. *et al.*, 2016; Dagdas, Y. F. *et al.*, 2018). In the meantime, there were studies supported the importance of Joka2 mediated autophagy in plants to fight against bacterial and viral pathogens (Hafren, Anders *et al.*, 2017; Ustun, S. *et al.*, 2018). In this chapter, I showed that elevated plant immunity by Joka2, is at least in part due to the interaction of Joka2 with PTI signalling cascade proteins MAPK3/6 and their upstream kinase MEK2. I have investigated the domain that is responsible for this interaction and ended up showing that the NBR1 domain was required for MAPK3 and an unknown region was for MAPK6. This finding supported the notion that Joka2 might be a scaffold for the enhanced signalling. Joka2 might accumulate MAPKs and their signalling partners at the host-pathogen interface to facilitate and intensify the signal generated by the receptors. This is supported by the observation that MAPK3/6 were not degraded by Joka2 overexpression. Moreover, loss of Joka2's impact on increased plant immunity upon removal of NBR1 domain was consistent with the view that MAPK3 might be crucial for defence-related autophagy.

However, as scientific findings raise more questions, there are still things to be investigated in the future. For example, physical evidence of MAPK-NBR1 domain interaction should be provided as all co-IP experiments presented in this thesis were done *in planta*. Secondly, I have not ruled out the possibility that Joka2 might be also a target of MAPK signalling. Although I showed Joka2 might not be destabilized by MEK2, its stabilization by PAMP treatment and additional protein bands observed after WB suggest that Joka2 might be post-translationally modified. The possible Joka2 phosphorylation by this MAPK signalling should be investigated. While I have attempted to find out if Joka2 is phosphorylated upon PAMP treatment of $MEK2^{DD}$ activity or not, I could not optimise the procedure, so I have not added these experiments in this thesis.

CHAPTER 6 - GENERAL DISCUSSION AND FUTURE PERSPECTIVES

The mechanism of self-eating , i.e., autophagy is a fundamental process in all eukaryotic organisms. This mechanism has a physiological relevance to the health of both humans and plants, as perturbation of autophagy in these organisms negatively impacts their well-being. For example, involvement of autophagy in neurodegenerative and infectious diseases has been studied in humans (Leary, A. Y. *et al.*, 2018) (Green, D. R. *et al.*, 2014; Wu, M. Y. *et al.*, 2018). The cellular defence mediated by autophagic machinery contributes to overall systemic immunity, and has been reported in various eukaryotic kingdoms of life against a broad range of pathogens, from viruses to intra/extracellular organisms (Chapter 1). With studies focusing on selective autophagy, we have come to an understanding that this process is not just for bulk recycling of the cellular components but is also required for defence against pathogens. Autophagy related proteins (ATGs) and autophagy cargo receptors have been implicated in plant resistance to fight against biotic stresses in recent decades (Leary, A. Y. *et al.*, 2019).

A special interest on a plant autophagy cargo receptor, Joka2 (NBR1 in mammals), has started with a finding that an effector protein from a filamentous pathogen, *P. infestans*, was antagonising Joka2 to bind core autophagy protein ATG8 (Figure 1.3) (Dagdas, Y. F. *et al.*, 2016). Although Joka2 and PexRD54, the effector protein, were binding several ATG8s, their binding affinity towards ATG8CL was higher. When either Joka2 or PexRD54 was mutated on its binding region (AIM) to ATG8CL, the protein loses its function to enhance (Joka2) or hinder (PexRD54) plant immunity.

The mechanisms by which PexRD54 might be leading to increased susceptibility of the plant to pathogen invasion has been studied in both our and colleagues' laboratories (Pandey, P. *et al.*, 2020). I, however, focused on the Joka2's part in plant immunity. Although, Joka2 has been implicated in immunity from viruses to bacteria and oomycetes, the underlying mechanism how Joka2 enhances the resistance is still unclear, particularly against extracellular filamentous pathogens. The aim of the studies in this thesis was to illuminate the molecular and cellular mechanisms of how Joka2 manages to elevate host resistance. I have summarised the main finding in a summary figure (Figure 6.1).

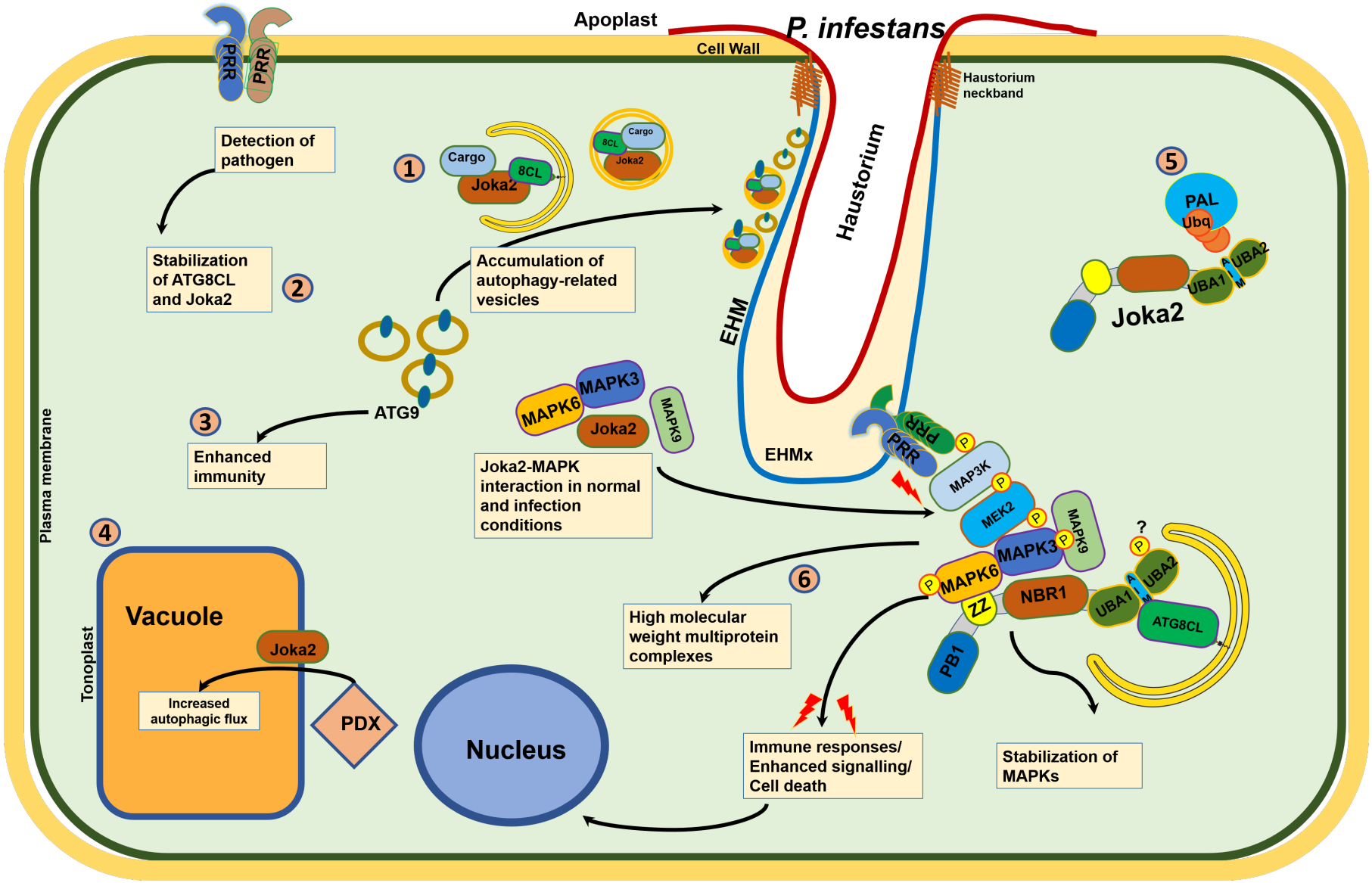

Apoplast
P. infestans
Cell Wall
Haustorium neckband
Haustorium
EHM
EHMx
Plasma membrane
PRR
Detection of pathogen
Stabilization of ATG8CL and Joka2
1
2
Cargo
8CL
Joka2
Accumulation of autophagy-related vesicles
ATG9
3
Enhanced immunity
MAPK6
MAPK3
MAPK9
Joka2
Joka2-MAPK interaction in normal and infection conditions
4
Vacuole
Tonoplast
Joka2
Increased autophagic flux
PDX
Nucleus
5
PAL
Ubq
UBA2
UBA1
Joka2
MAP3K
MEK2
6
High molecular weight multiprotein complexes
NBR1
ZZ
PB1
ATG8CL
Immune responses/ Enhanced signalling/ Cell death
Stabilization of MAPKs

Figure 6.1. Summary figure of how Joka2-mediated antimicrobial autophagy might function. 1) Joka2 and other autophagy related proteins such as ATG8 and ATG9 (2) vesicles are diverted to pathogen site to elevate plant immunity. 3) Autophagy switches from degradation to antimicrobial mechanism. 4) Potential interactor of PDX is not confirmed for association with Joka2 however, it increases autophagic flux to direct Joka2 into vacuole. 5) PAL is ubiquitinated and interacts with Joka2 through its UBA domains, which might regulate its function in production of precursors for salicylic acid and cell wall components. 5) Joka2 interacts with MAPK3, MAPK6 and MAPK9, maybe to form a multiprotein complex. MAPK3 association is established through NBR1 domain and MAPK6 might be interacting between ZZ and NBR1. Joka2 facilitates cell death caused MEK2-MAPK3/6 signalling cascade. Losing NBR1 domain aborts Joka2's impact on plant resistance against P. infestans. This might suggest that Joka2-mediated immunity functions through coordination of autophagy and PTI signalling.

In the first result chapter (Chapter 3), I demonstrated with confocal imaging that fluorescently-tagged autophagy related proteins, ATG8CL and ATG9, and puncta formed by Joka2 are diverted to the host-pathogen site (**1**). It was found that wild type Joka2, which is diverted to the pathogen-host interface, manages to reduce pathogen growth whereas an AIM mutant (incapable of binding to ATG8CL) or a truncated form, ΔPZ (unable to accumulate around haustoria), failed to show the same effect. After utilising various truncated versions of Joka2, I found that the region required for Joka2's diversion to the perihaustorial region was between the ZZ and NBR1 domains. The function of this area of Joka2 is still not known in the literature. However, just after PB1 domain, the algorithm predicts there is a region possessing relatively ordered structure. This region can be investigated in the future to test if Joka2 is diverted to infection site by proteins associated to that region. However, it should be in consideration that Joka2's interactions with other proteins can also lead the Joka2 puncta to perihaustorial region. As mammalian ATG8 homolog, MAP1LC3, for example, is known for its interactions with motor proteins, Joka2's intracellular movement can be through interaction with ATG8s. Historically, ATG8 homologs in mammals were discovered because of their association with the cytoskeleton. MAPK1LC3 stands for Microtubule-associated proteins 1A/1B light chain 3 (Mann, S. S. *et al.*, 1996). Therefore Joka2' association with ATG8s and other unknown proteins can divert Joka2 puncta in the cells

With regards to the expression of Joka2 and its mutants in the wild type *N. benthamiana* plants, the endogenous Joka2 must be kept in mind and its presence might be

interfering with some of the results as Joka2 can iteract with other proteins through PB1 and UBA domains. Therefore, those experiments regarding the traffcking of Joka2 puncta can be validated in Joka2 knock-out plants.

Considering accumulation of ATG9 vesicles around haustoria and its boosting effect on immunity, it can be concluded that autophagy functions as a focal antimicrobial pathway at the cellular level (**2**). It is still not completely clear if ATG9 contributes to immunity through solely autophagy dependent means or if it is also utilised by various endocytic pathways. ATG9's contribution to immunity can be through helping the biogenesis of autophagosomes by supplying new membranes. The frequent co-localisation of ATG8 autophagosomes and ATG9 puncta can be result of this biogenesis event. Since I have not used early autophagy protein markers in my experiments, my data do not fully support new autophagosome biogenesis. More focused experiments have to be designed to investigate if ATG9 vesicles contribute to autophagosome formation at the pathogen entry site.

All the autophagy related proteins, Joka2, ATG8CL and ATG9 accumulate around haustoria during pathogen infection. This finding necessitates further studies to find out how those autophagosome and autophagy related proteins contribute to plant focal immunity. Like these host proteins, *P. infestans* co-opts autophagy and exploits it to establish the infection on solanaceous plants by secreting PexRD54. This pathway of how PexRD54 reverses the function of autophagy at EHM also requires more detailed investigation.

Having shown that sensing of pathogens by plants has a stabilising effect on autophagy proteins such as ATG8CL and Joka2, prompted me to hypothesise that the host cells can convert autophagy from a degradation process to a mechanism where autophagy components support the fight against the pathogen (**3**). This phenomenon can be called antimicrobial autophagy and it is observed in many host organisms from eukaryotic kingdoms against many pathogen types, from viruses to parasitic plants.

Having shown that the trafficking of Joka2 was an important aspect of Joka2-mediated immunity, I continued my study to dissect what Joka2 could be carrying to the pathogen

site. My first prediction was that Joka2 puncta/autophagosomes might degrade negative regulators of immunity, or those vesicles might carry antibacterial compounds or enzymes to the EHMx. Therefore, I selected the potential proteins and enzymes that could be providing these potential immune responses after a proteomic screen of Joka2 pull down upon infection and normal conditions.

I chose PDX, PAL, MAPK3, MAPK6 and MAPK9 as probable cargoes of Joka2. Interestingly, PDX did not show any co-localisation or interaction with Joka2 through the experiments (**4**). Therefore, I have not gone further with PDX to investigate its effect on defence-related autophagy. However, its effect on Joka2's localisation to central vacuole in the preliminary experiment suggests that it might have a regulatory role on Joka2 or, in general, on autophagy. In my experiments I have not confirmed that PDX was either a cargo or an interactor of Joka2, even though it had the highest hit counts compared to PAL or MAPKs in the IP/MS proteomics screen (Table 4.1). Alternative experiments to detect protein-protein interactions could be used to validate Joka2-PDX association, if is an association. Yeast two-hybrid screening or eukaryotic protein expression and purification may help in this regard.

In contrast to PDX, I showed that PAL was targeted by Joka2 and that they interact through Joka2's UBA domains (**5**). This interaction profile means PAL is probably regulated by its degradation through Joka2. However, confocal images did not suggest that Joka2-PAL interaction. Although PAL has a bright signal under the microscope, there was no significant co-localisation with Joka2 punta. That suggest that PAL and Joka2 might be interacting in the cytosol and this part of the association needs to be elucidated. PAL had the most striking result regarding its infection assay when endogenous PAL was knocked down. Hemibiotrophic pathogen *P. infestans* revealed a more biotrophic spread than a necrotrophic one. This effect of PAL can be utilised to investigate biotrophic-necrotrophic life cycles of the pathogens, as we do not know entirely how these lifestyles affect pathogen and host sides. This effect can be studied by using the pathogen Peronospora tabacina (tobacco blue mold) which is an obligate biotrophic oomycete pathogen that can infect *N. benthamiana* (Fodor, J. *et al.*, 2018). The observation that I made after silencing PAL might be due to a perturbation in

production of either SA or cell wall precursors. Further experiments to detect the SA levels or indirect effects of SA triggered plant responses such as PR1 expression can be detecting by using RT-PCR or western blotting techniques.

I showed that MAPK3, MAPK6, and MAPK9, interact with Joka2 via subsequent confocal microscopy and co-IP experiments (**6**). Although *MAPK6* and *MAPK9* did not show an initial effect on plant immunity when they were silenced, *MAPK3* increased plant immunity against *P. infestans*. Joka2 might be regulating MAPK9 stability, however, Joka2 did not reduce protein levels of MAPK3 and MAPK6 overall. It is obvious that when there is a constant signalling by autoactive MEK2, Joka2 even caused higher protein stability. The protein stability by Joka2 might be provided by formation of protein complexes upon activation of MAPKs so that these MAPKs have higher affinity to Joka2. This interaction can lead docking of MAPK3/6 and other unknown MAPK elements (such as MEK2) or some phosphorylases around the pathogen site with the help of scaffolding effect of Joka2. This higher molecular complex might protect MAPKs from degradation. As I discussed in Chapter 5, there are examples of such cases where scaffold proteins bind to MAPKs and cell surface receptors, slowing down the degradation of receptors and enhancing MAPK signalling cascades (Mardakheh, F. K. *et al.*, 2010; Mardakheh, F. K. *et al.*, 2009).

Joka2's ortholog NBR1, but not p62, contain an uncharacterised NBR1 domain, which is the reason why the protein is called NBR1 in mammals. Since the function of this domain is a mystery to us, showing that Joka2 interacts through this region and loses its immune boosting effect upon truncating NBR1 is a substantial contribution to a function of a protein domain. Although it has been known that Joka2 orthologs had effect on some MAPKs in mammals, I studied and hopefully found convincing results that Joka2 might be contributing to MAPK signalling *in planta*.

Although I managed to show a specific domain of Joka2, (NBR1) interacts with MAPK3, I could not show a single domain interacting with MAPK6. When the domains are found for those MAPKs, alanine mutagenesis experiments on Joka2 can be conducted to search for individual residues required for the interactions. After finding the docking site for Joka2 to MAPKs, mutants of Joka2 can be generated to dissect the functional link

between Joka2 mediated autophagy and immune signalling. *In vitro* binding assays, such as gel filtration chromatography, are also required to determine the scaffolding ability of Joka2 for MAPKs.

The missing part of this MAPK-Joka2 interaction is that I could not show if MAPKs regulate Joka2-mediated autophagy related immunity. I had a few observations that Joka2 might be translationally modified upon MAPK and PAMP treatment, but I could not show it through experimental set up. I, for example, attempted to utilise Phos-tag polyacrylamide gel system to determine if Joka2 was phosphorylated by MAPKs. However, I could not optimise the procedure when I finished. Phosphorylation could also be checked through IP/MS before and after activation of MAPK3/6 specifically.

Findings regarding NBR1-MAPK interaction can be even used to enhance our understanding in human neurodegenerative diseases (Lamark, T. *et al.*, 2009). In neuroscience, scientists are trying to find ways of inducing aggrephagy to degrade the aggregated proteins in Alzheimer's disease, for instance (Malampati, S. *et al.*, 2020). If this link that I found in plants can be validated in mammals, potential MAPKs can be regulated with drugs to induce autophagy, which might reverse the progression of the neurodegenerative diseases.

In conclusion, results obtained during this project supported autophagy's and Joka2's role in immunity against the Irish famine pathogen, *P. infestans*. The main finding of my work suggests that one of the modes of action of Joka2 might contribute to resistance by operating as a scaffold protein for MAP kinases that are involved in pathogen-triggered immunity. This way, Joka2 can modulate the downstream signalling transduced by MAPKs upon recognition of an attack, therefore, the scaffolding property of Joka2 may enhance the signalling capacity of PTI. However, the interaction between Joka2 and MAPKs might also feedback defence-related autophagy. Activation of autophagy might be through this interaction, which might divert some of the degradation autophagy to defence-related autophagy. Elements in MAPK signalling and autophagy machinery are highly conserved among different organisms. Therefore, data obtained from this study are not limited to plant immunity against the potato blight disease, on the contrary, they can be implemented in other pathogen and host systems.

I mentioned many studies where I exemplified how plants impede pathogen growth by using autophagy components and how pathogens hijack host autophagy for their benefits (Chapter 1). As autophagy and PTI/ETI signalling cascade are crucial for plant immune responses, and these cellular processes are targeted by pathogens through many means, I have contributed to explore the unknown regions of molecular plant pathology.

APPENDIX

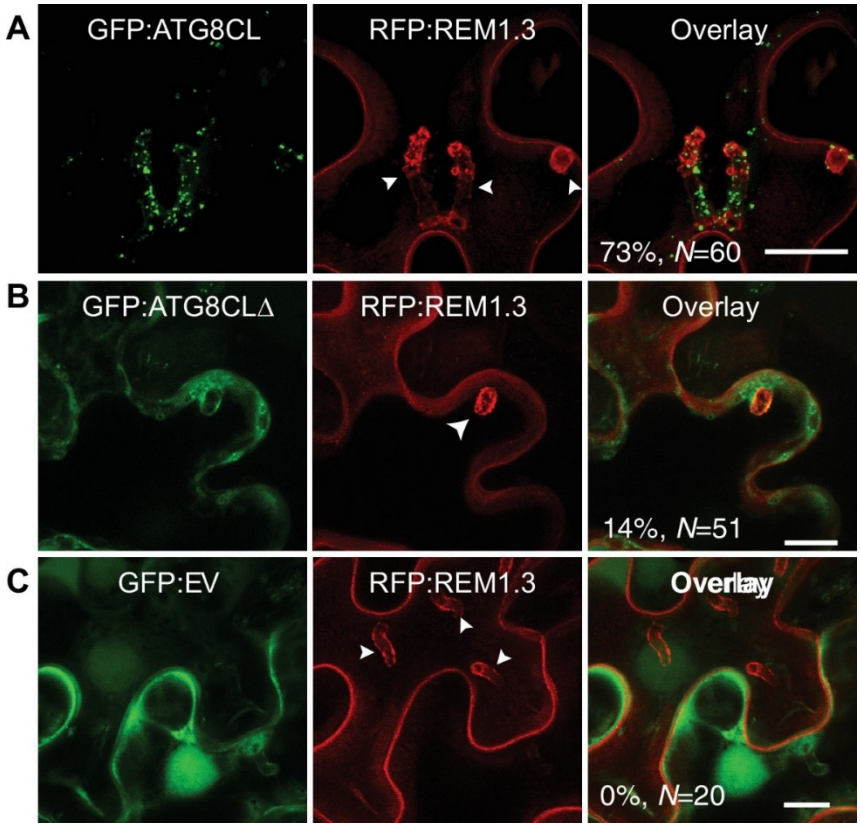


Figure 7.1. ATG8CL autophagosomes localize to perihaustorial region *in planta*. Infected *N. benthamiana* epithelial cells transiently co-expressing GFP-tagged ATG8CL, ATG8CLΔ, or ATG8IL with EHM marker RFP:REM1.3 are monitored via confocal laser scanning microscopy. Empty vector is utilized as a negative control. Percentage of haustoria surrounded by autophagosomes is determined 3-4 days post infection (dpi). (A) Although wild type GFP:ATG8CL-labelled autophagosomes were frequently around haustoria, (B) autophagy deficient GFP:ATG8CLΔ -positive puncta looked to be randomly distributed in the cytoplasm. (C) GFP tag itself did not generate puncta, therefore, only labelled perihaustorial cytoplasm. (D) GFP-tagged Clade-II type ATG8, ATG8IL, was mostly present in the cytoplasm and rarely marked perihaustorial puncta. Whilst taking confocal images, multiple optical planes were obtained to cover visualized haustoria and puncta around them. Images are maximal projections of 16, 10, 15, and 11 frames with 1 µm steps for the top, upper middle, lower middle and bottom rows, respectively. White arrow heads are pointing to haustoria. Scale bars of the images represent 10 µm.

Transiently expressed GFP:ATG8CL was monitored in *N. benthamiana* leaf abaxial epidermal cells during *P. infestans* infection. To visualize the haustoria, EHM and cytoplasmic membrane marker RFP-tagged Remorin 1.3 (RFP:REM1.3) was co-expressed with other marker proteins. 73% of the haustoria was surrounded or associated with GFP:ATG8CL-labelled autophagosomes (N=60) (Figure 7.1A), whereas in uninfected cells ATG8CL labelled randomly distributed puncta and the central vacuole. Autophagy deficient GFP:ATG8CLΔ mutant, which was constructed by replacing the last glycine with alanine in order to avoid phosphatidylethanolamine (PE) conjugation, failed to accumulate around the haustoria (Figure 7.1B). Unlike wild type ATG8CL, GFP:ATG8CLΔ formed less autophagosomes and the observed puncta were randomly distributed in the cytosol. Only 14% of the observations were positive for GFP:ATG8CΔ-haustoria association (N = 51) (Figure 7.1B). The control construct, GFP:EV, showed expected cytoplasmic signal and therefore did not form puncta that accumulate around haustoria (0% N = 20) (Figure 7.1C). As Dagdas *et al.* showed previously, both Joka2 and PexRD54 do not bind as strongly to ATG8IL compared to ATG8CL, therefore, I monitored the subcellular localization of autophagosomes formed by ATG8IL. Unlike GFP:ATG8CL puncta (73%), GFP:ATG8IL was found in only 28% of the imaged haustoria (*N* = 65), typically with no more than a few puncta per haustorium, which supports the idea that ATG8 variants may have specialized for different functions (Zess, E. K. *et al.*, 2019).

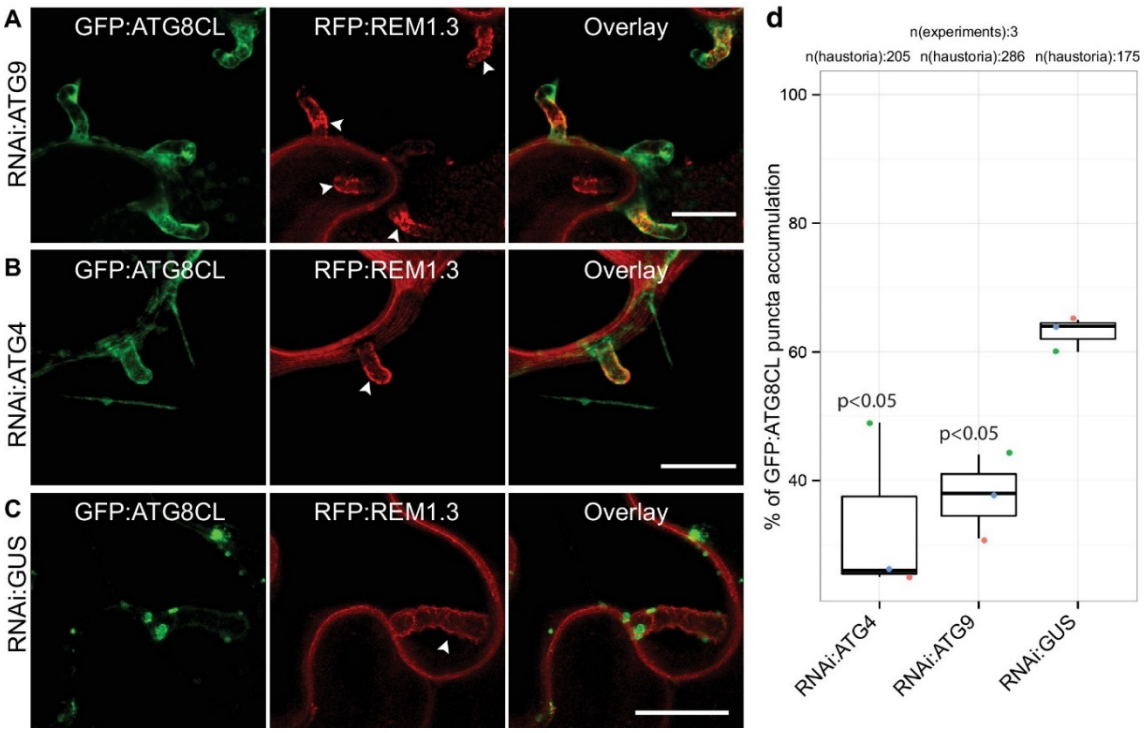


Figure 7.2. Expression of ATG4 and ATG9 is required for proper accumulation of ATG8CL puncta around haustoria. GFP:ATG8CL is co-expressed with EHM marker RFP:REM1.3 in infected *N. benthamiana* epithelial cells. Accumulation of ATG8CL puncta around the haustoria is observed when *ATG4*, *ATG9* or control *GUS* mRNAs are knocked down. Silencing of *ATG9* (A) and *ATG4* (B) significantly reduced the number of ATG8CL autophagosomes surrounding haustoria compared to *GUS* silencing (C). (D) Quantification of percentage perihaustorial ATG8CL puncta accumulation upon silencing of *ATG9*, *ATG4* and *GUS*. Images are maximal projections of 12, 10, and 9 frames with 1 µm intervals (from top to bottom rows in order, A-C). Images were taken 3-4 days post infection. Scale bars represent 10 µm.

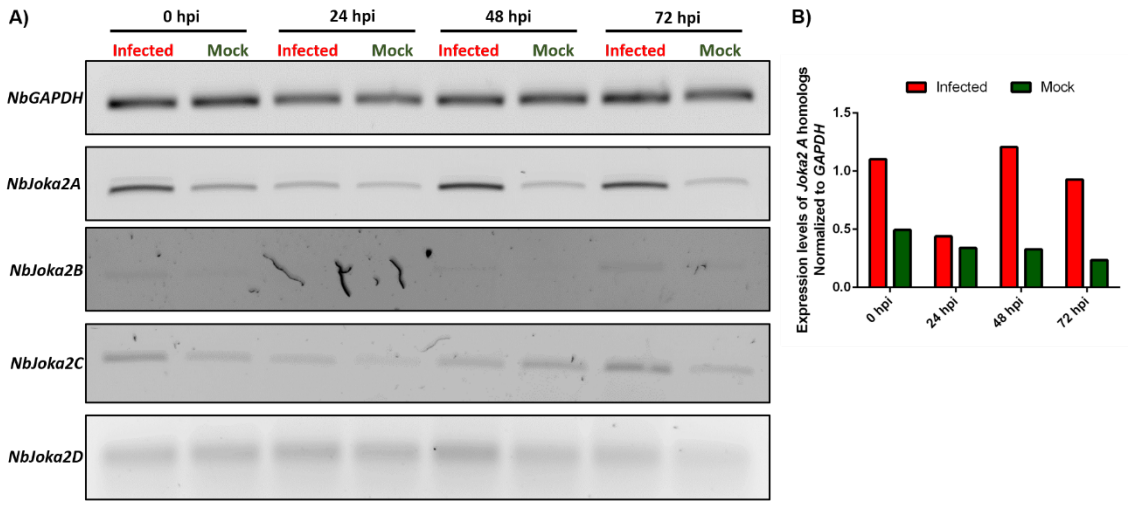


Figure 7.3. Joka2 mRNA levels, specifically NbJoka2A, increases upon infection of *N. benthamiana*. A) Semiquantitative reverse-transcription PCR results (RT-PCR) of four homologs of *NbJoka2* and housekeeping gene *NbGAPDH* in time course infection. B) Bar graph showing analysis of relative signal intensity of NbJoka2A normalized to *NbGAPDH* in different time points. Although the signal intensity of *N. benthamiana Joka2* homologs B, C, and D are not clear enough, *NbJoka2A* shows higher signal intensity when the plant is infected compared to the mock infected control.

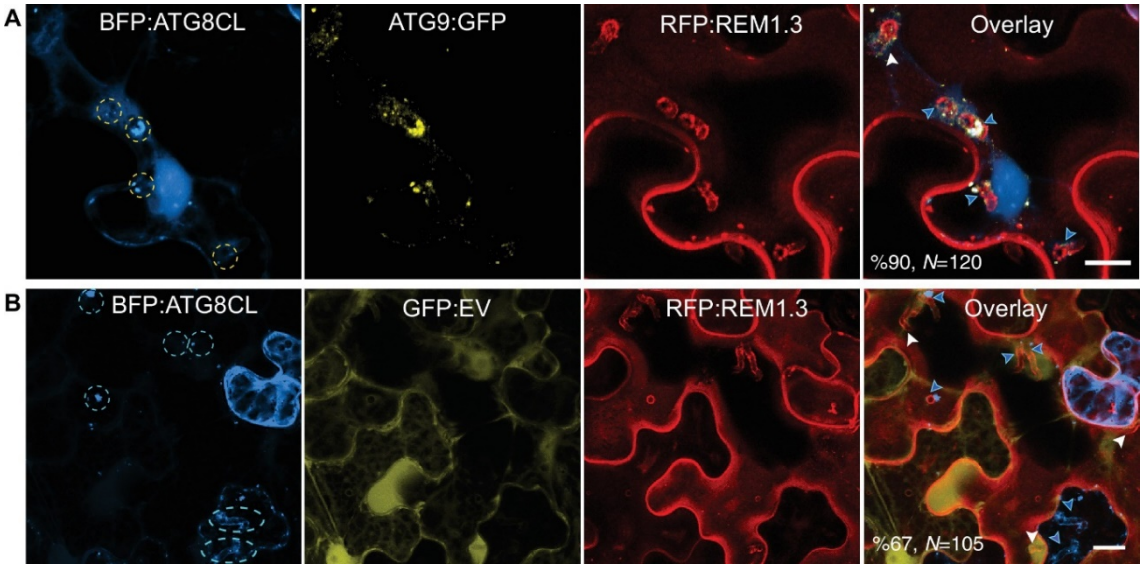


Figure 7.4. Overexpression of ATG9 increases the frequency of haustoria surrounded by ATG8CL-autophagosomes. BFP tagged ATG8CL and RFP-tagged REM1.3 are either transiently co-expressed with ATG9:GFP or GFP:EV in infected *N .benthamiana* cells. (A-B) Confocal images of epithelial cells showing haustoria which are associated with BFP:ATG8CL labelled autophagosomes substantially increase when ATG9:GFP is overexpressed (%90, *N* = 120) compared to GFP:EV control (%67, *N* = 105). Blue arrow heads point to haustoria that associate with BFP:ATG8CL-autophagosomes. White arrow heads, on the other

hand, label the haustoria that lack BFP:ATG8CL-autophagosomes. Images shown are maximal projections of 10, and 22 frames with 1 µm steps from top to bottom rows, respectively. Scale bars represent 10 µm.

To determine the stability of MAPK9 and potential interactors in the presence and absence of Joka2, we overexpressed Joka2 *in N. benthamiana* plants. GFP-tagged MAPK9 was coexpressed with Joka2:BFP and BFP:EV side by side on the same leaf. Unlike in the case of silencing Joka2, overexpression of Joka2 consistently gave similar results; decreased MAPK9 protein levels (Figure 7.5). GFP:EV levels did not change with Joka2:BFP overexpression. Primary results suggest that MAPK9 protein levels appear to be regulated by Joka2. Although the observation that Joka2 overexpression reduces MAPK9 protein stability is an interesting result, for the remainder of this work I chose to focus on MAPK3/6 as these are better described in the literature.

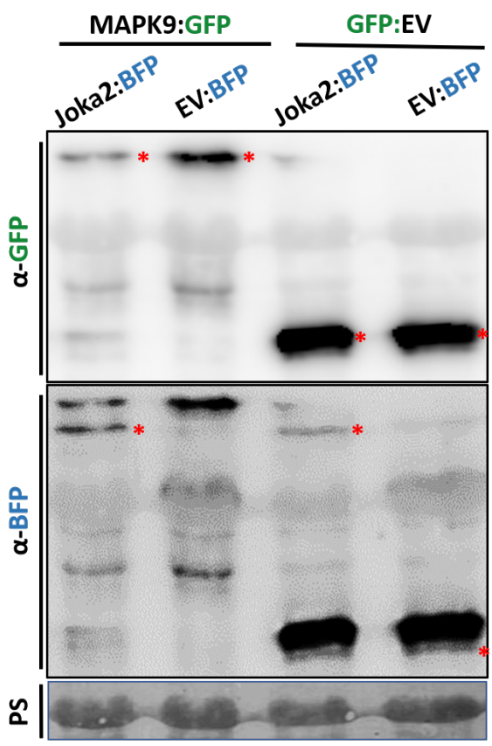


Figure 7.5. Overexpression of Joka2 destabilises MAPK9. MAPK9:GFP coexpressed with Joka2:BFP or BFP:EV showed different protein levels in immunoblots. Unlike GFP control, MAPK9:GFP revealed less protein stability when coexpressed with Joka2:BFP. Western blots obtained with anti-GFP and anti-BFP antiserum and total protein extracts were immunoblotted with appropriate antisera. Membranes were stained with Ponceau S (PS) to show loading levels. Red asterisks indicate the expected protein bands.

In order to test if MAPK3 alters Joka2 protein levels, a similar experiment was carried out by expressing MAPK3:GFP and EV:GFP on opposite sides of the leaves together with Joka2:RFP or GUS:RFP (Figure 7.6). The results suggested that overexpression of MAPK3 does not influence Joka2 protein levels.

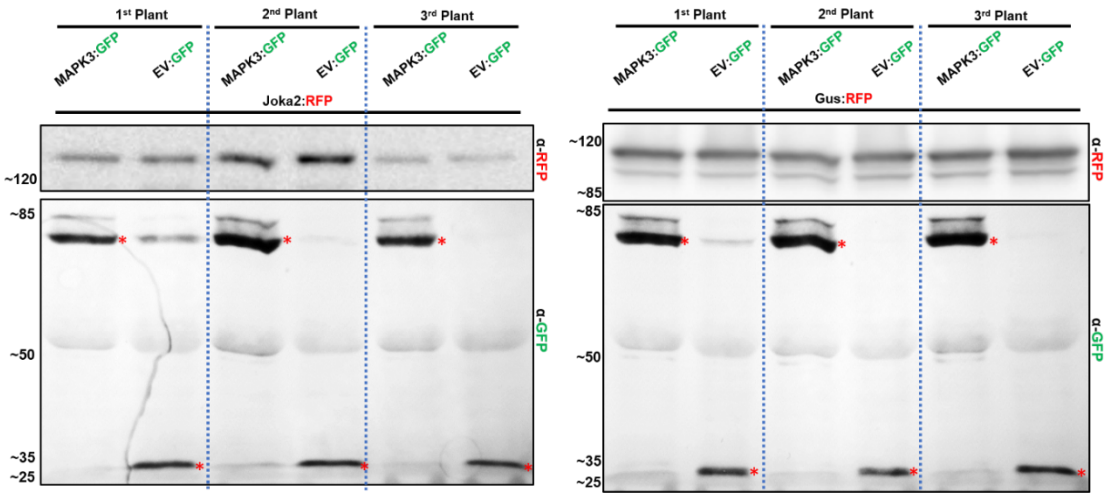


Figure 7.6. Joka2 or Gus protein levels do not change with MAPK3 overexpression. Joka2:RFP or Gus:RFP was co-expressed with MAPK3:GFP or EV:GFP in 3-4 weeks old *N. benthamiana* leaves. Protein levels in total extracts were determined three days post agroinfiltration. Protein levels Joka2:RFP or Gus:RFP were not affected by overexpression of MAPK3 suggesting MAPK3 is not regulating Joka2 levels. Total protein extracts were immunoblotted with appropriate antisera. Red asterisks indicate the expected protein bands.

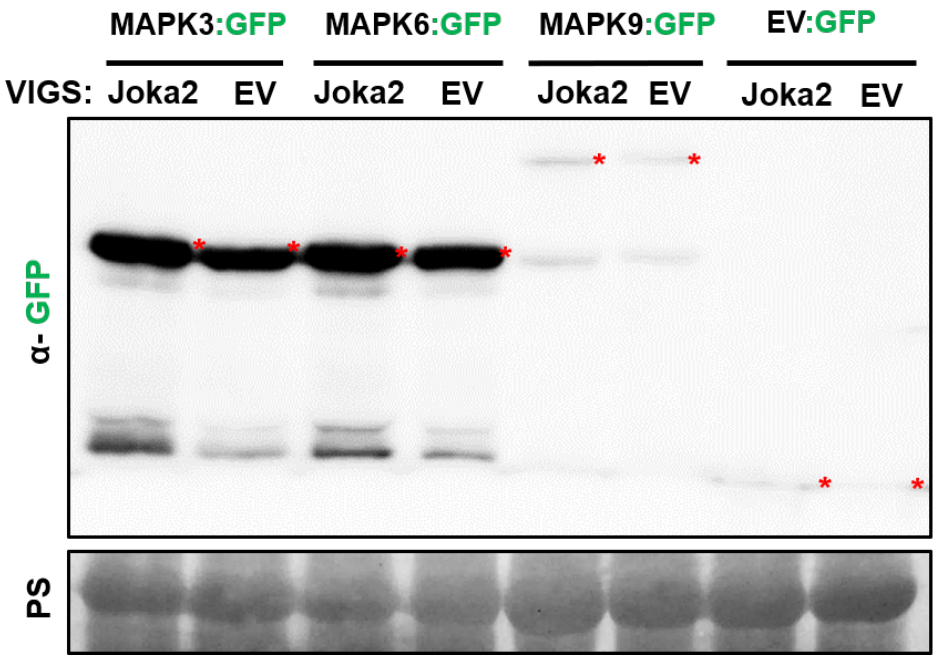


Figure 7.7. Silencing *NbJoka2* might be affecting MAP kinase protein levels. MAPK3:GFP, MAPK6:GFP, MAPK9:GFP or EV:GFP was transiently overexpressed in plants knocked down for Joka2 or EV (mock silencing). 3-4 weeks old *N. benthamiana* leaves were agroinfiltrated and protein levels in total extracts were determined three days post agroinfiltration. MAPK protein levels seem to increase upon silencing Joka2 *in planta*. However, the level of control GFP was also higher in TRV2:Joka2 plants. Leaf tissues from three individual plants were used per sample to get average protein levels. Total protein extracts were immunoblotted with appropriate antisera. Gels were stained with Ponceau S (PS) to show equal loading. Red asterisks indicate the expected protein bands.

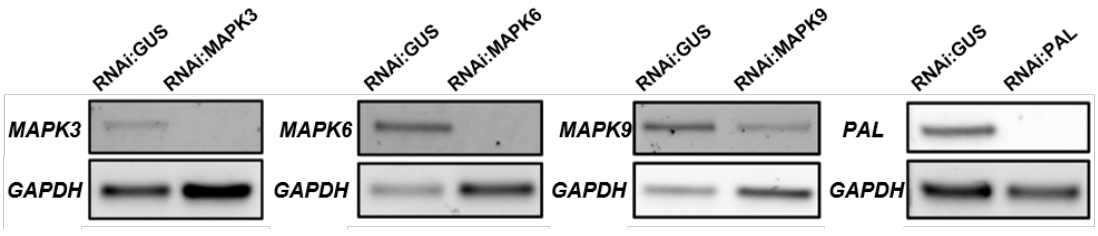


Figure 7.8. RNAi-mediated silencing constructs of *MAPK3, MAPK6, MAPK9* and *PAL* successfully silenced target genes in plant. Specific primers of MAPK3, MAPK6 and PAL-A were used to amplify the corresponding gene in plant cDNA silenced by RNAi MAPK3, RNAi MAPK6, RNAi MAPK9, RNAi PAL-A and RNAi GUS respectively. Glyceraldehyde 3-phosphate dehydrogenase (GAPDH) was used as internal control for silencing.

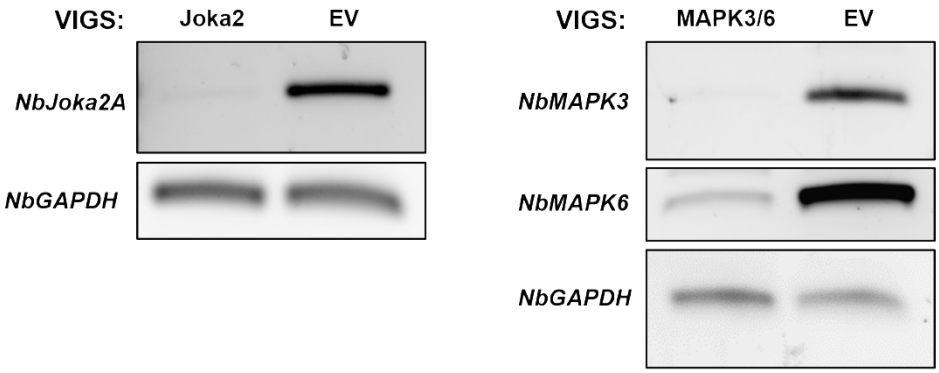


Figure 7.9. Validation of silencing of *NbJoka2A* and double silencing of *NbMAPK3* and *NbMAPK6*. Total RNA was extracted from plants agroinfiltrated with constructs carrying TRV1 together with TRV2Joka2, TRV2:MAPK3/6 or TRV2:EV. RT-PCR was carried out to test mRNA levels of *Joka2A*, *MAPK3*, *MAPK6* and *GAPDH* levels of *N. benthamiana* leaves. All of the tested genes were significantly silenced with their VIGS constructs.

REFERENCES

Agius, C., Eamens, A. L., Millar, A. A., Watson, J. M., & Wang, M. B. (2012). RNA silencing and antiviral defence in plants. *Methods Mol Biol, 894*, 17-38. doi:10.1007/978-1-61779-882-5_2

Anderson, R. G., Deb, D., Fedkenheuer, K., & McDowell, J. M. (2015). Recent Progress in RXLR Effector Research. *Mol Plant Microbe Interact, 28*(10), 1063-1072. doi:10.1094/MPMI-01-15-0022-CR

Asai, T., Tena, G., Plotnikova, J., Willmann, M. R., Chiu, W. L., Gomez-Gomez, L., Boller, T., Ausubel, F. M., & Sheen, J. (2002). MAP kinase signalling cascade in Arabidopsis innate immunity. *Nature, 415*(6875), 977-983. doi:10.1038/415977a

Aslam, B., Basit, M., Nisar, M. A., Khurshid, M., & Rasool, M. H. (2017). Proteomics: Technologies and Their Applications. *J Chromatogr Sci, 55*(2), 182-196. doi:10.1093/chromsci/bmw167

Axe, E. L., Walker, S. A., Manifava, M., Chandra, P., Roderick, H. L., Habermann, A., Griffiths, G., & Ktistakis, N. T. (2008). Autophagosome formation from membrane compartments enriched in phosphatidylinositol 3-phosphate and dynamically connected to the endoplasmic reticulum. *J Cell Biol, 182*(4), 685-701. doi:10.1083/jcb.200803137

Bequette, C. J., Hind, S. R., Pulliam, S., Higgins, R., & Stratmann, J. W. (2018). MAP kinases associate with high molecular weight multiprotein complexes. *Journal of Experimental Botany, 69*(3), 643-654. doi:10.1093/jxb/erx424

Birch, P. R., Boevink, P. C., Gilroy, E. M., Hein, I., Pritchard, L., & Whisson, S. C. (2008). Oomycete RXLR effectors: delivery, functional redundancy and durable disease resistance. *Curr Opin Plant Biol, 11*(4), 373-379. doi:10.1016/j.pbi.2008.04.005

Bjorkoy, G., Lamark, T., & Johansen, T. (2006). p62/SQSTM1: a missing link between protein aggregates and the autophagy machinery. *Autophagy, 2*(2), 138-139. doi:10.4161/auto.2.2.2405

Boller, T., & Felix, G. (2009). A renaissance of elicitors: perception of microbe-associated molecular patterns and danger signals by pattern-recognition receptors. *Annu Rev Plant Biol, 60*, 379-406. doi:10.1146/annurev.arplant.57.032905.105346

Bozkurt, T. O., Belhaj, K., Dagdas, Y. F., Chaparro-Garcia, A., Wu, C.-H., Cano, L. M., & Kamoun, S. (2015). Rerouting of Plant Late Endocytic Trafficking Toward a Pathogen Interface. *Traffic, 16*(2), 204-226. doi:10.1111/tra.12245

Bozkurt, T. O., Belhaj, K., Dagdas, Y. F., Chaparro-Garcia, A., Wu, C. H., Cano, L. M., & Kamoun, S. (2015). Rerouting of plant late endocytic trafficking toward a pathogen interface. *Traffic, 16*(2), 204-226. doi:10.1111/tra.12245

Bozkurt, T. O., & Kamoun, S. (2020). The plant-pathogen haustorial interface at a glance. *J Cell Sci, 133*(5). doi:10.1242/jcs.237958

Bozkurt, T. O., Richardson, A., Dagdas, Y. F., Mongrand, S., Kamoun, S., & Raffaele, S. (2014). The Plant Membrane-Associated REMORIN1.3 Accumulates in Discrete Perihaustorial Domains and Enhances Susceptibility to Phytophthora infestans. *Plant Physiol, 165*(3), 1005-1018. doi:10.1104/pp.114.235804

Bozkurt, T. O., Richardson, A., Dagdas, Y. F., Mongrand, S., Kamoun, S., & Raffaele, S. (2014). The Plant Membrane-Associated REMORIN1.3 Accumulates in Discrete Perihaustorial Domains and Enhances Susceptibility to Phytophthora infestans. *Plant Physiology, 165*(3), 1005-1018. doi:10.1104/pp.114.235804

Bozkurt, T. O., Schornack, S., Banfield, M. J., & Kamoun, S. (2012). Oomycetes, effectors, and all that jazz. *Current Opinion in Plant Biology, 15*(4), 483-492. doi:10.1016/j.pbi.2012.03.008

Bozkurt, T. O., Schornack, S., Win, J., Shindo, T., Ilyas, M., Oliva, R., Cano, L. M., Jones, A. M. E., Huitema, E., van der Hoorn, R. A. L., & Kamoun, S. (2011). Phytophthora infestans effector AVRblb2 prevents secretion of a plant immune protease at the haustorial interface. *Proceedings of the National Academy of Sciences of the United States of America, 108*(51), 20832-20837. doi:10.1073/pnas.1112708109

Cai, Q., Qiao, L. L., Wang, M., He, B. Y., Lin, F. M., Palmquist, J., Huang, S. N. D., & Jin, H. L. (2018). Plants send small RNAs in extracellular vesicles to fungal pathogen to silence virulence genes. *Science, 360*(6393), 1126-1129. doi:10.1126/science.aar4142

Caillaud, M. C., Wirthmueller, L., Sklenar, J., Findlay, K., Piquerez, S. J. M., Jones, A. M. E., Robatzek, S., Jones, J. D. G., & Faulkner, C. (2014). The Plasmodesmal Protein PDLP1 Localises to Haustoria-Associated Membranes during Downy Mildew Infection and Regulates Callose Deposition. *Plos Pathogens, 10*(11). doi:ARTN e1004496

10.1371/journal.ppat.1004496

Cardinale, F., Meskiene, I., Ouaked, F., & Hirt, H. (2002). Convergence and divergence of stress-induced mitogen-activated protein kinase signalling pathways at the level of two distinct mitogen-activated protein kinase kinases. *Plant Cell, 14*(3), 703-711. doi:10.1105/tpc.010256

Chen, J. S., Dagdas, Y. S., Kleinstiver, B. P., Welch, M. M., Sousa, A. A., Harrington, L. B., Sternberg, S. H., Joung, J. K., Yildiz, A., & Doudna, J. A. (2017). Enhanced proofreading governs CRISPR-Cas9 targeting accuracy. *Nature, 550*(7676), 407-410. doi:10.1038/nature24268

Cheng, X., & Wang, A. (2017). The Potyvirus Silencing Suppressor Protein VPg Mediates Degradation of SGS3 via Ubiquitination and Autophagy Pathways. *J Virol, 91*(1). doi:10.1128/JVI.01478-16

Cheng, Z., Li, J. F., Niu, Y., Zhang, X. C., Woody, O. Z., Xiong, Y., Djonovic, S., Millet, Y., Bush, J., McConkey, B. J., Sheen, J., & Ausubel, F. M. (2015). Pathogen-secreted proteases activate a novel plant immune pathway. *Nature, 521*(7551), 213-216. doi:10.1038/nature14243

Chowdappa, P., Kumar, N. B. J., Madhura, S., Kumar, M. S. P., Myers, K. L., Fry, W. E., Squires, J. N., & Cooke, D. E. L. (2013). Emergence of 13_A2 Blue Lineage ofPhytophthora

infestanswas Responsible for Severe Outbreaks of Late Blight on Tomato in South-West India. *Journal of Phytopathology, 161*(1), 49-58. doi:10.1111/jph.12031

Colcombet, J., & Hirt, H. (2008). Arabidopsis MAPKs: a complex signalling network involved in multiple biological processes. *Biochem J, 413*(2), 217-226. doi:10.1042/BJ20080625

Coll, N. S., Smidler, A., Puigvert, M., Popa, C., Valls, M., & Dangl, J. L. (2014). The plant metacaspase AtMC1 in pathogen-triggered programmed cell death and aging: functional linkage with autophagy. *Cell Death and Differentiation, 21*(9), 1399-1408. doi:10.1038/cdd.2014.50

Collinge, D. B. (2009). Cell wall appositions: the first line of defence. *J Exp Bot, 60*(2), 351-352. doi:10.1093/jxb/erp001

Cui, H., Tsuda, K., & Parker, J. E. (2015). Effector-triggered immunity: from pathogen perception to robust defence. *Annu Rev Plant Biol, 66*, 487-511. doi:10.1146/annurev-arplant-050213-040012

Dagdas, Y. F., Belhaj, K., Maqbool, A., Chaparro-Garcia, A., Pandey, P., Petre, B., Tabassum, N., Cruz-Mireles, N., Hughes, R. K., Sklenar, J., Win, J., Menke, F., Findlay, K., Banfield, M. J., Kamoun, S., & Bozkurt, T. O. (2016). An effector of the Irish potato famine pathogen antagonizes a host autophagy cargo receptor. *Elife, 5*. doi:10.7554/eLife.10856

Dagdas, Y. F., Pandey, P., Tumtas, Y., Sanguankiattichai, N., Belhaj, K., Duggan, C., Leary, A. Y., Segretin, M. E., Contreras, M. P., Savage, Z., Khandare, V. S., Kamoun, S., & Bozkurt, T. O. (2018). Host autophagy machinery is diverted to the pathogen interface to mediate focal defence responses against the Irish potato famine pathogen. *eLife, 7*. doi:ARTN e37476 10.7554/eLife.37476

Deretic, V., & Levine, B. (2009). Autophagy, Immunity, and Microbial Adaptations. *Cell Host & Microbe, 5*(6), 527-549. doi:10.1016/j.chom.2009.05.016

Derevnina, L., Petre, B., Kellner, R., Dagdas, Y. F., Sarowar, M. N., Giannakopoulou, A., De la Concepcion, J. C., Chaparro-Garcia, A., Pennington, H. G., van West, P., & Kamoun, S. (2016). Emerging oomycete threats to plants and animals. *Philosophical Transactions of the Royal Society B: Biological Sciences, 371*(1709), 20150459. doi:10.1098/rstb.2015.0459

Derrien, B., Baumberger, N., Schepetilnikov, M., Viotti, C., De Cillia, J., Ziegler-Graff, V., Isono, E., Schumacher, K., & Genschik, P. (2012a). Degradation of the antiviral component ARGONAUTE1 by the autophagy pathway. *Proceedings of the National Academy of Sciences of the United States of America, 109*(39), 15942-15946. doi:10.1073/pnas.1209487109

Derrien, B., Baumberger, N., Schepetilnikov, M., Viotti, C., De Cillia, J., Ziegler-Graff, V., Isono, E., Schumacher, K., & Genschik, P. (2012b). Degradation of the antiviral component ARGONAUTE1 by the autophagy pathway. *Proc Natl Acad Sci U S A, 109*(39), 15942-15946. doi:10.1073/pnas.1209487109

Devendrakumar, K. T., Li, X., & Zhang, Y. L. (2018). MAP kinase signalling: interplays between plant PAMP- and effector-triggered immunity. *Cellular and Molecular Life Sciences, 75*(16), 2981-2989. doi:10.1007/s00018-018-2839-3

Djamei, A., Pitzschke, A., Nakagami, H., Rajh, I., & Hirt, H. (2007). Trojan horse strategy in Agrobacterium transformation: abusing MAPK defence signalling. *Science, 318*(5849), 453-456. doi:10.1126/science.1148110

Doczi, R., Okresz, L., Romero, A. E., Paccanaro, A., & Bogre, L. (2012). Exploring the evolutionary path of plant MAPK networks. *Trends Plant Sci, 17*(9), 518-525. doi:10.1016/j.tplants.2012.05.009

Ekengren, S. K., Liu, Y., Schiff, M., Dinesh-Kumar, S. P., & Martin, G. B. (2003). Two MAPK cascades, NPR1, and TGA transcription factors play a role in Pto-mediated disease resistance in tomato. *Plant J, 36*(6), 905-917. doi:10.1046/j.1365-313X.2003.01944.x

Feng, Y., He, D., Yao, Z., & Klionsky, D. J. (2014). The machinery of macroautophagy. *Cell Res, 24*(1), 24-41. doi:10.1038/cr.2013.168

Fernandez-Pozo, N., Menda, N., Edwards, J. D., Saha, S., Tecle, I. Y., Strickler, S. R., Bombarely, A., Fisher-York, T., Pujar, A., Foerster, H., Yan, A., & Mueller, L. A. (2015a). The Sol Genomics Network (SGN)--from genotype to phenotype to breeding. *Nucleic Acids Res, 43*(Database issue), D1036-1041. doi:10.1093/nar/gku1195

Fernandez-Pozo, N., Rosli, H. G., Martin, G. B., & Mueller, L. A. (2015b). The SGN VIGS tool: user-friendly software to design virus-induced gene silencing (VIGS) constructs for functional genomics. *Mol Plant, 8*(3), 486-488. doi:10.1016/j.molp.2014.11.024

Fodor, J., Kaman-Toth, E., Danko, T., Schwarczinger, I., Bozso, Z., & Pogany, M. (2018). Description of the *Nicotiana benthamiana*-Cercospora *Nicotiana*e Pathosystem. *Phytopathology, 108*(1), 149-155. doi:10.1094/PHYTO-12-16-0448-R

Fu, S., Xu, Y., Li, C., Li, Y., Wu, J., & Zhou, X. (2018). Rice Stripe Virus Interferes with S-acylation of Remorin and Induces Its Autophagic Degradation to Facilitate Virus Infection. *Mol Plant, 11*(2), 269-287. doi:10.1016/j.molp.2017.11.011

Galluzzi, L., & Green, D. R. (2019). Autophagy-Independent Functions of the Autophagy Machinery. *Cell, 177*(7), 1682-1699. doi:10.1016/j.cell.2019.05.026

Gaude, N., Bortfeld, S., Duensing, N., Lohse, M., & Krajinski, F. (2012). Arbuscule-containing and non-colonized cortical cells of mycorrhizal roots undergo extensive and specific reprogramming during arbuscular mycorrhizal development. *Plant J, 69*(3), 510-528. doi:10.1111/j.1365-313X.2011.04810.x

Giraldo, M. C., & Valent, B. (2013). Filamentous plant pathogen effectors in action. *Nat Rev Microbiol, 11*(11), 800-814. doi:10.1038/nrmicro3119

Godfray, H. C. J., Beddington, J. R., Crute, I. R., Haddad, L., Lawrence, D., Muir, J. F., Pretty, J., Robinson, S., Thomas, S. M., & Toulmin, C. (2010a). Food Security: The Challenge

of Feeding 9 Billion People. *Science, 327*(5967), 812-818. doi:10.1126/science.1185383

Godfray, H. C. J., Crute, I. R., Haddad, L., Lawrence, D., Muir, J. F., Nisbett, N., Pretty, J., Robinson, S., Toulmin, C., & Whiteley, R. (2010b). The future of the global food system. *Philosophical Transactions of the Royal Society B-Biological Sciences, 365*(1554), 2769-2777. doi:10.1098/rstb.2010.0180

Green, D. R., & Levine, B. (2014). To be or not to be? How selective autophagy and cell death govern cell fate. *Cell, 157*(1), 65-75. doi:10.1016/j.cell.2014.02.049

Gutierrez, M. G., Master, S. S., Singh, S. B., Taylor, G. A., Colombo, M. I., & Deretic, V. (2004). Autophagy is a defence mechanism inhibiting BCG and Mycobacterium tuberculosis survival in infected macrophages. *Cell, 119*(6), 753-766. doi:10.1016/j.cell.2004.11.038

Gutjahr, C., & Parniske, M. (2013). Cell and Developmental Biology of Arbuscular Mycorrhiza Symbiosis. In R. Schekman (Ed.), *Annual Review of Cell and Developmental Biology, Vol 29* (Vol. 29, pp. 593-617).

Haas, B. J., Kamoun, S., Zody, M. C., Jiang, R. H., Handsaker, R. E., Cano, L. M., Grabherr, M., Kodira, C. D., Raffaele, S., Torto-Alalibo, T., Bozkurt, T. O., Ah-Fong, A. M., Alvarado, L., Anderson, V. L., Armstrong, M. R., Avrova, A., Baxter, L., Beynon, J., Boevink, P. C., Bollmann, S. R., Bos, J. I., Bulone, V., Cai, G., Cakir, C., Carrington, J. C., Chawner, M., Conti, L., Costanzo, S., Ewan, R., Fahlgren, N., Fischbach, M. A., Fugelstad, J., Gilroy, E. M., Gnerre, S., Green, P. J., Grenville-Briggs, L. J., Griffith, J., Grunwald, N. J., Horn, K., Horner, N. R., Hu, C. H., Huitema, E., Jeong, D. H., Jones, A. M., Jones, J. D., Jones, R. W., Karlsson, E. K., Kunjeti, S. G., Lamour, K., Liu, Z., Ma, L., Maclean, D., Chibucos, M. C., McDonald, H., McWalters, J., Meijer, H. J., Morgan, W., Morris, P. F., Munro, C. A., O'Neill, K., Ospina-Giraldo, M., Pinzon, A., Pritchard, L., Ramsahoye, B., Ren, Q., Restrepo, S., Roy, S., Sadanandom, A., Savidor, A., Schornack, S., Schwartz, D. C., Schumann, U. D., Schwessinger, B., Seyer, L., Sharpe, T., Silvar, C., Song, J., Studholme, D. J., Sykes, S., Thines, M., van de Vondervoort, P. J., Phuntumart, V., Wawra, S., Weide, R., Win, J., Young, C., Zhou, S., Fry, W., Meyers, B. C., van West, P., Ristaino, J., Govers, F., Birch, P. R., Whisson, S. C., Judelson, H. S., & Nusbaum, C. (2009). Genome sequence and analysis of the Irish potato famine pathogen Phytophthora infestans. *Nature, 461*(7262), 393-398. doi:10.1038/nature08358

Hafren, A., Macia, J.-L., Love, A. J., Milner, J. J., Drucker, M., & Hofius, D. (2017). Selective autophagy limits cauliflower mosaic virus infection by NBR1-mediated targeting of viral capsid protein and particles. *Proceedings of the National Academy of Sciences of the United States of America, 114*(10), E2026-E2035. doi:10.1073/pnas.1610687114

Hafren, A., Macia, J. L., Love, A. J., Milner, J. J., Drucker, M., & Hofius, D. (2017). Selective autophagy limits cauliflower mosaic virus infection by NBR1-mediated targeting of viral capsid protein and particles. *Proc Natl Acad Sci U S A, 114*(10), E2026-E2035. doi:10.1073/pnas.1610687114

Hafren, A., Ustun, S., Hochmuth, A., Svenning, S., Johansen, T., & Hofius, D. (2018). Turnip Mosaic Virus Counteracts Selective Autophagy of the Viral Silencing Suppressor HCpro. *Plant Physiol, 176*(1), 649-662. doi:10.1104/pp.17.01198

Hailey, D. W., Rambold, A. S., Satpute-Krishnan, P., Mitra, K., Sougrat, R., Kim, P. K., & Lippincott-Schwartz, J. (2010). Mitochondria supply membranes for autophagosome biogenesis during starvation. *Cell, 141*(4), 656-667. doi:10.1016/j.cell.2010.04.009

Haldar, A. K., Piro, A. S., Pilla, D. M., Yamamoto, M., & Coers, J. (2014). The E2-like conjugation enzyme Atg3 promotes binding of IRG and Gbp proteins to Chlamydia- and Toxoplasma-containing vacuoles and host resistance. *Plos One, 9*(1), e86684. doi:10.1371/journal.pone.0086684

Havaux, M., Ksas, B., Szewczyk, A., Rumeau, D., Franck, F., Caffarri, S., & Triantaphylides, C. (2009). Vitamin B6 deficient plants display increased sensitivity to high light and photo-oxidative stress. *BMC Plant Biol, 9*, 130. doi:10.1186/1471-2229-9-130

Hayashi-Nishino, M., Fujita, N., Noda, T., Yamaguchi, A., Yoshimori, T., & Yamamoto, A. (2009). A subdomain of the endoplasmic reticulum forms a cradle for autophagosome formation. *Nat Cell Biol, 11*(12), 1433-1437. doi:10.1038/ncb1991

Hoehenwarter, W., Thomas, M., Nukarinen, E., Egelhofer, V., Rohrig, H., Weckwerth, W., Conrath, U., & Beckers, G. J. M. (2013). Identification of Novel in vivo MAP Kinase Substrates in Arabidopsis thaliana Through Use of Tandem Metal Oxide Affinity Chromatography. *Molecular & Cellular Proteomics, 12*(2), 369-380. doi:10.1074/mcp.M112.020560

Hofius, D., Munch, D., Bressendorff, S., Mundy, J., & Petersen, M. (2011). Role of autophagy in disease resistance and hypersensitive response-associated cell death. *Cell Death & Differentiation, 18*(8), 1257-1262. doi:10.1038/cdd.2011.43

Hofius, D., Schultz-Larsen, T., Joensen, J., Tsitsigiannis, D. I., Petersen, N. H., Mattsson, O., Jorgensen, L. B., Jones, J. D., Mundy, J., & Petersen, M. (2009). Autophagic components contribute to hypersensitive cell death in Arabidopsis. *Cell, 137*(4), 773-783. doi:10.1016/j.cell.2009.02.036

Hofius, D., Schultz-Larsen, T., Joensen, J., Tsitsigiannis, D. I., Petersen, N. H. T., Mattsson, O., Jorgensen, L. B., Jones, J. D. G., Mundy, J., & Petersen, M. (2009). Autophagic Components Contribute to Hypersensitive Cell Death in Arabidopsis. *Cell, 137*(4), 773-783. doi:10.1016/j.cell.2009.02.036

Huang, J., & Brumell, J. H. (2014). Bacteria-autophagy interplay: a battle for survival. *Nature Reviews Microbiology, 12*(2), 101-114. doi:10.1038/nrmicro3160

Huang, J., Gu, M., Lai, Z., Fan, B., Shi, K., Zhou, Y. H., Yu, J. Q., & Chen, Z. (2010). Functional analysis of the Arabidopsis PAL gene family in plant growth, development, and response to environmental stress. *Plant Physiol, 153*(4), 1526-1538. doi:10.1104/pp.110.157370

Hyun, M. W., Yun, Y. H., Kim, J. Y., & Kim, S. H. (2011). Fungal and Plant Phenylalanine Ammonia-lyase. *Mycobiology, 39*(4), 257-265. doi:10.5941/MYCO.2011.39.4.257

Ichimura, K., Casais, C., Peck, S. C., Shinozaki, K., & Shirasu, K. (2006). MEKK1 is required for MPK4 activation and regulates tissue-specific and temperature-dependent cell death in Arabidopsis. *J Biol Chem, 281*(48), 36969-36976. doi:10.1074/jbc.M605319200

Ichimura, K., Shinozaki, K., Tena, G., Sheen, J., Henry, Y., Champion, A., Kreis, M., Zhang, S. Q., Hirt, H., Wilson, C., Heberle-Bors, E., Ellis, B. E., Morris, P. C., Innes, R. W., Ecker, J. R., Scheel, D., Klessig, D. F., Machida, Y., Mundy, J., Ohashi, Y., Walker, J. C., & Grp, M. (2002). Mitogen-activated protein kinase cascades in plants: a new nomenclature. *Trends in Plant Science, 7*(7), 301-308. doi:10.1016/S1360-1385(02)02302-6

Ishida, T., & Kinoshita, K. (2007). PrDOS: prediction of disordered protein regions from amino acid sequence. *Nucleic Acids Res, 35*(Web Server issue), W460-464. doi:10.1093/nar/gkm363

Jammes, F., Song, C., Shin, D., Munemasa, S., Takeda, K., Gu, D., Cho, D., Lee, S., Giordo, R., Sritubtim, S., Leonhardt, N., Ellis, B. E., Murata, Y., & Kwak, J. M. (2009). MAP kinases MPK9 and MPK12 are preferentially expressed in guard cells and positively regulate ROS-mediated ABA signalling. *Proc Natl Acad Sci U S A, 106*(48), 20520-20525. doi:10.1073/pnas.0907205106

Jammes, F., Yang, X., Xiao, S., & Kwak, J. M. (2011). Two Arabidopsis guard cell-preferential MAPK genes, MPK9 and MPK12, function in biotic stress response. *Plant Signal Behav, 6*(11), 1875-1877. doi:10.4161/psb.6.11.17933

Ji, C. H., & Kwon, Y. T. (2017). Crosstalk and Interplay between the Ubiquitin-Proteasome System and Autophagy. *Molecules and Cells, 40*(7), 441-449. doi:10.14348/molcells.2017.0115

Jiang, S., Dupont, N., Castillo, E. F., & Deretic, V. (2013). Secretory versus Degradative Autophagy: Unconventional Secretion of Inflammatory Mediators. *Journal of Innate Immunity, 5*(5), 471-479. doi:10.1159/000346707

Jones, J. D., & Dangl, J. L. (2006). The plant immune system. *Nature, 444*(7117), 323-329. doi:10.1038/nature05286

Kabbage, M., Williams, B., & Dickman, M. B. (2013). Cell death control: the interplay of apoptosis and autophagy in the pathogenicity of Sclerotinia sclerotiorum. *Plos Pathogens, 9*(4), e1003287. doi:10.1371/journal.ppat.1003287

Kalapos, B., Hlavova, M., Nadai, T. V., Galiba, G., Bisova, K., & Doczi, R. (2019). Early Evolution of the Mitogen-Activated Protein Kinase Family in the Plant Kingdom. *Sci Rep, 9*(1), 4094. doi:10.1038/s41598-019-40751-y

Katsiarimpa, A., Kalinowska, K., Anzenberger, F., Weis, C., Ostertag, M., Tsutsumi, C., Schwechheimer, C., Brunner, F., Huckelhoven, R., & Isonoa, E. (2013). The Deubiquitinating Enzyme AMSH1 and the ESCRT-III Subunit VPS2.1 Are Required for Autophagic Degradation in Arabidopsis. *Plant Cell, 25*(6), 2236-2252. doi:10.1105/tpc.113.113399

Kaur, J., & Debnath, J. (2015). Autophagy at the crossroads of catabolism and anabolism. *Nature Reviews Molecular Cell Biology, 16*(8), 461-472. doi:10.1038/nrm4024

Kellner, R., De la Concepcion, J. C., Maqbool, A., Kamoun, S., & Dagdas, Y. F. (2016). ATG8 Expansion: A Driver of Selective Autophagy Diversification? *Trends in Plant Science*. doi:10.1016/j.tplants.2016.11.015

Kerppola, T. K. (2008). Bimolecular fluorescence complementation (BiFC) analysis as a probe of protein interactions in living cells. *Annu Rev Biophys, 37*, 465-487. doi:10.1146/annurev.biophys.37.032807.125842

Khokon, M. A., Salam, M. A., Jammes, F., Ye, W., Hossain, M. A., Uraji, M., Nakamura, Y., Mori, I. C., Kwak, J. M., & Murata, Y. (2015). Two guard cell mitogen-activated protein kinases, MPK9 and MPK12, function in methyl jasmonate-induced stomatal closure in Arabidopsis thaliana. *Plant Biol (Stuttg), 17*(5), 946-952. doi:10.1111/plb.12321

Klionsky, D. J. (2007). Autophagy: from phenomenology to molecular understanding in less than a decade. *Nature Reviews Molecular Cell Biology, 8*(11), 931-937. doi:10.1038/nrm2245

Klionsky, D. J., Baehrecke, E. H., Brumell, J. H., Chu, C. T., Codogno, P., Cuervo, A. M., Debnath, J., Deretic, V., Elazar, Z., Eskelinen, E. L., Finkbeiner, S., Fueyo-Margareto, J., Gewirtz, D., Jaattela, M., Kroemer, G., Levine, B., Melia, T. J., Mizushima, N., Rubinsztein, D. C., Simonsen, A., Thorburn, A., Thumm, M., & Tooze, S. A. (2011). A comprehensive glossary of autophagy-related molecules and processes (2(nd) edition). *Autophagy, 7*(11), 1273-1294. doi:10.4161/auto.7.11.17661

Koh, S., Andre, A., Edwards, H., Ehrhardt, D., & Somerville, S. (2005). Arabidopsis thaliana subcellular responses to compatible Erysiphe cichoracearum infections. *Plant Journal, 44*(3), 516-529. doi:10.1111/j.1365-313X.2005.02545.x

Korolchuk, V. I., Mansilla, A., Menzies, F. M., & Rubinsztein, D. C. (2009). Autophagy Inhibition Compromises Degradation of Ubiquitin-Proteasome Pathway Substrates. *Molecular Cell, 33*(4), 517-527. doi:10.1016/j.molcel.2009.01.021

Lai, Z., Wang, F., Zheng, Z., Fan, B., & Chen, Z. (2011). A critical role of autophagy in plant resistance to necrotrophic fungal pathogens. *Plant J, 66*(6), 953-968. doi:10.1111/j.1365-313X.2011.04553.x

Lamark, T., Kirkin, V., Dikic, I., & Johansen, T. (2009). NBR1 and p62 as cargo receptors for selective autophagy of ubiquitinated targets. *Cell Cycle, 8*(13), 1986-1990. doi:10.4161/cc.8.13.8892

Lamark, T., Perander, M., Outzen, H., Kristiansen, K., Overvatn, A., Michaelsen, E., Bjorkoy, G., & Johansen, T. (2003). Interaction codes within the family of mammalian Phox and Bem1p domain-containing proteins. *Journal of Biological Chemistry, 278*(36), 34568-34581. doi:10.1074/jbc.M303221200

Lamb, C. A., Yoshimori, T., & Tooze, S. A. (2013). The autophagosome: origins unknown, biogenesis complex. *Nat Rev Mol Cell Biol, 14*(12), 759-774. doi:10.1038/nrm3696

Larue, H., & Zhang, S. (2019). SCREAM in the making of stomata. *Nat Plants, 5*(7), 648-649. doi:10.1038/s41477-019-0460-6

Lassowskat, I., Bottcher, C., Eschen-Lippold, L., Scheel, D., & Lee, J. (2014). Sustained mitogen-activated protein kinase activation reprograms defence metabolism and phosphoprotein profile in Arabidopsis thaliana. *Frontiers in Plant Science, 5*. doi:ARTN 554 10.3389/fpls.2014.00554

Latijnhouwers, M., de Wit, P. J. G. M., & Govers, F. (2003). Oomycetes and fungi: similar weaponry to attack plants. *Trends in Microbiology, 11*(10), 462-469. doi:DOI 10.1016/j.tim.2003.08.002

Le Bot, N. (2012). Atg9 vesicles make up autophagosomes. *Nature Cell Biology, 14*(9), 909-909. doi:10.1038/ncb2583

Le Fevre, R., Evangelisti, E., Rey, T., & Schornack, S. (2015). Modulation of Host Cell Biology by Plant Pathogenic Microbes. In R. Schekman (Ed.), *Annual Review of Cell and Developmental Biology, Vol 31* (Vol. 31, pp. 201-229).

Leary, A. Y., Sanguankiattichai, N., Duggan, C., Tumtas, Y., Pandey, P., Segretin, M. E., Linares, J. S., Savage, Z. D., Yow, R. J., & Bozkurt, T. O. (2018). Modulation of plant autophagy during pathogen attack. *Journal of Experimental Botany, 69*(6), 1325-1333. doi:10.1093/jxb/erx425

Leary, A. Y., Savage, Z., Tumtas, Y., & Bozkurt, T. (2019). Contrasting and emerging roles of autophagy in plant immunity. *Current Opinion in Plant Biology, 52*, 46-53. doi:10.1016/j.pbi.2019.07.002

Lenz, H. D., Haller, E., Melzer, E., Kober, K., Wurster, K., Stahl, M., Bassham, D. C., Vierstra, R. D., Parker, J. E., Bautor, J., Molina, A., Escudero, V., Shindo, T., van der Hoorn, R. A. L., Gust, A. A., & Nuernberger, T. (2011). Autophagy differentially controls plant basal immunity to biotrophic and necrotrophic pathogens. *Plant Journal, 66*(5), 818-830. doi:10.1111/j.1365-313X.2011.04546.x

Li, F., Zhang, C., Li, Y., Wu, G., Hou, X., Zhou, X., & Wang, A. (2018). Beclin1 restricts RNA virus infection in plants through suppression and degradation of the viral polymerase. *Nat Commun, 9*(1), 1268. doi:10.1038/s41467-018-03658-2

Li, H., Xu, H., Zhou, Y., Zhang, J., Long, C., Li, S., Chen, S., Zhou, J. M., & Shao, F. (2007). The phosphothreonine lyase activity of a bacterial type III effector family. *Science, 315*(5814), 1000-1003. doi:10.1126/science.1138960

Liu, T. L., Song, T. Q., Zhang, X., Yuan, H. B., Su, L. M., Li, W. L., Xu, J., Liu, S. H., Chen, L. L., Chen, T. Z., Zhang, M. X., Gu, L. C., Zhang, B. L., & Dou, D. L. (2014). Unconventionally secreted effectors of two filamentous pathogens target plant salicylate biosynthesis. *Nature Communications, 5*. doi:Artn 4686 10.1038/Ncomms5686

Loake, G., & Grant, M. (2007). Salicylic acid in plant defence--the players and protagonists. *Curr Opin Plant Biol, 10*(5), 466-472. doi:10.1016/j.pbi.2007.08.008

Long, J., Garner, T. P., Pandya, M. J., Craven, C. J., Chen, P., Shaw, B., Williamson, M. P., Layfield, R., & Searle, M. S. (2010). Dimerisation of the UBA domain of p62 inhibits

ubiquitin binding and regulates NF-kappaB signalling. *J Mol Biol, 396*(1), 178-194. doi:10.1016/j.jmb.2009.11.032

Lu, K., Guo, W., Lu, J., Yu, H., Qu, C., Tang, Z., Li, J., Chai, Y., & Liang, Y. (2015). Genome-Wide Survey and Expression Profile Analysis of the Mitogen-Activated Protein Kinase (MAPK) Gene Family in Brassica rapa. *Plos One, 10*(7), e0132051. doi:10.1371/journal.pone.0132051

Lu, Y. J., Schornack, S., Spallek, T., Geldner, N., Chory, J., Schellmann, S., Schumacher, K., Kamoun, S., & Robatzek, S. (2012). Patterns of plant subcellular responses to successful oomycete infections reveal differences in host cell reprogramming and endocytic trafficking. *Cell Microbiol, 14*(5), 682-697. doi:10.1111/j.1462-5822.2012.01751.x

Maher, E. A., Bate, N. J., Ni, W., Elkind, Y., Dixon, R. A., & Lamb, C. J. (1994). Increased disease susceptibility of transgenic tobacco plants with suppressed levels of preformed phenylpropanoid products. *Proc Natl Acad Sci U S A, 91*(16), 7802-7806.

Malampati, S., Song, J. X., Chun-Kit Tong, B., Nalluri, A., Yang, C. B., Wang, Z., Gopalkrishnashetty Sreenivasmurthy, S., Zhu, Z., Liu, J., Su, C., Krishnamoorthi, S., Iyaswamy, A., Cheung, K. H., Lu, J. H., & Li, A. M. (2020). Targeting Aggrephagy for the Treatment of Alzheimer's Disease. *Cells, 9*(2). doi:10.3390/cells9020311

Mamun, M. A., Tang, C., Sun, Y., Islam, M. N., Liu, P., Wang, X., & Kang, Z. (2018). Wheat Gene TaATG8j Contributes to Stripe Rust Resistance. *Int J Mol Sci, 19*(6). doi:10.3390/ijms19061666

Mann, S. S., & Hammarback, J. A. (1996). Gene localization and developmental expression of light chain 3: a common subunit of microtubule-associated protein 1A(MAP1A) and MAP1B. *J Neurosci Res, 43*(5), 535-544. doi:10.1002/(SICI)1097-4547(19960301)43:5<535::AID-JNR3>3.0.CO;2-J

Mao, G., Meng, X., Liu, Y., Zheng, Z., Chen, Z., & Zhang, S. (2011). Phosphorylation of a WRKY transcription factor by two pathogen-responsive MAPKs drives phytoalexin biosynthesis in Arabidopsis. *Plant Cell, 23*(4), 1639-1653. doi:10.1105/tpc.111.084996

Mardakheh, F. K., Auciello, G., Dafforn, T. R., Rappoport, J. Z., & Heath, J. K. (2010). Nbr1 Is a Novel Inhibitor of Ligand-Mediated Receptor Tyrosine Kinase Degradation. *Molecular and Cellular Biology, 30*(24), 5672-5685. doi:10.1128/Mcb.00878-10

Mardakheh, F. K., Yekezare, M., Machesky, L. M., & Heath, J. K. (2009). Spred2 interaction with the late endosomal protein NBR1 down-regulates fibroblast growth factor receptor signalling. *Journal of Cell Biology, 187*(2), 265-277. doi:10.1083/jcb.200905118

Mari, M., Griffith, J., Rieter, E., Krishnappa, L., Klionsky, D. J., & Reggiori, F. (2010). An Atg9-containing compartment that functions in the early steps of autophagosome biogenesis. *Journal of Cell Biology, 190*(6), 1005-1022. doi:10.1083/jcb.200912089

Mauch-Mani, B., & Slusarenko, A. J. (1996). Production of Salicylic Acid Precursors Is a Major Function of Phenylalanine Ammonia-Lyase in the Resistance of Arabidopsis to Peronospora parasitica. *Plant Cell, 8*(2), 203-212. doi:10.1105/tpc.8.2.203

Mendgen, K., & Nass, P. (1988). The Activity of Powdery-Mildew Haustoria after Feeding the Host-Cells with Different Sugars, as Measured with a Potentiometric Cyanine Dye. *Planta, 174*(2), 283-288. doi:Doi 10.1007/Bf00394782

Meng, X., & Zhang, S. (2013). MAPK cascades in plant disease resistance signalling. *Annu Rev Phytopathol, 51*(1), 245-266. doi:10.1146/annurev-phyto-082712-102314

Micali, C. O., Neumann, U., Grunewald, D., Panstruga, R., & O'Connell, R. (2011). Biogenesis of a specialized plant-fungal interface during host cell internalization of Golovinomyces orontii haustoria. *Cellular Microbiology, 13*(2), 210-226. doi:10.1111/j.1462-5822.2010.01530.x

Mooney, S., Leuendorf, J. E., Hendrickson, C., & Hellmann, H. (2009). Vitamin B6: a long known compound of surprising complexity. *Molecules, 14*(1), 329-351. doi:10.3390/molecules14010329

Nakahara, K. S., Masuta, C., Yamada, S., Shimura, H., Kashihara, Y., Wada, T. S., Meguro, A., Goto, K., Tadamura, K., Sueda, K., Sekiguchi, T., Shao, J., Itchoda, N., Matsumura, T., Igarashi, M., Ito, K., Carthew, R. W., & Uyeda, I. (2012). Tobacco calmodulin-like protein provides secondary defence by binding to and directing degradation of virus RNA silencing suppressors. *Proc Natl Acad Sci U S A, 109*(25), 10113-10118. doi:10.1073/pnas.1201628109

Nakatogawa, H., Suzuki, K., Kamada, Y., & Ohsumi, Y. (2009). Dynamics and diversity in autophagy mechanisms: lessons from yeast. *Nat Rev Mol Cell Biol, 10*(7), 458-467. doi:10.1038/nrm2708

Noda, N. N., Kumeta, H., Nakatogawa, H., Satoo, K., Adachi, W., Ishii, J., Fujioka, Y., Ohsumi, Y., & Inagaki, F. (2008). Structural basis of target recognition by Atg8/LC3 during selective autophagy. *Genes Cells, 13*(12), 1211-1218. doi:10.1111/j.1365-2443.2008.01238.x

Nowicki, M., Fooled, M. R., Nowakowska, M., & Kozik, E. U. (2012). Potato and Tomato Late Blight Caused by Phytophthora infestans: An Overview of Pathology and Resistance Breeding. *Plant Disease, 96*(1), 4-17. doi:10.1094/Pdis-05-11-0458

Ogawa, M., Yoshimori, T., Suzuki, T., Sagara, H., Mizushima, N., & Sasakawa, C. (2005). Escape of intracellular Shigella from autophagy. *Science (New York, N.Y.), 307*(5710), 727-731. doi:10.1126/science.1106036

Pandey, P., Leary, A. Y., Tümtas, Y., Savage, Z., Dagvadorj, B., Tan, E., Khandare, V., Duggan, C., Yusunov, T., Madalinski, M., Mirkin, F. G., Schornack, S., Dagdas, Y., Kamoun, S., & Bozkurt, T. O. (2020). The Irish potato famine pathogen subverts host vesicle trafficking to channel starvation-induced autophagy to the pathogen interface. *bioRxiv*, 2020.2003.2020.000117. doi:10.1101/2020.03.20.000117

Pankiv, S., Clausen, T. H., Lamark, T., Brech, A., Bruun, J. A., Outzen, H., Overvatn, A., Bjorkoy, G., & Johansen, T. (2007). p62/SQSTM1 binds directly to Atg8/LC3 to facilitate

degradation of ubiquitinated protein aggregates by autophagy. *J Biol Chem, 282*(33), 24131-24145. doi:10.1074/jbc.M702824200

Panstruga, R., & Dodds, P. N. (2009). Terrific Protein Traffic: The Mystery of Effector Protein Delivery by Filamentous Plant Pathogens. *Science, 324*(5928), 748-750. doi:10.1126/science.1171652

Papinski, D., Schuschnig, M., Reiter, W., Wilhelm, L., Barnes, C. A., Maiolica, A., Hansmann, I., Pfaffenwimmer, T., Kijanska, M., Stoffel, I., Lee, S. S., Brezovich, A., Lou, J. H., Turk, B. E., Aebersold, R., Ammerer, G., Peter, M., & Kraft, C. (2014). Early steps in autophagy depend on direct phosphorylation of Atg9 by the Atg1 kinase. *Mol Cell, 53*(3), 471-483. doi:10.1016/j.molcel.2013.12.011

Park, E., Woo, J., & Dinesh-Kumar, S. P. (2014). Arabidopsis ATG4 cysteine proteases specificity toward ATG8 substrates. *Autophagy, 10*(5), 928-929. doi:10.4161/auto.28280

Patel, S., & Dinesh-Kumar, S. P. (2008). Arabidopsis ATG6 is required to limit the pathogen-associated cell death response. *Autophagy, 4*(1), 20-27. doi:DOI 10.4161/auto.5056

Pitzschke, A., Schikora, A., & Hirt, H. (2009). MAPK cascade signalling networks in plant defence. *Current Opinion in Plant Biology, 12*(4), 421-426. doi:10.1016/j.pbi.2009.06.008

Pumplin, N., Zhang, X., Noar, R. D., & Harrison, M. J. (2012). Polar localization of a symbiosis-specific phosphate transporter is mediated by a transient reorientation of secretion. *Proceedings of the National Academy of Sciences of the United States of America, 109*(11), E665-E672. doi:10.1073/pnas.1110215109

Qiu, J. L., Fiil, B. K., Petersen, K., Nielsen, H. B., Botanga, C. J., Thorgrimsen, S., Palma, K., Suarez-Rodriguez, M. C., Sandbech-Clausen, S., Lichota, J., Brodersen, P., Grasser, K. D., Mattsson, O., Glazebrook, J., Mundy, J., & Petersen, M. (2008). Arabidopsis MAP kinase 4 regulates gene expression through transcription factor release in the nucleus. *EMBO J, 27*(16), 2214-2221. doi:10.1038/emboj.2008.147

Raffaele, S., Win, J., Cano, L. M., & Kamoun, S. (2010). Analyses of genome architecture and gene expression reveal novel candidate virulence factors in the secretome of Phytophthora infestans. *BMC Genomics, 11*, 637. doi:10.1186/1471-2164-11-637

Randow, F., MacMicking, J. D., & James, L. C. (2013). Cellular Self-Defence: How Cell-Autonomous Immunity Protects Against Pathogens. *Science, 340*(6133), 701-706. doi:10.1126/science.1233028

Ravikumar, B., Moreau, K., Jahreiss, L., Puri, C., & Rubinsztein, D. C. (2010). Plasma membrane contributes to the formation of pre-autophagosomal structures. *Nat Cell Biol, 12*(8), 747-757. doi:10.1038/ncb2078

Real, E., Rodrigues, L., Cabal, G. G., Enguita, F. J., Mancio-Silva, L., Mello-Vieira, J., Beatty, W., Vera, I. M., Zuzarte-Luis, V., Figueira, T. N., Mair, G. R., & Mota, M. M. (2018). Plasmodium UIS3 sequesters host LC3 to avoid elimination by autophagy in hepatocytes. *Nat Microbiol, 3*(1), 17-25. doi:10.1038/s41564-017-0054-x

Reggiori, F., Shintani, T., Nair, U., & Klionsky, D. J. (2005). Atg9 cycles between mitochondria and the pre-autophagosomal structure in yeasts. *Autophagy, 1*(2), 101-109. doi:DOI 10.4161/auto.1.2.1840

Rodriguez, M. C., Petersen, M., & Mundy, J. (2010). Mitogen-activated protein kinase signalling in plants. *Annu Rev Plant Biol, 61*, 621-649. doi:10.1146/annurev-arplant-042809-112252

Savary, S., Ficke, A., Aubertot, J. N., & Hollier, C. (2012). Crop losses due to diseases and their implications for global food production losses and food security. *Food Security, 4*(4), 519-537. doi:10.1007/s12571-012-0200-5

Schornack, S., Huitema, E., Cano, L. M., Bozkurt, T. O., Oliva, R., van Damme, M., Schwizer, S., Raffaele, S., Chaparro-Garcia, A., Farrer, R., Segretin, M. E., Bos, J., Haas, B. J., Zody, M. C., Nusbaum, C., Win, J., Thines, M., & Kamoun, S. (2009). Ten things to know about oomycete effectors. *Molecular Plant Pathology, 10*(6), 795-803. doi:10.1111/j.1364-3703.2009.00593.x

Shahid, S., Kim, G., Johnson, N. R., Wafula, E., Wang, F., Coruh, C., Bernal-Galeano, V., Phifer, T., dePamphilis, C. W., Westwood, J. H., & Axtell, M. J. (2018). MicroRNAs from the parasitic plant Cuscuta campestris target host messenger RNAs. *Nature, 553*(7686), 82-+. doi:10.1038/nature25027

Sievers, F., Wilm, A., Dineen, D., Gibson, T. J., Karplus, K., Li, W., Lopez, R., McWilliam, H., Remmert, M., Soding, J., Thompson, J. D., & Higgins, D. G. (2011). Fast, scalable generation of high-quality protein multiple sequence alignments using Clustal Omega. *Mol Syst Biol, 7*, 539. doi:10.1038/msb.2011.75

Somssich, I. E., & Hahlbrock, K. (1998). Pathogen defence in plants - a paradigm of biological complexity. *Trends in Plant Science, 3*(3), 86-90. doi:Doi 10.1016/S1360-1385(98)01199-6

Song, J., Win, J., Tian, M., Schornack, S., Kaschani, F., Ilyas, M., van der Hoorn, R. A., & Kamoun, S. (2009). Apoplastic effectors secreted by two unrelated eukaryotic plant pathogens target the tomato defence protease Rcr3. *Proc Natl Acad Sci U S A, 106*(5), 1654-1659. doi:10.1073/pnas.0809201106

Stolz, A., Ernst, A., & Dikic, I. (2014). Cargo recognition and trafficking in selective autophagy. *Nature Cell Biology, 16*(6), 495-501. doi:10.1038/ncb2979

Strange, R. N., & Scott, P. R. (2005). Plant disease: A threat to global food security. *Annual Review of Phytopathology, 43*, 83-116. doi:10.1146/annurev.phyto.43.113004.133839

Su, J., Xu, J., & Zhang, S. (2015). RACK1, scaffolding a heterotrimeric G protein and a MAPK cascade. *Trends Plant Sci, 20*(7), 405-407. doi:10.1016/j.tplants.2015.05.002

Suarez-Rodriguez, M. C., Adams-Phillips, L., Liu, Y., Wang, H., Su, S. H., Jester, P. J., Zhang, S., Bent, A. F., & Krysan, P. J. (2007). MEKK1 is required for flg22-induced MPK4 activation in Arabidopsis plants. *Plant Physiol, 143*(2), 661-669. doi:10.1104/pp.106.091389

Suchanek, M., Radzikowska, A., & Thiele, C. (2005). Photo-leucine and photo-methionine allow identification of protein-protein interactions in living cells. *Nat Methods, 2*(4), 261-267. doi:10.1038/nmeth752

Tambasco-Studart, M., Tews, I., Amrhein, N., & Fitzpatrick, T. B. (2007). Functional analysis of PDX2 from Arabidopsis, a glutaminase involved in vitamin B6 biosynthesis. *Plant Physiol, 144*(2), 915-925. doi:10.1104/pp.107.096784

Tang, J., & Bassham, D. C. (2018). Autophagy in crop plants: what's new beyond Arabidopsis? *Open Biol, 8*(12). doi:10.1098/rsob.180162

Tattoli, I., Philpott, D. J., & Girardin, S. E. (2012). The bacterial and cellular determinants controlling the recruitment of mTOR to the Salmonella-containing vacuole. *Biol Open, 1*(12), 1215-1225. doi:10.1242/bio.20122840

Teh, O. K., & Hofius, D. (2014). Membrane trafficking and autophagy in pathogen-triggered cell death and immunity. *J Exp Bot, 65*(5), 1297-1312. doi:10.1093/jxb/ert441

Thurston, T. L., Wandel, M. P., von Muhlinen, N., Foeglein, A., & Randow, F. (2012). Galectin 8 targets damaged vesicles for autophagy to defend cells against bacterial invasion. *Nature, 482*(7385), 414-418. doi:10.1038/nature10744

Titiz, O., Tambasco-Studart, M., Warzych, E., Apel, K., Amrhein, N., Laloi, C., & Fitzpatrick, T. B. (2006). PDX1 is essential for vitamin B6 biosynthesis, development and stress tolerance in Arabidopsis. *Plant Journal, 48*(6), 933-946. doi:10.1111/j.1365-313X.2006.02928.x

Tonnessen, B. W., Manosalva, P., Lang, J. M., Baraoidan, M., Bordeos, A., Mauleon, R., Oard, J., Hulbert, S., Leung, H., & Leach, J. E. (2015). Rice phenylalanine ammonia-lyase gene OsPAL4 is associated with broad spectrum disease resistance. *Plant Mol Biol, 87*(3), 273-286. doi:10.1007/s11103-014-0275-9

Tsukada, M., & Ohsumi, Y. (1993). Isolation and characterization of autophagy-defective mutants of Saccharomyces cerevisiae. *FEBS Lett, 333*(1-2), 169-174. doi:10.1016/0014-5793(93)80398-e

Ustun, S., Hafren, A., Liu, Q., Marshall, R. S., Minina, E. A., Bozhkov, P. V., Vierstra, R. D., & Hofius, D. (2018). Bacteria Exploit Autophagy for Proteasome Degradation and Enhanced Virulence in Plants. *Plant Cell, 30*(3), 668-685. doi:10.1105/tpc.17.00815

Vanderschuren, H., Boycheva, S., Li, K. T., Szydlowski, N., Gruissem, W., & Fitzpatrick, T. B. (2013). Strategies for vitamin B6 biofortification of plants: a dual role as a micronutrient and a stress protectant. *Front Plant Sci, 4*, 143. doi:10.3389/fpls.2013.00143

Wang, H., Ngwenyama, N., Liu, Y., Walker, J. C., & Zhang, S. (2007). Stomatal development and patterning are regulated by environmentally responsive mitogen-activated protein kinases in Arabidopsis. *Plant Cell, 19*(1), 63-73. doi:10.1105/tpc.106.048298

Wang, S., Boevink, P. C., Welsh, L., Zhang, R., Whisson, S. C., & Birch, P. R. J. (2017). Delivery of cytoplasmic and apoplastic effectors from Phytophthora infestans haustoria by

distinct secretion pathways. *New Phytologist, 216*(1), 205-215. doi:10.1111/nph.14696

Wanner, L. A., Li, G., Ware, D., Somssich, I. E., & Davis, K. R. (1995). The phenylalanine ammonia-lyase gene family in Arabidopsis thaliana. *Plant Mol Biol, 27*(2), 327-338. doi:10.1007/BF00020187

Waterhouse, A. M., Procter, J. B., Martin, D. M., Clamp, M., & Barton, G. J. (2009). Jalview Version 2--a multiple sequence alignment editor and analysis workbench. *Bioinformatics, 25*(9), 1189-1191. doi:10.1093/bioinformatics/btp033

Waters, S., Marchbank, K., Solomon, E., Whitehouse, C., & Gautel, M. (2009). Interactions with LC3 and polyubiquitin chains link nbr1 to autophagic protein turnover. *FEBS Lett, 583*(12), 1846-1852. doi:10.1016/j.febslet.2009.04.049

Wawra, S., Trusch, F., Matena, A., Apostolakis, K., Linne, U., Zhukov, I., Stanek, J., Kozminski, W., Davidson, I., Secombes, C. J., Bayer, P., & van Westa, P. (2017). The RxLR Motif of the Host Targeting Effector AVR3a of Phytophthora infestans Is Cleaved before Secretion. *Plant Cell, 29*(6), 1184-1195. doi:10.1105/tpc.16.00552

Wei, Y., Liu, W., Hu, W., Liu, G., Wu, C., Liu, W., Zeng, H., He, C., & Shi, H. (2017). Genome-wide analysis of autophagy-related genes in banana highlights MaATG8s in cell death and autophagy in immune response to Fusarium wilt. *Plant Cell Rep, 36*(8), 1237-1250. doi:10.1007/s00299-017-2149-5

Whisson, S. C., Boevink, P. C., Moleleki, L., Avrova, A. O., Morales, J. G., Gilroy, E. M., Armstrong, M. R., Grouffaud, S., van West, P., Chapman, S., Hein, I., Toth, I. K., Pritchard, L., & Birch, P. R. J. (2007). A translocation signal for delivery of oomycete effector proteins into host plant cells. *Nature, 450*(7166), 115-+. doi:10.1038/nature06203

Whisson, S. C., Boevink, P. C., Wang, S., & Birch, P. R. J. (2016). The cell biology of late blight disease. *Current Opinion in Microbiology, 34*, 127-135. doi:10.1016/j.mib.2016.09.002

Whitehouse, C. A., Waters, S., Marchbank, K., Horner, A., McGowan, N. W. A., Jovanovic, J. V., Xavier, G. M., Kashima, T. G., Cobourne, M. T., Richards, G. O., Sharpe, P. T., Skerry, T. M., Grigoriadis, A. E., & Solomon, E. (2013). Neighbor of Brca1 gene (Nbr1) functions as a negative regulator of postnatal osteoblastic bone formation and p38 MAPK activity (vol 107, pg 12913, 2010). *Proceedings of the National Academy of Sciences of the United States of America, 110*(11), 4428-4428. doi:10.1073/pnas.1300714110

Wildermuth, M. C., Dewdney, J., Wu, G., & Ausubel, F. M. (2001). Isochorismate synthase is required to synthesize salicylic acid for plant defence. *Nature, 414*(6863), 562-565. doi:10.1038/35107108

Win, J., Chaparro-Garcia, A., Belhaj, K., Saunders, D. G., Yoshida, K., Dong, S., Schornack, S., Zipfel, C., Robatzek, S., Hogenhout, S. A., & Kamoun, S. (2012). Effector biology of plant-associated organisms: concepts and perspectives. *Cold Spring Harb Symp Quant Biol, 77*, 235-247. doi:10.1101/sqb.2012.77.015933

Wu, M. Y., Song, J. X., Wang, S. F., Cai, C. Z., Li, M., & Lu, J. H. (2018). Selective autophagy: The new player in the fight against neurodegenerative diseases? *Brain Res Bull, 137*, 79-90. doi:10.1016/j.brainresbull.2017.11.009

Yamamoto, H., Kakuta, S., Watanabe, T. M., Kitamura, A., Sekito, T., Kondo-Kakuta, C., Ichikawa, R., Kinjo, M., & Ohsumi, Y. (2012). Atg9 vesicles are an important membrane source during early steps of autophagosome formation. *Journal of Cell Biology, 198*(2), 219-233. doi:10.1083/jcb.201202061

Yan, P., Shen, W., Gao, X., Li, X., Zhou, P., & Duan, J. (2012). High-throughput construction of intron-containing hairpin RNA vectors for RNAi in plants. *Plos One, 7*(5), e38186. doi:10.1371/journal.pone.0038186

Yan, Y., Wang, P., He, C., & Shi, H. (2017). MeWRKY20 and its interacting and activating autophagy-related protein 8 (MeATG8) regulate plant disease resistance in cassava. *Biochem Biophys Res Commun, 494*(1-2), 20-26. doi:10.1016/j.bbrc.2017.10.091

Yang, M., Zhang, Y., Xie, X., Yue, N., Li, J., Wang, X. B., Han, C., Yu, J., Liu, Y., & Li, D. (2018). Barley stripe mosaic virus gammab Protein Subverts Autophagy to Promote Viral Infection by Disrupting the ATG7-ATG8 Interaction. *Plant Cell, 30*(7), 1582-1595. doi:10.1105/tpc.18.00122

Yi, M., & Valent, B. (2013). Communication between filamentous pathogens and plants at the biotrophic interface. *Annu Rev Phytopathol, 51*, 587-611. doi:10.1146/annurev-phyto-081211-172916

Yoshimoto, K., Jikumaru, Y., Kamiya, Y., Kusano, M., Consonni, C., Panstruga, R., Ohsumi, Y., & Shirasu, K. (2009). Autophagy negatively regulates cell death by controlling NPR1-dependent salicylic acid signalling during senescence and the innate immune response in Arabidopsis. *Plant Cell, 21*(9), 2914-2927. doi:10.1105/tpc.109.068635

Yu, Z. Q., Ni, T., Hong, B., Wang, H. Y., Jiang, F. J., Zou, S. S., Chen, Y., Zheng, X. L., Klionsky, D. J., Liang, Y. H., & Xie, Z. P. (2012). Dual roles of Atg8-PE deconjugation by Atg4 in autophagy. *Autophagy, 8*(6), 883-892. doi:10.4161/auto.19652

Yue, J., Sun, H., Zhang, W., Pei, D., He, Y., & Wang, H. (2015). Wheat homologs of yeast ATG6 function in autophagy and are implicated in powdery mildew immunity. *BMC Plant Biol, 15*, 95. doi:10.1186/s12870-015-0472-y

Zaffagnini, G., Savova, A., Danieli, A., Romanov, J., Tremel, S., Ebner, M., Peterbauer, T., Sztacho, M., Trapannone, R., Tarafder, A. K., Sachse, C., & Martens, S. (2018). p62 filaments capture and present ubiquitinated cargos for autophagy. *EMBO J, 37*(5). doi:10.15252/embj.201798308

Zeng, H., Xie, Y., Liu, G., Lin, D., He, C., & Shi, H. (2018). Molecular identification of GAPDHs in cassava highlights the antagonism of MeGAPCs and MeATG8s in plant disease resistance against cassava bacterial blight. *Plant Molecular Biology, 97*(3), 201-214. doi:10.1007/s11103-018-0733-x

Zess, E. K., Jensen, C., Cruz-Mireles, N., De la Concepcion, J. C., Sklenar, J., Stephani, M., Imre, R., Roitinger, E., Hughes, R., Belhaj, K., Mechtler, K., Menke, F. L. H., Bozkurt, T., Banfield, M. J., Kamoun, S., Maqbool, A., & Dagdas, Y. F. (2019). N-terminal beta-

strand underpins biochemical specialization of an ATG8 isoform. *PLoS Biol, 17*(7), e3000373. doi:10.1371/journal.pbio.3000373

Zhang, J., Shao, F., Cui, H., Chen, L. J., Li, H. T., Zou, Y., Long, C. Z., Lan, L. F., Chai, J. J., Chen, S., Tang, X. Y., & Zhou, J. M. (2007). A Pseudomonas syringae effector inactivates MAPKs to suppress PAMP-Induced immunity in plants. *Cell Host & Microbe, 1*(3), 175-185. doi:10.1016/j.chom.2007.03.006

Zhang, S., & Klessig, D. F. (1998). Resistance gene N-mediated de novo synthesis and activation of a tobacco mitogen-activated protein kinase by tobacco mosaic virus infection. *Proc Natl Acad Sci U S A, 95*(13), 7433-7438.

Zhang, S., & Klessig, D. F. (2001). MAPK cascades in plant defence signalling. *Trends in Plant Science, 6*(11), 520-527.

Zhang, Y., Jin, X., Ouyang, Z., Li, X., Liu, B., Huang, L., Hong, Y., Zhang, H., Song, F., & Li, D. (2015). Vitamin B6 contributes to disease resistance against Pseudomonas syringae pv. tomato DC3000 and Botrytis cinerea in Arabidopsis thaliana. *J Plant Physiol, 175*, 21-25. doi:10.1016/j.jplph.2014.06.023

Zhang, Y., Liu, B., Li, X., Ouyang, Z., Huang, L., Hong, Y., Zhang, H., Li, D., & Song, F. (2014). The de novo biosynthesis of vitamin B6 is required for disease resistance against Botrytis cinerea in tomato. *Mol Plant Microbe Interact, 27*(7), 688-699. doi:10.1094/MPMI-01-14-0020-R

Zhuang, X., Chung, K. P., Cui, Y., Lin, W., Gao, C., Kang, B. H., & Jiang, L. (2017). ATG9 regulates autophagosome progression from the endoplasmic reticulum in Arabidopsis. *Proc Natl Acad Sci U S A, 114*(3), E426-E435. doi:10.1073/pnas.1616299114

Zientara-Rytter, K., Lukomska, J., Moniuszko, G., Gwozdecki, R., Surowiecki, P., Lewandowska, M., Liszewska, F., Wawrzynska, A., & Sirko, A. (2011). Identification and functional analysis of Joka2, a tobacco member of the family of selective autophagy cargo receptors. *Autophagy, 7*(10), 1145-1158. doi:10.4161/auto.7.10.16617

Zientara-Rytter, K., & Sirko, A. (2014). Selective autophagy receptor Joka2 co-localizes with cytoskeleton in plant cells. *Plant Signalling & Behavior, 9*(5). doi:10.4161/psb.28523

Zientara-Rytter, K., & Sirko, A. (2014). Significant role of PB1 and UBA domains in multimerization of Joka2, a selective autophagy cargo receptor from tobacco. *Front Plant Sci, 5*, 13. doi:10.3389/fpls.2014.00013